
**PHD**

# The characterisation of next generation ceramic bearings for orthopaedic hip applications

Insley, Gerard M.

*Award date:*
2003

*Awarding institution:*
University of Bath

# The Characterisation of Next Generation Ceramic Bearings for Orthopaedic Hip Applications

Submitted By Gerard M. Insley
For the degree of PhD
At the University of Bath
2003



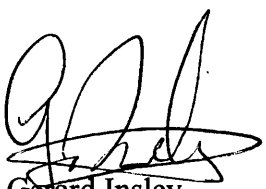

Gerard Insley





ProQuest LLC
789 East Eisenhower Parkway
P.O. Box 1346
Ann Arbor, MI 48106-1346

## Abstract

Two zirconia toughened alumina ceramic materials were characterised for application as bearing surfaces for hip joint arthroplasty. Both ceramics were supplied by orthopaedic ceramic suppliers in the form of flat discs, flexural strength bars and finished ball heads and cups. Analysis techniques involved standard and novel test methods in order to gauge the suitability of the ZTA for this application. These included mechanical strength testing, phase composition analysis by x-ray diffraction, accelerated and real time stability testing, friction testing and hip simulator testing under standard and non-standard conditions. Alumina was used as a control in all testing.

The results show the ZTA materials to be 50 to 75% stronger and up to 25% tougher than the alumina. Both materials differ in terms of their processing, microstructure and crystalline phase composition, however both showed no tetragonal to monoclinic degradation after both accelerated and real time ageing.

The friction and wear tests show the ZTA to be performing as well as the alumina in normal test conditions. However, when microseparation is introduced into the hip simulator testing the ZTA ceramics wear significantly less than the alumina. Clinical analysis of a series of explanted heads showed that microseparation definitely occurs in the clinical situation with wear scars observed in eleven out of sixteen components.

Zirconia toughened alumina is suitable as a fourth generation bearing surface for hip joint arthroplasty.

# Acknowledgements

I would like to thank my PhD supervisor Dr. Irene Turner for her supervision, knowledge and above all else patience.

I am extremely grateful to all my industrial supervisors throughout the term of this project. I would like to thank Christina Doyle for encouraging me to start this work and ensuring I kept at it! Ian Brown for putting a bomb under me at the appropriate time and my current boss Robert Streicher for his support.

I would also like to take this opportunity to thank the staff and technicians of the school of materials science, University of Bath, specifically Frank for all his help. Likewise the postgraduate students I have had the pleasure of working with; namely Brian Casey and Bernd Grimm.

Special thanks goes to Matthew Murphy, Todd Stewart, Roger Morrell and Bill Walter for their input and advice.

I would like to thank my wife Patricia for all her support and understanding over the last five years.

Finally, to my parents without whom none of this work would have been possible.


*Humanity needs practical men, who get the most out of their work, and, without forgetting the general good, safeguard their own interests. But humanity also needs dreamers, for whom the disinterested development of an enterprise is so captivating that it becomes impossible for them to devote their care to their own material profit.*

*Without doubt, these dreamers do not deserve wealth, because they do not desire it. Even so, a well-organized society should assure to such workers the efficient means of accomplishing their task, in a life freed from material care and freely consecrated to research.*

Marie Curie

# The Characterisation of Next Generation Ceramic Bearings for Orthopaedic Hip Applications.

## Table Of Contents

# List of Figures

# 1.0 Introduction.

At present the vast majority of orthopaedic hip implants have a polished metal bearing surface articulating against an ultra-high molecular weight polyethylene (UHMWPE) acetabular cup. In the majority of cases, this bearing surface is extremely successful, but there is a growing body of evidence which shows that wear debris produced by this bearing can migrate into the periprosthetic tissue and cause osteolysis [1,2,3, 4].

The resulting aseptic loosening of the hip joint is the main limiting factor affecting the long-term success of modern hip joint arthroplasty.

Two approaches have been taken to improve this outcome:

1. Improve the wear resistance of the UHMWPE through cross-linking the polymer chains.
2. Use hard on hard type bearings i.e. ceramic on ceramic and metal on metal.

Cross-linking of the UHMWPE has been shown to increase the wear resistance of this material [5]. However the wear resistance has been increased at the expense of other material properties and the effect of decreasing the toughness of the material due to varying degrees of cross-linking has been reported [6]. Also the same inherent debris problem still remains with these enhanced materials. UHMWPE debris, although present in small amounts, is still produced with these bearings, and work by Ingham et al [7] has shown that it is the size range as well as the population of this debris that is the important factor with regard to osteolytic potential.

The use of hard-on-hard bearings remains the most promising development in solving this problem for orthopaedic joints applications. Ceramics, because of their high hardness, excellent wear properties and their biological tolerance in the body, are extremely good bearing materials, and will form the main subject of this research.

Alumina and zirconia are the currently used orthopaedic bearing ceramics. Since their introduction in 1969, there have been over two million alumina heads and 300,000 alumina

liners implanted [8]. Zirconia was first implanted later in 1985, and there have been over 300,000 recorded implantations [9]. The use of ceramics for bearing applications has had a difficult history and early components, even though they showed very low wear rates, failed due to poor material, inadequate design and surgical technique. These failures are now well understood and through improvements in the material properties and processing, the use of the modular cups and greater surgical knowledge, the current so called third generation ceramics show excellent short to mid-term clinical outcomes [10].

These ceramics do have inherent disadvantages that can limit them from widespread use as orthopaedic bearing materials. Alumina is extremely hard but brittle and fracture rates, even though small (1 in 25,000, [11]), are unacceptable to some surgeons. Alumina is not a very forgiving material because of this brittleness and requires careful attention to detail in all aspects of its implantation by the surgeon, from handling to correct alignment in order to guarantee a successful outcome. Its mechanical properties limit the number of size ranges that can be offered to the surgeon with 28mm, 32mm and 36 mm heads being the optimal range. Alumina is also generally restricted for use on CoCr stems as this combination is not strong enough to pass the FDA ultimate compression test required for all ceramics prior to use in the body.

Zirconia is a tougher more fracture resistant material. However, because it is in a metastable crystalline state at room temperature, its stability is an issue and is the subject of considerable research [12,9,13]. The toughening mechanism of the yttria-stabilised zirconia depends on the transformation of its metastable tetragonal phase to monoclinic phase and the resulting volume increase acting to close the crack tip. However this transformation can happen spontaneously for a variety of reasons, which will be discussed later, to cause uncontrolled microcracking that can grow to form macrocracks and lead to a reduction in mechanical properties [14]. The low thermal diffusion value of this material can also contribute to this phenomenon. Zirconia fracture rates are typically lower than alumina, however they have been reported [15].

Therefore the main disadvantage of ceramics remains their brittleness or low resistance to fracture; they have $K_{IC}$ values which are roughly one fiftieth of those of ductile metals [16]. The strength of ceramic materials depends on the presence of flaws or cracks in the material.

These flaws are always present and are most commonly caused by the processing methods such as forming, sintering and surface machining. As the design strength of a material is given by the fracture toughness $K_{IC}$ divided by the size of the largest flaw $a_m$, then there are two possible ways to increase the strength of these materials [16]:

1. decrease $a_m$ by careful quality control
2. increase $K_{IC}$ by alloying.

It is the latter solution that is the focus of this research.

The aim of this research was to increase the fracture resistance and strength of alumina without losing its high hardness and stability. Mixing alumina and zirconia has been shown to be promising in achieving these goals [14]. Zirconia toughened alumina has enjoyed widespread use as an engineering ceramic for non-biomedical applications. The focus of this work was to investigate the potential of this material for application as a biomedical grade bearing material for hip joint arthroplasty. The optimum mix composition was selected to give the desired properties and this material was then fabricated and tested using both standard and novel test methods to ensure the objectives were met.

Ultimately, it was hoped that a recommendation could be made with respect to the to use of this composite material as a fourth generation ceramic bearing replacement for clinical applications.

# 2.0 Literature review.

## 2.1 Introduction.

A material scientist working in the field of orthopaedics faces many challenges. The development of new improved materials for application in this field is a long detailed process due to the nature of the safety risks involved in implanting foreign materials into the human body. New materials are first rigorously tested in the laboratory and unsuccessful materials are screened out at this point. Longer term laboratory testing then involves using the material in the design application intended for it. In the case of bearing materials this would be hip simulator testing. Biocompatibility of the material is also checked through a series of standard ISO specified tests. If the material passes through these stages successfully, it can then be considered for pre-clinical animal trials or limited clinical application. In the latter case, the material/implant is followed up closely at a number of key surgical centers for a minimum of five years before it is considered safe for general use. Even at this stage, it is hard to estimate if the material is successful as at least 10 to 15 years clinical use is considered necessary to judge this. Therefore, from the initial conception, it can take 15 to 20 years to know if the new material is a genuine step forward or improvement in terms of added benefit to the patient.

For these reasons it is difficult to assess the success of ceramics for orthopaedic bearing applications. There have been many material, processing and design changes since they were first used in the seventies [17]. The current third generation ceramics have good medium term outcomes and show extremely good survivorship curves [10,17,] however, as more and more surgeons are using ceramic-on-ceramic bearings for younger and more active patients, the design limitations of the current generation orthopaedic ceramics are being reached and exceeded in some cases [18,19,20,21]

Success or failure of a particular material or design of implant is multi-factorial and does not depend on the skill of the material scientist or engineer alone. The surgeon and end user also play a big part in the outcome, success or failure. Early Mittelmeier cups were of a

monolithic design where the whole cup was made of alumina and was screwed directly into the bone, Figure 1.

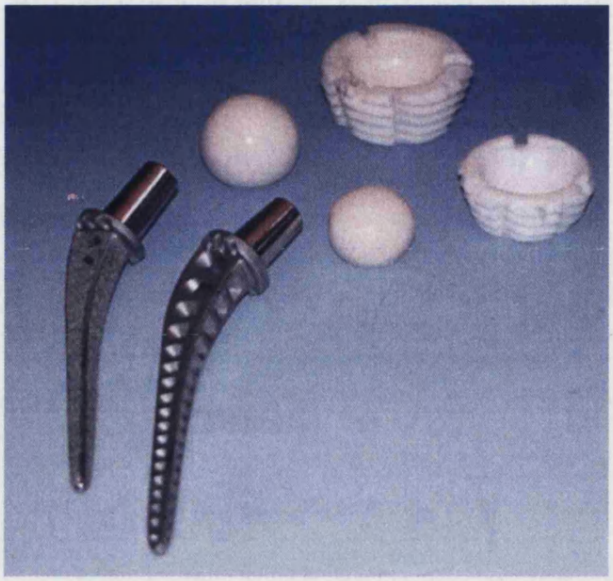

Figure 1: Examples of the early Mittelmeier ceramic on ceramic hip joints [22].

The success of these cups was generally unsatisfactory. Alumina is a bio-tolerant material and hence there was no interaction or natural bone ingrowth between these cups and the surrounding bone, so they failed, due to loosening and migration. However, when these cups were implanted with very good primary fixation i.e. the ceramic was implanted tightly in the surrounding bone, they performed well and showed satisfactory survival curves [23]. This illustrates that even with a poor design a surgeon has the scope to compensate and achieve good results. However the contrary is also true.

Scientists therefore, can only concentrate on designing a material with the optimum properties and then work in partnership with clinicians to ensure the outcomes are optimised to the patients' benefit.

## 2.2 Alumina-on-alumina bearings.

What is the clinical demand that has led to the development of the alumina-on-alumina bearing? The main concern in orthopaedics today is UHMWPE debris induced osteolysis and subsequent loosening of the implant [24,25,26,27,28]. The problem is illustrated in Figure 2, an x-ray of a hip replacement in 1993 and the follow up x-ray at 1997 [29]. There is a clear osteolytic void at the back of the acetabular cup.

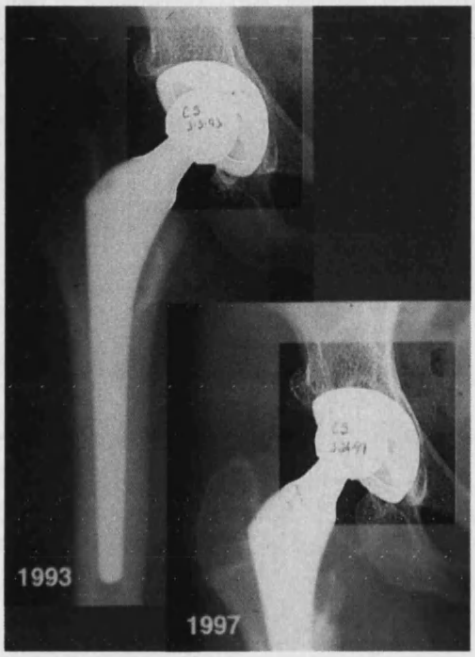


Figure 2: Clinical x-rays post –op and after four years showing development of osteolytic void [29].

The surgeon subsequently revised this hip and the intra-operative picture of the void is clear, Figure 3.

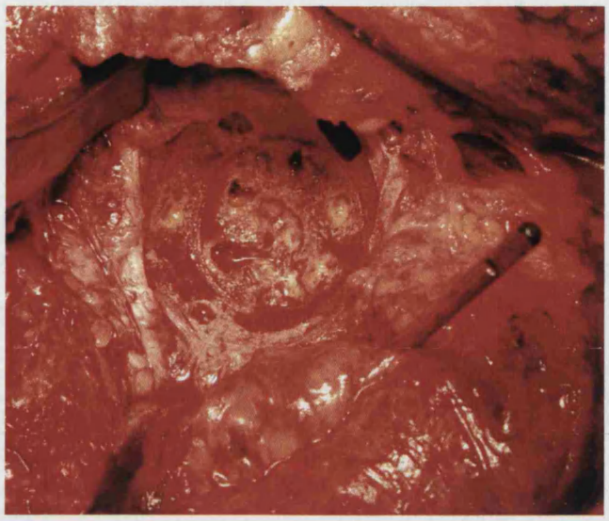

Figure 3: Intra-operative picture of osteolytic void in the acetabulum [29].

Alumina-on-alumina bearings are seen therefore as a suitable bearing combination to avoid this problem of osteolytic loosening. [30, 31] The trend in orthopaedics is such that more and more people are living longer, healthier lives and demand more and more performance from artificial joints, Figure 4.

Figure 4: An example of the increasing demand patients put on their hips [29].

With this increased activity comes an increased demand on the artificial joints, especially the bearing surfaces; more cycles and higher loading are clearly not going to suit the conventional metal polyethylene bearings.

Alumina is a hard material (1900 Hv) [32], that can be polished to extremely low surface roughness (0.01Nm $R_a$) and is hydrophilic [8] making it an ideal low wear bearing combination for hip arthroplasty. The wear results for this bearing are well reported [33,34,35] and generally are found to be $>0.1mm^3/10^6$cycles from *in-vitro* standard simulator testing and between 1-5$mm^3$/year *in-vivo* [36]. Alumina is bio-tolerant and studies show a relatively benign reaction to the small amount of debris produced by this bearing combination [37,38,39].

As discussed previously, alumina-on-alumina has had a chequered past in terms of performance in orthopaedics. When Boutin first used it in 1969, even though the wear was extremely low, the components failed due to loosening, cup migration and fracture [40]. Designs, especially on the cup side were not optimum. The material quality was also variable. The average grain size of these components was typically around 5µm but the deviation was high with grains up to eight or nine microns frequently measured [41]. Residual porosity in the ceramic was also a problem.

As these shortfalls in the material were understood, process changes were introduced to improve the quality of the material. Hot isostatic pressing (HIPing) was the most significant change made to the processing of alumina ball heads and cups for orthopaedic applications. HIPing is a high temperature, high pressure, process that grain refines the alumina and closes any residual porosity thus increasing the strength of the ceramic. This and other process improvement changes, laser engraving, surface polish and 100% proof testing have led to the alumina ceramic now produced, being the state of the art with regard to reliability, repeatability and strength. Figure 5, shows the improvement in the microstructure achieved by the third generation alumina components.

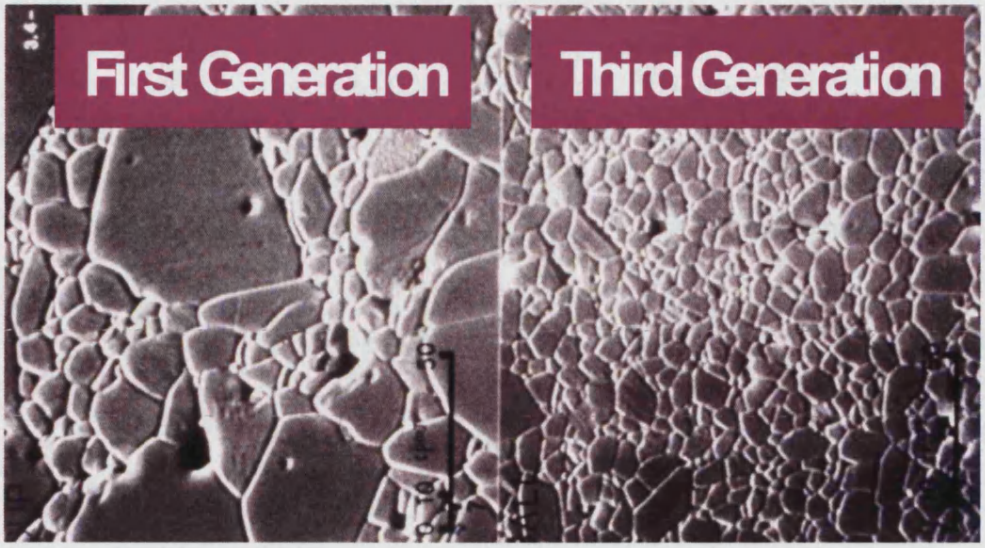


Figure 5: Microstructure differences in first and third generation alumina components [42].

Alongside these material/process improvements, the product designs were optimised. Changes included: modular titanium shells to hold the ceramic cups, optimised taper design on both the cup and heads for improved locking and optimised head offsets. Likewise, the surgeons' knowledge and experience with handling and implanting these components was improved.

All these advances led to much better outcome and survival curves for third generation alumina components, Figure 6.

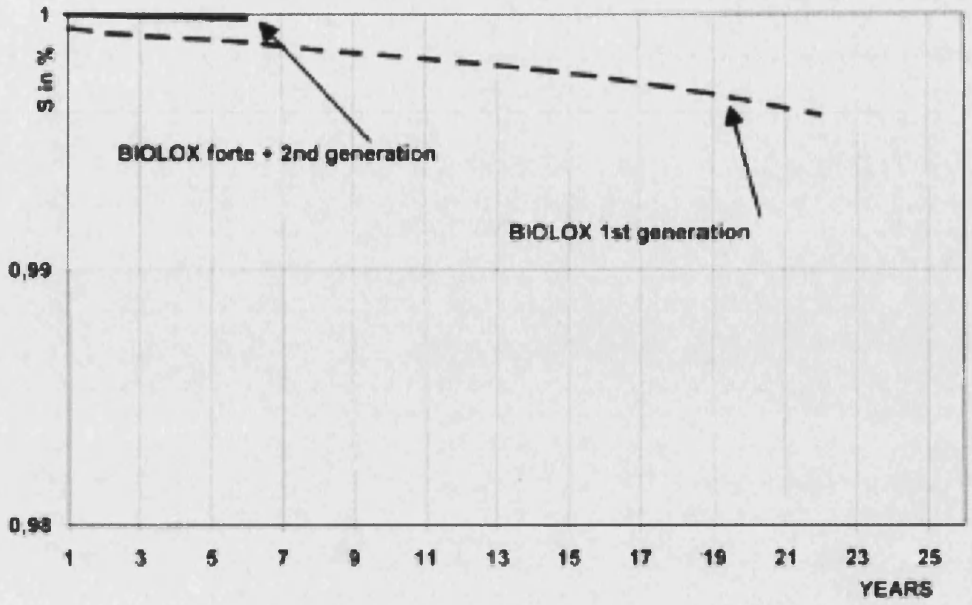


Figure 6: Survival curves comparison for the different generation alumina components [43].

The use of alumina-on-alumina today in orthopaedics is a success story, with many excellent short to mid-term results being reported. The FDA, on a clinical trial basis, has allowed use of the products in the US since 1998 [44] and they are now awaiting approval for general clinical use there. One of these trials that has been successfully reported has shown excellent clinical results for 345 alumina-on-alumina components after a mean follow up of 35.2 months [45]. 514 hips were implanted, 345 alumina on alumina and 169 metal-on-polyethylene. Even though these results are early in the follow-up, the alumina-on-alumina components are performing as well as the metal on polyethylene controls and there have been no cases of alumina fracture. The results from this study show that one of the control metal-on-polyethylene components has shown evidence of a radiolucent line in Gruen zone 1 [45].

Alumina-on-alumina bearings therefore, are a wonderful technology and are appropriate for implantation in young active patients, however this is not to say that they are contra-indicated for older less active patients. Other aspects such as commercial cost play a part in choosing implants for this group.

However, despite this success there are still inherent limitations with the application of alumina-on-alumina in orthopaedics. From a customer perspective, there is a limitation on

the type of stem material alumina can be safely implanted with. Alumina is strong enough to be used on titanium and stainless steel hips but it is not strong enough to pass the FDA strength requirements [46] on cobalt chromium stems. Alumina heads are only available in the 28 to 36mm size range and this is restrictive when a small head (22-26mm) is required. Alumina is a relatively unforgiving material due to its brittleness.

Some surgeons and researchers feel that alumina-on-alumina bearings constitute too much of a hard bearing and that there is no shock absorption present in this joint. It has been proposed that this can lead to weakening of the fixation to the bone and loosening of the implant. Indeed some surgeons [47] will not implant ceramic on ceramic bearings unless the patient has excellent healthy bone to receive the implant. This has led to the design of so-called cushion bearings where a polyethylene liner is sandwiched between the ceramic and the metal shell as shown in Figure 7. It is doubtful however if this small piece of UHMWPE will have any measurable effect as a shock absorber, even though some advantage has been proven [48]. In this regard, it is more relevant what the patient wears on his or her feet. This also has the disadvantage of re-introducing a material (polyethylene) that the alumina-on-alumina bearings are designed to eliminate. Even though the material is not acting as a bearing in this case, micro-movement between the surfaces may lead to wear and debris production from the polyethylene.

CeraLock® combination BIOLOX®forte/metal back.

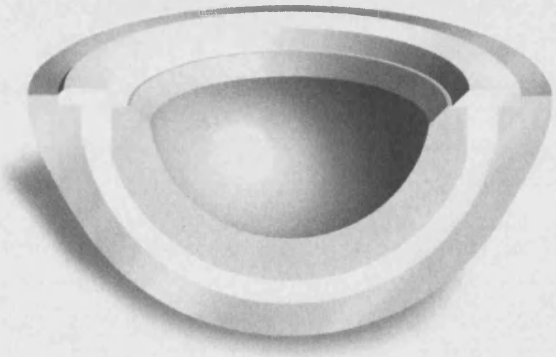

Sandwich construction.

Figure 7: Ceramic shell liner system with and without the UHMWPE sandwich [49].

As researchers in this field have shown, it is clear then that there are obvious improvements that can be made to this bearing combination that will further enhance its clinical success.

## 2.3 Zirconia bearings

Zirconia ($ZrO_2$) or zirconium oxide was first implanted in 1985 [50] as a ball head articulating against a polyethylene liner. The actual chemical form used for the manufacture of ball heads is yttria-tetragonal zirconia polycrystals (Y-TZP). This ceramic material differs to alumina in terms of chemical composition and mechanical/physical properties. Table 1 below shows a comparison of the main properties for both ceramics.

| Property | Alumina | Zirconia |
|---|---|---|
| **Chemical composition** | 99.9% $Al_2O_3$ MgO doping | 97% $ZrO_2$ 3%$Y_2O_3$ |
| **Density** | ≥3.97 g/cm$^3$ | ≥6.0g/cm$^3$ |
| **Porosity** | 0.1% | 0.1% |
| **Bending strength** | 500MPa | 500-1000MPa |
| **Compression strength** | 4100MPa | 2000MPa |
| **Youngs modulus** | 380 GPa | 210 GPa |
| **Poissons ratio** | 0.23 | 0.3 |
| **Fracture Toughness** | 4 MPa √m | ≤ 10 MPa √m |
| **Coeff. Thermal expansion** | 8 x10$^{-6}$K$^{-1}$ | 11 x 10$^{-6}$K$^{-1}$ |
| **Thermal conductivity** | 30 W/mK | 2 W/mK |
| **Hardness** | ≤ 2200 HV0.1 | 1200 HV0.1 |

Table 1: Comparison of main mechanical/physical properties of zirconia and alumina [17].

The chemistry of zirconia is much more involved than medical grade alumina, which is largely a one-phase material of alpha-alumina or corundum and this phase is thermodynamically stable up to 2000°C [51]. Alumina does have less than 0.1% grain boundary impurities which are carefully controlled to avoid excessive glass formation at the grain boundaries through careful control of the sintering cooling cycle. Zirconia on the other hand can exist in three different phases depending on the temperature and to a lesser extent the environment. These phases are monoclinic, tetragonal and cubic zirconia. The transformation temperatures are monoclinic to tetragonal 1950-1200°C and tetragonal to cubic 2677°C [52]. On cooling from sintering temperatures, a pure zirconia block will change from the tetragonal form to the monoclinic form and the whole structure will crack. This is because this transformation is associated with a 3-5% volume increase in the lattice cell.

However this tetragonal to monoclinic transformation and its associated volume increase can be used to improve the toughness and strength of the zirconia [52]. Stabilising agents such as MgO, CaO and $Y_2O_3$ added to the zirconia in small amounts (3-5%) stabilise the tetragonal and cubic phase to room temperature thus avoiding the cracking associated with the volume expansion. Taking this theory one step forward, if insufficient stabilising agent is

added the zirconia becomes what is termed partially stabilised or metastable. It was first realised by Garvie et al [53, 54] that by utilising the tetragonal to monoclinic transformation of metastable tetragonal particles, induced by the effect of a stress field ahead of a crack, the toughness of the ceramic could be increased. The volume expansion associated with the transformation acts on the crack to increase the ceramics resistance to its propagation, Figure 8.

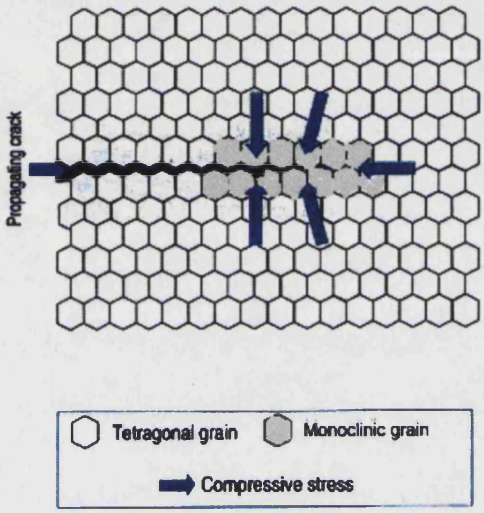


Figure 8: Schematic of phase transformation toughening in zirconia ceramics [50].

Logically then, it was found that as the amount of tetragonal particles retained in the microstructure increased the toughness increased. This led to the development of a ceramic consisting of almost 100% tetragonal zirconia polycrystals (TZP) [54]. By controlling the sintering temperatures to below 1400°, ensuring the starting powder is chemically homogeneous and the grain size of the zirconia is controlled below 0.7 µm a ceramic with high toughness, strength and mechanical properties can be produced [54].

Orthopaedic grade zirconia contains 93.5 wt% $ZrO_2$ with 5.2 wt% $Y_2O_3$, 2 wt% $HfO_2$ and <0.5 wt% $Al_2O_3$ [55]. More than 95% of the zirconia is in the metastable tetragonal phase (TZP) the remainder is either cubic or monoclinic zirconia. The microstructure of the

zirconia grains is controlled to below 0.5µm to ensure that the tetragonal phase remains stable in physiological conditions, Figure 9.

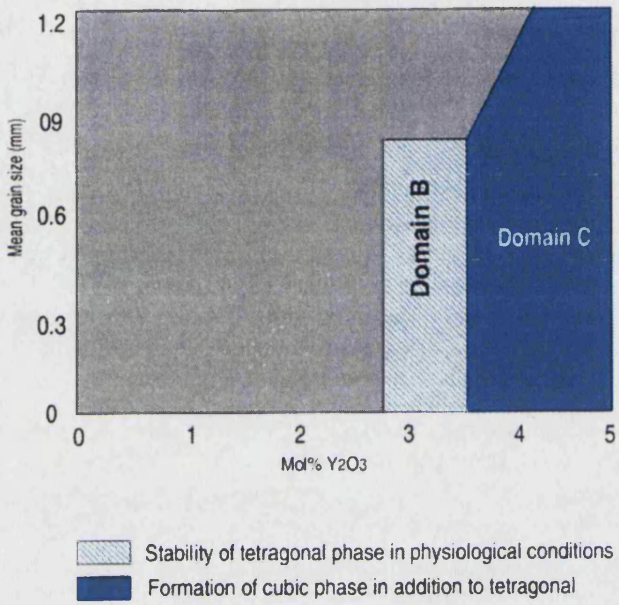


Figure 9 Schematic stability diagram of Y-TZP ceramic in physiological conditions. [50]

Zirconia because of its high strength and good wear resistance has been used widely as a ball head in orthopaedics. Zirconia has the advantage over alumina in cases where small head sizes are required and 22mm zirconia heads are now routinely implanted. It is also suitable for any type of hip spigot material as it passes the FDA requirements for strength on cobalt chrome and stainless steel [56].

The wear performance of zirconia against polyethylene is well reported [57,58,59]. Most authors concur that because of the high hardness and scratch resistance of the zirconia the wear on the polyethylene is reduced. McKellop et al [60] found the wear rate of zirconia against polyethylene to be 10.9 $mm^3/10^6$ cycles as opposed to 15.7 $mm^3/10^6$ cycles for cobalt chromium heads articulating against polyethylene in a joint simulator. The surprising finding from this work was that they discovered the alumina heads produced the highest wear of all the heads tested with 17.9 $mm^3/10^6$ cycles. The authors propose that this may be due to surface roughness variation from different manufacturers of ceramic ball heads, however there was no as-received roughness values presented in the paper to support this theory.

The mechanism by which the ceramic heads articulating against polyethylene reduce wear has to be due to their high resistance to damage and scratching. Metal heads, even though they are much harder than the polyethylene, gradually roughen due to four main processes: (1) surface wettability changes (2) oxidative wear (3) miroabrasion of metal surfaces from oxide film damage and (4) surface abrasion from 3rd body particles such as bone cement or bone debris [61]. Hard stable ceramic heads will maintain their surface finish and thus reduce the overall wear in the long term. Minakawa et al [62] explored the effect of scratching the surfaces of 10 sets each of cobalt chrome, stainless steel and zirconia heads, on the wear rate in a simulator. The type, amount and depth of scratches were determined in each case by measuring representative scratches on retrieved clinical components. The results from this analysis show the ceramic clinical components to have significantly lower $R_{pm}$ values (mean height of the scratches above the mean line). The ceramic heads had a mean $R_{pm}$ of 0.02 μm compared to 0.98 μm for the cobalt chrome heads. The authors present the effect on wear of polyethylene from severely damaged heads and heads with little or no damage. It is clear that the resistance to damage has a large influence on the amount of wear seen, with a 50% reduction in linear and volumetric wear and wear debris produced for the low damaged heads. Therefore, the high hardness and scratch resistance of zirconia ceramic heads results in lower polyethylene wear.

However, the explanted ceramic heads used in this study had a significantly lower implantation time compared to the cobalt chrome heads (14.4 years as opposed to 4.8 years). The authors have not adequately discussed this. It can be proposed however that the $R_{pm}$ value is not likely to change very much for the ceramics after fourteen years implantation, therefore the wear rate should remain low.

Controversy exists however over the use of zirconia in hard-on-hard bearings. As discussed before, the main problem that causes joint failure lies in the wear debris produced by the polyethylene bearing causing osteolysis and loosening. Even though using zirconia heads articulating against polyethylene reduces the wear, the polyethylene particles are still being produced in the joint space. Bigsby et al [63] looked at metal against polyethylene and zirconia against polyethylene in a hip simulator. They found where there is no damage to the

heads and no third body particles present, the wear rates are similar, i.e. they found no advantage to using zirconia articulating against polyethylene.

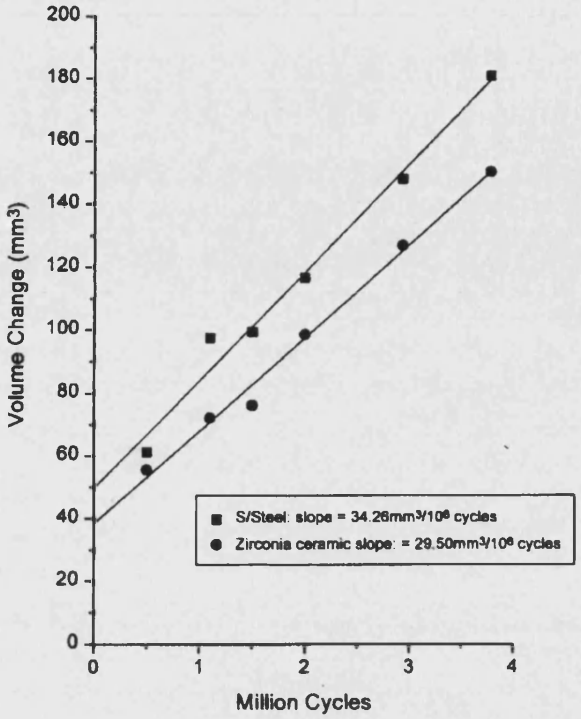


Figure 10: Regression analysis of the volumetric wear of 32mm cups articulating against zirconia ceramic and stainless steel heads [63].

Figure 10, shows the regression analysis plots of the wear rates from this study. The zirconia head produced a polyethylene wear rate of 29.50 $mm^3/10^6$cycles and the stainless steel head produced a wear rate of 34.26 $mm^3/10^6$cycles. The difference is not statistically significant.

Therefore, the use of a zirconia head articulating against polyethylene will only delay the osteolytic mechanism not prevent it. Zirconia-on-zirconia bearings have been proposed and used clinically as an option to alumina-on-alumina bearings [64]. Examining the literature, there are mixed results reported. Amin et al [65] examined the wear of zirconia-zirconia (Y-TZP) in a pin on plate assembly and examined the effect of different lubricants on the wear rate. The authors concluded that the system was very sensitive to the lubricant used. Dry sliding in air caused cracking and delamination of the surface. Water as the lubricant caused wear by an adhesive mode with a transfer film evident on the plate. Oil was found to

produce acceptable wear rates. Nevelos et al [22] found in a pin-on-plate study, comparing zirconia-on-zirconia to various other combinations, this couple had a wear rate that was an order of magnitude higher than any other couple tested. These were tested in bovine serum and the result led to the authors discarding this couple from further studies. Willmann et al [66,67] also demonstrated high wear for zirconia-on-alumina and zirconia-on-zirconia couples when compared to alumina-on-alumina in ISO6474 pin-on-plate testing.

Even though the above results show zirconia-on-zirconia to be a disastrous wear couple, engineers and scientists at different centres have persevered with the combination. The problem with pin-on-plate testing is that it is a simple configuration-screening test. It bears no resemblance to the shape, form, design or lubrication regime that the couple will experience *in-vivo*. As hip simulator studies are long and expensive and resources or centers that can adequately carry them out are limited, most researchers were willing to disregard the zirconia-on-zirconia couple at this stage.

Clarke et al [68] carried the combination into full bovine serum lubricated hip simulator studies. The authors tested zirconia against alumina and zirconia against zirconia. The former couple is interesting as it is mainly the alumina head in the alumina-on-alumina bearings that is likely to fracture and alumina heads have a restricted size range available i.e.28-32mm. Using a zirconia head articulating against an alumina cup would theoretically solve these restrictions. Clarke found very low wear rates for this couple and the zirconia-on-zirconia couple at five million cycles compared to alumina [68]. The author continued to run the simulator out to 15 million cycles and found the same wear trend.

Rieker [69] looked at the zirconia-on-zirconia, alumina-on-alumina and metal on metal wear in the simulator. It was found that the ceramic bearings wore the least, 0.6 µm per million cycles as opposed to 5.6 µm per million cycles for metal. Again, the simulation was run in bovine serum and the zirconia heads performed well.

Taking this couple one step further, Banon [70] reports on a radomised trial of 163 cases where the zirconia-on-alumina couple was implanted. The reported outcomes are for an extremely short implantation time, 1-24 months, however no problems were reported on the Harris hip score or radiological evaluation with any of the patients. Pitto et al [71, 72]

looked at a smaller scale trial with ten alumina-on-alumina patients and five zirconia-on-alumina patients. Again, the follow up time is short, however audible squeaking was noted in one of the five patients.

These short clinical trials are by no means proof that the zirconia-on-alumina couple is safe. Both surgeons concluded that there were still some concerns about the use of the couple and that further careful investigation was required. The trials were limited and badly set up. The ceramic components used in both cases were a mix and match of designs, ceramic supplier and sizes, even within patients. It would be very difficult to derive conclusions from either of these trials. The audible squeaking noted in one of the five patients in Pitto's study is worrying. This could be due to the mix of designs causing sub-optimal lubrication.

Overall, there is still a lingering doubt about the performance of zirconia in a hard-on-hard bearing. In any given wear situation articulating surfaces have a regime of parameters within which the wear rate is optimum. Go outside these parameters and whatever the bearing material, it will break down. This is also true of the hip bearing system. The parameters that are important in this system are the lubrication regime, the applied load and the type of loading. Hip simulator testing is "best case" testing where all these parameters are optimised. However the clinical situation is different, sub-optimised lubrication can occur (diseased synovium), higher than normal loading (jumping, running, stair climbing) and various types of loading (point contact due to steep cup angles, impingement) can occur regularly. Ceramic bearings have to be capable of performing under these harsh conditions as well as the optimum conditions. The alumina-on-alumina couple has a proven track record under such conditions, and has been tested in water and dry in the hip simulator [73]. The wear has increased in these conditions but it was not disastrous runaway wear. It can be deduced then that the alumina-on-alumina system has a large envelope of resistance to damage in adverse conditions. The zirconia hard-on-hard system on the other hand has a much smaller envelope of resistance to damage under adverse conditions. This is why there are different results reported on the system. The pin-on-plate testing represents sub-optimised lubrication and point contact conditions that the zirconia-on-zirconia bearing cannot handle. Likewise, it will run up to 15 million cycles in a simulator under ideal conditions showing very little wear [68], however it is a disastrous couple when water is used in the simulator instead of bovine serum [74]. Ideal conditions cannot be guaranteed in

the clinical situation and this will potentially lead to performance problems for zirconia in the hard-on-hard application.

Spontaneous transformation from the tetragonal to the monoclinic phase has been shown to occur on the surface of these ceramic ball heads *in-vivo* and this is termed transformation ageing [75, 76]. The associated volume increase results in the surface becoming roughened and this is followed by high polyethylene wear [75]. This phenomenon has been extensively studied in the literature [77,78,79,80,81]. The most extensive review of all the data has been completed by Lawson [82] who reviewed over one hundred publications on the environmental degradation of zirconia ceramics, examining the mechanisms and suggesting techniques to retard or prevent the transformation. As discussed previously, the TZP zirconia is in a metastable tetragonal form due to the addition of rare earth oxides such as yttria. Research has found that this metastable tetragonal phase can transform to monoclinic phase, and hence age, in the presence of aqueous fluids over a temperature range of 65-500°C [82]. During this ageing, degradation in mechanical properties such as bending strength and toughness can occur. Clearly, this ageing is not a desirable attribute of the material and the aim is to first understand the mechanism of how it occurs so that it can be avoided altogether. From Lawson's experimental work and review of the literature, a number of material based variables are outlined that, if not controlled, can lead to ageing. The grain size, stabiliser content and composition of the zirconia all affect the rate and/or occurrence of ageing. It has been suggested that the optimum grain size for TZP materials (3 mol% Y) is between 0.3 to 0.6 μm to retard ageing [50]. Lawson also agrees with this, the effect of grain size is dependent on the yttria content; above a certain grain size, certainly at grain sizes above 1 μm, the material exhibits a large amount of tetragonal – monoclinic transformation and decreases in strength. Also, below a grain size of 0.4μm it can be shown that no transformation occurs at all, leading to a decrease in the toughness values for these ceramics. Figure 11 below shows this relationship and Figure 12 outlines the effect of the yttria content on the critical grain size for ageing.

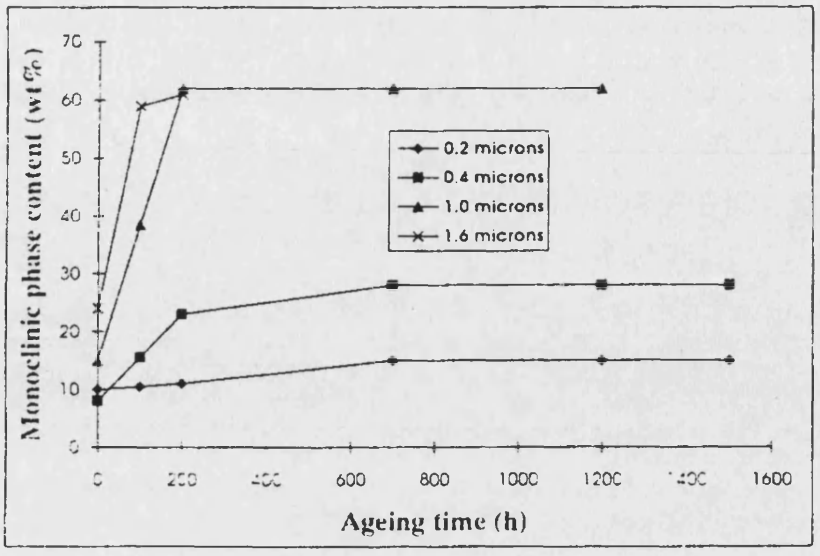


Figure 11: Grain size dependence of surface phase transformation on a 3Y-TZP aged at 230°C in air [82].

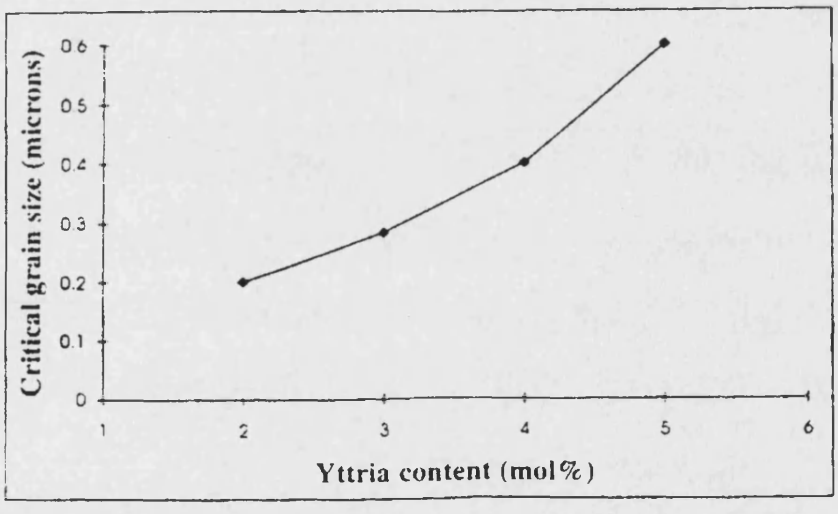


Figure 12: Critical grain size as a function of yttria content when aged in air at 300°C for 100h [82].

Stabiliser content has a large effect on the ageing resistance of these ceramics [82]. Again, there is a critical amount above which the cubic zirconia phase is increasingly formed in

preference to the tetragonal phase with an associated loss in strength. At the lower end, too little stabiliser and the t-m transformation will occur readily.

There is much debate on how the ageing mechanism starts and proceeds in these ceramics. Again Lawson [82] reviews and summarises the various theories adequately. It is generally accepted that the tetragonal grains transform to the monoclinic form at the grain boundaries and then move into the centre of the grain. From optical microscopy studies and XRD measurements the monoclinic phase generally starts at the surface of the material and proceeds into the bulk. With this in mind, there are three main mechanisms for ageing of TZP zirconia proposed:

1. corrosion mechanisms
2. destabilisation mechanisms
3. stress induced transformations.

Corrosion mechanisms are mainly based on the attack of the Zr-O-Zr bonds by water – either at a crack tip or at the free surface. This mechanism is demonstrated in Figure 13 below:

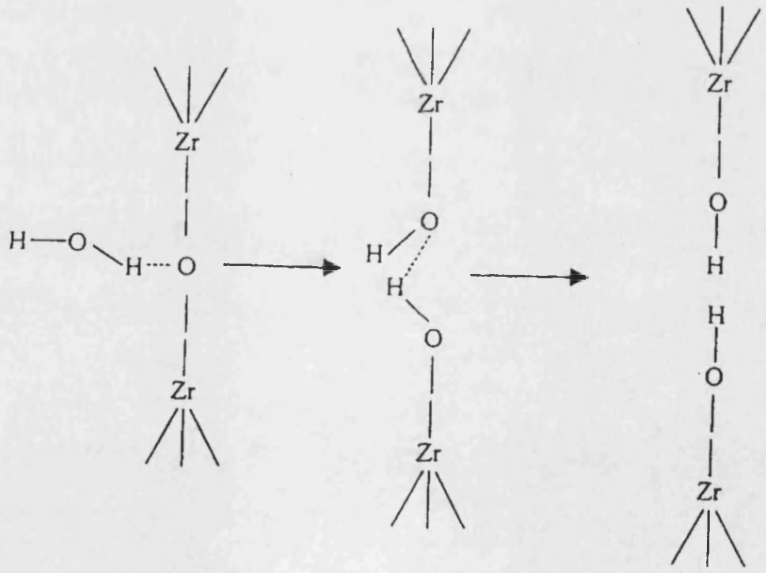


Figure 13: Reaction scheme expected for the reaction between water and Zr-O-Zr bonds at the crack tip [83].

This reaction has been proposed to release the strain in the zirconia grains, which stabilises the tetragonal phase, thus allowing the t-m transformation to occur. A more plausible corrosion based mechanism is proposed by Yoshimura [82] who noted an increase in the crystal lattice associated with the t-m transformation. It was also found that the original lattice parameters could be restored almost immediately by annealing the ceramic at 400°C for six hours in a vacuum. The authors concluded that this reversible change was the result of the inclusion of $OH^-$ in the lattice. This was confirmed by Raman spectroscopy measurements. The mechanism is described schematically in Figure 14 and can be summarised as follows:

1. Chemical adsorption of $H_2O$ at the surface.
2. The formation of Zr-OH and or Y-OH bonds at the surface, at which point stressed sites are created.
3. The accumulation of strain by the migration of $OH^-$ ions at the surface and in the lattice, to prepare nucleation defects.
4. The nucleation of the monoclinic phase in the tetragonal – monoclinic transformation yields micro and macro cracking. [82]

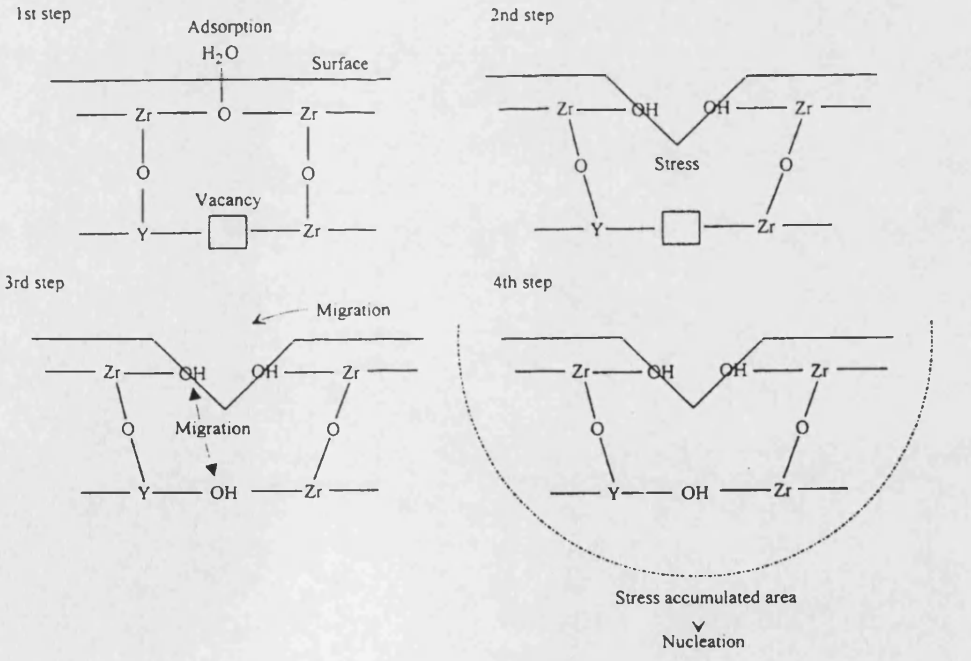


Figure 14: Proposed degradation process of Y-TZP by the $OH^-$ trigger mechanism. [82]

Destabilisation mechanisms for ageing of the TZP materials mainly involve the depletion of yttrium in specific areas of the microstructure due to the action of the water vapor. This occurs first on the surface and as the yttrium is drawn out the locally effected zirconia grains transform. If these grains are a critical size then this transformation is associated with micro-cracking which in turn opens up more of the microstructure to the action of the water vapor [82]. This mechanism is not prevalent in orthopaedic grade zirconia as the diffusion rate of yttria is minimal at anything lower than 1000°C.

Stress induced transformation ageing is also reported in the literature [83]. Lawson [82] outlines an experiment where 2 mol % Y-TZP samples were prepared for TEM analysis. The sample was analysed in the TEM before and after annealing at 250°C in humid air for 6 hours. As is shown in Figure 15 only the protruding unconstrained grain in position 4 remains untransformed. This indicates that the local stress situation prevalent for each grain has a large bearing on its stability.

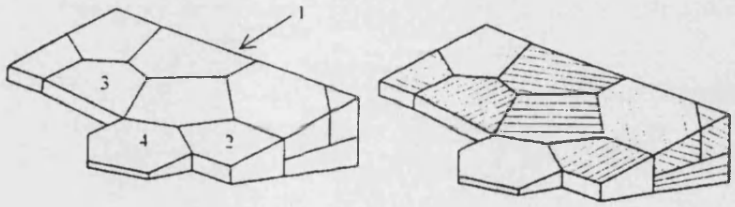


Figure 15: TEM experiment showing the effect of ageing for 168h, at 250°Cin humid air, on constrained and unconstrained grains in 2Y-TZP. [82].

It is known that shear and tensile stresses are destabilising forces whereas compressive stresses are stabilising forces [14]. Another mechanism not reported in the literature involves the grain boundary impurities present in the zirconia. Silica is present in small amounts and is highly water soluble. As the silica dissolves, the constraint on the tetragonal grains is reduced and transformation occurs. The addition of small amounts of alumina to the material decreases the solubility of the silica thus stabilising the material.

How do these mechanisms manifest themselves in the orthopaedic application of the material? Cales et al have written extensively on this subject [84,85]. Their studies have monitored and measured the transformation through *in-vitro* artificial ageing in an autoclave to analysing retrieved explants. Their main findings show that the transformation does occur on the surface of zirconia ceramics but to a small degree. This amount of transformation does not affect the wear properties [84] or the strength properties [84,85]. The proposal is that the modern HIPped zirconia ceramic has less than 5% monoclinic transformation on the surface. This is maintained at a low level through tight control over the critical grain size as shown previously in Figure 9, and the use of pure starting powders, the even dispersion of yttria throughout the matrix and the addition of small levels of $Al_2O_3$ to the material. These findings were also echoed by Shimizu et al [86] who looked at *in-vitro* and *in-vivo* time dependent changes in the mechanical properties of the zirconia. They found no monoclinic content over 5-mol % after ageing in saline and in a rabbit model for three years. The bending strength of the ceramic did not change in any of the experiments. The authors concluded that the material was therefore safe for orthopaedic applications. One limitation to their findings has to be the unloaded, unstressed nature of the implants in the *in-vivo* animal model. Flexural strength bars were simply implanted in the medullary cavity of the rabbit tibia. These implants would have been exposed to the corrosion action of the body fluids, however they would not experience the shear stresses experienced at a bearing surface. As demonstrated previously the stress induced ageing mechanism plays a large part in the ageing behavior of these ceramics [82]. A similar study by Christel et al [87] echoed the same results. Murray et al [88] looked at the *in-vivo* and *in-vitro* ageing of zirconia and reported very little t-m transformation or drop in strength of the ceramic after 1.5 years *in-vivo* and 300 days *in-vitro*.

Thomson and Rawlings looked at this ageing behaviour and found a detrimental drop in bending strength after exposure of the Y-TZP material to saline ageing [89,90,91]. The authors concluded that the extent of the surface monoclinic formation and the subsequent loss in hardness and fracture toughness makes these materials unsuitable for orthopaedic use. These are strong conclusions and therefore the data warrants close investigation. The materials used for this study were produced on a laboratory scale by the authors. The properties of these materials were not adequately addressed in the data to assess how they compare to today's commercially produced material. The grain size was controlled at

0.5μm, by sintering between 1400-1500°C. The components were not HIPped and therefore could not have been at the optimum density. In addition, dispersion or chemical purity of the starting raw material powders was not outlined in the data. All these attributes can have a large bearing on the ageing of the zirconia and have not been discussed in this work.

Drummond [92] reported similar results to Rawlings. His study looked at the strength of zirconia aged in Ringer's solution for exposure times up to 453 days. The zirconia used in this study showed a 13-22% drop in strength.

In summary, the zirconia ceramic has many advantages over alumina for use as an orthopaedic bearing surface. Its high fracture toughness makes it suitable for use with the full range of orthopaedic hip joint materials, spigots and sizes (22-36mm). There are however disadvantages or limitations with the material – its use in a hard-on-hard bearing needs further research, the phenomenon of transformation ageing is of concern and the low thermal conductivity of the material may further add to these problems.

A fresh look at these limitations of both alumina and zirconia was required and this led to the use of zirconia toughened alumina as a bearing material for hip joint arthroplasty.

## 2.4 Zirconia Toughened Alumina

Zirconia added to alumina as a grain-refining agent in ppm levels is a well-established practice, however the addition of large quantities of zirconia in order to toughen the alumina is a relatively new development [54]. These ceramics have become known as zirconia toughened alumina (ZTA). The addition of discrete particles of zirconia to the alumina matrix (typically in the range 5-45vol %) gives the resulting ceramic material increased toughness (10-12 MPa $m^{0.5}$ as opposed to 3 MPa $m^{0.5}$ for alumina) and increased strength (1000-1100 MPa as opposed to 450 MPa for alumina)[54]. The advantages for orthopaedics are immediately obvious. Even though the industry has been well served by the alumina and zirconia ceramics there is scope to improve their performance and the ZTA materials have generated a lot of attention for possible orthopaedic use.

The main part of this thesis is involved with the characterisation of these materials for orthopaedic hip joint bearing surfaces. The first step was to review the information already available on these materials from other industries in order to ascertain what form would be the most suitable for hip bearing applications. The main variables that needed to be decided were the form of zirconia added i.e. unstabilised tetragonal zirconia, monoclinic zirconia or partially stabilised zirconia particles or a mixture of all three, and the volume fraction in which these should be added to the material. The best processing route for these materials was also briefly explored.

In an excellent review of the technology, Wang and Stevens [54] outlined the toughening mechanisms that operate in the ZTA, which relates directly to the type and shape and volume of zirconia crystals added. The main toughening mechanisms at play are:

1. stress induced transformation toughening
2. microcrack toughening
3. crack deflection/ formation of a compressive surface layer.

The authors continued to review four different types of ZTA ceramics and related their microstructure to their mechanical properties. These included:

1. alumina with dispersed unstabilised zirconia
2. alumina with dispersed PSZ
3. alumina with PSZ agglomerates
4. alumina –zirconia duplex structures.

Alumina with dispersed unstabilised zirconia showed a number of interesting features. When the alumina was dispersed with zirconia grains slightly larger than the critical size for spontaneous t-m transformation, the toughness was increased up to 11 MPa $m^{0.5}$. The main mechanism for toughening was shown to be microcrack nucleation and propagation [54].
The volume of unstabilised zirconia added to the alumina was found to have a large effect on the properties. The strength of the ZTA increased for additions up to 12 vol % zirconia after which there was a marked drop in the strength as measured by three-point bend testing, Figure 16.

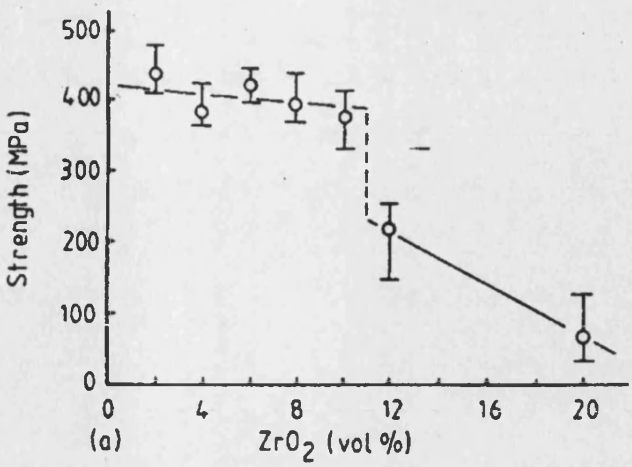


Figure 16: Three-point bend strength of alumina with well dispersed unstabilised zirconia particles as a function of zirconia addition. Note the drop in strength at 12 vol% zirconia additions [54].

This was explained by Wang & Stevens as microcrack coalescence, where the volume of zirconia additions gets to a level that the t-m transformation creates such a high density of microcracks that they spontaneously join to form a critical size defect. The effect on indentation fracture toughness was similar. Figure 17 shows that the indentation fracture toughness increased rapidly with increased additions of unstabilised zirconia particles however at 12 vol % zirconia additions the value increased very little.

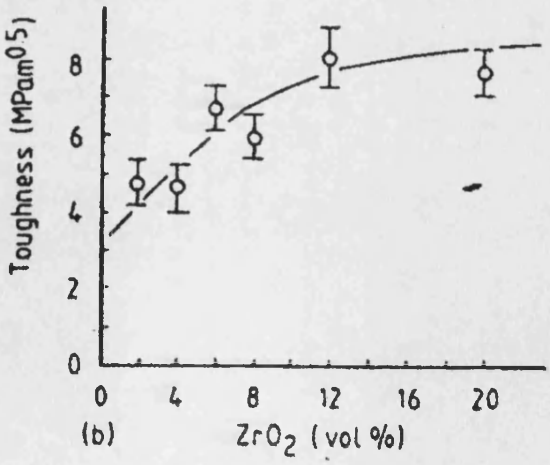


Figure 17: Indentation fracture toughness of alumina with well-dispersed unstabilised zirconia particles [54].

Alumina with dispersed partially stabilised zirconia particles is the natural progression from the above structures and is the most interesting from an orthopaedics perspective. Wang et al [54] report work completed by Claussen et al that shows increases in fracture toughness and fracture strength with the addition of tetragonal zirconia to the alumina matrix. The authors found that as the vol% of the PSZ additions was increased up to 40% the fracture toughness increased up to 10 MPa $m^{0.5}$ and the fracture strength increased up to 1000 MPa. However, the hardness of the material decreased from 18 GPa to below 15 GPa for the same volume fraction additions. The authors concluded that the main toughening mechanism was a combination of stress induced transformation toughening and the grain refining effect of the zirconia particles.

Alumina with dispersed PSZ agglomerates have also been studied and show an increase in fracture toughness of up to 13 MPa $m^{0.5}$ [54]. The microstructure consists of large (5-25 μm) agglomerations of PSZ particles in the matrix. The authors concluded there were two different toughening mechanisms occurring in these materials – transformation toughening within the agglomerates and crack deflection at the boundaries of the agglomerates [54].

It is clear then, from the literature, that a large number of combinations in terms of phase, Vol.% and dispersion of the zirconia can result in different mechanical properties. The properties that are important for use in hip joint bearing surfaces are high hardness, chemical stability, high strength and fracture toughness, and low wear. With this in mind, the work completed by Leriche and Orange et al [93,94] was closely examined in order to find the ideal ZTA composition that would fulfill all these requirements.

The authors examined the relationship between the mechanical properties of ZTA and their wear resistance [95,96,97,] for alumina and Y-TZP composites. The zirconia additions ranged from 5 to 45 vol % and the stabiliser content from 0-3mol% (yttria).

The authors first examined the optimum route to make these composites. In all cases, commercially available ceramic powders were used. The dispersion of the zirconia particles in the alumina was identified as critical with respect to achieving a good homogeneous microstructure. The research looked at three different mixing techniques:

1. Mechanical milling of the two powders using a technique called attrition milling where the powders are ground by zirconia balls in a plastic container in water for 18 hours.
2. Deflocculation of the zirconia and alumina particles in an aqueous environment such that a minimum of mixing gives a maximum dispersion of the particles.
3. A combination of the two processes above.

All of the resulting powders were further processed in a number of ways. Each of the slurries were spray dried and then either isostatically pressed at 400MPa, the binder was removed and pressureless sintered in air at 1600°C for 2h or uniaxially pressed into pellets, binder removed and hot pressed at 30 MPa in graphite dies at 1500°C for 15 minutes under vacuum.

The results showed the combination of electrochemical and mechanical milling to be optimal for producing the well-dispersed microstructure that would be required for optimum toughening of the ceramic. The addition of 3-mol % of yttria to the zirconia ensures that the largest amount of tetragonal zirconia was retained in the microstructure. Hot pressing was found to inhibit grain growth and the method produced a very small grain size for zirconia (0.6-0.9 μm) and alumina (0.9-1.6μm). However, pressureless sintering also resulted in very fine grain structures [94].

Based on these encouraging results, the authors continued to look at the mechanical and wear properties of these ceramics [94]. Fracture strength, elastic modulus and fracture toughness were examined. The wear rate was measured using a block-on ring arrangement (ceramic on steel) with water and air as the environments utilised.

The key results are summarised by the authors in Figure 18 below:

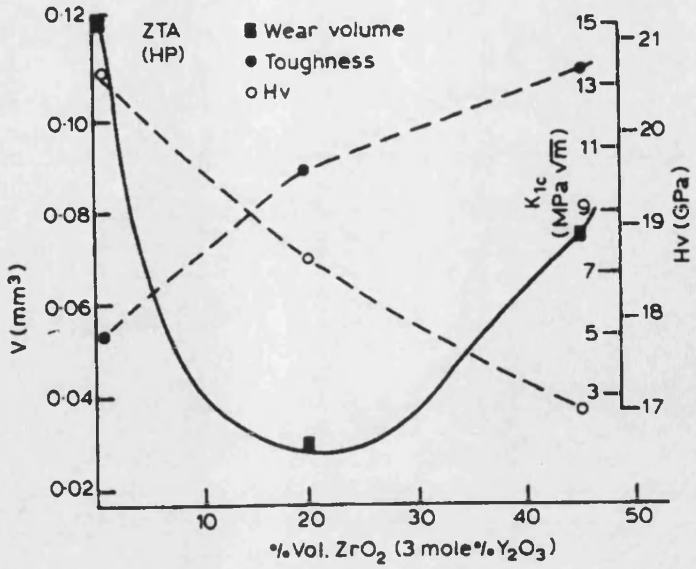


Figure 18: The effect of wear and fracture resistance on yttria-zirconia content [94].

This graph is a summary of the authors finding and looks at the effect of different vol% addition of Y-PSZ particle to alumina on the wear performance, toughness and hardness of the material.

The addition of the zirconia increases the wear resistance of the material and the wear reaches a minimum between 20-30 vol% additions. The authors explained this decrease by the combination of the alumina hardness and the toughening action of the zirconia which maintains the surface intact. Indeed, when the authors looked at a similar graph for additions of unstabilised zirconia it was found that anything above 10 vol % the composite surface wears badly. This was due to too much transformation resulting in microcracking on the surface and delamination [94].

The fracture toughness of the ceramic increased with increasing Y-PSZ additions, however this has to be balanced against the drop of hardness seen as the vol% of zirconia added is increased.

From an orthopaedic point of view, the addition of 3-mol% PSZ to the alumina is the best choice as both of these materials are already in clinical use. The optimum mixture for hip bearing applications would be between 20-30 vol% additions based on this research. To

optimise the fracture toughness and wear and maintain high hardness it was proposed to use a mixture of 75wt % alumina with 25wt% yttria TZP as shown in Figure 18.

Based on this research a number of experimental batches of ZTA material were commissioned from an orthopaedic ceramic supplier, Norton Demarquest, and then characterised using various test methods that will be outlined below. In parallel with this, a commercial grade ZTA currently in orthopaedic use was also characterised.

## 2.5 Analysis Techniques – Orthopaedic ceramics.

### 2.5.1 Fracture Toughness testing.

Fracture toughness testing measurement of oxide ceramics is often regarded as ambiguous and questions remain as to which technique gives the most realistic and reliable result for a particular material [98]. Two different types of analysis are typically used to measure fracture toughness of ceramics: Indentation fracture toughness and single edge notched beam (SENB) testing.

Indentation fracture toughness testing is generally believed to be a good qualitative way of comparing the fracture toughness difference of differently treated ceramics rather than an absolute measurement of fracture toughness [99]. There are many reviews of the advantages and disadvantages of this method for assessing the fracture toughness of various ceramics [99,100,101] and the main considerations are as follows:

1. The technique is quick and economical on the amount of material required.
2. The test surfaces do not have to be flat and spheres, rods etc. can be measured.
3. On the other hand, the test surface needs to be prepared to a mirror finish to allow for crack length measurement.
4. To be sure of crack lengths SEM analysis is often required. Sub-critical crack growth (SCCG) can continue on the specimen as it is being transferred giving a false reading for fracture toughness.
5. The indentation behaviour of the ceramic needs to be well understood prior to the analysis. The loading rate, top load and indenter geometry need to be carefully selected in order to ensure a well defined radial median crack system.

6. It is important to ensure that there are no pre-existing stresses in the surface of the ceramic prior to testing.
7. It is difficult to measure the fracture toughness of ceramics such as zirconia because of the nature of its transformation toughening mechanism. It is usual to over-estimate the toughness of these ceramics due to the large amount of transformation occurring around the indent, thus restricting crack growth artificially.

Indentation fracture toughness, single edge notched beam (SENB) fracture toughness testing and chevron notched beam testing (CNB) were all compared as techniques by Mukhopadhyay et al [102]. The authors tested different structural ceramics, including alumina, using each technique and compared the results. This comprehensive study also examined the effect of different test variables on the outcomes from each test. Loading rate, notch radius and notch length were all varied during the testing of each candidate material.

The results show differences between each technique to be significant. Essentially the $K_{IC}$ measured by CNB is consistently greater for a given blade width and loading rate and both these techniques are higher (1.7 times) than the indentation fracture toughness method [102]. The authors also found the SENB testing sensitive to notch width and loading rate, with an increase in toughness with an increase in these variables.

Wang et al [98], also considered the effects of notch width on the SENB toughness of oxide ceramics, the authors compared three types of alumina, with varying grain size 2.6-6.3 μm, zirconia with varying yttria content, 2-3-mol %, and two ZTA materials.

The results for the alumina (fine grain) gave a SENB fracture toughness of 4MPa $m^{0.5}$ and this decreased slightly to just over 3MPa $m^{0.5}$ as the notch width increased, figure 19. The TZP ceramics showed an increase in fracture toughness as the notch width is increased. This can be explained by the fact that the transformation zone is increased as the notch width is increased. Looking at the results for the 3-mol% yttria stabilised zirconia, the SENB fracture toughness for the material increased from just over 12MPa $m^{0.5}$ for a notch width of 200μm to 20MPa $m^{0.5}$ for a notch width of 1800μm, Figure 20.

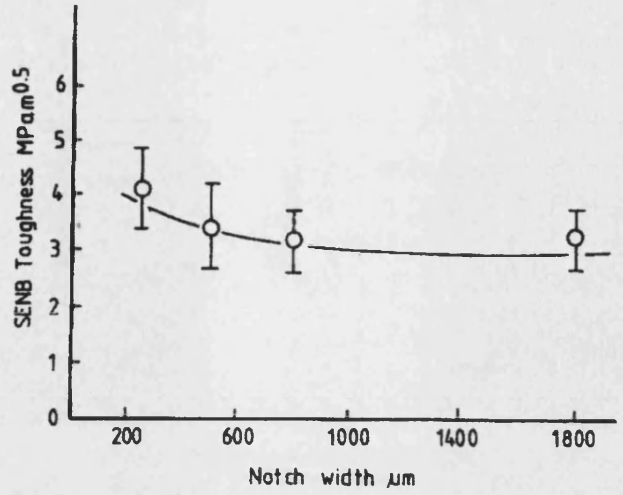


Figure 19: The SENB fracture toughness as a function of notch width for alumina [98].

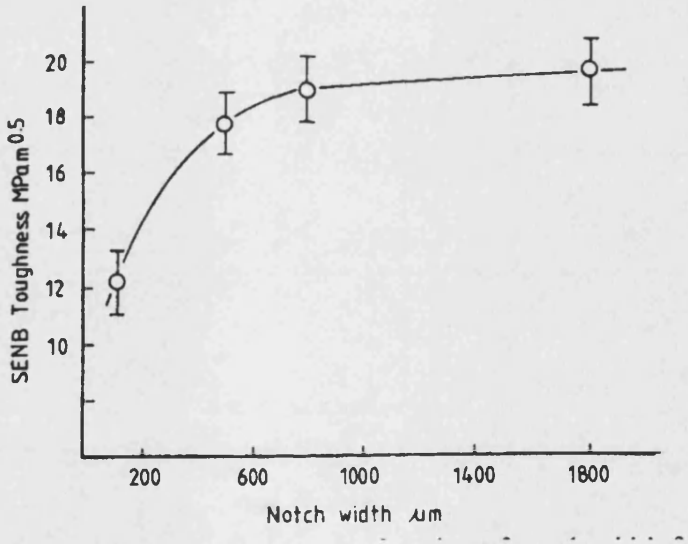


Figure 20. The SENB fracture toughness as a function of notch width for 3-mol% Y-TZP [98].

The ZTA materials tested in this work showed SENB fracture toughness values ranging from just under 4MPa $m^{0.5}$ to just under 6MPa $m^{0.5}$ for a notch width range of 200µm to 18000µm, Figure 21.

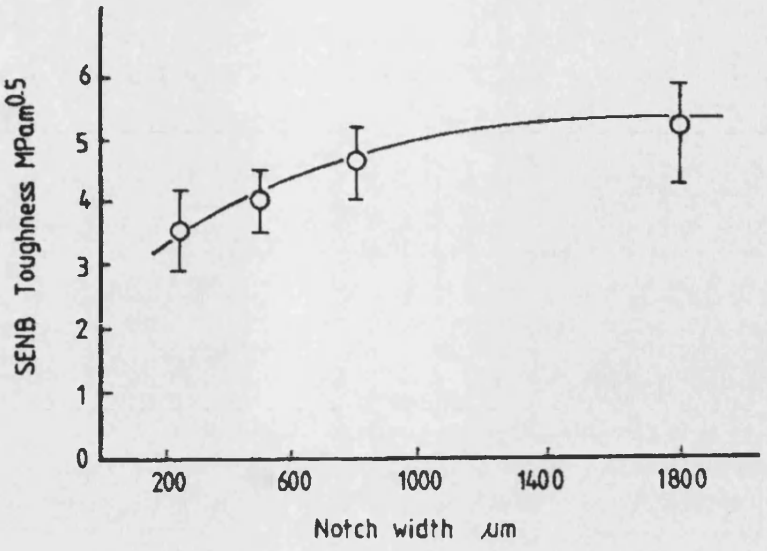


Figure 21: The SENB fracture toughness as a function of notch width for ZTA [98].

There are many other variations on the SENB test method reported in the literature [103,104,105], however one recent study by De Aza et al [106] proved extremely relevant to orthopaedic ceramics. The authors examined the conventional wisdom of measuring $K_{IC}$ and proposed that this is the wrong measurement to make when looking at the reliability of ceramic heads *in –vivo*. $K_{IC}$ is essentially the point at which fast crack growth occurs and the ceramic body fractures, however there are cases where ceramic heads fail even when the applied stresses are under the $K_{IC}$ value [106]. As $K_{IC}$ represents a critical value, ceramics are susceptible to sub-critical crack growth at values of $K_I$ below $K_{IC}$. This relationship can be demonstrated schematically by producing a V (crack velocity) versus $K_I$ (stress intensity factor) diagram, figure 22. For each stage of the diagram, a power law can fit the speed at which a crack propagates when stressed, given by:

$$V = AK_I^n$$

Where A and n are constants depending on the material's properties and environmental variables [106]. Environmental conditions are critical because it is known that SCCG is assisted by stress corrosion at the crack tip. The authors point out that there is experimental evidence of a region $K_0$ where no crack growth occurs. It is this threshold that should be established in order to define a perfectly safe region of operation for ceramic heads [106].

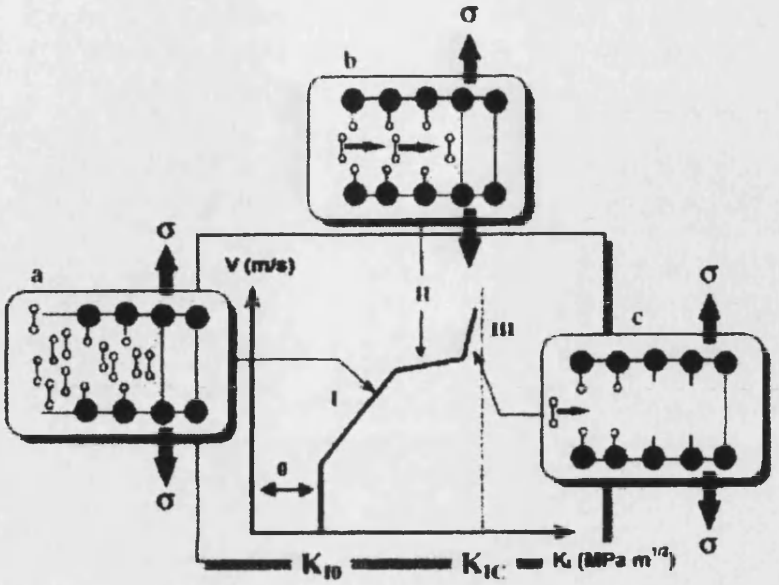


Figure 22: Schematic representation summarising the different crack velocity regions observed in experimental V-$K_I$ curves [106].

The authors used the double torsion technique, figure 23, to measure the SCCG behaviour of three ceramics – alumina, zirconia and zirconia toughened alumina.

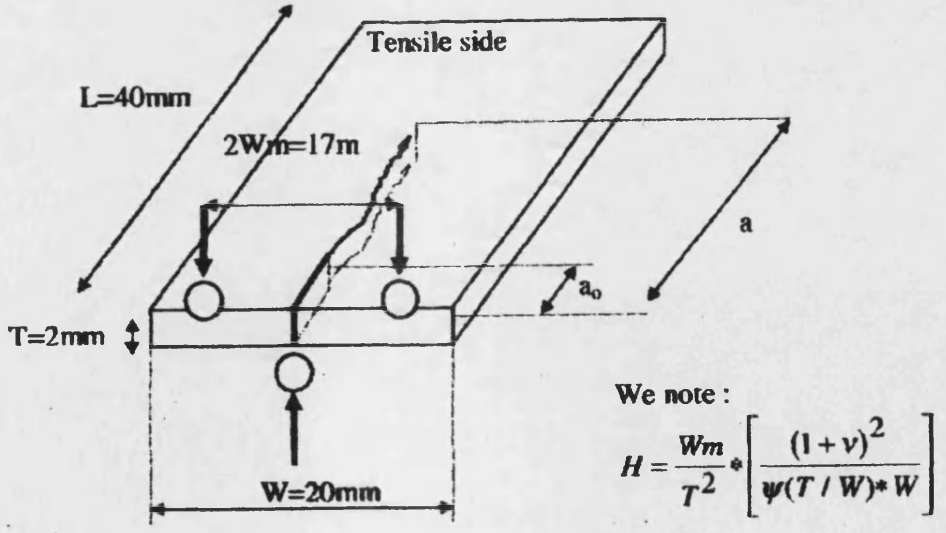


Figure 23: Specimen dimensions and loading configuration for the double torsion test [106].

The results showed the ZTA material to have the highest $K_0$, $K_I$ values. The ZTA material could operate at loads two times higher than alumina and still have no SCCG. Figure 24 shows the authors' results for the three ceramics.

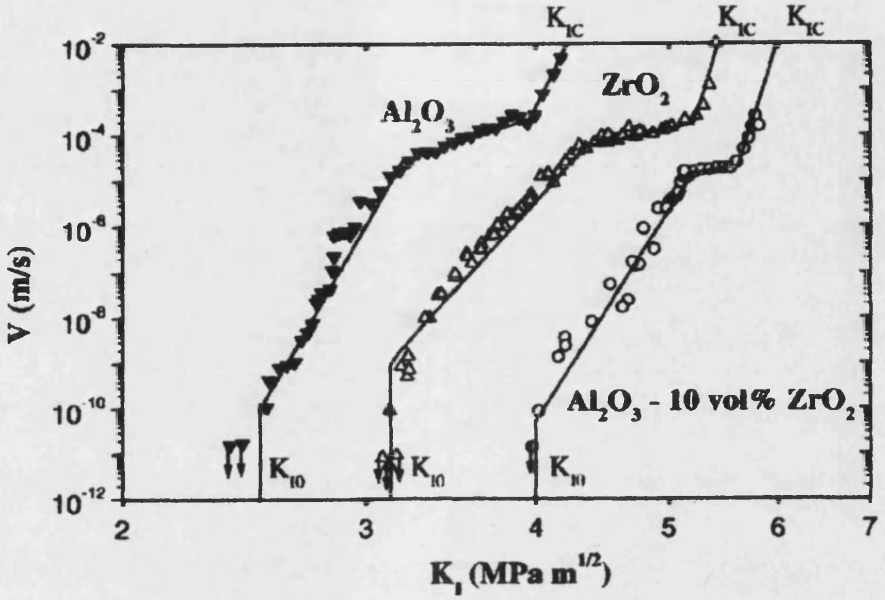


Figure 24: Crack velocity (V) versus stress intensity factor ($K_I$) for biomedical grade alumina, zirconia and zirconia toughened alumina [106].

The proposal of using $K_{I0}$ i.e. the stress intensity below which no crack growth occurs, as a reliability measure below which no SCCG occurs is very interesting for scientists and engineers designing hip ball heads.

### 2.5.2 Friction Testing.

Friction analysis of the interaction of the two bearings in an articulating artificial joint has historically been the first consideration for researchers in the development of hip joints. The natural human synovium joint has a friction coefficient of about 0.02 and exhibits wear factors of $10^{-6}mm^3/Nm$ [107]. The joint space is made up of hard structural cortical bones covered in soft cartilage material. The cartilage acts as the bearing surface and is extremely smooth. The surfaces are for the most part separated by a liquid called synovium, which is a water-based, tacky, viscous liquid made up of hyluronic acid and proteins. This means that

the natural joint articulates under a lubrication regime known as full fluid film lubrication [108].

The trouble starts when this natural joint becomes diseased or worn and needs replacing. Very few man-made materials or designs can hope to come close to the natural joint in terms of friction and wear performance. The main lubrication regime operating in artificial joints is what is termed mixed lubrication where the roughness asperities of the articulating materials are in contact. This means wear is occurring at all times thus limiting the lifetime of man-made joints.

Friction torque reduction was the main reason Sir John Charnley used a small head (22mm) articulating against a thick acetabular liner. The use of the disastrous polytetraflouroethylene (PTFE or Teflon) was also with a view to reducing the friction in the joint space.

Hall and Unsworth reviewed this logic in their paper on friction in hip prostheses paper [109]. The authors relate the need for an understanding and measurement of the friction in prosthesis design, especially where new bearing surfaces were being developed. Even though frictional torque values may not be high when compared to the torque required to remove a well cemented acetabular cup from its socket, the cyclic nature of this torque is liable to have an effect on the subsequent loosening of the joint if it is not controlled.

The authors continue to review the various methods for measuring friction values between candidate orthopaedic materials. The use of screening test rigs such as pin-on-plate testers to measure friction have a number of fundamental shortcomings. Due to the very simplistic nature of these machines, the results gained may not be representative of *in-vivo* behaviour due to the difference in tribological conditions [109].

There are a number of such studies worth looking at more closely. Sawae et al [110] used a pin-on-plate friction rig to measure the effect of different composition synovia on the friction and wear of polyethylene. The authors used both stainless steel and ceramic pins and used saline and bovine serum with different additions of the protein albumin and sodium hyluronate. The saline solution alone produced a transfer film of polyethylene on the metal during the testing, however when albumin was used in the lubricant this transfer film was

suppressed. The albumin solution performed the same in terms of friction and wear rate to that of the bovine serum, however the wear mechanisms in both types of lubricant were not similar. Additions of hyluronic acid to the saline solution successfully reduced the friction and wear rate of the polyethylene. The study demonstrated the importance of lubricant type and composition in determining the friction and subsequent wear of the bearings. Young et al [111] looked at measuring the reduction in friction by testing surface patterned polyethylene disks in a pin-on-plate friction testing rig. The polyethylene had machined holes, 0.16mm in diameter and 0.32mm deep, across the articulating surface of 6 of the 12 specimens tested. The authors found that the patterned samples had friction values 43% lower than the unpatterned specimens. The authors explain that is probably due to the holes holding more lubricant at the articulating surface and thus reducing the friction. The wear rate for this surface did not experience the same relative reduction as the friction value.

Zhou et al [112] examined the start up and steady state friction of alumina against alumina in a pin-on-disc friction testing rig. The results show that the type of lubricant used has a large affect on the friction value. The start up friction value was 30 times less when using a carboxy methyl cellulose (CMC) lubricant when compared to distilled water. The authors also discuss a number of other factors that were found to effect the friction values, these were: resting time, load, sliding velocity, acceleration time and the influence of machining and fit of the pin and disc components. Zhou [112] also outlines the limitations of using a pin-on-disc type friction tester:

1. The pin-on-disc testing machine cannot accurately simulate the load and motion of an artificial hip joint.
2. The geometry selected in this test was such that the spherical radius of the pin and disc was much smaller than a full hip joint bearing surface. This will mean the hydrodynamic effect seen in the simulator would be smaller.
3. CMC does not contain proteins and lipids etc. unlike synovium.
4. The sliding velocity of the tester is high compared to joint speeds *in-vivo.*

A much more successful way of measuring the friction is the use of friction hip simulators. These are single station hip simulators with a single axis of rotation (flexion/extension), with a loading force that represents the main loading seen in a hip joint during walking. A friction transducer usually measures the friction.

These simulators have an advantage over the pin-on-plate testers in that they simulate more closely the joint design and hence its contact area, loading and lubrication regime.

The friction simulators most commonly quoted in the literature are those developed at Leeds, Durham and Helsinki [109]. It is the Durham simulator design that is used in this work to measure friction.

The mode of operation for this simulator will be covered in more detail in the methods section. The most common way of presenting the results from a particular bearing combination is by plotting a Stribeck curve [109]. This is produced by plotting the coefficient of friction (or the friction factor) against a dimensionless Sommerfield parameter Z, which is defined as:

$$Z = \frac{\eta \mu r}{L}$$

Where $\eta$ is the viscosity of the lubricant (carboxymethylcellulose, CMC), $\mu$ is the entraining velocity, r is the radius of the head and L is the load. By varying the viscosity of the fluid a range of Sommerfield numbers are produced.

The authors analysed the lubrication regimes and relative friction values for metal/polyethylene, ceramic/polyethylene and ceramic-on-ceramic joints. The results showed that metal polyethylene joints operate in a mixed lubrication regime i.e. the friction factor decreases as the Sommerfield number increases. The ceramic/polyethylene combination also acts in a mixed lubrication regime; however the friction factors are on the whole lower than those measured for the metal/polyethylene components. Scholes et al [113] continued with the research and investigated ceramic-on-ceramic and metal-on-metal bearings. Their results show the ceramic-on-ceramic joints to have extremely low friction values with the suggestion that this bearing articulates under full fluid film lubrication. Table 2 below is a summary of the reported results.

| Femoral component | Acetabular component | Friction factor |
|---|---|---|
| Cobalt Chromium | Polyethylene | 0.059 |
| Alumina | Polyethylene | 0.047 |
| Alumina | Alumina | 0.002 |
| Metal | Metal | 0.26 |

Table 2: Comparison of the friction factors for main orthopaedic bearings [113].

As can be seen from Table 2, the metal-on-metal on metal components showed the highest friction factor of all bearings measured. This value was found to decrease by approximately one half when bovine lubricant was used in the friction rig instead of CMC. The authors proposed that this was due to protein adsorption on the surface of the metal from the bovine serum, which set up a boundary lubrication regime.

One large study conducted using the Durham friction-testing rig, looked at the friction of 54 explanted Charnley joints and compared them to 32 new joints [114]. The authors also examined the effect of the presence and absence of lubrication, different material combinations and head diameter. The research showed that the explanted Charnley joints showed a friction factor that was higher for the explanted joints than for the new joints, both in dry and lubricated conditions. The estimated frictional torque for these explants ranged from 1 to 4.5 Nm, and there was no correlation between the higher torques and implant loosening as implants with low torque values also failed. All joints operated under a mixed lubrication regime [114].

Some recent work carried out by Dowson et al [115], attempted to measure the extent of the fluid film present in articulating joints, real time in a simulator. The researchers used the electrical resistance or voltage drop between the femoral head and the acetabular cup of a metal-on metal prosthesis. The study was relative to the ceramic-on-ceramic bearings, in that they were of the hard-on-hard bearing category. The factors that affect the lubrication film in theses metal-on metal bearings are likely to effect the ceramic-on-ceramic to the same extent. To carry out the study the metal components were electrically insulated from the testing rig, and a simple electrical circuit, with the head and cup in the loop, was set up. The electrical resistivity was measured using an oscilloscope during the walking cycle.

When the head and joint were completely separated the maximum voltage drop across the joint was 50mV [115]. When contact occurred between the components, a very small current flowed. The authors also examined the wear of the components across a range of head sizes, 16mm, 22mm, 28mm and 36mm. The results showed that the mode of lubrication with these joints is very dependent on the head size. The smaller head sizes, 16 and 22mm, showed no detectable voltage drop between the head and cup, indicating mixed lubrication. The wear rate for these components was high and increased with increasing head size Figure 25. The bearings in this size range were reported to be operating in the boundary lubrication regime. As the head size increased the authors measured a dramatic decrease in the wear rate, 6.3 $mm^3/10^6$ cycles for 22mm to 0.54 $mm^3/10^6$c cycles for the 28 mm heads. They also measured a drop in the voltage between the head and cup throughout the walking cycle. The measured voltage decreased i.e. the separation increased, as the measured clearance between head and cup increased [115]. This indicates that the larger diameter bearings were tending to operate in a more mixed lubrication regime.

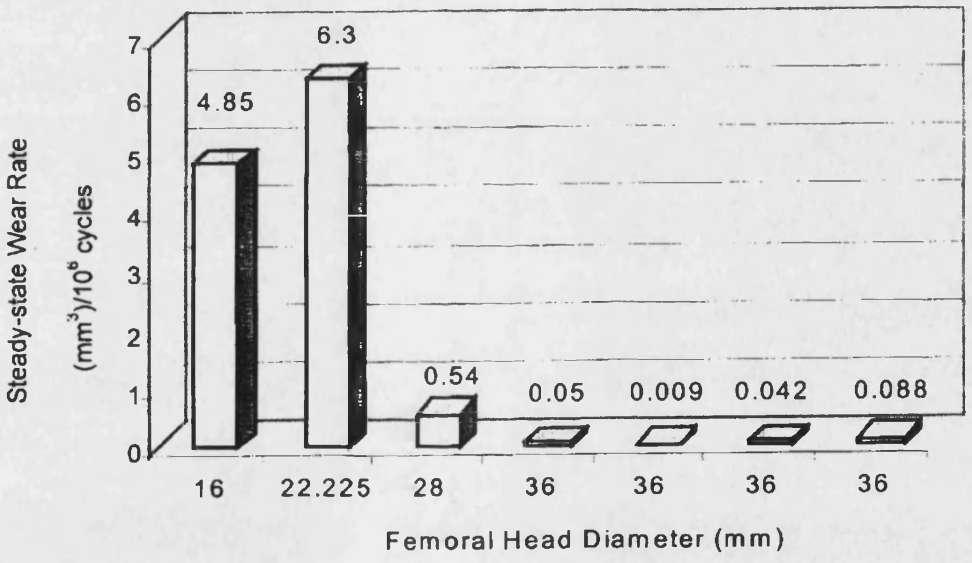


Figure 25: Measured volumetric wear rates for various femoral head diameters when subjected to the simplified walking cycle [115].

Indeed Scholes et al [116] in a recent study confirmed these findings for metal on metal articulation. The authors went on to propose that hard bearings such as metal-on-metal and

ceramic-on-ceramic relied on close radial clearance and highly polished surfaces to attain full fluid film lubrication.

### 2.5.3 Wear testing

As discussed earlier, the majority of total hip prostheses currently implanted consist of a metal femoral head (Cobalt Chrome, nitrogen strengthened stainless steel) articulating against an ultra-high molecular weight polyethylene (UHMWPE) acetabular cup. Typical wear rates of 40-100 $mm^3$/year have been reported corresponding to a penetration rate of the femoral head into the acetabular component of less than 0.25mm year [117]. Even though the majority of these implants are successful there is a growing volume of evidence that shows wear debris from this combination leads to the eventual failure of the prosthesis [119,120]. It is generally believed that UHMWPE wear debris generated at the articulating surface enters the periprosthetic tissue where it triggers a number of defense mechanisms in the bone cells. The result is osteoclastic bone resorption, leading to osteolysis and eventual loosening of the prosthesis. It is not only the volume of wear particles that is important in this mechanism but the number of particles and their size range. Research has shown that particles in the size range 0.2-0.8μm cause the greatest biological response in the body [7].

Wear rates of early alumina-on-alumina hip prostheses manufactured from 1st generation alumina have been shown to be low *in vivo*, ranging from 1 to 5 $mm^3$/year [121]. The vast majority of retrieved components showed similar characteristic features within the worn bearing surfaces. These included:

1. an elliptical wear stripe on the head with maximum penetration up to 100μm
2. a worn area in the cup with evidence of rim wear
3. an intergranular fracture wear mechanism.

Characteristically these early prostheses were retrieved because of loosening of the acetabular cup, which was partly attributed to the poor fixation of the acetabular component to the bone.

In contrast, simulator testing of ceramic on ceramic hip prostheses reported extremely low wear rates (< 0.1$mm^3$/million cycles), an order of magnitude lower than those reported *in*

*vivo*. Bearing surfaces were undamaged with no noticeable change in surface roughness [119].

The wear stripes found in first generation ceramics were believed to be related to the inferior quality of the ceramic material. Developments such as hot isostatic pressing (HIPing) and grain refinement, to increase the density and strength of the alumina, were considered to alleviate this problem. However, recently two modern alumina/alumina hip prostheses manufactured from 2nd generation HIPped alumina retrieved after only one year showed wear patterns similar to those found in the early retrieved components, with a small elliptical wear stripe on the femoral head 2-5µm deep and a small amount of wear on the rim of the acetabular cup [123]. These two prostheses (Figure 26) were both retrieved due to trauma and were anatomically positioned and well fixed prior to retrieval [123]. Wear volumes for these components have been measured to be approximately 0.5 $mm^3$.

Figure 26 Wear stripes of explanted HIPed Alumina/Alumina components after 1 year [**Error! Bookmark not defined.**].

Wear patterns and mechanisms found clinically were not replicated in standard *in-vitro* simulator tests.

Mallory *et al* [124] examined the fluoroscopic images of up to ten patients walking on a treadmill and found the head and cup separated a small amount during the swing phase. They reported that the maximum separation was 2.8mm and the minimum was 0.8mm with an average separation seen at 1.2mm. They also found that while the femoral head separated

from the cup it remained in contact with the rim and postulated that high contact stresses would occur at this point with the application of load at heel strike.

From this research it was hypothesized that microseparation of the head and cup could occur with any joint replacement and that this could be a factor in wear initiation for ceramic – ceramic systems such as seen *in vivo*. Typically, with these systems, there is a very small clearance between the head and cup, in the order of 40μm, and it is these tight clearances that allow the femoral head to contact the rim of the cup with only limited translation (Figure 27). Contact would occur with lateral and inferior displacements of less than 1mm for a well-positioned prosthesis. Upon heel strike, the head would translate superiorly and contact the rim before relocating. This rim contact would occur under very high stress and could initiate surface damage and hence accelerate wear [125].


Figure 27: Schematic of the stages of microseparation during the walking cycle [122].

*In-vitro* microseparation was first reproduced by Nevelos *et al* using the Leeds MKII physiological hip joint simulator [123]. Under standard conditions this simulator applied a small positive swing phase load that ensured the head remained located correctly in the insert throughout the gait cycle. To achieve joint separation a small lateral to medial load was applied to the acetabular insert, which, during the swing phase when the joint load was reduced, produced medial and superior translation of the insert relative to the head. Joint separation was limited by the radial clearance between the articulating components and ceased when the superior rim of the insert contacted the head after approximately 0.5mm of translation. Further impact of the head and cup occurred with reapplication of the joint load

at heel-strike. The load was momentarily supported by the small contact at the rim before the head relocated in the insert, thus modelling the clinical observations shown in Figure 27.

The microseparation technique reproduced for the first time, clinically relevant levels of wear in ceramic-ceramic hip prostheses. The technique produced stripe wear with alumina/alumina via a similar intergranular fracture wear mechanism (Figure 28) as seen *in vivo*. For additional validation of the technique, debris collected from the simulator was compared to debris from retrieved tissues, both were found to contain predominantly nanometer sized ceramic particles with the addition of a few larger ceramic particles attributed to microseparation [123].

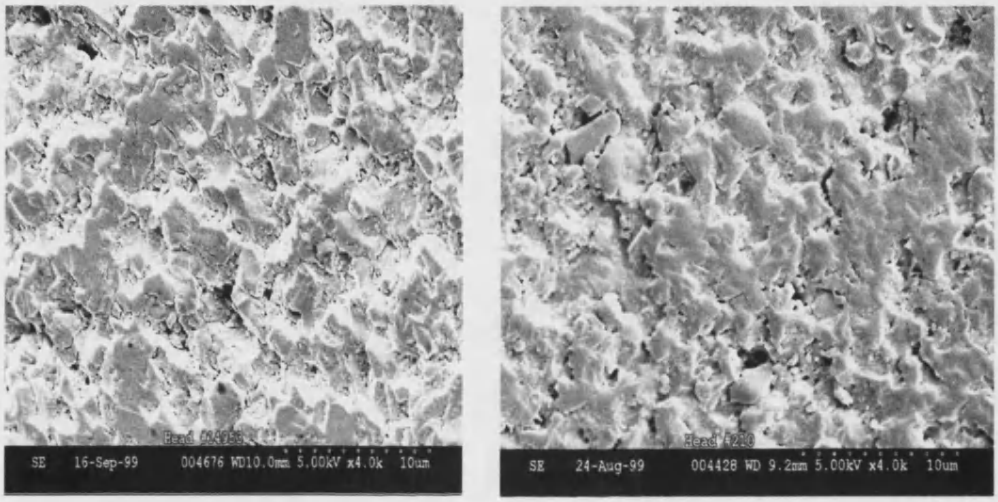


Figure 28: SEM of Retrieved (left) and in vitro microseparation (right) head wear stripes [123].

Further research by Stewart *et al* showed that when the swing phase load in the simulator was reduced it becomes easier for the medial separation force to both overcome friction and to produce superior translation between the head and insert [118]. This increased the velocity of the insert and upon impact of the insert and head, produced an increased momentum and impact energy, which resulted in a more severe microseparation condition. Therefore, by decreasing the swing phase load, greater levels of joint laxity were modelled.

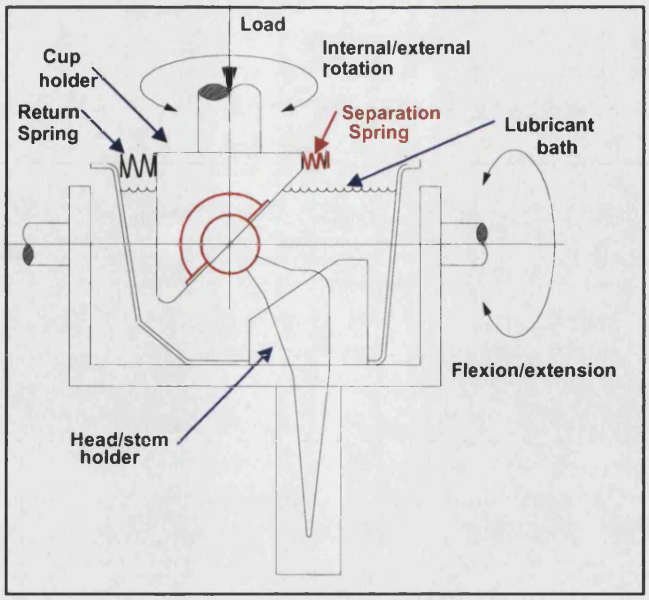


Figure 29: Schematic of the Leeds Mk II physiological hip joint simulator with microseparation [123]

The volumetric wear from standard simulation testing of alumina ceramic on ceramic bearings has generally been reported as < 0.1mm³/million cycles. Microseparation simulation has been shown to increase this by a factor of 10, approaching clinical levels of wear as seen in retrieved 1st generation alumina hip prostheses (figure 30).

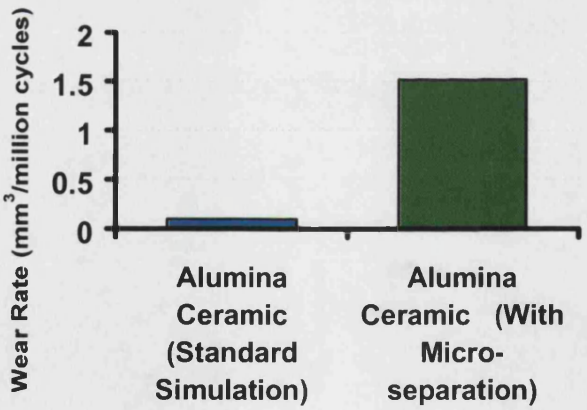


Figure30: *In-vitro* ceramic wear, standard versus microseparation simulation [123].

Microseparation simulator studies have only, been reported from one centre [125]. The findings so far support its use as a means to evaluate ceramic bearing materials in a more physiological manner.

For the current alumina materials under severe microseparation, wear was characterised by an initially higher wear period during which a characteristic wear stripe on the femoral head and the rim wear on the cup were initiated. The wear then decreased to a lower steady state value with no signs of runaway wear observed. The severity of testing had a significant difference on the resulting wear rates of the alumina material, emphasising the need for careful control of experiments.

Thus, clinically relevant wear rates and mechanisms can be simulated for the first time *in-vitro*. This is important for characterising different candidate bearing materials and the test will be used for the ZTA materials in this study.

# 3.0 Experimental Techniques.

## 3.1 Materials

Two candidate ZTA materials were considered for this research – Biolox Delta (AZTA; *CeramTec*, Plochingen, Germany) and another ZTA material (BZTA; Norton Desmarquest Fine Ceramics, Evereux, France).

Biomedical grade alumina (Al; *CeramTec*, Plochingen, Germany) and zirconia (Zr; Norton Desmarquest Fine Ceramics, Evereux, France) were used as controls, where possible, for all the experimental techniques.

The Norton Desmarquest supplied material (BZTA) is a binary ceramic consisting of 25 wt.% Y-PSZ (yttria partially stabilised zirconia) dispersed in a 75 wt.% alumina ($Al_2O_3$) matrix. The material has a white appearance (Figure 31).

The CeramTec material (AZTA) is a pentary ceramic consisting of 24 wt% Y-PSZ in a 75 wt.% alumina matrix with an addition of 0.3 wt.% chromium oxide ($Cr_2O_3$) for hardness and 0.8 wt.% strontium oxide (SrO) for increased toughness. The material has a pink appearance (Figure 31).

Specimens were obtained from both manufacturers in the form of:

- polished, flat, rectangular coupons (20 x 10 x 5 mm in size),
- rectangular bars in accordance with ASTM C1161-94 for flexural tests (4 x 3 x 45 mm in size),
- ball heads, 28 mm in diameter and ceramic liners, 28 mm internal diameter/ 36 mm outside diameter.

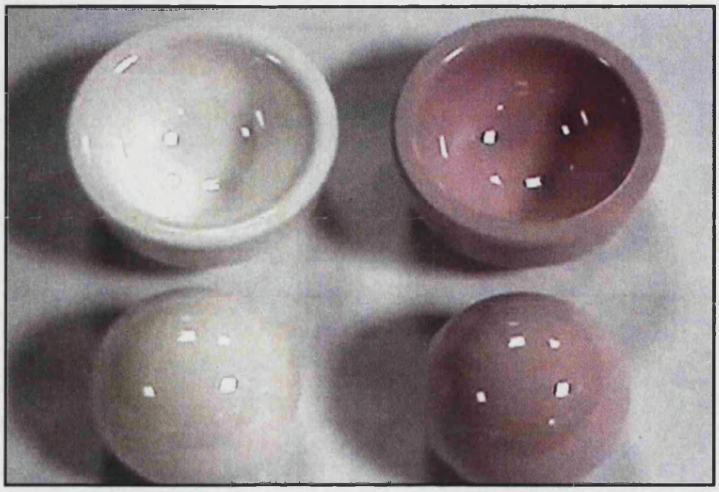

Figure 31: ZTA ball and cup hip components – BZTA & AZTA (pink).

## 3.2. Manufacturing Process.

The development and process details for these ZTA ceramics are not available from the ceramic suppliers however, the manufacturing processes are largely similar to the standard alumina and zirconia ceramics currently on the market.

The manufacturing process for these ceramics involves first mixing the raw materials, in the required ratios, in a milling tumbler. The raw materials used are the biomedical grade powders used for making the current bioceramics –alumina and zirconia. The mixture is then spray dried and compressed (1200bar) into a large rod shape by cold isostatic pressing (CIP). This rod of ZTA ceramic is next biscuit fired. This low temperature fire (prefire) has two main purposes:

- to burn out any organic binders used in the primary green manufacturing process and;
- to consolidate the powder to a level of density where it can be premachined into the final desired shape prior to sintering.

The firing or sintering of these ceramic components usually happens in a bottom loaded batch furnace as shown in Figure 32 however. The temperature range is typically between 1350 to 1650°C to achieve a sintered density of 4.31g/cm$^3$ for alumina and 5.9g/cm$^3$ for zirconia.

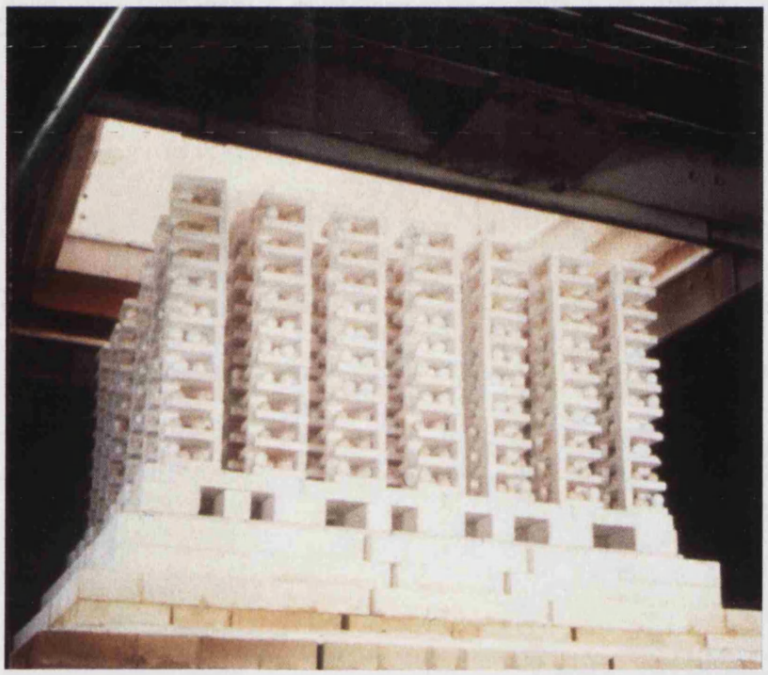

Figure 32: Bottom loaded batch sintering furnace for zirconia [29].

The desired outcome from the sintering cycle is an optimised grain size and fully dense ceramic. This cannot be achieved in the same sintering cycle therefore orthopaedic ceramic manufacturers employ a two stage sintering process. A lower sintering cycle is used to first optimise the grain size – typically averaging less than 1.8 μm for alumina and 0.5μm for zirconia.

After this cycle, the sintered ceramic components contain approximately 0.5 – 2% closed porosity in the form of microscopic voids. As these components require extremely high strength, fracture resistance and good surface finish, it is essential that even this small amount of porosity is removed. To achieve almost theoretical density the components are sent for hot isostatic pressing (H.I.P.). The combination of high-pressure gas (usually Argon) and high temperature (below sintering temperature) is successful in removing the

residual porosity. Final polishing of the components is achieved through various proprietary methods but typically involves rumbling (ball milling or vibration milling) and fixed grit diamond machining, Figure 33. The components are finished to a surface finish of >0 .001µm.

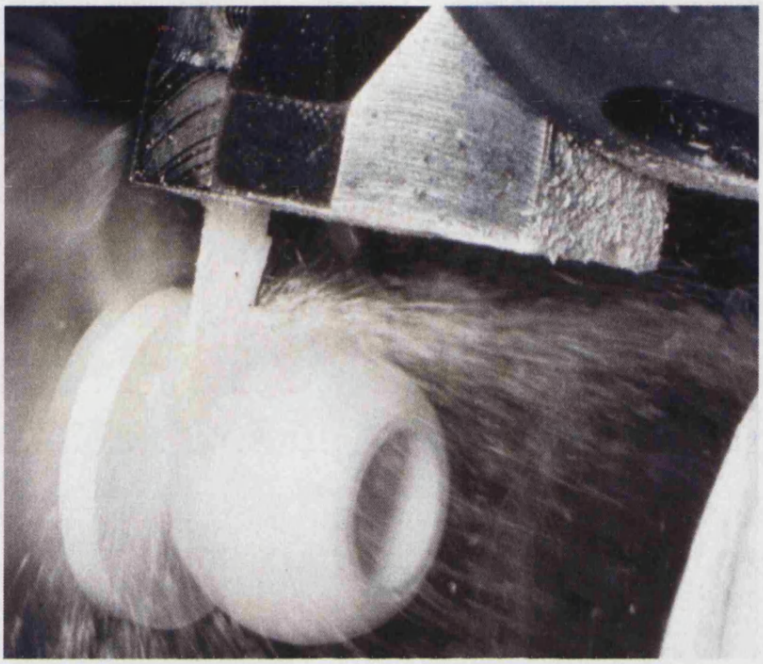

Figure 33: Fixed grit diamond machining of alumina ceramic ball heads [29].

All components produced have to pass extremely precise dimensional tolerances in terms of sphericity and surface finish. Dye penetrant inspection is used to detect any surface flaws or imperfections. All dimensional tolerances are measured by sophisticated co-ordinate measurement machines (CMM) as shown in Figure 34.

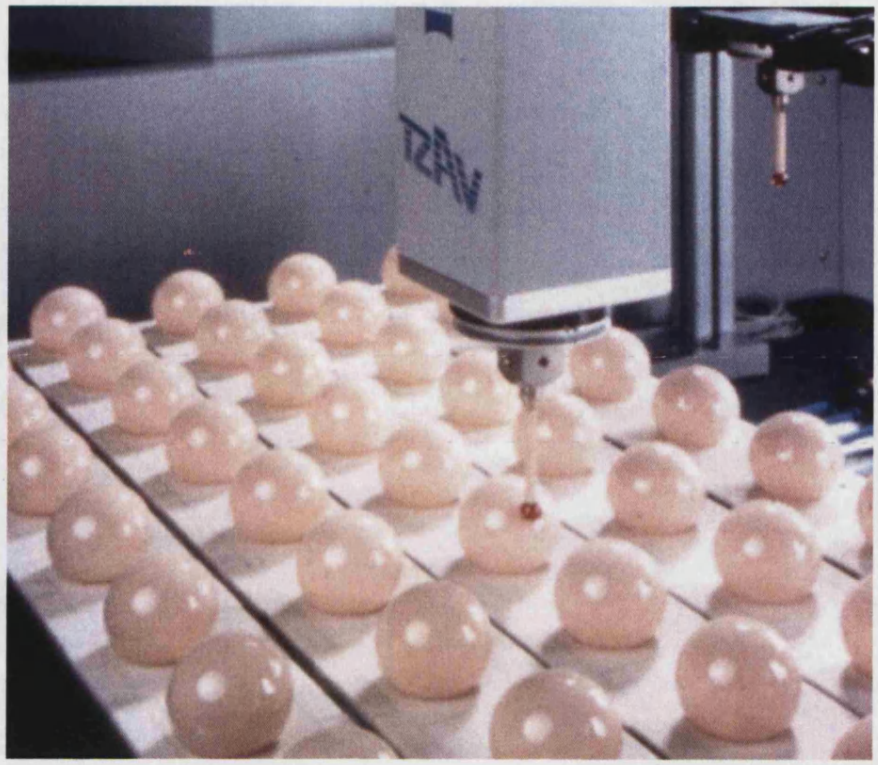


Figure 34: CMM analysis of alumina ball heads [29].

One of the most important developments in the quality control of ceramics for clinical use has been the introduction of the proof test. All components produced are subjected to a load that is typically some fraction of its failure load thus allowing the manufacturer to identify any components with internal flaws.
Prior to shipment, all ceramics are laser marked to ensure full traceability to the customer.

## 3.3. Test sample condition.

The ceramic samples were tested in a number of different conditions. These were as follows:

- air – as received,
- accelerated aged (AA) – These samples were aged in a steam autoclave at 2 bar for 5 hours at 134°C. - this has been shown to be equivalent to 20 years *in vivo*,
- physiologically aged (SA) – This involved immersion of the ceramics in standard Ringer's solution at 37°C ± 0.1°C, pH = 7, for 6 and 12 months.

## 3.4 Physical Characterisation.

### 3.4.1 X-ray diffraction (XRD).

XRD analysis was carried out before and after accelerated ageing to determine the chemical phase composition of the material and also to measure any change in the volume fraction of monoclinic zirconia phase present in the ceramic.

AZTA & BZTA flexural bars and flat coupons were examined by x-ray diffraction using a Rigaku Dmax 3 diffractometer. Diffraction scans were run with a generator voltage of 40V and a generator current of 40 mA. Each diffraction scan was run with an angle of 2θ from 27° to 37° with a fixed time of 1.00 second and a sampling interval of 0.10° using copper Kα radiation.

Zirconia flexural bars and hip ball heads were also measured by XRD as a negative control. Ten flexural bars and three flat coupons of each candidate material were measured each time.

Each spectra was analysed to measure quantitatively the amount of monoclinic phase present in the ceramic. The monoclinic phase has a characteristic peak present at 2θ = 28.2° whereas the 100% intensity peak for the tetragonal crystalline phase is present at 2θ = 30.4°. To calculate the quantity of monoclinic phase present the relative peak intensities are measured and the amount calculated using the following formula as proposed by Thomson & Rawlings [89].

$$M\% = \frac{1.68 \times I(11-1)m}{I(111)t + 1.68 \times I(11-1)m}$$

Where (111) t and (11-1) are the intensities of the tetragonal and monoclinic phases respectively.

### 3.4.2 Grain size analysis.

The microstructures of the candidate ceramics were analysed using scanning electron microscopy (SEM). The samples were thermally etched at 1400°C for 60 minutes prior to analysis. The microstructures were checked for an even dispersion of zirconia throughout the alumina matrix and the average grain size for each phase was measured.

Three flexural strength bars, three coupons and one ball head were analysed for each ceramic material.

## 3.5 Mechanical Characterisation.

### 3.5.1 Flexural Strength testing.

Flexural strength testing was used to measure the bending strength of the candidate ceramics and to measure any change in this strength due to ageing.

The testing was carried out using a minimum of 10 rectangular bar specimens each of AZTA, BZTA, Al and Zr. The bars were 40mm x 3mm x 4mm and were prepared according to the standard specification ASTM C 1161.

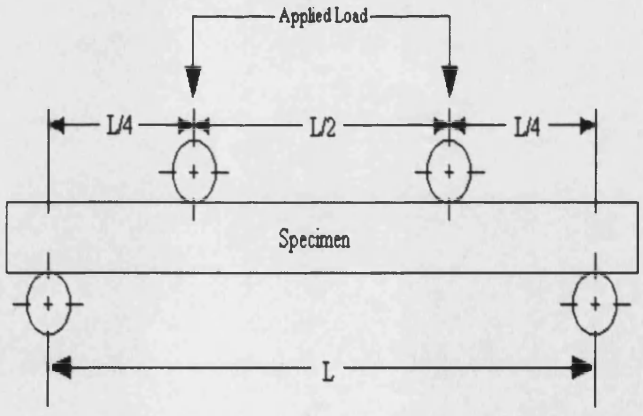


Figure 35: Four-point bend testing set up as per ASTM C1161-94. (L=40mm).

A detailed drawing of the test set-up is outlined in Figure 35. The samples were tested using an Instron tensometer with a 5KN load cell and a crosshead speed of 0.5mm/min.

Each test specimen was measured using calibrated verniers. The average of eight measurements was taken for the breadth and width (b and d) in each case.
The flexural strength was calculated using the following formula:

$$S = \frac{3PL}{4bd^2}$$

where: P= breakload, L=Outer support span, b= specimen width, d=Specimen thickness.

The fractured samples were collected, labelled and stored. The highest and lowest strength test bars from each series were then examined under a light microscope and fracture analysis carried out.

### 3.5.2 Microhardness (HV).

Microhardness tests were carried out on 3 rectangular specimens each of AZTA, BZTA and Al to determine if there was any drop in the hardness of the alumina due to the addition of the softer zirconia. Vickers hardness results were obtained using a standard Vickers hardness machine (Vickers Limited, Crawford, Kent). Three samples were loaded to 30 kg with the dwell time being approximately 30 s. Three tests were carried out per sample.
The Vickers hardness number (Hv) being determined by the following equation:

$$\mathbf{Hv = 2(L/(2a)^2)}$$

where;

L is the applied load normal to the sample surface in Newtons,

2a is the length of the diagonal from the resultant indent in millimeters.

### 3.5.3 Indentation fracture toughness $K_{IC}$.

The fracture toughness of both the ZTA materials was measured using indentation fracture toughness. This was carried out using a standard Vickers hardness indenter. The indentation load ranged from 10 to 30 kg with a dwell time of 20 seconds on one specimen each of AZTA, BZTA and alumina. The crack length was measured immediately after indentation using a high power optical microscope. The indentation fracture toughness, $k_{IC}$, was calculated using the equation proposed by Anstis [99]:

$$K_{IC} = 0.016*[E/H^{1/2}]*[L*c^{-3/2}]$$

with E = Young's modulus, H = Vickers Hardness, L = Load (N) and c = half the diagonal crack length.

The criteria for acceptable cracks were:

all cracks emanated from the corner of the Vickers indent,
the presence of only four radial cracks,
no crack chipping,
no crack branching.

### 3.5.4 Single edge V-notch fracture toughness testing.

Fracture toughness was measured by the single edge V-notch beam method. A V-shaped notch was machined on one narrow edge of each bar. This was done by first machining a notch 0.5mm deep with a 300μm diamond blade. The V-notch was then produced by placing the bar in a fixture that generated a back and forth movement with a sharp steel blade. The blade was smeared with a diamond paste and located in the 300μm slot in the bar and moved back and forth for 1000 cycles. The bars were then fractured in a 4-point bend loading arrangement in a Loyd LR50K mechanical testing machine with a 500N calibrated load cell. The maximum load to failure was

recorded for each sample and the notch depths were measured by optical microscopy. The fracture toughness was calculated according to the following equations:

$$k_{IC} = \frac{F}{B\sqrt{W \times S_0}} - \frac{S_i}{w \times 3\sqrt{\alpha 2(1-\alpha)^{1.5xy}}}$$

and

$$\alpha = \frac{a}{W}$$

and

$$Y = 1.9887 - 1.326\alpha - (3.49 - 0.68\alpha + 1.35\alpha^2) \times \alpha(1-\alpha)(1+\alpha)^{-2}$$

Where:

$K_{IC}$ = Fracture toughness ($MPa.m^{0.5}$)

F = Fracture load (N)

B = Specimen width (m)

W = Specimen height (m)

A = Notch depth (m)

$S_o$ = Support (outer) span (m)

$S_i$ = Loading (inner) span (m)

Y = Stress intensity shape factor

## 3.6 Data analysis.

All data was analysed by descriptive statistics and where applicable statistical significance was determined by Student's t-test with a significance level of $p < 0.05$

## *3.7* Component testing.

### *3.7.1* Burst strength, Uniaxial compression strength (UCS).

Flexural strength is a good indicator of the strength of candidate ceramics however the real test for suitability of purpose of a ceramic is to test the component in the actual final design form and application. Therefore, both the ceramics were tested as ball heads and liners in uniaxial compression testing (UCS). Testing was carried out on 28 mm diameter ball heads on CoCr (Vitallium), nitrogen strengthened steel (Orthinox) and beta-Ti-alloy (TMZF) standard spigots.

### *3.7.2* Friction testing.

The friction experiments were carried out on a Plint friction simulator (Plint and Partners Ltd, Berkshire, England) at the Applied Research Laboratory Stryker Howmedica Osteonics Limerick. The apparatus is shown in Figure 36 . The simulator consists of a fixed frame with an upper oscillating arm to provide the motion cycle. The simulator was controlled by a data acquisition software system – Compend 2000.

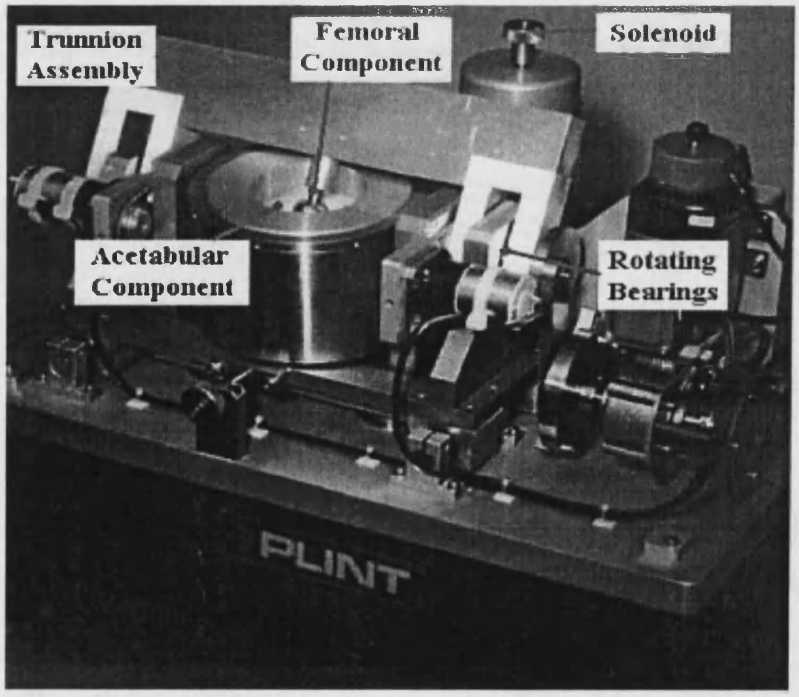


Figure 36: Plint Friction simulator.

The prostheses were mounted anatomically inverted with the femoral component held in the upper oscillating frame and the acetabular component held below in a friction measuring carriage. The friction measuring carriage is mounted into a holder that pivots in low friction contra-rotating bearings about the centre line of rotation of the upper component. These bearings are designed to have an extremely low coefficient of friction. The frictional torque developed during the testing of the ceramic couples was measured using a piezoelectric force transducer.

During testing, sinusoidal motion was imposed on the femoral component in the flexion extension plane with nominal amplitude of ±25 °. The cycle frequency was 0.8 Hz, during which the load, frictional torque and angular displacement were measured. For each sample, at least two experimental runs were required. The load was first applied in one direction of the femoral component motion, then in the reverse direction in order to eliminate any small alignment errors. Each measurement run involved first running the component four hundred times before a measurement was made in either direction. This allowed the components to bed-in and stabilise. After 400 cycles, the software is programmed to measure 600 data points.

The friction simulator has an applied load range of between 100 to 2500N. The majority of the experiments were carried out at a load of 2500N that is equivalent to about two and a half times body weight.

During each run, the average torque, produced between the couples tested, was measured. This was recorded for both the forward run and the backward run, $T_f$ and $T_b$. From these values the control software calculates the true frictional torque, T.

$$T = \frac{|Tb - Tf|}{2}$$

This value of torque was then used to calculate the friction factor f. The friction factor, f, is used rather than the coefficient of friction, μ, because the latter requires the specific pressure distribution to be known, and strictly speaking this is unknown

when using ball heads and liners. The frictional factor f is defined as the torque divided by the product of radius of the femoral head and load on the prosthesis.

$$f = \frac{T}{r.L}$$

In order to simulate different viscosities, different aqueous solutions of carboxy-methyl-cellulose (CMC) were used as the joint lubricant in each case. These synthetic solutions have been found to have similar rheological properties to those of synovial fluid. The viscosity range used for this work was 3.1, 9.10, 36.6, 80 and 139 cps. Each viscosity solution was made up by adding the required amount of water to known amounts of CMC. The viscosity was measured using a calibrated Brookfield digital viscometer. Combining a range of viscosities with known values of entraining velocity and radius of the head, a Sommerfield parameter, Z, can be calculated. This is described by the following formula:

$$Z = \frac{v.r.\eta}{L}$$

where v is the entraining velocity, r is the radius of the ball head and $\eta$ is the viscosity and L the applied load.

Analysis of the results took the form of a Stribeck curve that is produced by plotting the friction factor, f, against the Sommerfield parameter Z. Figure 37 shows an idealised Stribeck curve. The curve describes the different lubrication regimes that can exist between any given bearings and can be divided into three main areas:

1. *boundary lubrication* where essentially the bearing surfaces contact – usually due to high surface roughness (asperity contact) or low wettability of the surface by the lubricating fluid. This gives rise to high friction values and hence high wear,
2. *mixed lubrication* where the bearing surfaces are partially contacting and partially separated by the lubricating fluid. This is indicated on the curve as a fall in friction as the Sommerfield parameter increases,

3. *full fluid film lubrication* This is the point where the lubricating fluid is fully separating the bearing surfaces. The friction at this point is at its minimum and only slightly increases as the Sommerfield number increases due to the shear stress of the lubricant itself.

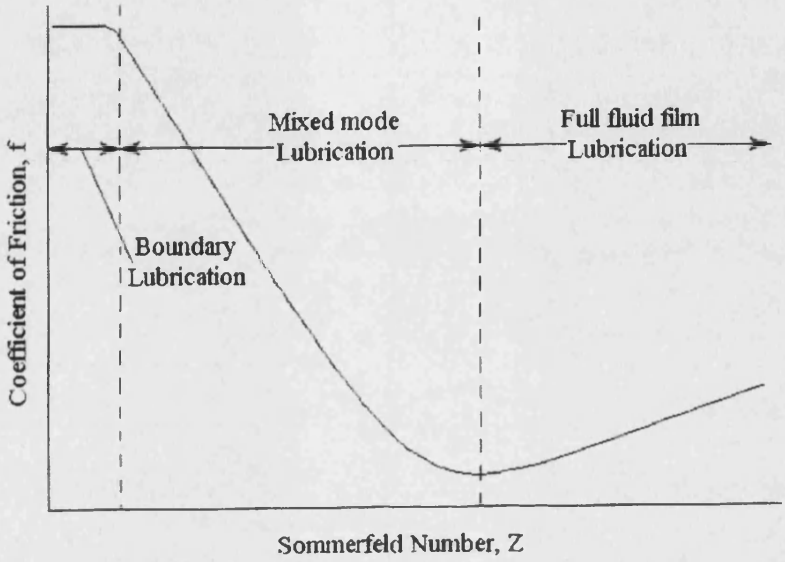


Figure 37. Idealised Stribeck plot.

The couples measured and the experimental conditions used are outlined in Table 4 below:

| Head | Cup | lubricant |
|---|---|---|
| Alumina | Alumina | CMC range |
| Orthinox | Polyethylene | CMC range |
| Alumina | Polyethylene | CMC range |
| CZTA | CZTA | CMC range |

Table 4: Combination of couples measured in friction testing.

Alumina/alumina was used as the control for the friction experiments and was run at least once a week during the testing to ensure that the machine was reproducing correct results in a repeatable form.

All ceramic components used in the study were supplied as per the standard requirements for surface roughness and head cup clearance.

### 3.7.3 Hip simulator wear testing.

Testing was carried out in collaboration with the University of Leeds on 28-mm combinations of ZTA femoral heads articulating with themselves and alumina.

This test was conducted using the Leeds MkII physiological hip simulator as shown in Figure 38. This simulator features internal/external (I/E) rotation and flexion/extension (F/E) motions.

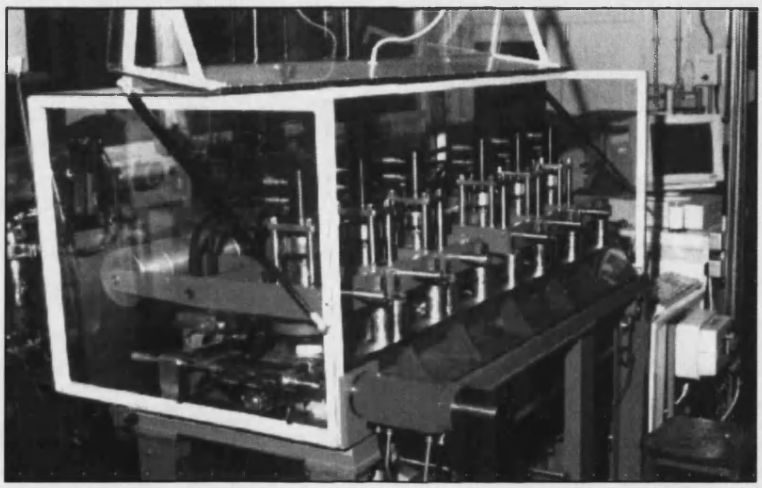

Figure 38: MkII Hip simulator [29].

Components were permanently labeled and coupled for the simulator test. A further diagram of the simulator is shown in Figure 39 outlining the orientation of the head and insert in the hip joint simulator.

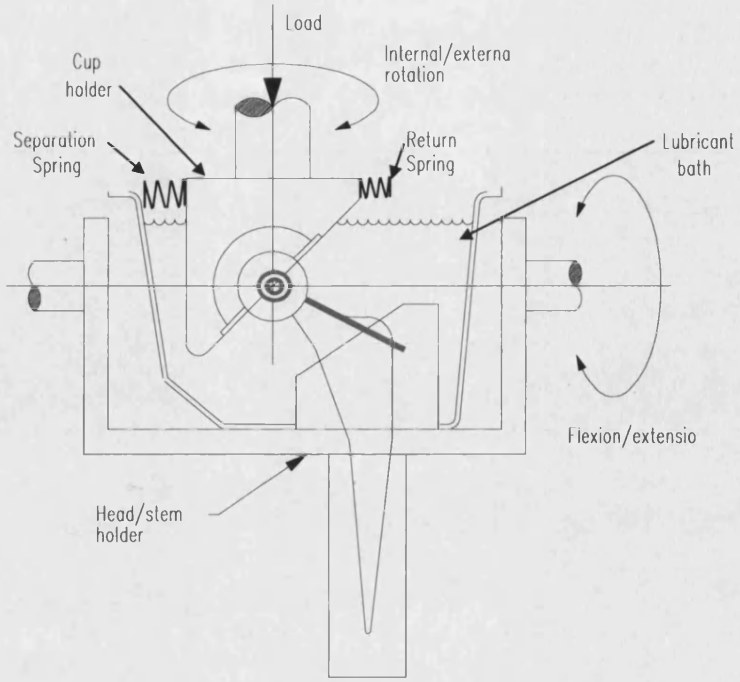


Figure 39. Schematic of a single test cell from the Leeds Mk II hip joint simulator incorporating microseparation [126].

Femoral stems were fixed into the stem holder with polymethylmethacrylate bone cement using a jig to ensure identical alignment was provided to each station. The simulator is a left hip and introduces 10° of anteversion into the setup. The simulator holds the components by allowing the femoral head to be pressed onto the stem taper, while the insert is pressed into a matching insert taper in the insert/cup holder. The heads and inserts were removed on several occasions for analysis purposes. To facilitate removal and replacement the components were carefully aligned. Femoral heads were aligned with the top centre of the stem as indicated by the solid line in Figure 39. Inserts were aligned with the centre of the cup holder at the position marked by the two dark circles (coming out of the page). This alignment ensured component relocation in the same position.

A simplified physiological loading pattern modeling the normal walking cycle developed by Barbour was utilised. The loading and motion are summarised in Figure 40 which demonstrates the elliptical path of the contact during motion.

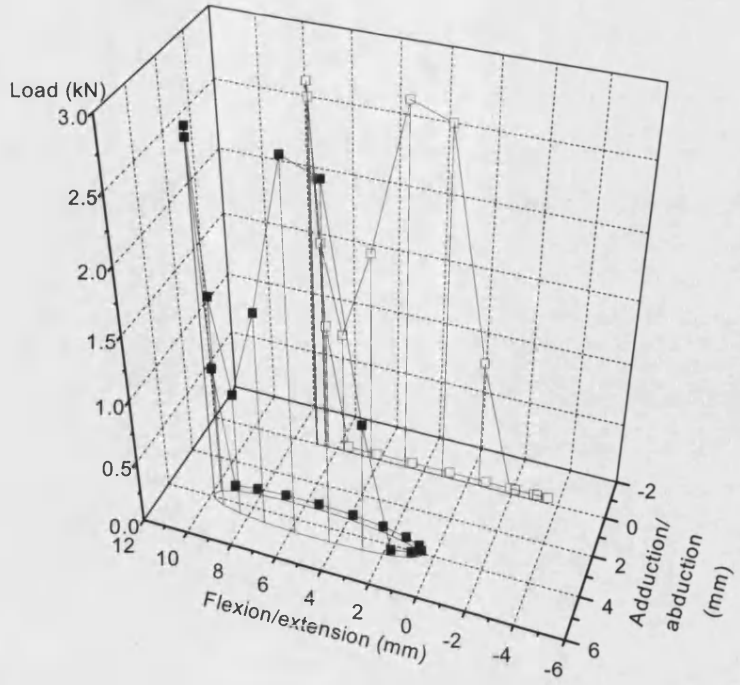


Figure 40: Load cycle and wear paths for the Leeds Mk II hip joint simulator [126].

Microseparation was achieved by applying a force of approximately 400N in the medial lateral (M/L) direction using a balanced spring system developed by Nevelos [22]. This, combined with a very low swing phase load of 50N, allowed the joint to separate.

The couples tested, the test duration and conditions are outlined in Table 5. The first test involved ZTA articulating against ZTA for 3 x $10^6$ cycles under standard simulator conditions and a further 2 x $10^6$ cycles under microseparation conditions. All tests were conducted at 1 Hz with components immersed in 25% bovine serum diluted with sodium azide to prevent degradation. The solution was changed every five days with samples kept for future analysis of wear debris.

| Couples tested | Test duration Million cycles | Test conditions |
|---|---|---|
| AZTA / AZTA | 3 | Standard |
| BZTA / BZTA | 3 | Standard |
| AZTA / AZTA | 2 | Micro separation |
| BZTA / BZTA | 2 | Micro separation |
| AZTA / AZTA | 5 | Micro separation |
| AZTA / AL | 5 | Micro separation |
| Zr / AL | 5 | Micro separation |

Table 5: Hip simulator runs.

The bearing components were removed at 1.0, 2.0, 3.0, 4.0 and 5.0 $x10^6$ cycles to evaluate their performance. Performance was quantified by gravimetric and surface analysis techniques. Gravimetrical analysis required components to be initially cleaned in glass cleanser (composition proprietary, Boots Cleanser and Steriliser Powder) and the tapers scrubbed to remove metal transfer from the stem. Components were then left in an atmosphere controlled room for 24 hours to dry and thermally stabilise. After initial calibration the components were weighed on a five figure microbalance. Weights were additionally adjusted according to the weight of a control alumina ceramic femoral head left permanently in the atmosphere controlled room for calibration purposes. Weights were converted to volumes using a specific gravity of 4.37 for the ZTA and 3.98 for the alumina ceramic materials.

Detailed surface analysis was completed using a form talysurf profilometer both parallel and perpendicular to the direction of motion.

# 4.0 Results

## 4.1 X-ray Diffraction Results.

X-ray diffraction analysis (XRD) was carried out on all materials as received. Figures 41 & 42, are the representative spectra for AZTA & BZTA respectively.

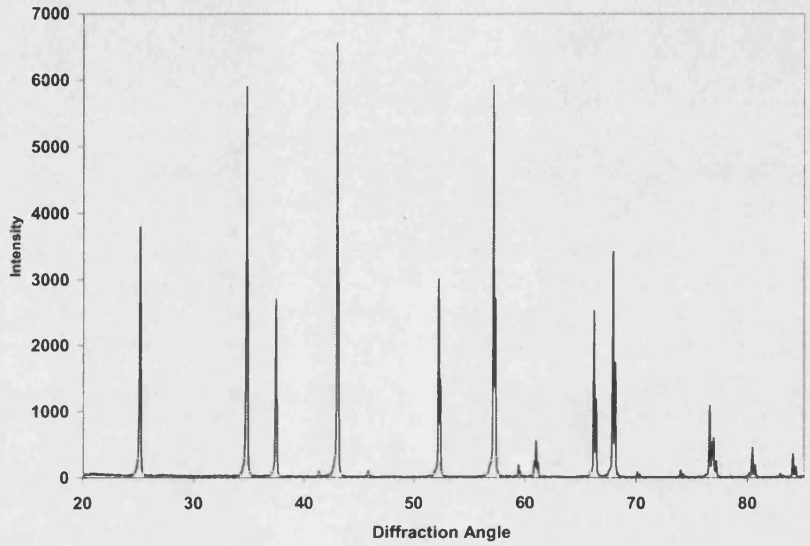


Figure 41: XRD trace for as received BZTA material.

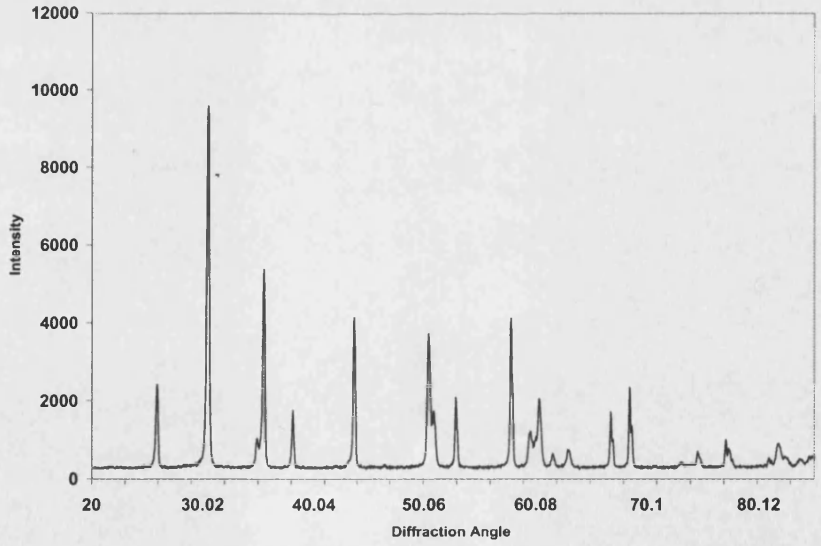


Figure 42: XRD trace for as received AZTA material.

Samples analysed were, where possible, in the form of flat rectangular plates in order to get the most accurate readings, however in the case of the AZTA material this was not possible. AZTA samples for analysis were in the form of flexural strength bars.

The BZTA materials were re-analysed after accelerated aging and the results presented below in Figure 43(a). In each case the XRD traces are shown for the region of interest for tetragonal to monoclinic transformation i.e. between $2\theta = 27° - 33°$.

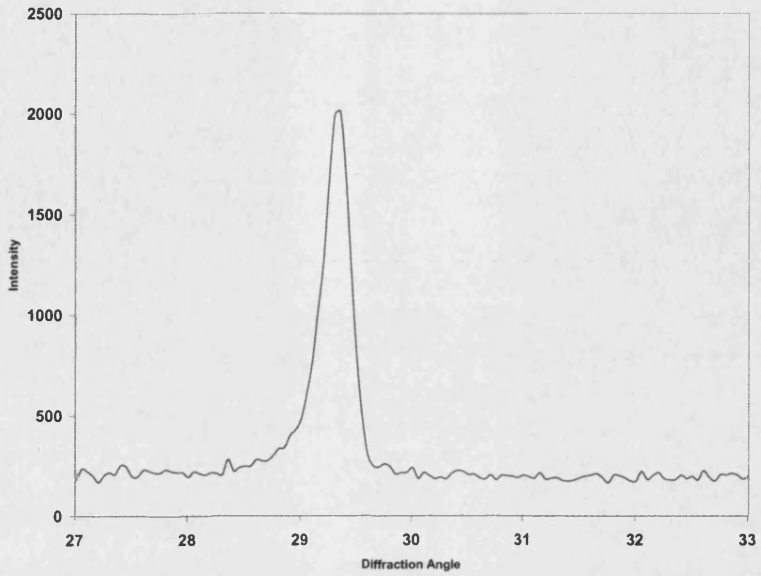


Figure 43(a): XRD trace for AZTA after accelerated ageing.

The same analysis was carried out on ten samples with no apparent change in the XRD traces. This indicates that no tetragonal to monoclinic transformation has occurred during the accelerated aging of the BZTA material. Figure 43(b) shows a representative sample of three of these XRD traces overlaid for comparative purposes. There is no scale on the y-axis as the traces have been staggered for ease of analysis.

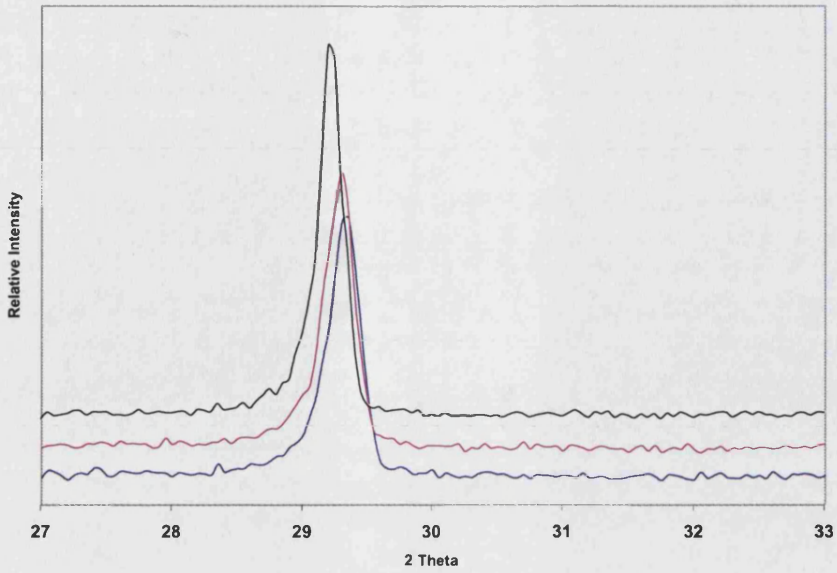


Figure 43 (b): XRD traces for three AZTA samples overlayed for comparative purposes.

Looking at the XRD traces for the AZTA material it can be seen that the material has a certain amount of monoclinic phase on the surface. Figures 44, shows the relevant area of the trace in more detail before and after aging. In the JCPDS standards, the two main peaks for the monoclinic phase appear at 2 theta 28.2° and 31.5 °. These are present in both cases on the AZTA XRD traces.

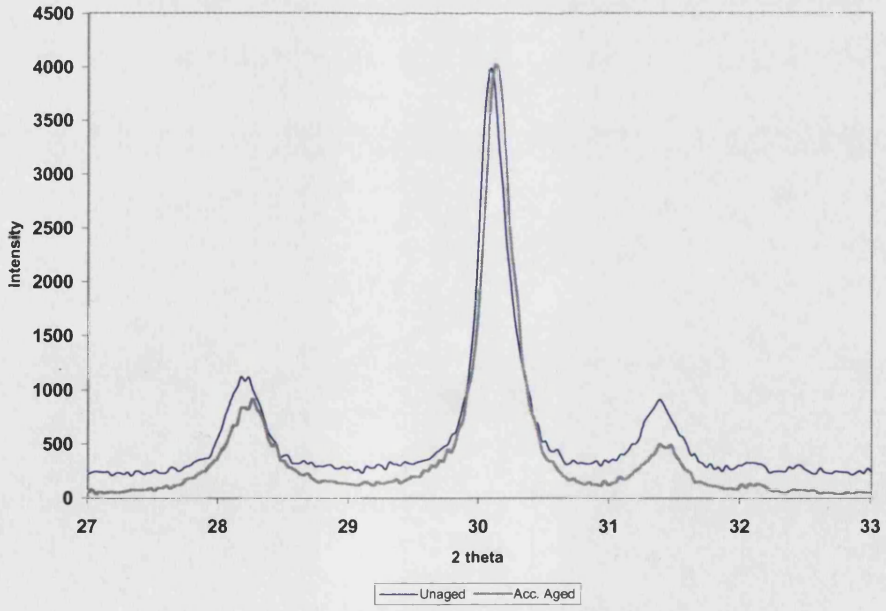


Figure 44: AZTA XRD analysis before and after accelerated aging.

Using the equation outlined in chapter three the amount of monoclinic phase present in the different material conditions can be calculated. These are presented in table 6.

| Sample No. | AZTA (AR) % monoclinic | AZTA (AA) % monoclinic |
|---|---|---|
| 1 | 27 | 26 |
| 2 | 29 | 27 |
| 3 | 30 | 24 |
| 4 | 27 | 31 |
| 5 | 28 | 24 |
| 6 | 26 | 26 |
| 7 | 27 | 28 |
| 8 | 25 | |
| 9 | 25 | 28 |
| 10 | 29 | 25 |

Table 6: Monoclinic content measurements for AZTA material.

The monoclinic content on the surface of the AZTA does not change after both accelerated aging in an autoclave at 134°C and after twelve months real time ageing. It is not possible to determine if this monoclinic phase is prevalent throughout the bulk of the material or if it is only a surface phenomenon. What can be stated from these results is that up to 30% of the zirconia on the surface of the BZTA is in the monoclinic form. This has either been introduced from the starting zirconia powder used or as an artefact of the processing of the ceramic. The significance of this will be discussed later however it seems that the structure is stable and no further transformation is occurring. This is probably due to the constraining nature of the alumina matrix that the zirconia grains are dispersed in.

## 4.2 Flexural Strength results.

The flexural strength results for each material and each material condition are presented in table and graphical form below.

| Sample ID | No. of Tests | Mean flex. strength MPa | Standard deviation |
|---|---|---|---|
| Al as received | 10 | 450.7 | ±107.4 |
| AL artificial age | 10 | 481.8 | ±109.1 |

Table 7: Flexural strength results measured for the alumina control specimens (AL).

| Sample ID | No. of Tests | Mean flex. strength MPa | Standard deviation |
|---|---|---|---|
| BZTA as received | 10 | 823.8 | ±136.4 |
| BZTA artificial age | 10 | 777.1 | ±128.8 |
| BZTA real time aged | 10 | 741.6 | ±122.2 |

Table 8: Flexural strength results for the BZTA material

| Sample ID | No. of Tests | Mean flex. strength MPa | Standard deviation |
|---|---|---|---|
| AZTA as received | 10 | 1188.2 | ±202.05 |
| AZTA artificial age | 10 | 1203.3 | ±101.15 |
| AZTA real time aged | 10 | 1162.8 | ±87.8 |

Table 9: Flexural strength results for the AZTA material.

All real time aged specimens are for a time period of 12 months.

Ten zirconia flexural strength bars were also tested in the as-received condition, giving a mean value of 15000 ± 128 MPa.

When the students t-test for difference of means of two populations is applied to the results there is no difference for any of the materials strength before and after aging at a 95% confidence level. Therefore, the overall average for each material can be reported as in table 10 below.

| Sample ID | No. of Tests | Mean flex. strength MPa | Standard deviation |
|---|---|---|---|
| Al | 20 | 466 | ±106 |
| AZTA | 30 | 1212 | ±130 |
| BZTA | 30 | 800 | ±131 |
| Zr | 10 | 1500 | ±128 |

Table 10: Flexural strength results for the CZTA material.

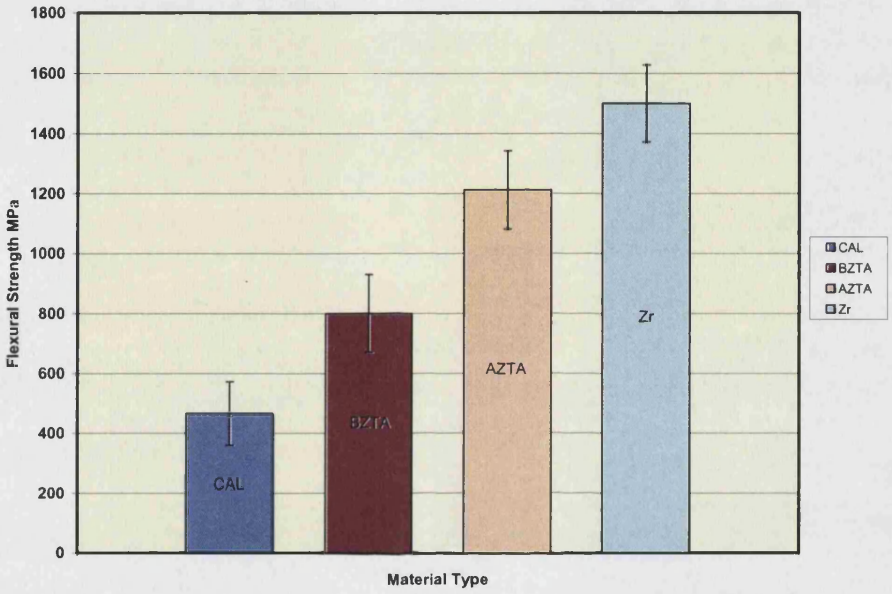


Figure 45: Flexural strength results for all ceramics tested.

As can be seen from the flexural strength results, Figure 45, the ZTA materials both show an increase in flexural strength over the alumina control. There is however a difference in strength when both ZTA materials are compared to each other. The AZTA is up to 25% stronger than the BZTA material. However, both materials are between 50 to 75% stronger than alumina.

Ageing (both artificial and real time) does not affect the mechanical properties of any of these ceramics. This indicates that there is no uncontrolled transformation during the simulated and real time aging that could affect the long-term strength. Both materials are stable.

## 4.3 Hardness testing.

The hardness results show both the ZTA materials to have the same hardness as alumina. AZTA 2014 HV, BZTA 2043 HV, alumina 2041 HV.

## 4.4 Fracture toughness results

*Indentation fracture toughness*

The indentation fracture toughness for the alumina and BZTA materials are shown in Table 11

| | Indentation Fracture toughness ($MPa.M^{1/2}$) | |
|---|---|---|
| **Test no.** | **Alumina** | **BZTA** |
| 1 | 2.78 | 4.35 |
| 2 | 2.79 | 4.2 |
| 3 | 2.78 | 4.1 |
| 4 | 2.8 | 4.3 |
| 5 | 2.65 | 3.8 |
| **Mean** | **2.76 ± 0.062** | **4.15 ± 0.21** |

Table 11. Indentation fracture toughness values.

Difficulties were encountered in measuring the resultant cracks under the light microscope and it was not possible to tell if the crack length was the true length or the limit of the resolution on the microscope. One indentation crack from each material was checked under the SEM and the crack lengths were found to correlate well with the measured values, Figures 46,47.

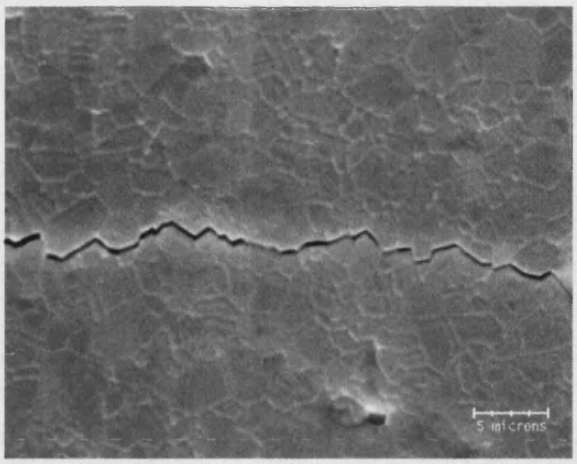


Figure 46: Indentation crack propagation for alumina sample.

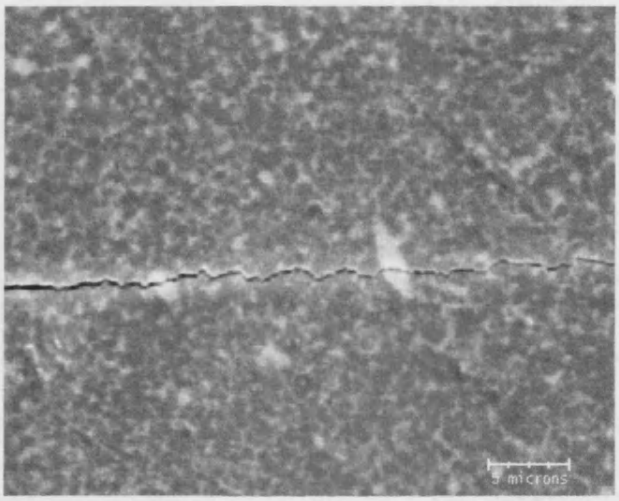


Figure 47: Indentation crack propagation for BZTA sample.

An interesting observation from these images is the difference in the grain structure of the two ceramics and its influence on the crack propagation behavior. The alumina material has a larger grain size and the crack propagates in an intergranular nature with very little resistance to its growth. The BZTA material has a much smaller grain size and has the addition of the zirconia in the matrix (seen as the lighter areas on the image). The crack propagation for this material exhibits both intergranular and transgranular growth. It also has to propagate through large areas of zirconia, which is an inherently tougher material; these areas also act as crack arresters.

*Single edge V-notch fracture toughness.*

The results for the single edge V-notch beam fracture toughness are shown in table 12 and are represented graphically in figure 48.

| Sample no. | AL<br>$K_{IC}$ (MPa.m½) | AZTA<br>$K_{IC}$ (MPa.m½) | BZTA<br>$K_{IC}$ (MPa.m½) |
|---|---|---|---|
| 1 | 3.60 | 6.1 | 5.47 |
| 2 | 3.68 | 5.89 | 4.62 |
| 3 | 3.66 | 6.31 | 4.64 |
| 4 | 4.1 | 6.40 | 4.71 |
| 5 | 3.89 | 6.26 | 4.36 |
| 6 | 3.83 | 6.46 | 4.55 |
| 7 | 4.25 | 6.63 | 4.46 |
| 8 | 3.97 | - | 5.56 |
| 9 | 3.93 | - | 4.71 |
| 10 | 3.92 | - | 4.53 |
| 11 | 3.65 | - | - |
| 12 | 3.92 | - | - |
| **Mean** | **3.86** | **6.29** | **4.76** |
| **Std. Dev.** | **0.2** | **0.24** | **0.41** |

Table 12: Single edge V-notch beam fracture toughness results

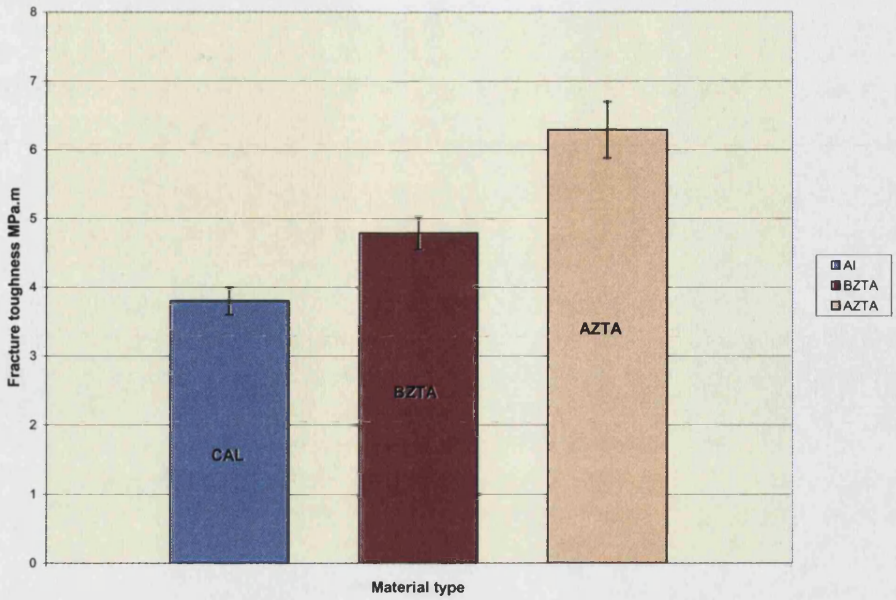


Figure 48 Single edge V-notch beam fracture toughness results.

The fracture toughness results show the same trend as the flexural strength results. The ZTA materials are both tougher than the alumina control however the AZTA is up to 23% tougher whereas the BZTA is 10% tougher.

## 4.5 Grain size analysis.

Energy dispersive x-ray (EDX) analysis was carried out on the microstructure to identify the zirconia and alumina grains. Figure 49 shows the micrograph and area analysed and the subsequent EDX traces are shown in Figures 50,51.

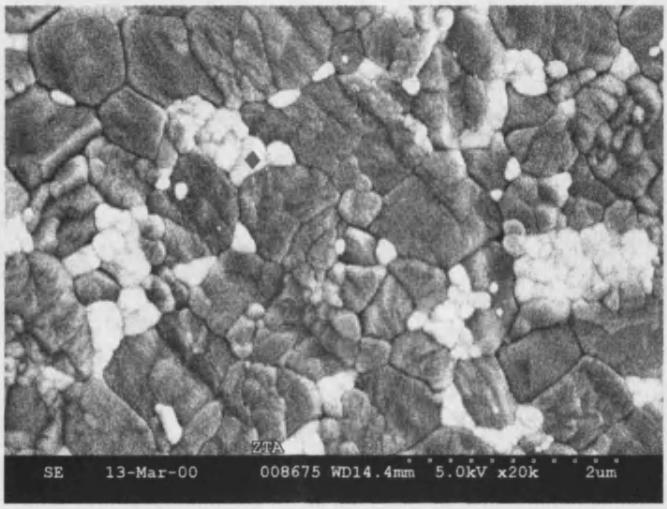


Figure 49: SEM micrograph of the BZTA material.

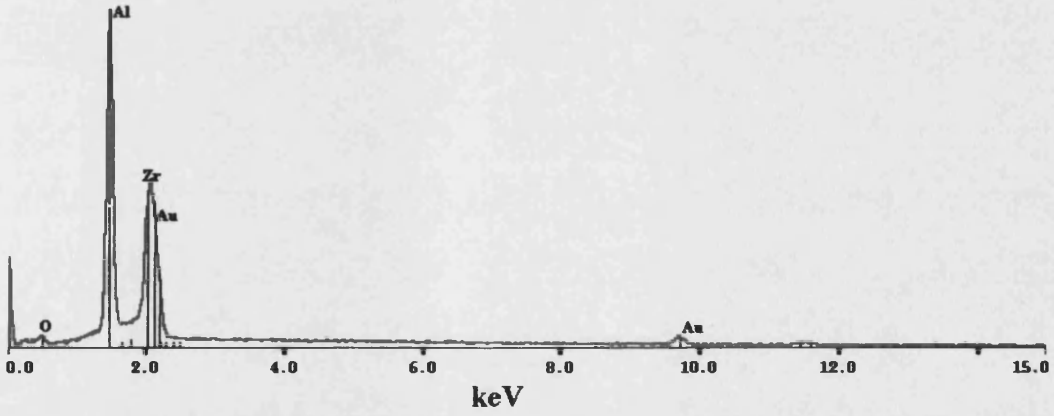


Figure 50 EDX analysis from area 1.

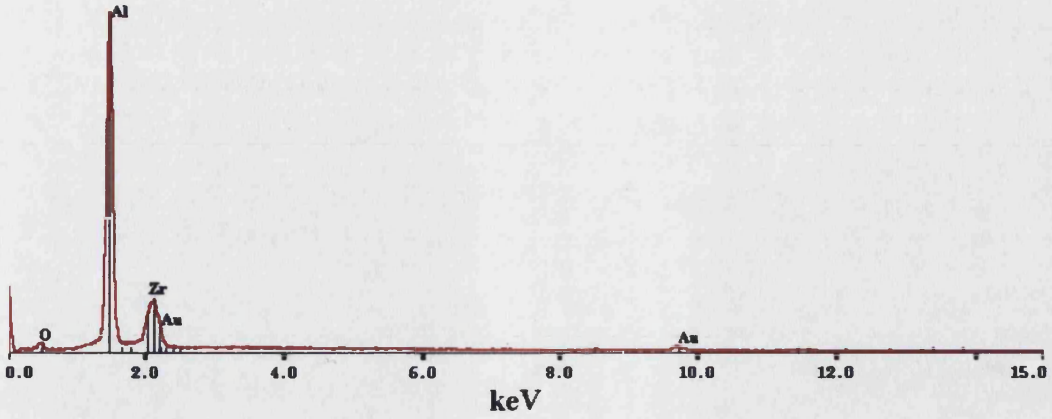


Figure 51. EDX analysis from area 2.

As can be seen from the EDX traces area 1 has a large amount of zirconia present indicating that the white areas are the zirconia grains. Alumina is present on the trace due to reflections from the surrounding grains that are predominately alumina. The EDX trace from area 2 on the other hand is predominantly alumina with very little zirconia present.

Table 13 shows the relative size of the grains for the two ZTAs. The AZTA material has a very fine alumina matrix with grains less than one micron in size. This is due to the grain refining action of the well-dispersed zirconia grains. The BZTA material, on the other hand, has a coarser alumina matrix with an average grain size just over one micron in size. Both materials pass the standard requirements for grain size outlined in ISO 6474.

| Material | BZTA | AZTA |
|---|---|---|
| **Zirconia size (µm)** | 0.265 ± 0.05 | 0.355 ± 0.09 |
| **Alumina size (µm)** | 1.105 ± 0.45 | 0.872 ± 0.26 |

Table 13: Grain size of the two ceramics.

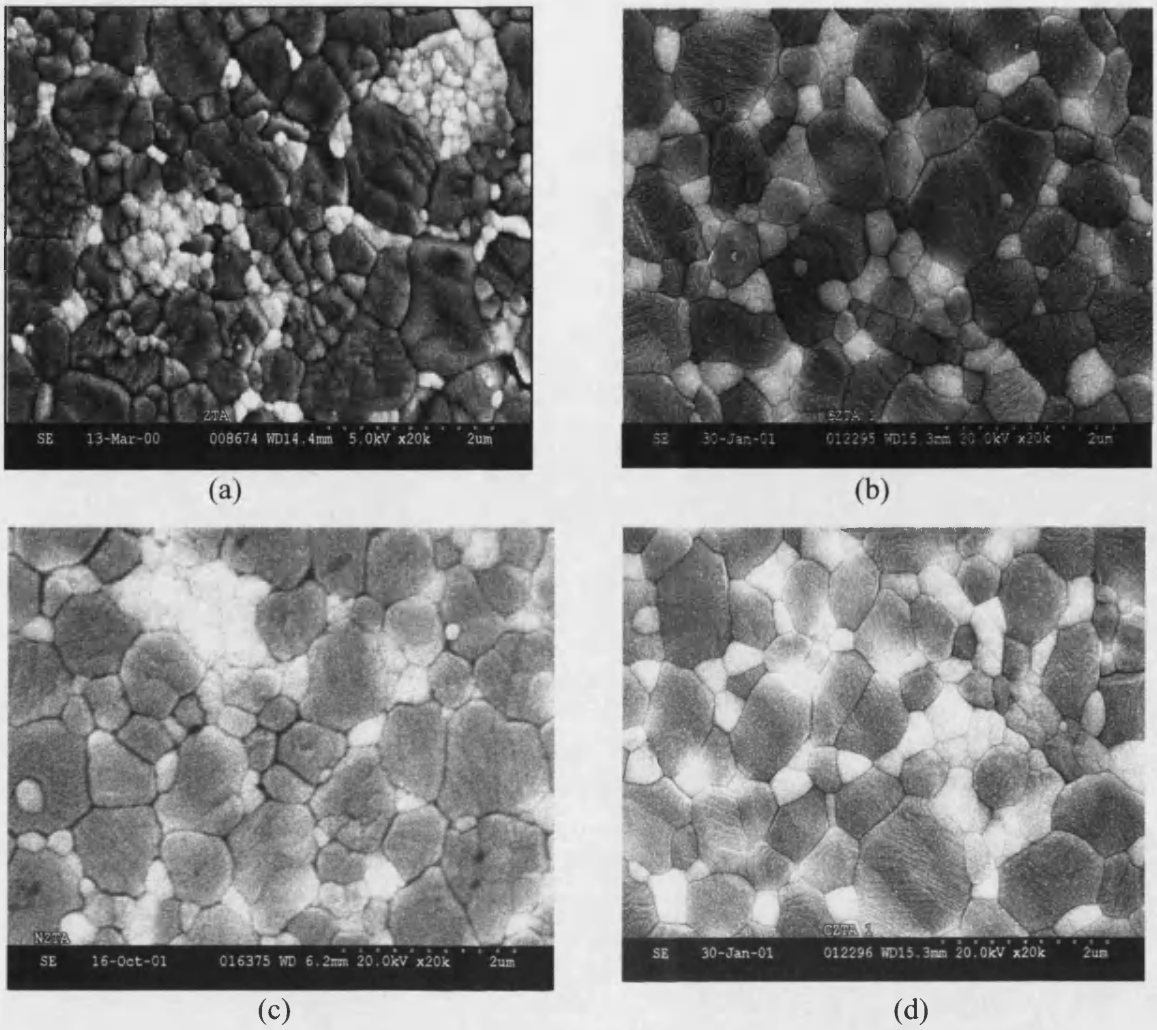


Figure 52. Representative SEM micrographs of both ceramic materials (a&c) BZTA (b&d) AZTA.

Figure 52 (a) shows the BZTA microstructure that consists of alumina grains with large agglomerates of sub-micron zirconia grains (lighter areas). In contrast, Figure 52 (b) shows the AZTA material (same magnification), which is made up of alumina grains with well-dispersed single zirconia grains throughout the matrix. Another point to note is the difference in grain sizes; BZTA has smaller average zirconia grain size whereas the AZTA has smaller average alumina grain size. This reflects the results reported in Table 13.

BZTA is a mixture of the standard zirconia and alumina powders used for the current biomaterials. The process of blending these powders prior to consolidation is currently at a

pilot plant stage. The resulting microstructure shows that this process has not been fully optimised. Looking at the micrograph Figure 52 (c) it can be seen that there is an uneven dispersion of zirconia throughout the matrix. This can be seen as the large agglomeration of white particles in the centre and left hand corner of the micrograph (c).

Analysis of the AZTA microstructure, Figure 52 (B, D) shows the material to have a good dispersion of zirconia grains throughout the alumina matrix. There is no apparent agglomeration of particles as seen in the BZTA. The Strontium platelets were not found on any of the samples examined.

## 4.6 Ultimate compression strength (UCS).

The results for the UCS testing for the ZTAs is shown in table 14. BZTA heads have a burst strength of 52.7 KN on CoCr for a 28 + 4mm spigot. AZTA has a burst strength of 67.7 KN on the same spigot. As expected, the burst strengths are much higher on the other spigot materials for BZTA.

| | CoCr taper | Stainless steel taper | Titanium taper | 46mm cup |
|---|---|---|---|---|
| BZTA (KN) | 52.7 ± 13.9 | 70.8 ± 12.5 | 82.2 ± 8.9 | 53.5 ± 20.9 |
| AZTA (KN) | 67.7 ± 17.9 | 74.5 ± 22.3 | 80.4 ± 15.1 | 107.9 ± 14.5 |

Table 14 UCS for V40 – 28 mm heads + 4 and 28/37 mm inserts.

The +25% difference in the flexural strength results for the ZTAs has equated to a 12% difference in actual product strength when the heads alone are compared. Looking at the results from the liners, there is a 50% difference in strength between the two ZTAs. Both ZTA ceramics passed the 46 KN compressive strength set by the FDA on all spigot materials with an improvement of over 20% in UCS compared to Al which gave only 40.5 ± 7.08 MPa on a CoCr spigot.

The burst strength of the liner was also within the FDA requirements at 53.9 KN for BZTA and 107.9 kN for AZTA when tested in a titanium shell.

## 4.7 Friction Results

The friction of the ceramic bearing materials was measured on a newly commissioned friction testing rig (Plint & partners). It was essential to ensure that the results achieved from this rig were the same as those reported by other authors using similar testing conditions and equipment.

Most of the work reported in the literature concerns the friction measurement of the CoCr / UHMPE bearing combination. CoCr heads 28mm in diameter were therefore tested against UHMWPE cups for a range of CMC viscosities using the Plint friction tester. The Stribeck plot measured is shown in figure 53 for this couple.

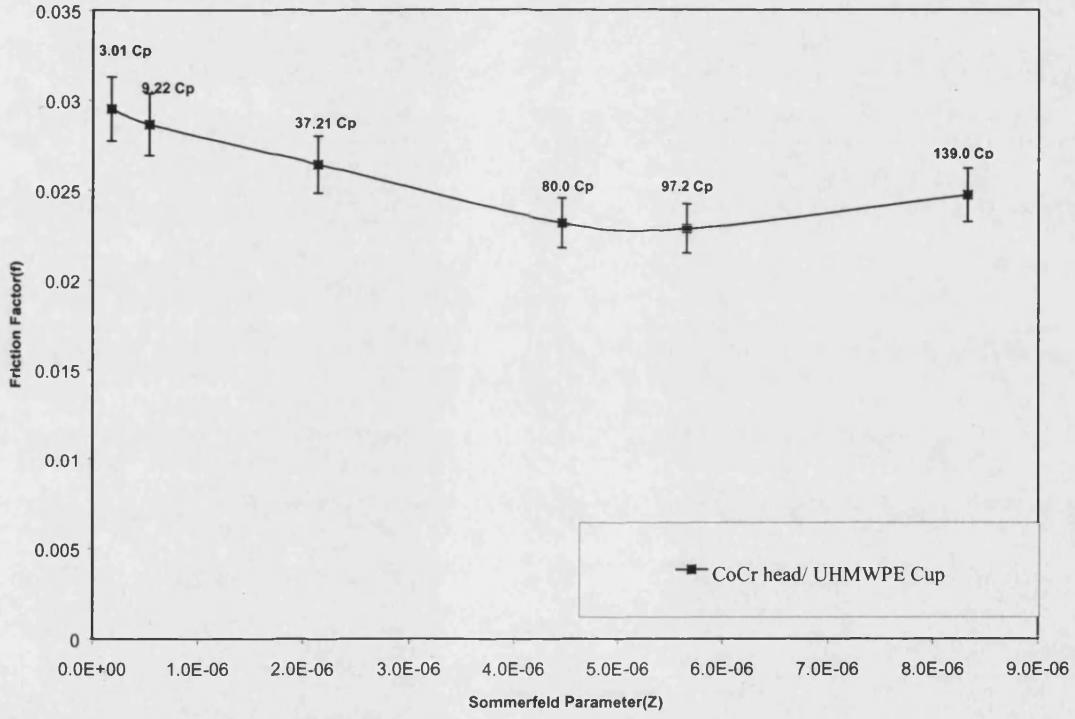


Figure 53: Stribeck plot for CoCr/UHMWPE couple (28mm) over a range of CMC viscosities.

The friction factor for this couple had a range of 0.03 to 0.023 over the range of CMC viscosities used (3.1-136 Cp). The plot shows an approximation to the theoretical Stribeck plot presented in the methods section in chapter 3. The friction factor values decrease as the Somerfield number or viscosity increases. This is indicative of a mixed lubrication regime. After a viscosity of between 80 to 97 Cp there is an increase in the friction factor up to the 136Cp value. This may be indicative of full fluid lubrication and will be discussed in more detail later.

This result compares well with friction factors reported by Unsworth et al [109] for similar testing conditions using 28mm CoCr heads and UHMWPE cups where friction factors in the range 0.037 to 0.015 were reported. The results also compare well with work completed by Smith et al [115] who recorded a friction factor of 0.025 for a viscosity of 1 Cp for a 28mm metal head and UHMWPE cup.

The results for all the combinations outlined in table 4 (methods section) are shown in Figure 54 (a-d) as a series of Stribeck plots.

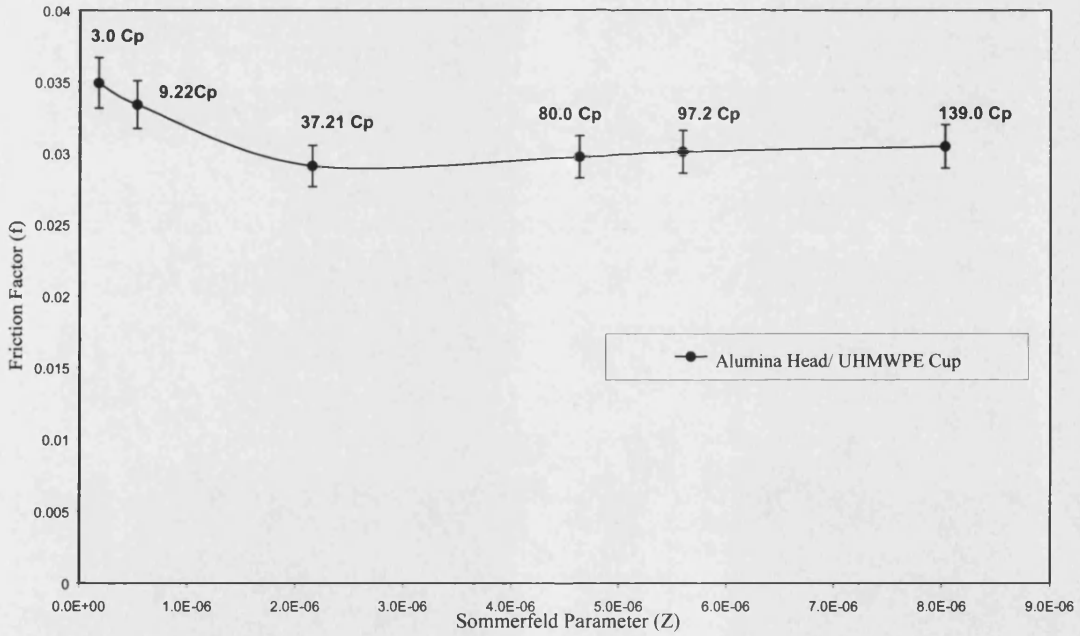


Figure 54 (a): Stribeck plot for alumina head / UHMWPE cup.

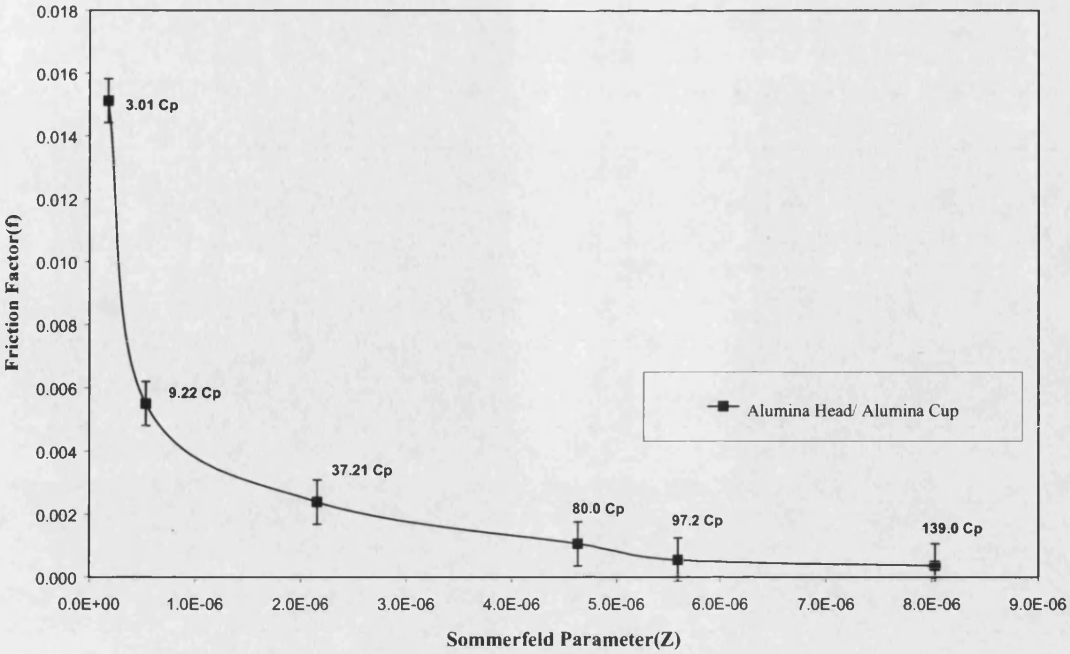


Figure 54 (b): Stribeck plot for alumina head / alumina cup.

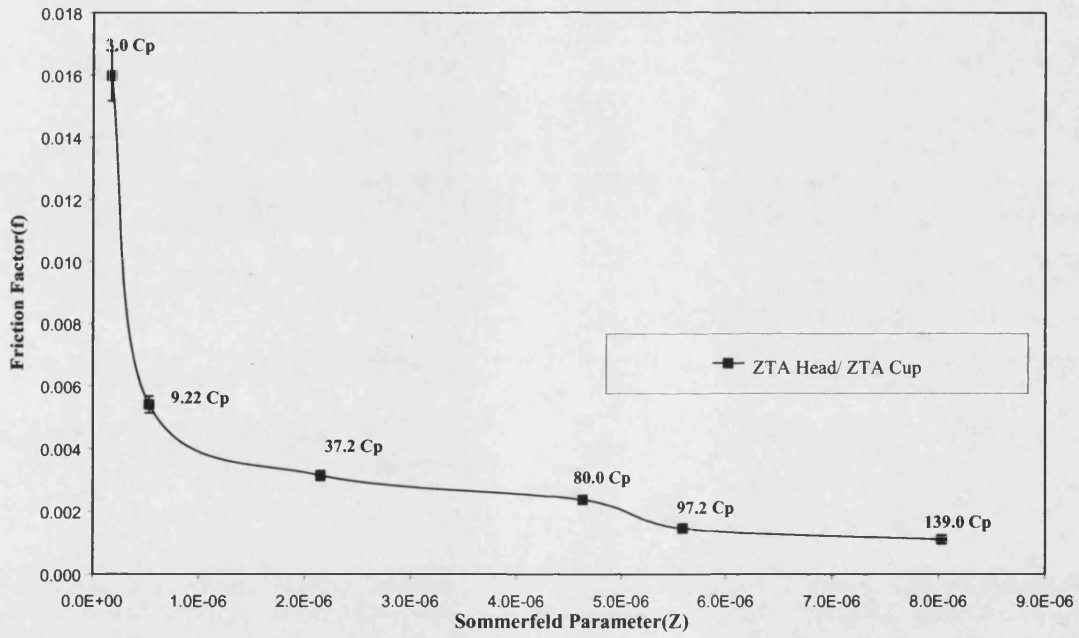


Figure 54 (c): Stribeck plot for CZTA head / CZTA cup.

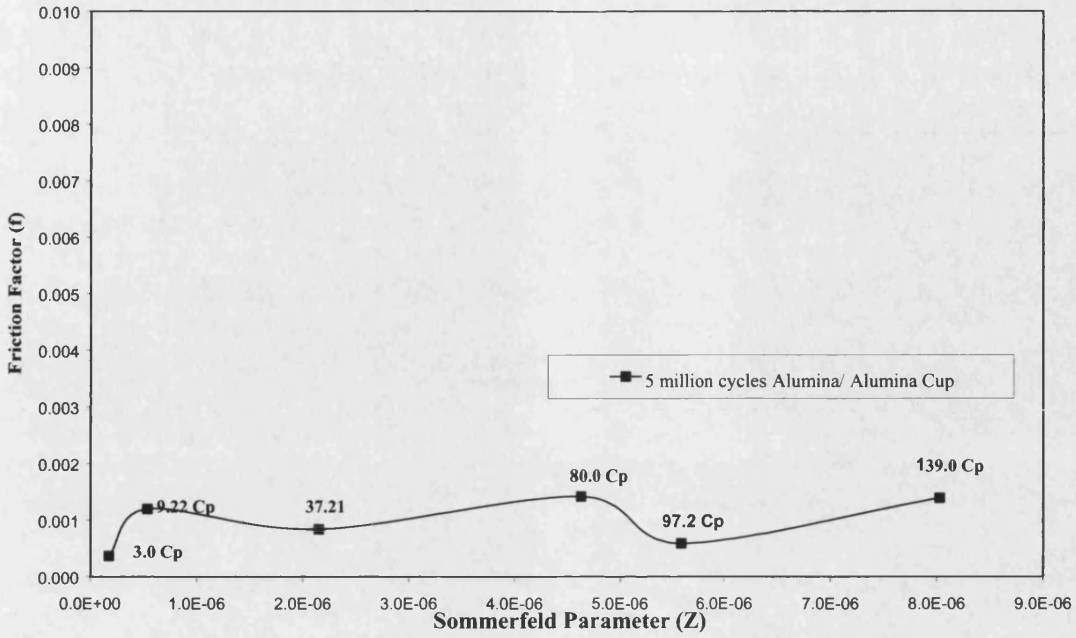


Figure 54 (d): Stribeck plot for alumina head / alumina cup post 5 million cycles in a hip simulator test.

The Stribeck plot for the alumina / UHMWPE (Figure 54 a) was very similar to that measured for the metal UHMWPE couple. No real improvement in friction was noted with the use of an alumina head and the combination had a friction factor that ranged between 0.035 and 0.02, which is slightly higher than the friction range measured for metal/UHMWPE. The Stribeck curve from this test showed a falling trend as the viscosity was increased which indicates mixed lubrication. The plot also showed a slight increase in friction factor at the higher viscosities as seen in the metal UHMWPE plot.

The alumina /alumina Stribeck plot (Figure 54 b) shows a large decrease in friction factor range when compared to the UHMWPE couples. The friction factor range for this combination was between 0.016 to below 0.002. The plot also shows a dramatic fall off as the viscosity is increased, indicating mixed lubrication, however unlike the previous two cases this continued to fall off over the full range of viscosities. The low friction

values would indicate that full fluid film lubrication has been achieved for this bearing couple over the viscosities used.

The ZTA / ZTA couple shows similar performance to the alumina / alumina couple (Figure 54 c). The friction factor range for this component is also between 0.016 to below 0.002. The plot shows a falling trend, which continues over the range of the viscosities measured.

The last combination to be tested involved an alumina / alumina combination that had undergone $5x10^6$ cycles in a standard hip simulator (Figure 54 d). These components are equivalent to a ceramic-ceramic hip replacement that was implanted for approximately five years. The Stribeck plot for this combination shows an extremely low friction factor range between 0.001 and 0.0005. The plot does show a slight increase in the friction factor as the viscosity of the lubricating fluid is increased

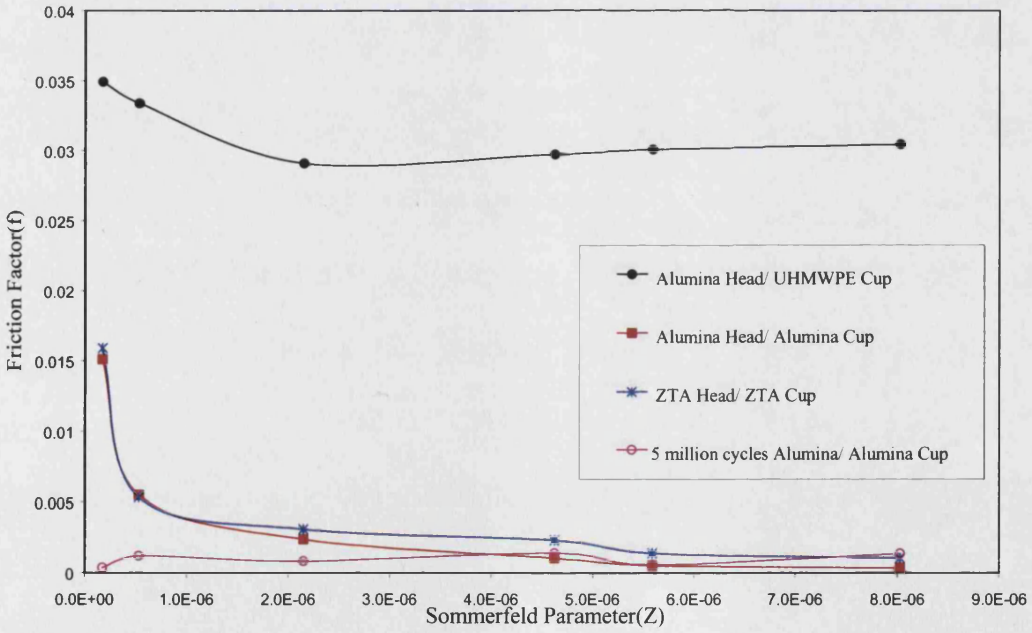


Figure 55: Stribeck plots for all the combinations tested normalised on one axis.

All the components tested with the exception of the alumina/alumina wear tested components, showed a falling trend as the Somerfield parameter increased, Figure 55. This is indicative of a mixed lubrication regime where there is some contact between the asperities or high points on the surfaces and this decreases as the viscosity of the fluid increases. This contradicts the findings of S.C. Scholes et al [113]. Using alumina /alumina components in the Durham hip simulator they found that the friction factor increased slightly over the viscosity range. They concluded that this trend indicated full fluid film lubrication. The friction factor range reported in this study were overall much lower in the low viscosity range. They reported for alumina/alumina a friction factor of 0.002 for a viscosity of 1-5centipoise as opposed to 0.015 in this present study. As the viscosity is increased, the numbers are in closer agreement, with both studies showing friction factors below 0.005 for viscosities in the range of 9 to 150 Cp.

The one area where the results are in agreement is in the case of the alumina/alumina components tested in this study that have undergone $5x10^6$ cycles in a wear simulator at Leeds. These results have almost the same friction range for those reported in the Scholes study. The results are up to 60-70% lower than the as received alumina-alumina components in the lower friction range and exhibit a slight upward trend as the viscosity of the lubricating film is increased. This is due to the nature of alumina-alumina wear mechanism, which is reported to be by self polishing in normal simulation testing [126]. The small level of asperities present on the as received ceramic heads and cups have been removed after five million cycles. Looking at the roughness results for these components table 15 (a) & (b) the $S_a$ and Sq values are up to 70% lower than for the new components.

| Alumina As Received | $S_a$ (nm) | $S_q$ (nm) | $S_{sk}$ (nm) |
|---|---|---|---|
| 1 | 3.22 | 4.09 | -0.62 |
| 2 | 3.1 | 3.84 | -0.23 |
| 3 | 3.46 | 4.24 | -0.1 |
| 4 | 3.04 | 3.9 | -0.32 |
| 5 | 3.22 | 4.22 | -0.4 |
| 6 | 3.11 | 3.89 | -0.3 |
| 7 | 3.87 | 5.02 | 0.34 |
| 8 | 4.19 | 5.23 | -0.56 |
| **MEAN** | **3.40** | **4.30** | **-0.27** |

Table 15(a): Wyko profilometry results for Alumina as received.

| Alumina 5 x $10^6$ cycles | $S_a$ (nm) | $S_q$ (nm) | $S_{sk}$ (nm) |
|---|---|---|---|
| 1 | 1.12 | 1.42 | 0.05 |
| 2 | 1.12 | 1.42 | 0.19 |
| 3 | 1.07 | 1.37 | -0.19 |
| 4 | 1.24 | 1.66 | -0.24 |
| 5 | 1.21 | 1.52 | -0.06 |
| 6 | 0.93 | 1.20 | 0.35 |
| 7 | 0.97 | 1.22 | 0.55 |
| 8 | 0.89 | 1.12 | -0.10 |
| **Mean** | **1.06** | **1.36** | **0.07** |

Table 15 (b): Wyko profilometry results for alumina after wear simulator testing.

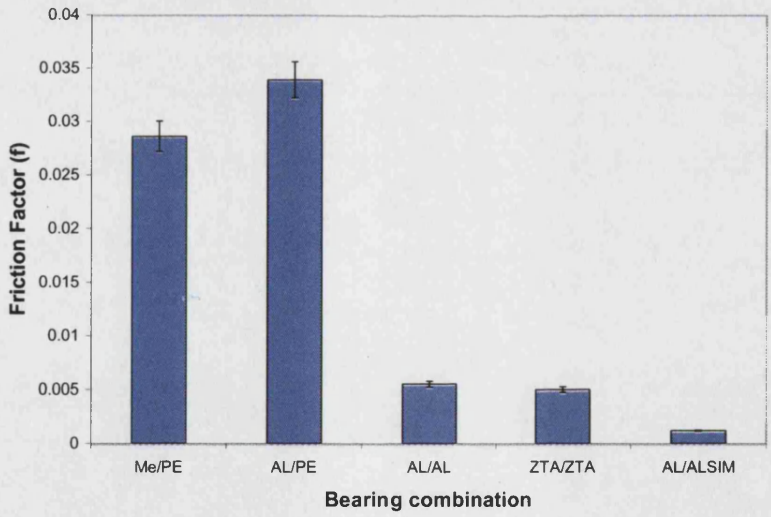


Figure 56: Friction factors of the various combinations tested at a viscosity of 9Cp i.e. healthy synovium.

Comparison of all the different bearings tested reveals, a number of differences. The highest friction was seen for the alumina/UHMWPE couple; this was very similar to the metal /UHMWPE combination. This is not a surprising result as there is usually very little difference in Stribeck plots for couples with UHMWPE cups regardless of the head material used [109]. One explanation is that regardless of the surface finish of whatever material used for the ball head the UHMWPE has a large $R_a$ value, which means large asperities override any friction benefit of using smoother counterfaces.

All the ceramic-ceramic components show a dramatic decrease in friction factor over metal-ceramic combinations against UHMWPE. Figure 56 is a comparison of the measured friction factors for the various bearings components tested at a CMC viscosity of 9 Cp, this is the closest approximation to the reported values for healthy human synovium. The value ranges from between a 60% - 70 % improvement in friction factor for the ceramic-ceramic couples. This clearly demonstrates the advantage of these components as low wear bearings.

## 4.8 Wear testing.

### 4.8.1 Wear Study 1.

This study was designed to investigate the relative wear resistance of AZTA and BZTA under both standard and microseparation conditions for 3 million and 2 million cycles respectively. Also investigated were the relative wear resistances of alumina heads against alumina cups.

At this stage in the testing the microseparation test set up was still experimental with only one previous run having been conducted. This involved CAL/CAL combination and was run out to 800,00 cycles. These initial results are therefore not as complete as later tests due to experimental error, gaining experience in setting the spring tension and fixing the components correctly.

Standard Conditions.

| Material | 0-1M Cycles ($mm^3$) | 1-2M Cycles ($mm^3$) | 2-3M Cycles ($mm^3$) | Average Wear Rate ($mm^3/10^6$ cycles) |
|---|---|---|---|---|
| **AZTA** | 0.04 | 0.05 | 0.00 | 0.03 |
| **BZTA** | 0.02 | 0.06 | 0.02 | 0.03 |

Table 16: Volumetric Wear under Standard Testing Conditions.

These results are in accordance with simulator data reported by Ceramtec for ZTA/ZTA with a wear rate of $0.034mm^3/10^6$ cycles ($0.15mg/10^6$ cycles). There was no change in surface roughness of the ceramic components at any stage during the testing with the Ra values remaining below $0.01\mu m$. The main wear mechanism was a slight relief grain polishing.

Microseparation Conditions.

Incremental volume loss data for each wear couple is shown in Table 17.

| Material | 500k Cycles ($mm^3$) | 5-800k Cycles ($mm^3$) | 800-1200k Cycles ($mm^3$) | 1200-2000k Cycles ($mm^3$) |
|---|---|---|---|---|
| AZTA 1 | 0.76 | 0.21 | 0.19 | 0.10 |
| AZTA 2 | 0.52 | 0.17 | 0.35 | 0.17 |
| BZTA 1 | 0.01 | 0.0 | 0.04 | 0.09 |
| BZTA 2 | 1.30 | 0.21 | 0.47 | 0.11 |
| CAL/CAL1 | 2.00 | 0.45 | | |
| CAL/CAL 2 | 1.70 | 0.0 | | |
| NAl/CAL 1 | | | 1.58 | 0.24 |
| NAl/CAL2 | | | 0.66 | 0.12 |

Table 17: Incremental Volume Loss Data for Micro-separation Testing.

In the BZTA1 station the microseparation was not achieved and, although the wear data is tabulated, it was excluded from further analysis. However, a very small wear stripe was visible. The results are shown graphically in Figure 57 below; alumina/alumina results are shown as dashed lines, the ZTA materials as solid lines.

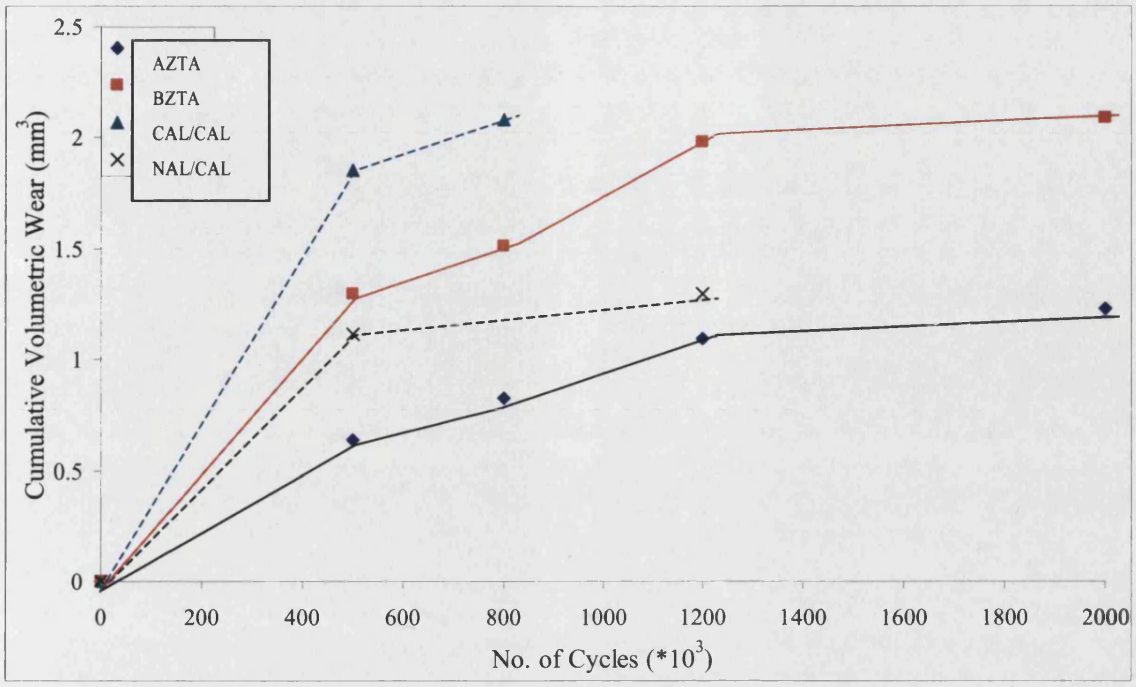


Figure 57: Cumulative volumetric wear for microseparation testing.

The ratio of head wear to cup wear for the different material combinations is shown in Table 18.

| Material Combination | Head Wear/Cup Wear |
|---|---|
| AZTA/AZTA | 1.2 |
| BZTA/BZTA (n=1) | 1.0 |
| NAl/CAL | 1.4 |
| CAL/CAL | 1.2 |

Table 18: Ratio of head wear to cup wear after micro-separation testing.

Standard and micro-separation results can be compared as average wear at 1 million cycles using interpolated data from Figure 57. This comparison is shown as Figure 58.

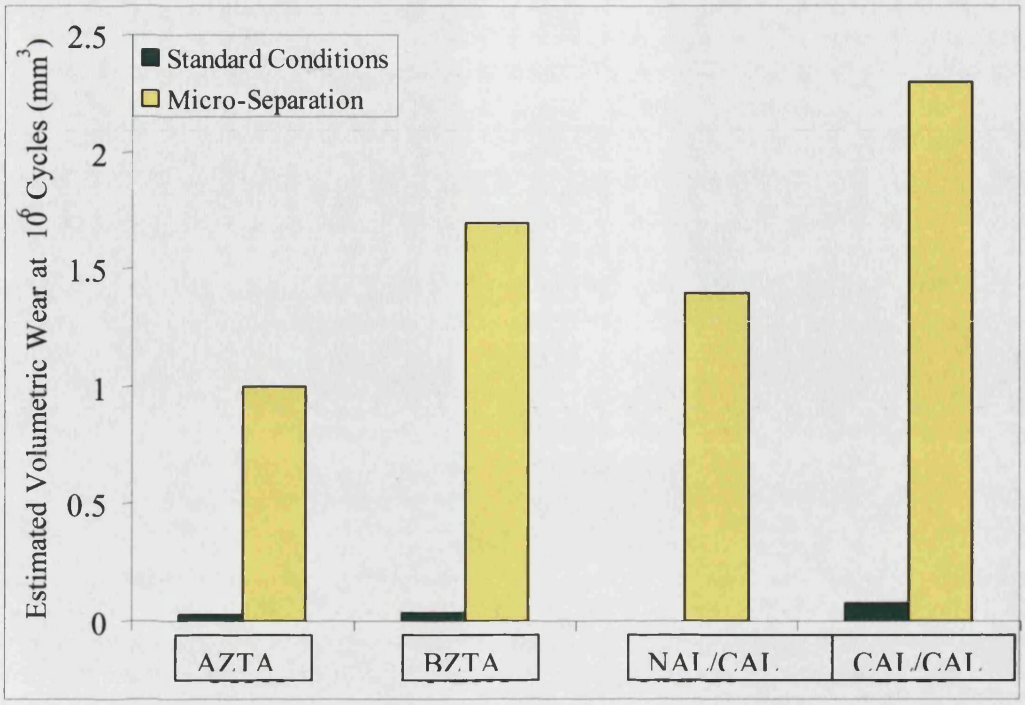


Figure 58: Comparative data from standard and microseparation testing.

Surface Analysis

All heads tested under microseparation conditions in this test showed a stripe wear scar on the head with a corresponding wear scar on the insert. The scars were similar to the scars seen in the retrieved components. These scars are shown in Figure 59 for the alumina components. The only way to photograph the scars is to rub them with a pencil; the graphite caught on the roughened surface allows sufficient contrast to show their extent.

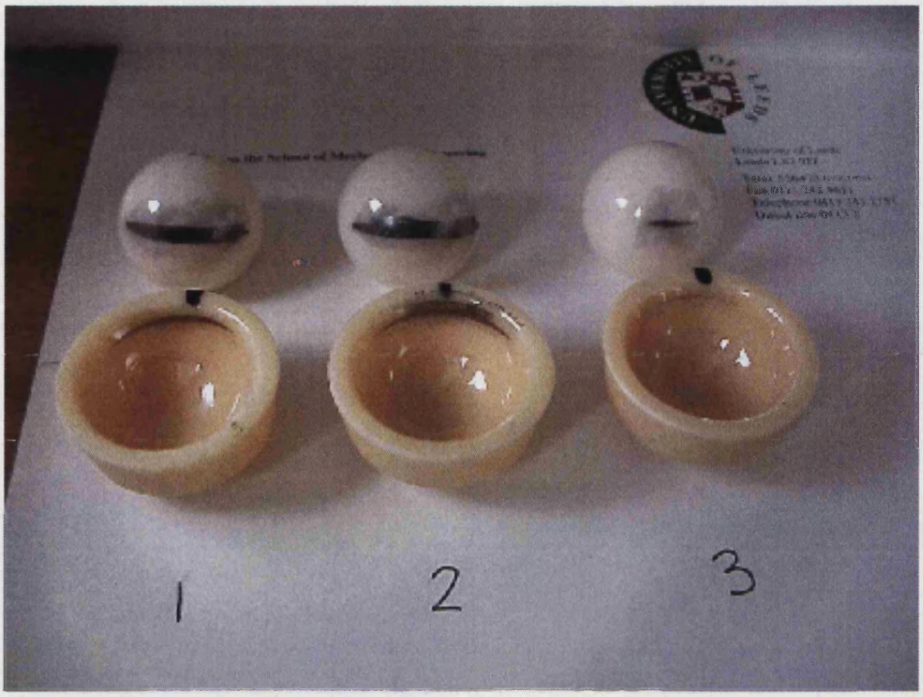


Figure 59: Wear stripes on the NAL/CAL components after 2 million cycles.

Talysurf surface roughness data on the worn areas of the heads at 800,000, 1.2M and 2M cycles in microseparation are shown in Tables 19 and 20.

| | **800k cycles** | **1.2M cycles** | **2M cycles** |
|---|---|---|---|
| **AZTA** | 0.012 | 0.017 | 0.017133 |
| **BZTA** | 0.013 | 0.026 | 0.32905 |
| **CAL** | 0.068 | | |
| **NAl** | | 0.079 | 0.137575 |

Table 19: Talysurf Data of Wear Stripes on Heads: Talysurf Roughness Average, Ra (μm).

| | 800k cycles | 1.2M cycles | 2M cycles |
|---|---|---|---|
| **AZTA** | 0.16 | 0.21 | 0.21 |
| **BZTA** | 0.24 | 0.70 | 0.74 |
| **CAL** | 1.68 | | |
| **NAl** | | 1.60 | 1.53 |

Table 20: Talysurf data of wear stripes on heads talysurf max peak to valley distance Rt (μm).

White light interferometry was also carried out on the worn areas of the heads of all four materials tested after microseparation testing was completed. This meant that the AZTA and BZTA heads had been tested for 2 million cycles, the NAl heads for 1.2 million cycles and the CAL heads for 800,000 cycles. However, the Talysurf data shows that the surface roughness parameters do not change greatly during the course of the testing.

Sa, Sq and St (area roughness average, root mean square roughness average and area maximum peak to valley height respectively) from the centres of the wear stripes are shown in Table 21.

| | Sa (μm) | Sq (μm) | St (μm) |
|---|---|---|---|
| **AZTA** | 0.05 | 0.07 | 1.37 |
| **BZTA** | 0.04 | 0.05 | 0.91 |
| **CAL** | 0.17 | 0.26 | 6.35 |
| **NAl** | 0.19 | 0.26 | 6.71 |

Table 21: Interferometry data of wear stripes on Heads: Sa, Sq and St.

Examples of the worn areas of AZTA and NAl are shown in both 2D and 3D in figures 60 and 61 respectively.

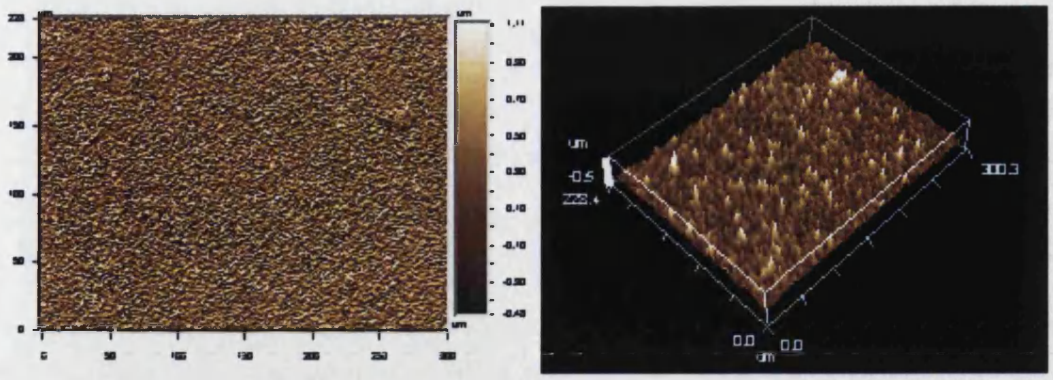

Figure 60: Interferometry Images of Centre of Wear Stripe for AZTA Head.

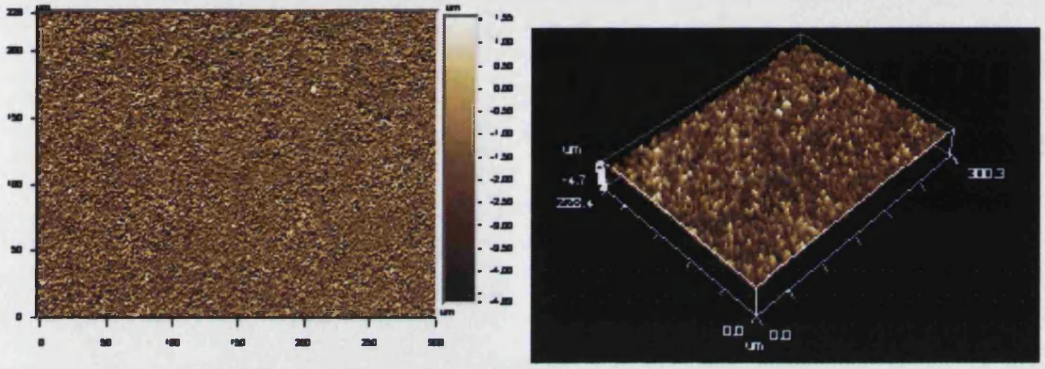

Figure 61: Interferometry Images of Centre of Wear Stripe for NAL Head.

From the data it can be seen that the zirconia toughened alumina materials (AZTA, BZTA) show consistently smoother surfaces than the alumina materials (NAl, CAL), however the differences between the like materials are not significant.

SEM analysis was carried out on the wear scars on the alumina heads only from this test. The ZTA scars were analysed in study 2&3. It was not possible to examine the scars on the rim of the inserts due to the geometry of the component.

The wear scar on the head shows two regions: an area of minimal damage at the edge of the scar and an area of total surface removal in the centre of the scar. Figure 62 below shows the first region where all that is evident are individual grain pullout voids in the surface. The size of these voids is close to the grain size of the components ~ 2-5 µm.

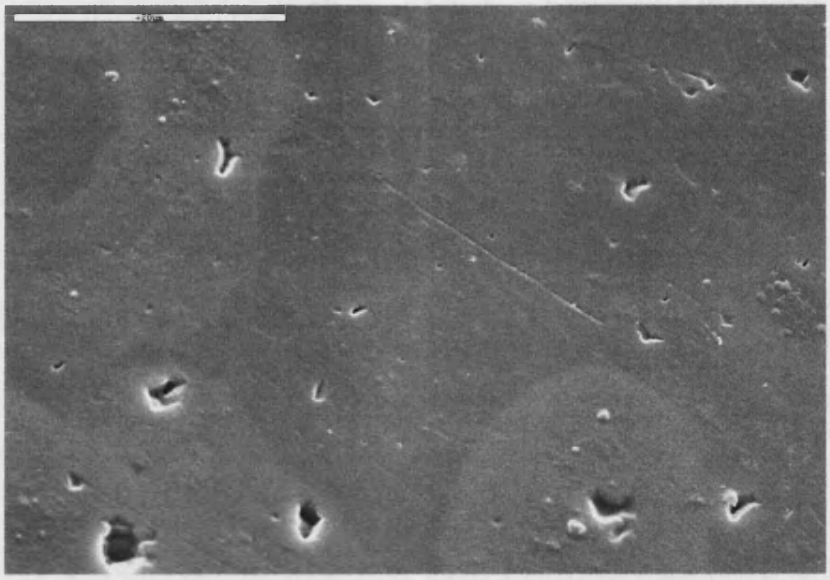

Figure 62: SEM image of sporadic grain pull-out at the edge of the scar.

Figure 63 on the other hand shows the extent of the damage at the centre of the scar. The original polished surface has been completely removed leaving a pattern of sharp voids (grain pull out through third body wear) and polished areas.

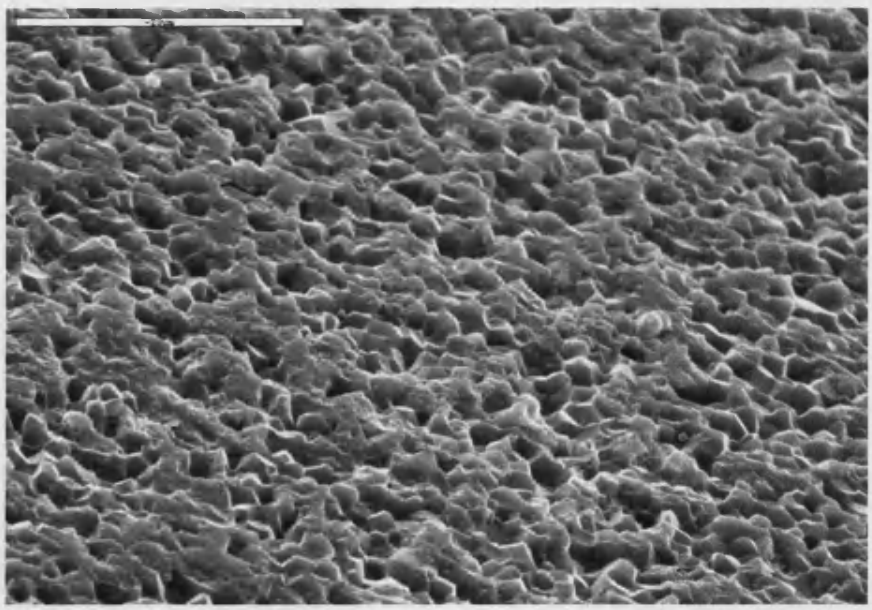

Figure 63: SEM image of the centre of a wear scar showing grain pull-out and polishing.

Standard conditions testing did show slightly lower wear for the zirconia toughened alumina materials although this was not statistically significant

From these initial results, there appears to be a distinction between the alumina and ZTA materials in that the surfaces of the ZTA remain much smoother during testing.
Further simulator studies were run to increase the statistical significance of the results from the microseparation testing.

### 4.8.2 Wear Study 2.

This study examined the relative wear of six pairs of components, three zirconia toughened alumina (AZTA) heads against alumina inserts (CAL) and three HIPed alumina heads against HIPed alumina inserts. The components are summarised in Table 22 for reference. The duration of the testing was set at 5 million cycles to provide significant information on the long-term effect of microseparation on the ceramic materials.

| Station | Heads - 28mm | Inserts - 28mm |
|---|---|---|
| 1-3<br>AZTA/CAL | CeramTec<br>Zirconia<br>Toughened<br>Alumina | CeramTec<br>HIPed Alumina |
| 4-6<br>CAL/CAL | CeramTec<br>HIPed<br>Alumina | CeramTec<br>HIPed Alumina |

Table 22: Component bearing combinations

Gravimetric Analysis

Gravimetric results for each increment of the 5 million cycle test duration are presented in Table 23 as wear volumes. The average results for each material are further presented in bar chart format in Figures 64a to 64b.

| Component ID | 1 x $10^6$ Cycles | 2 x $10^6$ Cycles | 3 x $10^6$ Cycles | 4 x $10^6$ Cycles | 5 x $10^6$ Cycles |
|---|---|---|---|---|---|
| **AZTA/CAL 1** | 1.198 | 0.668 | 0.518 | 0.464 | 0.589 |
| **AZTA/CAL 2** | 0.913 | 0.134 | 0.189 | 0.081 | *0.356 |
| **AZTA/CAL 3** | 0.851 | 0.345 | 0.263 | 0.565 | 0.246 |
| **CAL/CAL 1** | 3.383 | 1.198 | 1.998 | 0.881 | 0.761 |
| **CAL/CAL 2** | 5.144 | 3.437 | 1.496 | 0.949 | 1.275 |
| **CAL/CAL 3** | 3.436 | 1.501 | 0.975 | 0.457 | 0.812 |

Table 23: Incremental Volumetric Wear ($mm^3$), Heads plus Inserts.

The edge of insert CAL2 from AZTA/CAL2 was chipped on removal from the holder after 5 million cycles (marked by *). The weight of this insert was approximated by including the mass of the ceramic chip to determine the volume loss due to wear only.

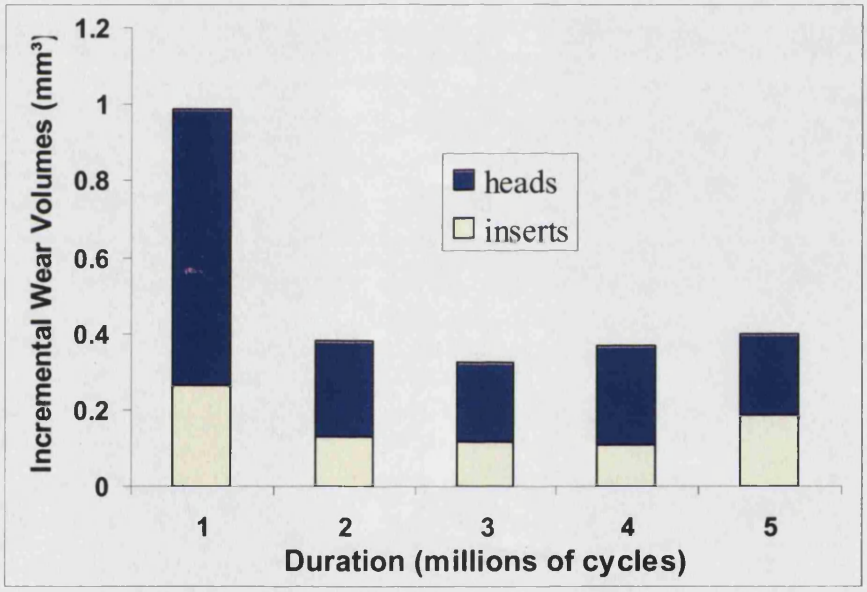


Figure 64 a: Average incremental volume losses of AZTA/CAL showing the contribution of head and insert

The average wear volume results in Figure 64 (a) above and Figure 64 (b) below clearly show significantly higher wear from the CAL/CAL compared to the CZTA/CAL, particularly during the first one million cycles.

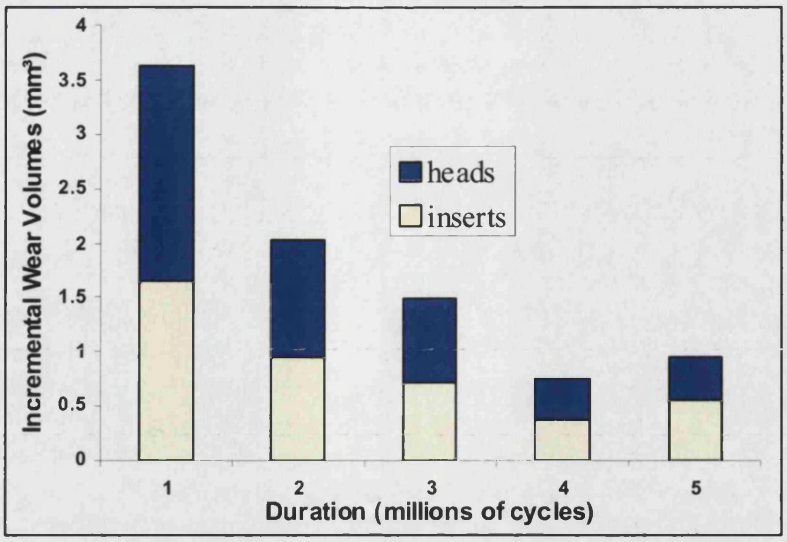


Figure 64 b: Average incremental volume losses of CAL/CAL showing the contribution of head and insert.

The proportion of wear from the heads and inserts is further summarised in Figure 65. The AZTA/CAL couples showed a greater percentage of wear on the heads (73%) compared to the CAL/CAL (55%) during the first 1 million cycles, a general trend which continued throughout the test.

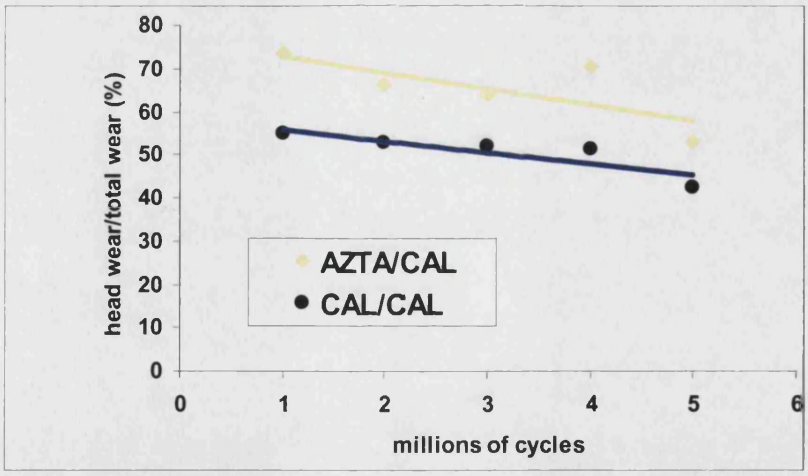


Figure 65: Percentage of wear from heads and inserts.

The incremental volumetric wear data from Table 23 is plotted in cumulative form as a line graph in Figure 66 below. The three CZTA/CAL pairs are shown as dashed lines, while the three CAL/CAL pairs are shown as solid lines. One of the CAL/CAL pairs dislocated at the

beginning of the study due to simulator malfunction (not included in Table 23). The dislocation caused localised intergranular fracture to the edge of the insert and severe stripe wear to the head. Both components were replaced and the test restarted.

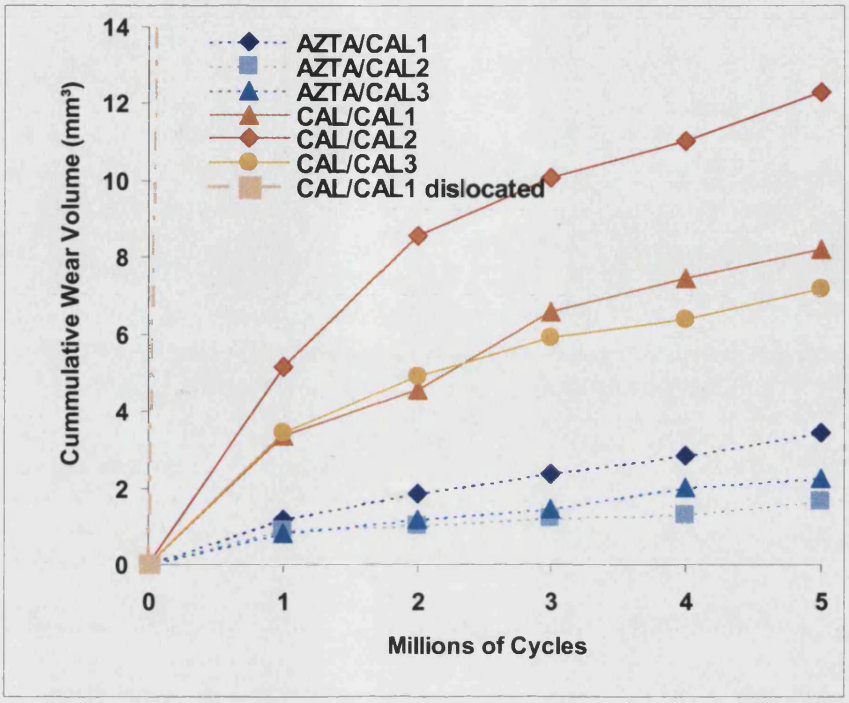


Figure 66: Cumulative Volumetric Wear of Articulating Pairs.

The spread of data from the CAL/CAL reflects the severity of the wear stripe, which formed on each femoral head and the corresponding wear on the rim of the insert. The three CZTA/CAL pairs displayed less damage and volume loss throughout the test duration.

The overall average wear of each material combination is further summarised in Figure 67.

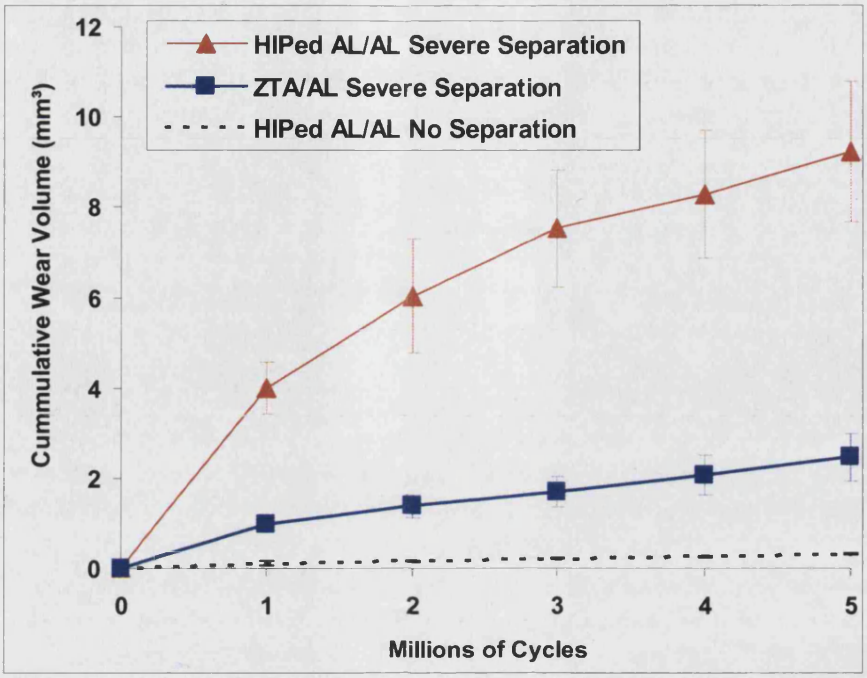


Figure 67: Average Cumulative Volumetric Wear ±standard error.

Surface Analysis

The severity of the damage to the surfaces caused because of rim contact during microseparation is best displayed visibly by rubbing the wear scars with a pencil as shown in Figure 68 (a and b).

Figure 68a: Wear stripes on the CAL/CAL components after 5 million cycles.

Figure 68 b: Wear stripes on the CZTA/CAL components after 5 million cycles.

The pencil rubbing revealed similar stripes in both CZTA and CAL heads, however, the severity of damage to the CAL/CAL is emphasised by the darkness of the stripes.

The surface damage to the components was evaluated using a Talysurf 5 surface profilometer for both the head and the insert with results listed in Table 24.

| | Femoral Head *Ra* (μm) | | Insert *Ra* (μm) |
|---|---|---|---|
| **Component** | **Contact** | **Stripe** | **Contact** |
| **AZTA/CAL1** | 0.0036 | 0.0588 | 0.0036 |
| **AZTA/CAL2** | 0.0042 | 0.0218 | 0.0033 |
| **AZTA/CAL3** | 0.0050 | 0.0804 | 0.0038 |
| **CAL/CAL1** | 0.0036 | 0.132 | 0.0034 |
| **CAL/CAL2** | 0.0044 | 0.0799 | 0.0054 |
| **CAL/CAL3** | 0.0040 | 0.0335 | 0.0040 |
| | | | |

Table 24. Component roughness after 5 million cycles.

Typical damage observed on the heads and inserts is shown in Figure 69 for the heads and inserts. While the depth/width of the head stripe can be measured with reasonable accuracy and confidence from the Talysurf trace, information from the worn rim is not as accurate due to differences in the curve fitting of the worn/unworn surfaces.

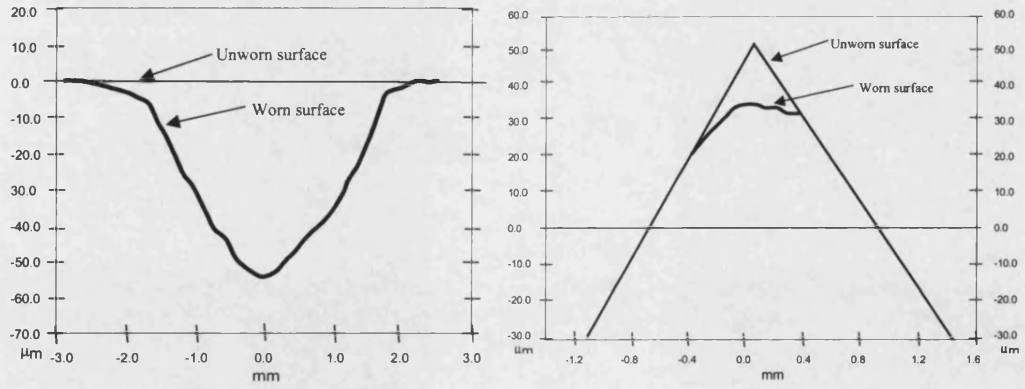


Figure 69: Typical stripe wear to the head (left) and rim (right).

Dimensions of the stripe areas are shown in Table 25 for reference.

| Component | Width (mm)±0.5 | Depth (μm)±10 |
|---|---|---|
| **AZTA/CAL1** | 4.5 | 53 |
| **AZTA/CAL2** | 6.0 | 17 |
| **AZTA/CAL3** | 4.0 | 43 |
| **CAL/CAL1** | 4.0 | 75 |
| **CAL/CAL2** | 6.0 | 130 |
| **CAL/CAL3** | 4.5 | 63 |

Table 25. Approximate femoral head stripe dimensions.

Stripe depth was deeper for the CAL/CAL, however the width was very similar to the AZTA/CAL.

Under SEM analysis the wear stripe for the AZTA also differed from the alumina stripe. There are areas of individual grain pullout as seen in Figure 70 outside the main stripe area however this time the pull out is of a much smaller dimension due to the smaller grain size.

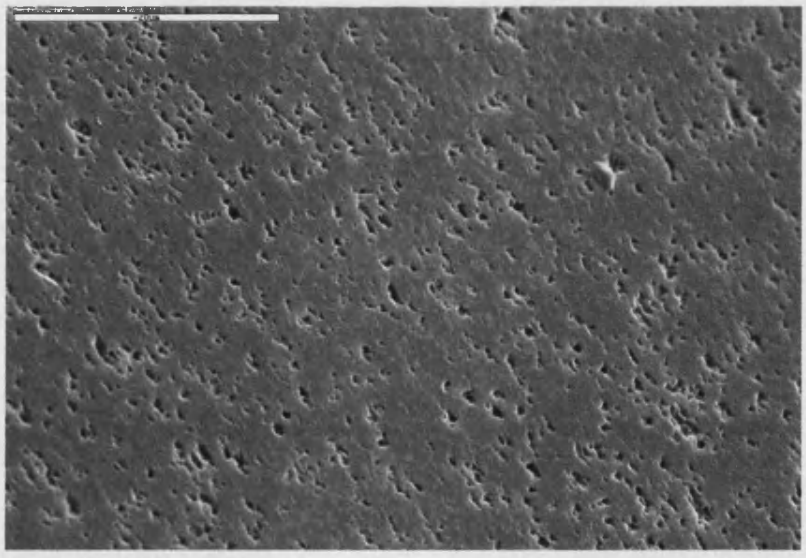

Figure 70: Grain pull out seen on AZTA heads outside stripe area.

Within the actual stripe wear area, the type of damage to the surface is also different to that reported for the alumina in study 1. Less evidence of intergranular fracture can be seen and the surface is made up of large areas of 'plastic deformation' suggesting more intragranular type failure, Figure 71 below.

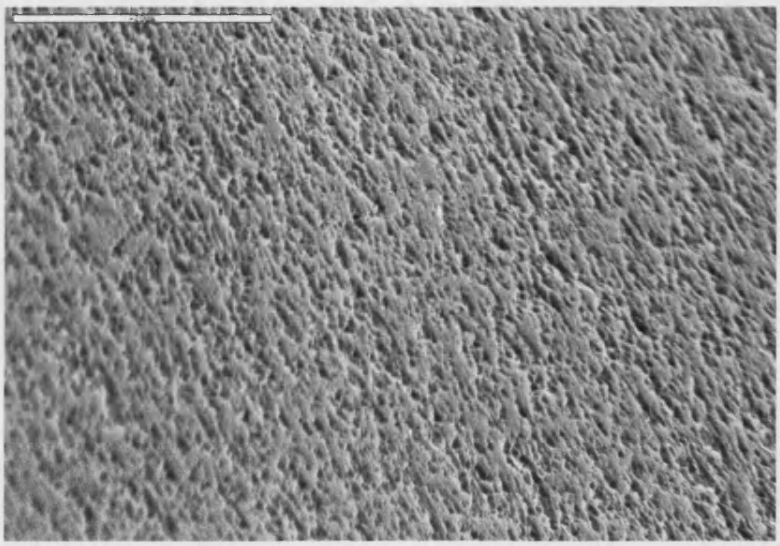

Figure 71: SEM of damage in stripe area of AZTA head.

Overall, the zirconia toughened alumina heads articulating against HIPed alumina inserts have shown a three-fold decrease in wear volume generated when compared to the HIPed alumina/alumina under severe microseparation conditions. All of the components tested in this study developed a significant stripe by 1 million cycles, marked by a noticeable increase in the wear volumes, as shown in Figure 72 below. The wear rate of the CZTA/CAL was 0.99 $mm^3$/million cycles during bedding-in which reduced to a lower steady-state wear of 0.37 $mm^3$/million cycles for the remainder of the study resulting in an overall average wear rate of 0.49 $mm^3$/million cycles. In comparison, the wear rate of the CAL/CAL was 4.0 $mm^3$/million cycles during bedding-in which reduced to a lower steady-state wear of 1.31 $mm^3$/million cycles for the remainder of the study resulting in an overall average wear rate of 1.85 $mm^3$/million cycles. No noticeable difference has been observed in the microseparation levels experienced by each couple and rotation of the couples to different stations produced no noticeable change.

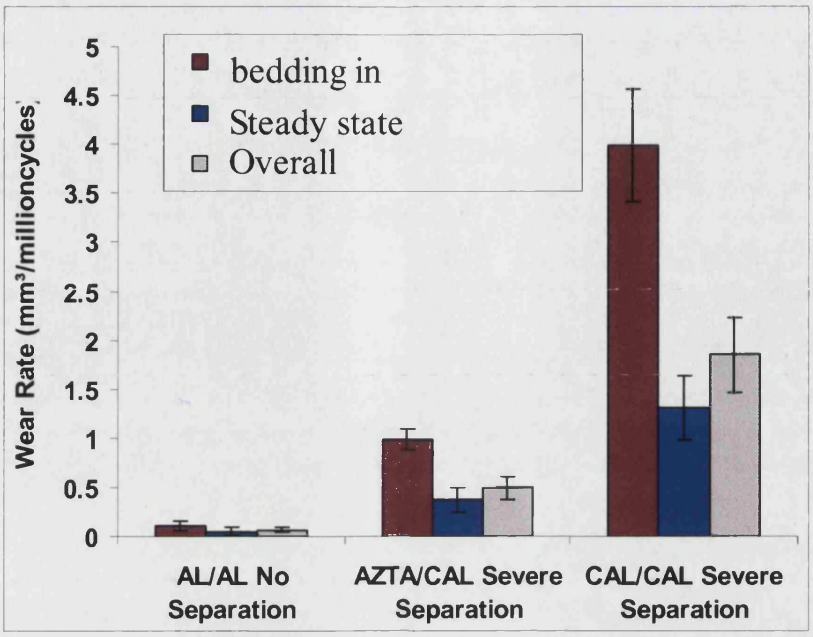


Figure 72: Overall Average Wear Rates.

The high wear resistance of the toughened alumina/normal alumina articulating couple may be due to the higher toughness of the zirconia toughened alumina head. Traditionally relative hardness between the articulating surfaces has been shown to be preferential in hard on hard bearings. Perhaps, for ceramics undergoing microseparation, a relative toughness may be beneficial between the materials. Nevertheless, the increased toughness and smaller grain size of the zirconia toughened alumina provided a greater resistance to intergranular fracture compared to the HIPed alumina and resulted in less wear to the acetabular insert.

### 4.8.3 Wear study 3.

Six pairs of components were tested in this study, three zirconia toughened alumina (ZTA) heads against ZTA inserts and three Zirconia heads against HIPed alumina inserts. The components are summarised in Table 25 for reference. The duration of the testing was set at 5 million cycles.

| Station | Heads - 28mm | Inserts - 28mm |
|---|---|---|
| 1-3<br>AZTA/CZTA | CeramTec<br>Zirconia<br>Toughened<br>Alumina | CeramTec<br>Zirconia<br>Toughened<br>Alumina |
| 4-6<br>ZR/CAL | Norton<br>Demarquest<br>Zirconia | CeramTec<br>HIPed Alumina |

Table 25: Component bearing combinations

The durability of the materials was evaluated based on the weight loss and surface analysis of the components.

Gravimetric Analysis

Gravimetric results for each increment of the 5 million cycle test duration are presented in table 26 as wear volumes. The average results for each material are further presented in bar chart format in Figures 74a to 74b.

| Component ID | 1 x $10^6$ Cycles | 2 x $10^6$ Cycles | 3 x $10^6$ Cycles | 4 x $10^6$ Cycles | 5 x $10^6$ Cycles |
|---|---|---|---|---|---|
| AZTA/AZTA1 | 0.719 | 0.456 | 0.280 | 0.015 | 0.077 |
| AZTA/AZTA2 | 0.043 | 0.037 | 0.070 | 0.018 | 0.055 |
| AZTA/AZTA3 | 0.197 | 0.129 | 0.273 | 0.003 | 0.047 |
| NZR/CAL1 | 18.219 | 13.540 | 8.462 | 4.107 | 1.281 |
| NZR/CAL2 | 10.239 | 2.942 | 0.565 cup fracture | 0.000 | 0.000 |
| NZR/CAL3 | 3.962 | 3.827 | 1.475 | 0.000 head fracture | 0.000 |

Table 26: Incremental volumetric wear ($mm^3$), heads plus inserts.

Insert CAL2 was cracked during testing and fractured on removal. Head NZR3 fractured while testing at ~3.3 million cycles. Average values are taken from remaining components where applicable, however, error bars are not used where the number of samples was below three.

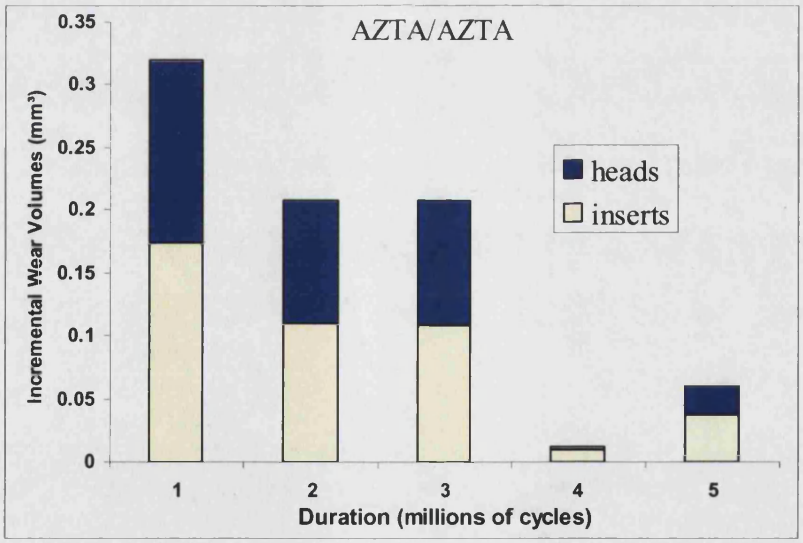


Figure 74a: Average incremental volume losses of CZTA/CZTA showing the contribution of head and insert.

The average wear volume results in Figure 74a and b clearly show significantly higher wear from the NZR/CAL compared to the AZTA/AZTA, throughout the test duration.

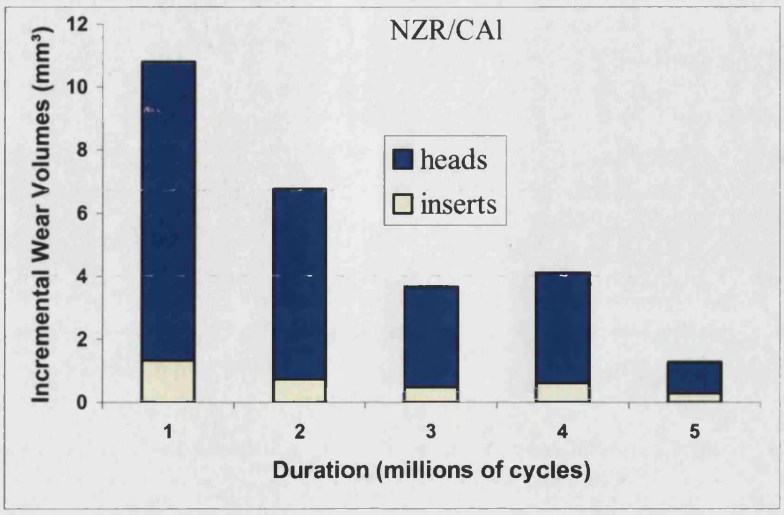


Figure 74b: Average incremental volume losses of NZR/CAL showing the contribution of head and insert.

The proportion of wear from the heads and inserts is further summarised in Figure 75. The NZR/CAL couples showed a greater percentage wear on the heads (~90%) compared to the CZTA/CZTA (~50%) during the first 1 million cycles, a general trend which continued throughout the test.

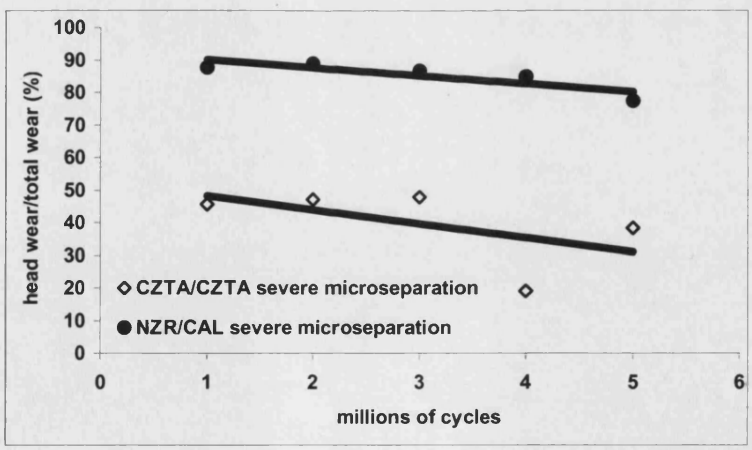


Figure 75: Percentage of wear from heads and inserts.

The incremental volumetric wear data from table 26 is plotted in cumulative form as a line graph in Figure 76 below. The three CZTA/CZTA pairs are shown as dashed lines, while the three NZR/CAL pairs are shown as solid lines.

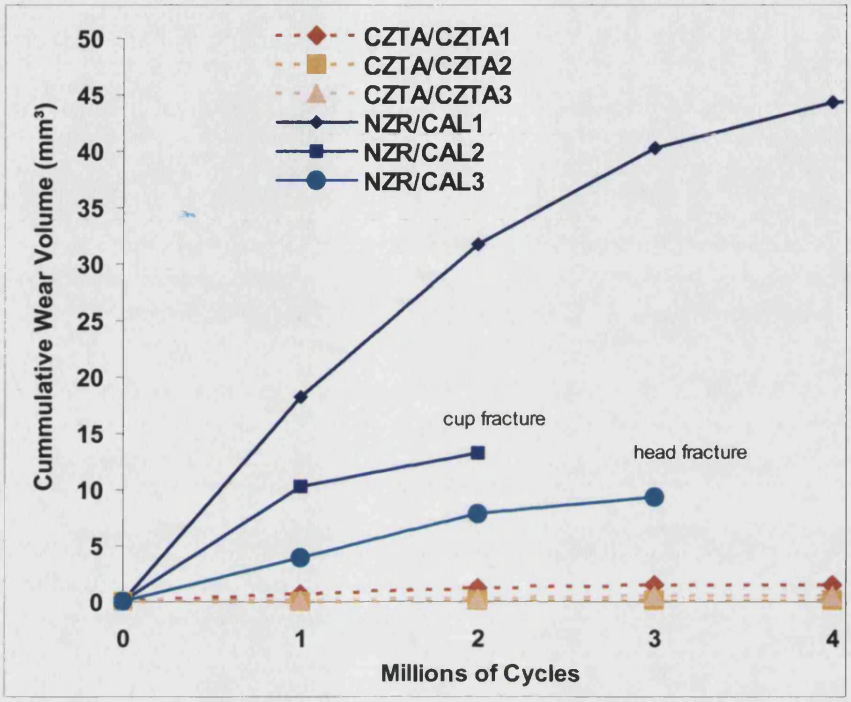


Figure 76: Cumulative Volumetric Wear of Articulating Pairs.

The spread of data from the NZR/CAL reflects the severity of the wear stripe, which formed on each femoral head and the corresponding wear on the rim of the insert. The three CZTA/CZTA pairs displayed less damage and volume loss throughout the test duration. The overall average wear of each material combination is further summarised in Figure 78.

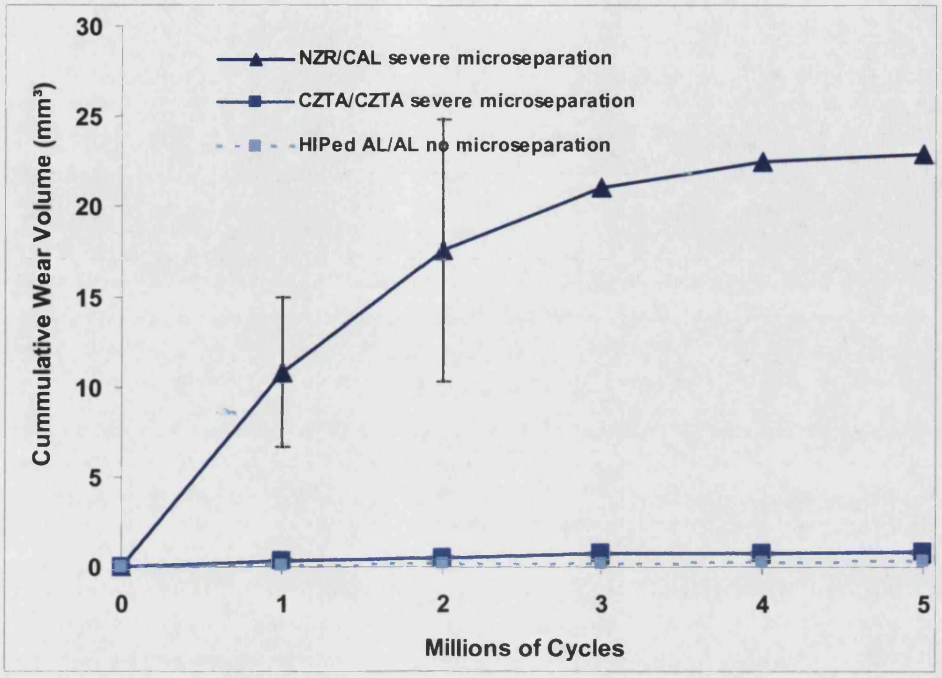


Figure 78: Average cumulative volumetric wear ±standard error.

Surface Analysis

The severity of the damage to the surfaces caused by rim contact during microseparation is best displayed visually by rubbing the visibly worn area with a pencil as shown in Figure 79 a and b.


Figure 79a: Wear stripes on the NZR/CAL components after 5 million cycles.


Figure 79 b: Wear stripes on the CZTA/CZTA components after 5 million cycles.

The pencil rubbing revealed only mild stripe wear to the CZTA heads, however, the severity of damage to the NZR is unmistakable.

In the as-received condition the *Ra* of the components was generally <0.005μm. The surface damage to the components was evaluated using a Talysurf 5 surface profilometer for both the head and the insert with results listed in Table 27.

| | Femoral Head *Ra* (μm) | | Insert *Ra* (μm) |
|---|---|---|---|
| **Component** | **Contact** | **Stripe** | **Contact** |
| **AZTA/AZTA1** | 0.0046 | 0.0266 | 0.0046 |
| **AZTA/AZTA2** | 0.0042 | 0.0226 | 0.0046 |
| **AZTA/AZTA3** | 0.0043 | 0.0103 | 0.0042 |
| **NZR/CAL1** | 0.0080 | 8.5095 | 0.0050 |
| **NZR/CAL2 *** | 0.0087 | 1.4506 | 0.0033 |
| **NZR/CAL3 *** | 0.0110 | 0.1607 | 0.0046 |

Note * component fracture 3m cycles

Table 27. Component roughness after 5 million cycles.

The average roughness (*Ra*) of the damaged AZTA heads was similar to that previously found in study2. R*a* measurements were not possible for the worn areas on the insert rims. The roughness of the NZR heads increased up to a value of 8 μm for *Ra* in the stripe area.

The depth/width of the head stripe can be measured with reasonable accuracy and confidence from the Talysurf trace, information from the worn rim is not as accurate to due to differences in the curve fitting of the worn/unworn surfaces. The dimensions of the stripe areas are shown in Table 28 for reference.

| Component | Width (mm)±0.5 | Depth (μm)±10 |
|---|---|---|
| **AZTA/AZTA** | | |
| **AZTA/AZTA1** | 5.0 | 16.5 |
| **AZTA/AZTA2** | 4.5 | 1.5 |
| **AZTA/AZTA2** | 4.0 | 8.5 |
| **NZR/CAL** | | |
| **NZR/CAL1** | 8.0 | 350 |
| **NZR/CAL2** | 5.0 | 125 |
| **NZR/CAL3** | 7.0 | 130 |

Table 28: Approximate femoral head stripe dimensions at 5 million cycles.

It can be seen that the stripe depth and width were significantly greater for the NZR/CAL, samples. SEM analysis reveals the scars to be similar to those seen on AZTA heads analysed in wear study two. Individual grain pull-out can be seen just outside the scars, Figure 80, with the interior of the scar showing extensive removal of the polished layer, Figure 81.

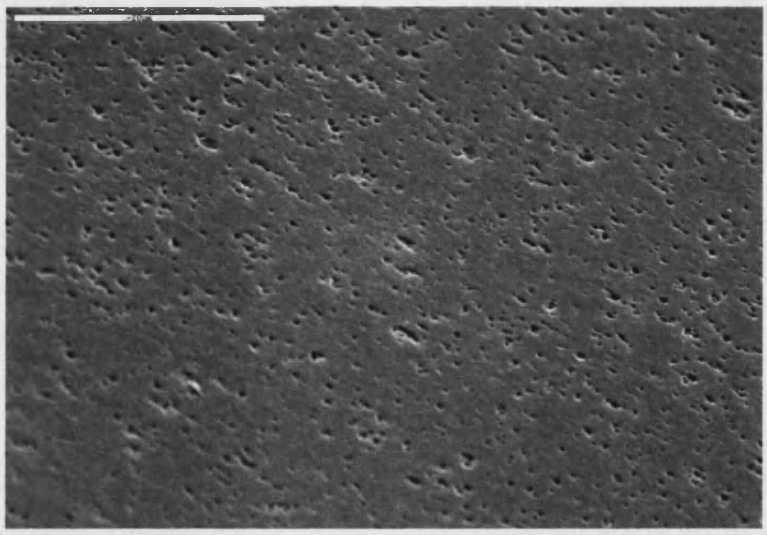

Figure 80: Grain pull out seen on AZTA heads outside stripe area.

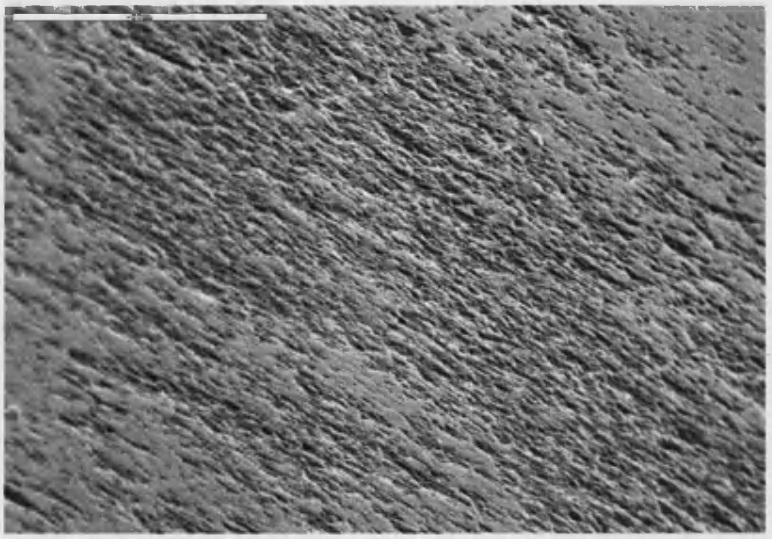

Figure 81. SEM of damage in stripe area of AZTA head.

Overall, the zirconia toughened alumina heads articulating against zirconia toughened alumina inserts have shown a ten fold decrease in wear volume generated compared to previously tested HIPed alumina/alumina under the same severe microseparation conditions. All of the components tested in this study developed a significant stripe by one million cycles, marked by a noticeable increase in the wear volumes, as shown in Figure 82. The wear rate of the AZTA/AZTA was 0.32 $mm^3$/million cycles during bedding-in which reduced to a lower steady-state wear of 0.12 $mm^3$/million cycles for the remainder of the study, resulting in an overall average wear rate of 0.16 $mm^3$/million cycles. In comparison, the wear rate of the NZR/CAL was 10.8 $mm^3$/million cycles during bedding-in which reduced to a lower steady-state wear of 3.9 $mm^3$/million cycles for the remainder of the study resulting in an overall average wear rate of 5.3 $mm^3$/million cycles. No noticeable difference has been observed in the microseparation levels experienced by each couple and rotation of the couples to different stations produced no noticeable change.

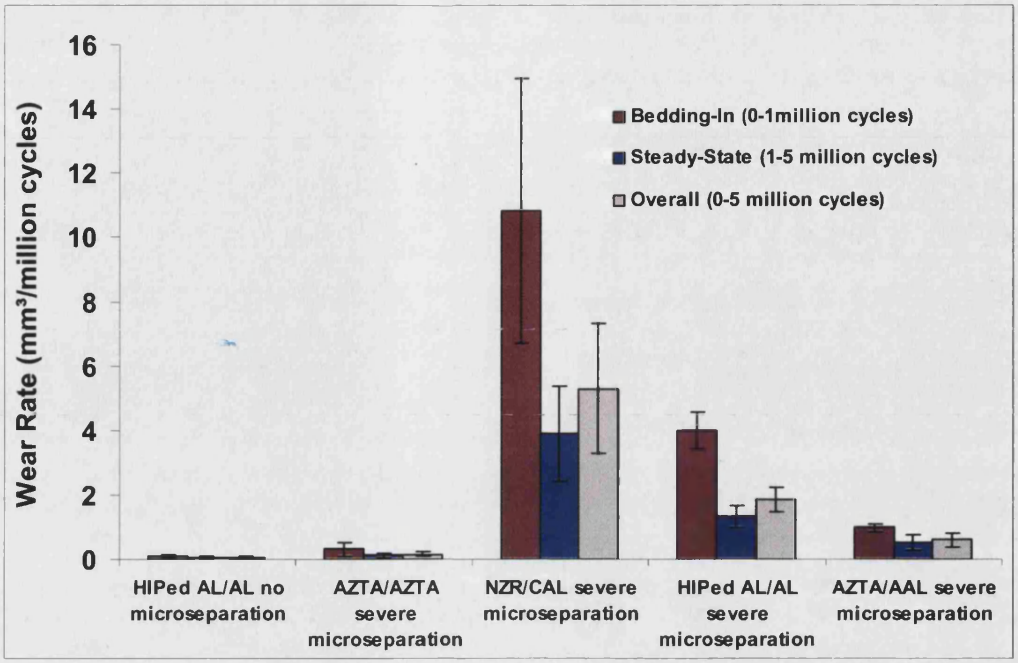


Figure 82: Average wear rates of severe microseparation studies.

The high wear resistance of the toughened alumina/toughened alumina articulating couple may be due to the higher toughness of the zirconia toughened alumina material as seen previously in study 2 with zirconia toughened alumina against HIPed alumina. With increased toughness and smaller grain size the zirconia toughened alumina may provide a greater resistance to intergranular fracture when compared to the HIPed alumina.

The poor wear resistance of the zirconia/HIPed alumina articulating couple was not surprising when compared to other reported wear simulator studies for this couple and Zr/Zr. When the simulator operates under normal simulator conditions, i.e. protein lubricant and standard articulation, this bearing couple shows remarkable wear performance. However, when any abnormal conditions are applied such as protein deficient lubrication, the wear rate of this bearing increases to extremely high levels. It is suggested that the abnormal separation during the walking cycle has put high point contact loads on the zirconia and this coupled with a lack of lubrication at this point has lead to the extremely high wear rates.

# 5.0 Clinical results

## 5.1 Introduction

It is not often in orthopaedic research that clinically used materials are made available for analysis. During the course of this research, just such an opportunity presented itself. Sixteen explanted ceramic-on-ceramic alumina bearings were made available for analysis.

The ceramics were part of a larger series of more than 1500 successful implants done by mainly one surgeon at The Orthopaedic Hospital Sydney, Australia. The majority of the bearings were removed during a routine re-operation for a variety of clinical conditions such as Psoas tendonitis, periprosthetic fracture and infection. The surgeon noticed that the surface of the heads had a slight loss of polish in some areas and this coincided with a similar mark on the cup. These areas were termed wear scars and the components were sent to Stryker for analysis.

The objective of the analysis was to characterize the wear scars in terms of their extent and the material failure mechanism that led to their formation and then determine if this was similar to the stripe wear seen from microseparation in the hip simulator studies.

## 5.2 Methods.

Sixteen explanted alumina-alumina couples were analysed in this study. Eleven components had evidence of wear scars (11 heads and 8 liners). The remaining components, which showed no wear scars, were used as controls. table 29 below, outlines all the components coded with the patient's initials along with all the relevant clinical data. Pre-revision x-rays were also available for analysis for all patients. The following dimensional and angular measurements of the scars were carried out to correlate the data with the available clinical information:

On the heads:

- the length of the scars and their maximum width,
- the latitude angle of the centre of the scar relative to the head equator ('inclination' angle, Figure 83 (a)).

- the angle of the long axis of the scar to a line of latitude running through the centre of the scar ('tilt' angle, Figure 83 (b)).

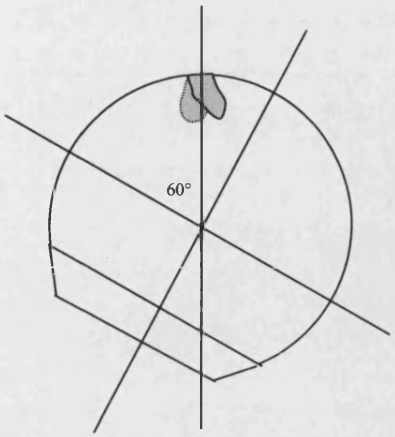


Figure 83 (a). Latitude angle of scar.

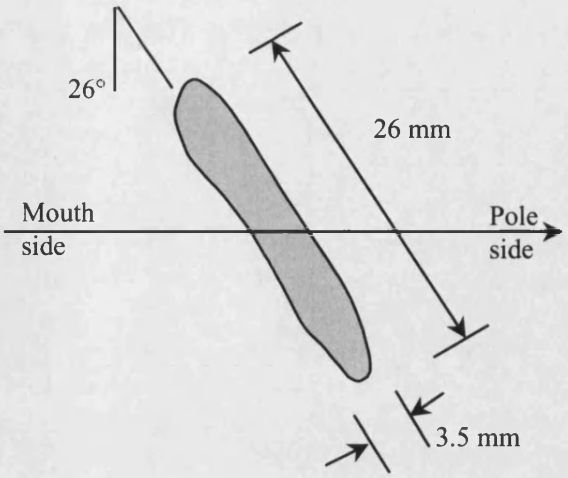


Figure 83 (b). Tilt angle of scar.

On the cups:

- The circumferential length of the scars and their maximum width.

These measurements were made visually using a ruler and protractor, and are thus somewhat subjective, especially on the cups. This is because the ends of the scars on the cups were not well defined. The obvious visual scar highlighted with ink was often significantly extended in both directions when viewed under a microscope. Therefore, only the size of the principal visual scar area is reported.

| Code | Months to revision | Wear scar | Reason for revision | Age | Sex | Weight, kg | Height, cm | Side | Cup incl., ° |
|---|---|---|---|---|---|---|---|---|---|
| DM | 18.0 | Y | Recurrent dislocation | 53 | M | 103 | 175 | L | 50 |
| ES | 2.5 | Y | Periprosthetic fracture, femur | 77 | F | 55 | 160 | R | 53 |
| GM | 18.6 | Y | Periprosthetic fracture, femur | 79 | F | 70 | 170 | L | 50 |
| JR | 12.3 | Y | Infection | 63 | M | 82 | 175 | R | 46 |
| MT | 6.0 | Y | Periprosthetic fracture, femur | 71 | F | 68 | 168 | L | 50 |
| RH | 8.2 | Y | Periprosthetic fracture, femur | 56 | F | 82 | 180 | L | 50 |
| SC1 | 32.9 | Y | Psoas tendonitis | 47 | F | 57 | 158 | R | 53 |
| SC2 | 10.3 | Y | Psoas tendonitis | 50 | F | 57 | 158 | R | 53 |
| TB | 34.1 | Y | Psoas tendonitis | 33 | F | 65 | 165 | R | 47 |
| WF | 32.4 | Y | Psoas tendonitis | 75 | M | 65 | 168 | L | ? |
| YP | 30.8 | Y | Infection | 67 | F | 86 | 175 | L | 49 |
| CA | 30.4 | N | Psoas tendonitis | 55 | F | 68 | 170 | R | 43 |
| DJ | 27.4 | N | Psoas tendonitis | 57 | F | 65 | 170 | L | 52 |
| JH | 10 | N | | | M | | | | |
| KB | 1.8 | N | Dislocation | 77 | M | 78 | 178 | R | 41 |
| PJ | 11.1 | N | Periprosthetic fracture, femur | 62 | F | 59 | 149 | R | 43 |

Table 29: Clinical data on explanted ceramic hip systems.

For examination at higher magnification, a conventional optical microscope was used. The principal problem was the curved surface to be examined. This resulted in variable illumination and focus over the field of view. To minimise this it was essential to

position the feature to be observed at the exact summit of the head surface. This was achieved by placing the head on a brass-loading ring used for mechanical testing of heads, which allowed the head to be rotated under the microscope without lateral movement of the summit. Various lenses were used to image the scars. Optical examination of cups proved problematical. It was impossible to obtain normal or near normal access to the wear scars with conventional lenses, so it was not possible to use direct reflection to illuminate scratches and other features within the scars. The small depth of field limited the value of photography at shallower angles.

For scanning electron microscopy, a small number of representative examples were chosen. The heads were mounted mouth down on the SEM stub using graphite adhesive, and the area of interest was lightly sputter-coated with gold/palladium to provide conductivity.

## 5.3 Results

It was immediately clear that a great variety of sizes and shapes of scar were found amongst the examined group.

| Patient | Cup Scar | | Head Scar | | | |
|---|---|---|---|---|---|---|
| | Length, mm. | Width, mm. | Length, mm. | Width, mm. | Tilt angle | Latitude |
| TB | 50 | 8 | 32 | 15 | 15 | 60 |
| SC1 | 33 | 4 | 25 | 8.5 | 15 | 36 |
| WF | - | - | 30 | 10 | 35 | 60 |
| YP | 35 | 6 | 30 | 14 | 30 | 45 |
| GM | - | - | 5 | 3 | 10 | 41 |
| DM | 15 | 1 | 10 | 7 | 12 | 35 |
| SC2 | 22 | 1.2 | 13.5 | 6 | 20 | 85 |
| RH | 30 | 1.5 | 16 | 2.8 | 16 | 30 |
| MT | 15 | 1 | 12 | 4 | 17 | 58 |
| JR | 35 | 4 | 36 | 10 | 2 | 0 |
| ES | - | - | 13 | 3 | 5 | 15 |

Table 30: Summary of head and cup scar measurements.

The following features appeared to be common to all explanted heads and cups showing localised wear scars:

- The worn areas on the heads are usually well defined with sharp boundaries, especially at the ends and on the trunnion side of the scar, Figure 84 (b). There tended to be more damage outside the main scar on the pole side than on the trunnion side, Figure 84 (c).

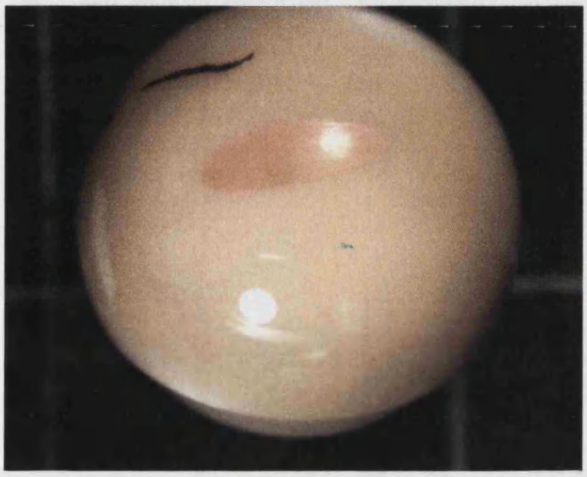

Figure 84 (a): Macro Picture of scar.

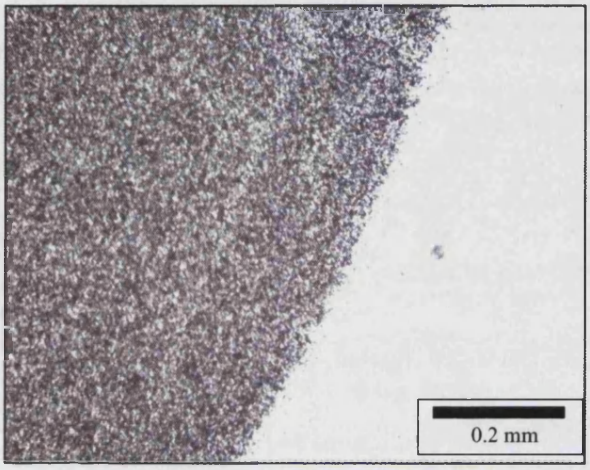


Figure 84 (b): Micrograph of well-defined Boundary

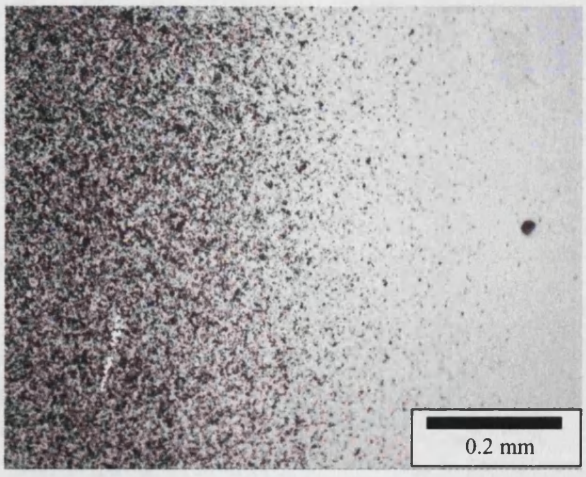


Figure 84 (c): Micrograph of more diffuse boundary on pole side of the scar.

- The worn areas on the cups were lens-shaped, generally narrower than on the matching head, and were usually located along the 'blend' line between the highly

polished hemispherical bearing surface and the less well-polished convexly curved chamfer near the cup edge, Figure 85 (a). In a number of cases, it was apparent that a very narrow scar existed over an extended length of the blend line outside the main lens-shaped scar, in one or both directions. In extreme cases, the scar was found to extend beyond this convexly curved region onto the conical chamfer region, along the outer blend line, Figure 85 (b).

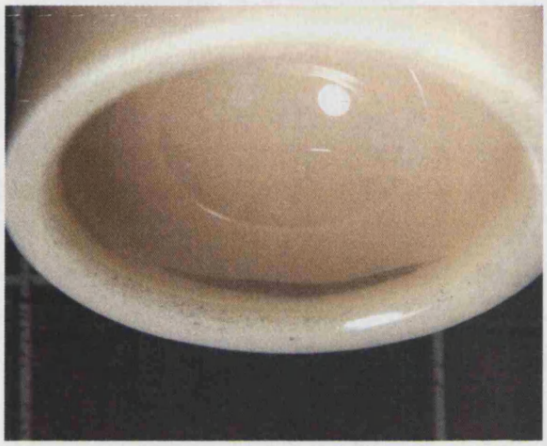

Figure 85 (a): Macrograph of narrow scar.

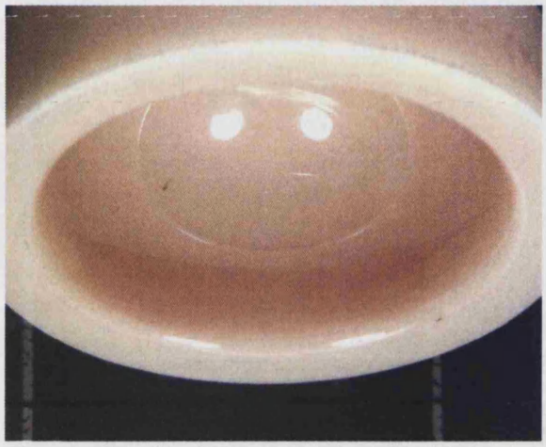

Figure 85 (b): Macrograph of wide scar.

- The lengths of the worn areas on the head and cup are similar, and increase in size with implantation time (Figure 86), suggesting that the initial non-conforming contact of the head on the cup rim becomes conforming with time and/or number of cycles of movement.

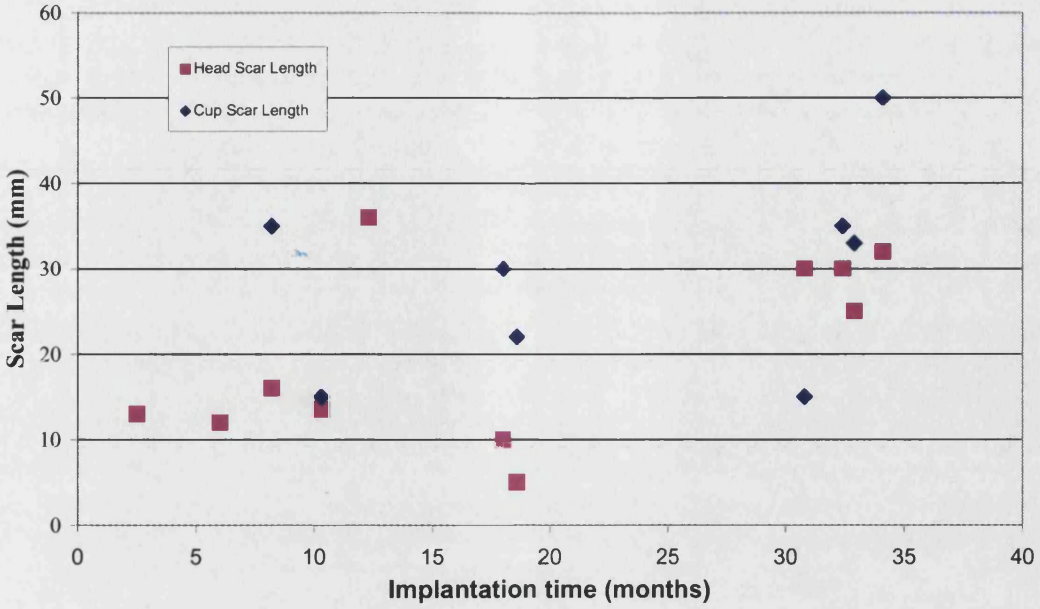


Figure 86: Correlation between wear scar length and implantation time.

- Under optical examination, the head scars appeared to comprise a high density of pits where grains had been removed. In the main scar area, the pits covered most of the surface and often there were signs that the original pitting was being re-polished by subsequent, more benign, wear processes almost like a 'wearing-in'.
- Both heads and cups exhibited scratches in the form of lines of pits both within and outside the main scar areas. Scratches were most prevalent on badly worn components. These could be parallel to the length of the scars, and/or at a steep angle across them. They were often in parallel sets, Figure 87 below.

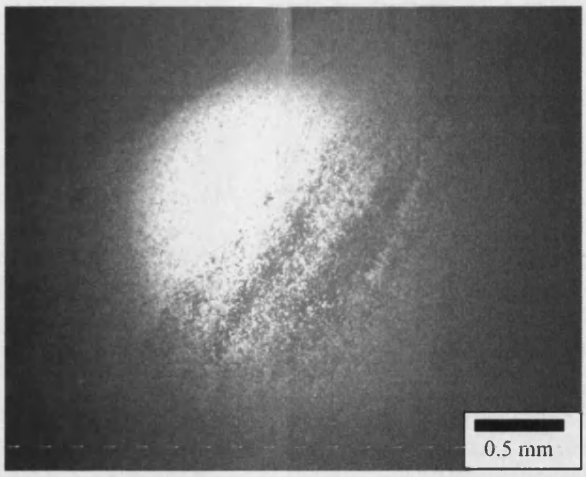


Figure 87: Micrograph of parallel sets of scratches within wear scar.

- There was a wide variation in the tilt angle of the scar to the lines of latitude on the head. Generally, the direction correlated with whether the implant was on the patient's left or right side. All scars showed a tilt direction that was retroverted i.e. tilting backwards in respect to the body.

- There was also a wide variation in inclination angle of the head scars to the head equator, from 0° to 60°.

- On the explanted heads, which showed no obvious wear scars; close examination revealed slight pitting and grain relief in the region of the pole where the maximum contact pressure would tend to be, and an absence of the scratching and intense pitting seen in the scarred heads.

The following components were examined: ES head, TB head, CA head, SC head, SC cup, and T4C5 simulator head and cup. Images obtained are shown in Figures 88 to 95, and are explained in the legends. The overriding feature of the scars is that they all comprised clear grain pluck-out with clear facetted sides to the remaining pits. In some cases, there was evidence of subsequent smoothing over of the surface, almost a partial re-polishing of the surface, with some fine-scale debris being trapped in the pits

Images of the pole area of the CA head (Figure 92), which did not have a scar, were taken as representative of 'normal' wear. In addition to the appearance of some pits not normally present in an as-received head, there is clear relief polishing showing that some slight wear is taking place at different rates in different grains. This is generally taken as being a result of crystallographic anisotropy of hardness.

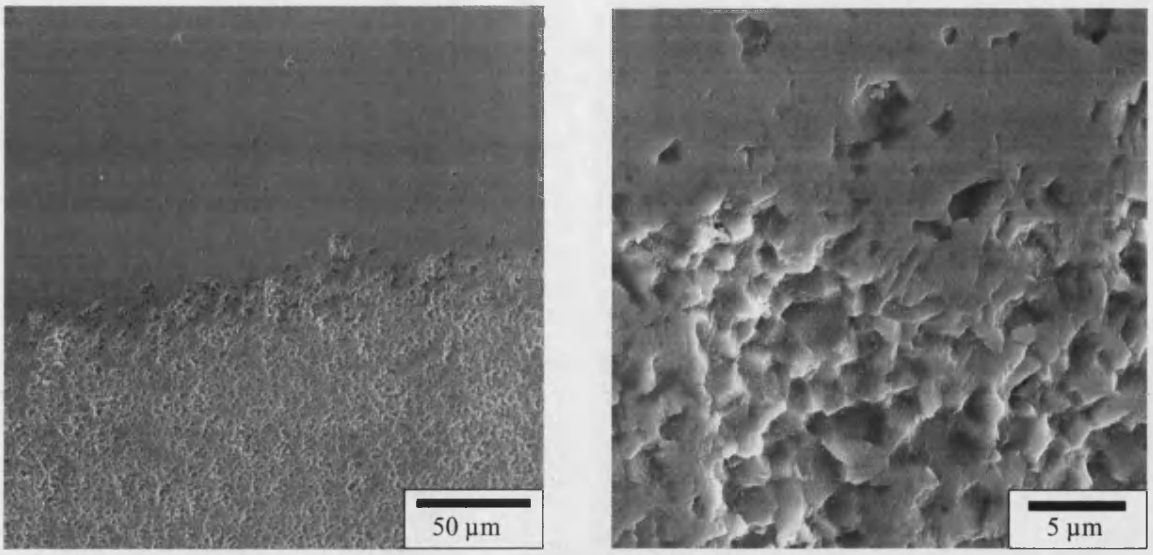


(a) (b)

Figure 88: ES head scar centre showing a distinct boundary to the scarred area.

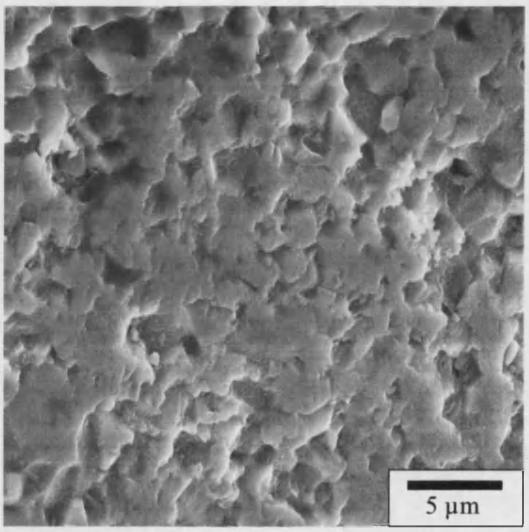


Figure 89: ES head scar centre region showing re-polished area with partially filled pits.

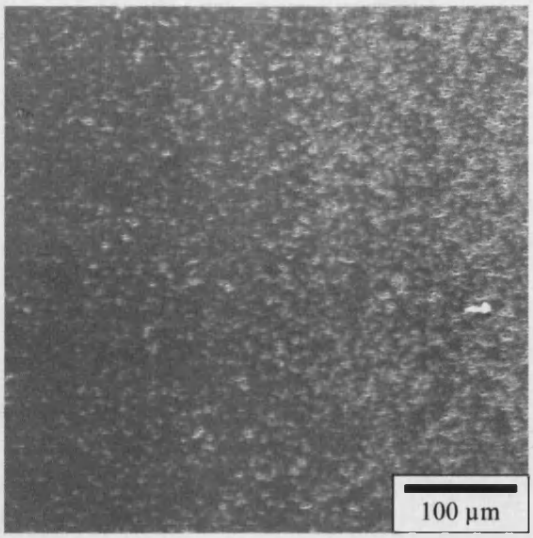


Figure 90: TB head, pole side of scar showing indistinct boundary.

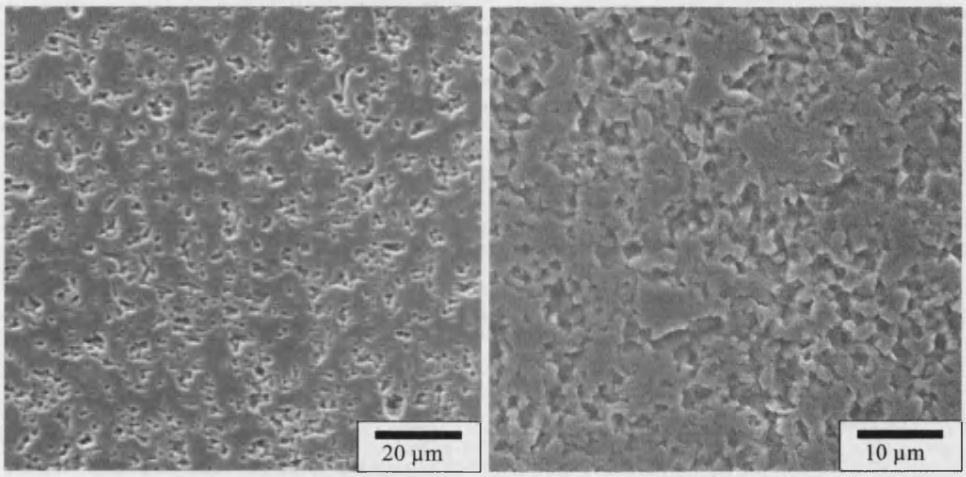


(a) (b)

Figure 91: TB head (a) near centre of scar, showing semi-polished appearance, and (b) near end of scar showing deeper pitting and fresher appearance.

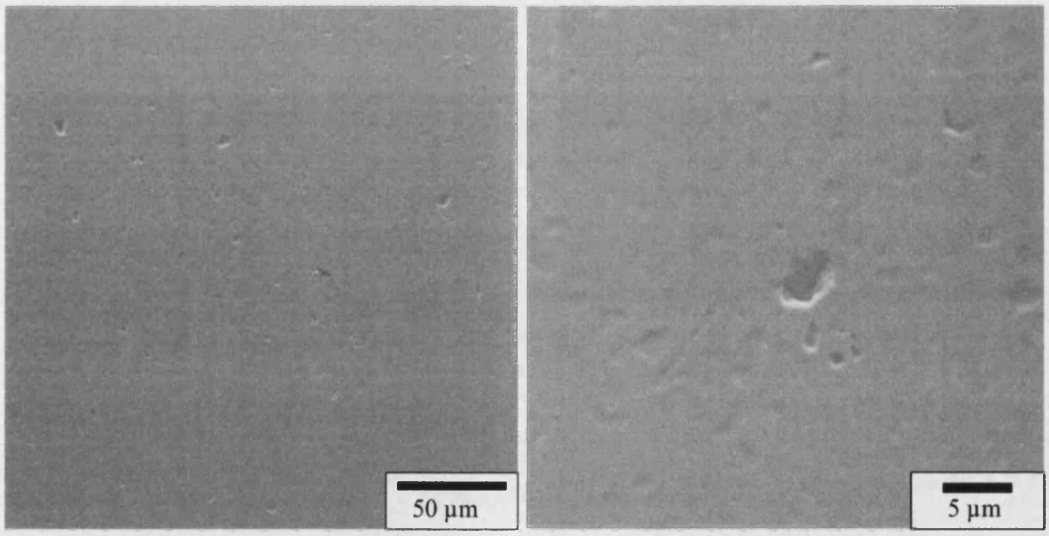


(a) (b)

Figure 92: CA head showing (a) low magnification view of the pole area with minor pitting, and (b) higher magnification image showing additionally some relief polishing of individual alumina grains.

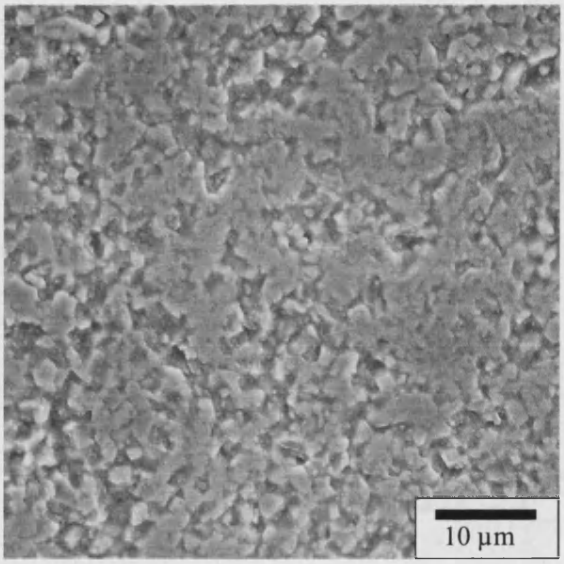


Figure 93: SC head, centre of scar, showing pitting and partial re-polishing, with some evidence of fine-scale debris within the pits.

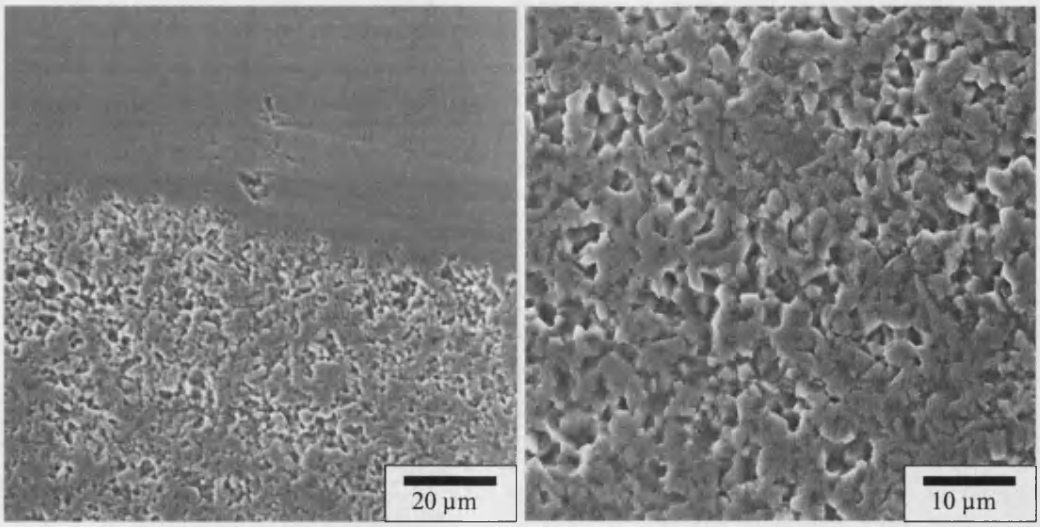


(a) (b)

Figure 94 SC cup (a) showing inner boundary of wear scar with some plastic grooving in the polished area (the banding evident in the top half of this image is due to charging in the SEM) and (b) central region of the scar with clear pitting and evidence of re-polishing.

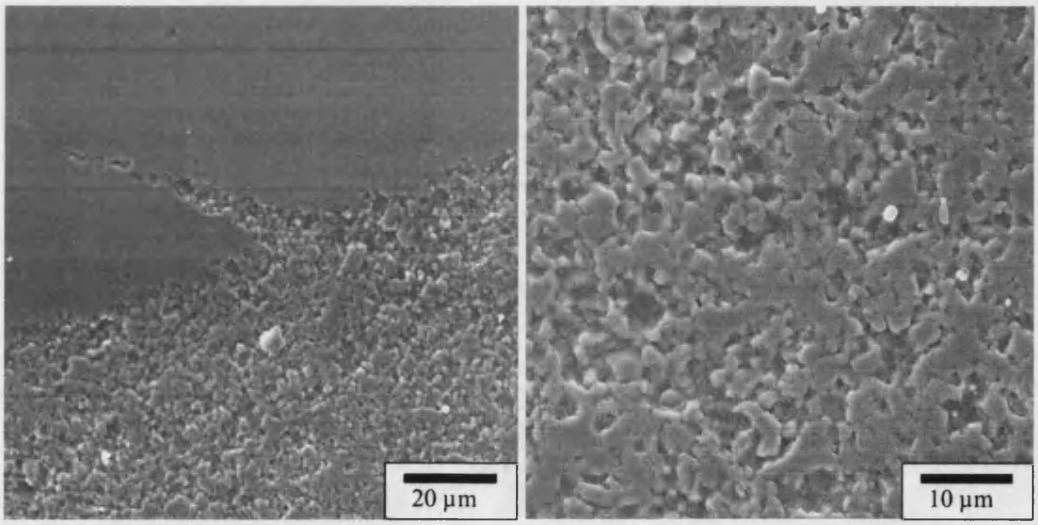


(a) (b)

Figure 95: Leeds T4C5 simulator head showing (a) the pole side boundary of the scar with a scratch and (b) the scar centre with evidence of re-polishing.

## 5.4 DISCUSSION

On analysis of the clinical information available on these components, three distinct groupings are apparent:

- heads and cups that were clinically stable and showed no stripe wear (6)
- heads and cups that were clinically stable (well fixed) and showed stripe wear (12)
- heads and cups that were not clinically stable (subsided femoral component) and showed stripe wear (2).

All wear scars had a tilt angle that was retroverted i.e. the scar sloped backwards when positioned in the body. However, the stable implants were more retroverted than the unstable components, 18.8° ±8.31 and 3.5°±2.1. The stable explants had a higher latitude measurement i.e. the scar was closer to the pole than the equator of the head, 50.1°±17.3 as opposed to 7.5°±10.4 for the unstable implants.

It was obvious when the stable heads and cups were physically brought together in the laboratory that the wear scar on the heads did not match the wear scar on the cups in terms of position. In fact, they run 90 degrees perpendicular to each other. The only way the wear scars line up, on these implants, is if the head is turned through 90 degrees, which equates to the patient being in a sitting position or steep stair climb. Therefore this type of stripe was not formed during the walking cycle as proposed but occurred at the moment the force is applied through the hip joint as the patient goes from a sitting to a standing position.

The two components with the lower tilt and latitude angles did in fact match with the heel strike theory and the scars match up with each other when the leg is at about the degree of flexion for heel strike. These components had subsided by up to two centimetres and there was clearly a lot of laxity in the joint. One of the surgeon's notes for one of these patients talked about a clicking sound being heard as the patient was walking.

On examination of the wear mechanisms an number of features were observed. The pitting type of wear, followed later by a smoothing process, is typical of highly localised contacts occurring initially between the head and cup rim over a localised area. As these contacts conform geometrically with increasing size of the scar, the wear process becomes less severe, and can even lead to partial re-polishing. The initial intense process seems to consist of individual grain 'pluck-out', followed later by groups of unsupported grains breaking away. It is thought that in the latter case this may cause the scratching to occur, as some will be trapped between the head and cup and will be dragged into the bearing surface by the relocation movement, becoming reduced in size in the process and eventually disappearing. The swinging movement of the head in the cup would tend to cause these scratches to be diagonal to the main scar length, which seems to correspond to the respective relocation contact zones of head on cup. They are in most cases quite short, suggesting the relocation movement may only be a fraction of a millimetre.

The SEM examination of representative components confirms the granular nature of the 'pop-out' and further, that under more benign conditions later in the process, some re-polishing of the pitted surface can occur, with some material partly filling the residual pits in an otherwise 'plateau-polished' surface. In addition, away from the main scar area towards the pole of the heads, relief polishing of individual grains in the head surface shows that a slow, so-called 'mild' wear mechanism is the normal process occurring here. Such regions do not seem badly affected by debris from the scarring process near the cup rim. No profilometry was conducted as part of this study, but this would be required to prove that re-polishing of worn areas was occurring.

It is possible that much of the debris from the edge impact process does not end up on the bearing surface but remains outside the joint, pumped out by the relocation process. This may account for the minimal damage to the main load-bearing contact areas during walking.

The heads from the hip simulator trials, Figure 95, showed similar damage to the clinical heads, with massive grain pull-out and some re-polishing observed. The depths of the simulator trial scars were visibly deeper than the clinically produced scars, which would indicate that this clinical microseparation does not occur in every single patient activity.

This analysis has been extremely useful for correlating the *in-vivo* wear scars with those obtained from the hip simulator trials with microseparation. The wear scars were similar

in terms of appearance, size and shape but were different in terms of orientation and depth indicating a different mechanism of formation. Two of the clinical heads matched very well with the heel strike theory however the remainder were clearly formed during the sitting to standing activity of the patients. There has been no other reported analysis of explanted heads as detailed as this and these results will be essential in further improving the way we test future candidate bearing materials.

# 6.0 Discussion

## 6.1 Introduction

The objectives of this research were clearly defined, namely to increase the fracture resistance and strength of orthopaedic grade alumina without compromising its high hardness and stability. This would result in real benefits in terms of improved implant lifetime and outcomes for the patient. Zirconia toughened alumina was proposed as a material that would be successful in achieving this goal. The focus of this work has been the investigation of this material for application as a biomedical grade bearing material.

In order to achieve this, the optimum material composition was selected and then fabricated into test samples and hip ball heads for characterisation using standard and novel test methods. These results have been presented and now the discussion will concentrate on analysing these results in the context of the objectives.

## 6.2 Mechanical properties of ZTA ceramics.

### 6.2.1 Microstructure.

In order to understand the mechanical properties of ceramic materials it is essential to go back to first principles and fully characterise the building blocks or foundations of the ceramic – the microstructure.

The starting powders used and the processing methods employed to fabricate the ceramic will affect the type, size and dispersion of the grains in the ceramic microstructure.

Two candidate ZTA materials were characterised for this research. The first a commercially available material, AZTA consisted of 24 wt.% Y-PSZ in a 75 wt.% alumina matrix with an addition of 0.3wt.% chromium oxide and 0.8 wt.% strontium oxide. The second material, BZTA, was a straight mix of existing alumina (75 wt.%) and zirconia (25 wt. %) powders currently used for production of hip heads. This material was an experimental batch processed material.

The processing details of the ceramics were not available for this research. However the critical aspect in producing this type of alloyed ceramic is to ensure proper dispersion of the zirconia throughout the alumina matrix. This aspect of ZTA fabrication was covered in-depth by Fantozzi et al [93,94,95] who found the ideal way to achieve good dispersion was to use a combination of electrochemical and mechanical milling techniques.

The two ZTA materials in this study differed in terms of their starting powders, composition, scale and probably type of processing, so it was no surprise that they also differed with respect to their microstructures.

The grain size analysis, Table 13, shows the AZTA material to have a finer alumina grain size than the BZTA, 0.872±0.26μm as opposed to 1.105±0.45μm. Conversely, the zirconia size range is slightly larger in the AZTA material than in the BZTA material, 0.355±0.09μm and 0.265±0.05μm respectively. However, this size range is within the region for stable tetragonal phase outlined by Cales [50].

The greatest difference in the microstructures of the two materials occurs however with the zirconia dispersion throughout the alumina matrix. The AZTA material has a well dispersed zirconia phase with no more than two or three zirconia grains at each alumina grain boundary, Figure 52 (b,d). The BZTA on the other hand contains a zirconia phase that is more agglomerated than dispersed throughout the alumina matrix, Figure 52 (a,c). Agglomerates of more than 20 zirconia grains can be seen in this ceramic. This material resembles an alumina with dispersed PSZ agglomerates as outlined by Wang and Stevens [14]. The size range of the agglomerates in the BZTA material is not as great as the 5-25μm reported by Wang [14] but is closer to 2-2.5 μm. Wang reported fracture toughness values up to 13 MPa $m^{½}$ with this material. This was achieved through a combination of transformation toughening within the agglomerates and crack deflection at the boundaries of the agglomerates.

The effect of this difference in zirconia dispersion will be examined now in terms of the strength and fracture toughness of the two ceramics.

### 6.2.2 Flexural Strength

The flexural strength of the candidate ceramics was measured in a number of material conditions, however the overall flexural strength results for the ceramics will be discussed in this section.

A considerable difference was seen between the flexural strengths of the two ZTA materials, with the AZTA being up to 25% stronger than the BZTA material, Figure 45. However, both materials were between 50% to 75% stronger than the alumina control. The zirconia dispersion difference seen in the microstructural analysis has had an effect on the flexural strength of the ZTA materials. The main reason for this has to be the fine grained alumina, already discussed, in the AZTA material. It is reported [14] that zirconia added to alumina has a large grain boundary pinning effect during sintering keeping the grains below one micron. This is predominantly the largest effect on the strength of the alumina, as shown by Willmann and Wang [8,14]. The grain refinement is more marked in the AZTA material because of the finer dispersion of the zirconia second phase.

The results demonstrate the powerful strengthening effect of adding zirconia to the alumina. However, the ZTA materials are not as strong as the zirconia which showed a flexural strength of 1500MPa.

### 6.2.3 Hardness

The addition of 25 wt% zirconia to the alumina has not decreased the hardness of alumina. The results show no difference between the ZTA ceramics and the alumina control which will be an important factor in maintaining the high wear resistance of the material.

### 6.2.4 Fracture toughness.

Indentation fracture toughness was used initially to gauge the relative toughness of the ZTA materials. BZTA was measured after the flexural strength testing to investigate if the strength increase observed in this test translated into a toughness increase in the ceramic.

Even though difficulties were encountered with this method of analysis, the results show the BZTA material to be 20% tougher than the alumina control. Looking at the work completed by other authors in this field there is very little reported on indentation fracture toughness of ZTA. All the main work concentrates on direct crack measurement techniques [98,102,103,105]. Thomson et al [90] reported indentation fracture toughness values for alumina and ZTA. The results were higher than that measured for AZTA and BZTA in this study. Indentation fracture toughness values of 4.5 ± 0.5 $MN/m^{3/2}$ and 10.9 ± 1.0 $MN/m^{3/2}$ were reported by Thomson for alumina and ZTA respectively. These results are an order of magnitude above the values reported in section 4.4 of this study. This difference may be due, in part, to the type of equation used to calculate the toughness value, which in the case of Thomson was a composite value of sixteen different equations not an absolute figure from one equation, as used in this study. The materials measured were also different, with the Thomson's materials being purely experimental, small-scale batch produced materials. In addition, the indentation fracture toughness values do not agree with the SENB fracture toughness values reported by Thomson. The SENB values were lower than the indentation fracture toughness values indicating that the latter technique over estimated the toughness of these materials.

This preliminary analysis on the BZTA material indicated that the zirconia additions to the alumina were having a significant effect on the material properties. The 25% flexural strength increase seen with BZTA material has translated into a 20% increase in indentation fracture toughness. On examining the microstructure around the cracks, observations can be made with regard to the crack propagation differences between the alumina and the BZTA. Figure 46 shows an indentation crack through the alumina, and it is clear that the crack follows a very contorted inter granular path. In contrast, the crack in the BZTA material is extremely straight with very little deviation. On first analysis, the latter case might be thought to be better, as crack propagation seems to be hindered by the large irregular grain boundaries. This is the main crack resistance or toughening mechanism at play in the alumina matrix. The BZTA material benefits from both the alumina fracture toughness mechanism and additionally the crack closing action of the PSZ particles.

Further fracture toughness measurements were carried out on alumina and both BZTA and AZTA materials using single edge v-notch fracture toughness testing. The results show that AZTA has a fracture toughness of 6.26 ± 0.24 MPa $m^{½}$ and BZTA is lower at 4.76 ± 0.41 MPa $m^{½}$. The AZTA and BZTA are between 24% and 10% tougher than

alumina at 3.86 ± 0.2 MPa $m^{½}$. The relative difference in toughness between the two ZTA materials may be explained again by considering their microstructures. The fine grained AZTA material has an even dispersion of zirconia throughout its matrix therefore any propagating crack will encounter two or three zirconia grains every half a micron as it propagates around the grain boundaries. In the BZTA material however a propagating crack will for the most part only encounter alumina grains and every couple of microns an agglomeration of zirconia grains. These zirconia grains are effective in exerting a crack closure effect through a transformation toughening mechanism on the propagating crack and hence the 10% increase in toughness. They are not of a large enough size to cause crack deflection and therefore achieve the higher toughness reported by Wang et al [14] for similar materials. Indeed, a closer look at the crack propagation through this material, Figure 47, shows the crack propagating through these agglomerates with no crack deviation or deflection evident.

These single edge v-notch toughness results, Table 12 compare favourable with the literature. Wang [14] reported SENB fracture toughness results of between 6 and 7 MPa $m^{½}$ for similar ZTA materials. In a further study on SENB fracture toughness testing Wang et al [79] reported a fracture toughness of between 4 and 3 MPa $m^{½}$ for alumina (grain size 2.5 μm) for a notch width between 200 to 300 μm. The ZTA material tested by the authors had a fracture toughness of between 3.5 and 5 MPa $m^{½}$ for similar notch widths.

Therefore, the ZTA materials show a distinct advantage in terms of fracture toughness over alumina.

### 6.2.5. Ultimate compression testing.

The flexural strength and fracture toughness test results are an indication of how strong and tough a candidate engineering ceramic is, however the final test of a ceramic has to be completed using the final design of the end product.

Ultimate compression testing involves testing the final design head and cup under static loading conditions. Table 14, shows that both ZTA materials are stronger than the required 46 KN for clinical applications. The cobalt chromium spigot is the hardest material and gives the lowest UCS values of all the tests. However, BZTA has a burst

strength of 52.7 ± 13.9 KN and AZTA shows a burst strength of 67.7 ±17.9 KN on the cobalt chromium spigot. It is interesting to note that the 25% difference in flexural strength seen for the ZTA materials only translated to a 12% difference in UCS for the ball heads on a cobalt chromium spigot.

## 6.3 Stability.

### 6.3.1 X-ray diffraction results.

X-ray diffraction measurements of the two ZTA ceramics demonstrated further differences. The BZTA material has no monoclinic phase. The zirconia fraction at the surface was in the tetragonal form only, Figure 43. The AZTA material was different in that its zirconia was made up of up to 30% monoclinic phase with the remaining percentage being tetragonal phase. This is illustrated in Figure 44 as peaks at 2 theta 28.2° and 31.5°.

The difference in zirconia phase between the two ceramics could be explained in a number of ways, either the zirconia in the AZTA material transformed on the surface due to mechanical stress i.e. polishing, or the starting zirconia powder has inconsistent dispersion of yttria i.e. stabilising agent. Either of these two theories would give reason for concern regarding the use of this material in biomedical bearing surfaces.

Both ceramics were re-tested after accelerated aging (134°C in an autoclave) and real time aging (12 months in Ringer's solution at 37°C) and no change was measured in either case. The BZTA zirconia remained in purely tetragonal form, Figure 43, with no transformation to the monoclinic phase evident. The AZTA material also remained largely unchanged with no further transformation above the 30% monoclinic measured before ageing.

If the AZTA material had an irregular dispersion of stabilising agent then the ageing conditions would have produced further transformation of the zirconia phase. This would have been recorded as an increase in the monoclinic peaks on the XRD trace. As this did not occur it is unlikely that this is the reason for the presence of the monoclinic phase.

The proposal that this monoclinic content could be caused by mechanical stress induced by grinding and polishing requires further investigation. The BZTA material was produced by a company whose focus is the production of zirconia heads; they are therefore extremely knowledgeable and experienced in the polishing of zirconia without causing a surface monoclinic transformation. The AZTA material was produced by a company whose focus is alumina production. There remains a possibility that the monoclinic phase was produced due to sub-optimised final machining and polishing. If this is the case, the transformation only occurs at the surface of the ceramic with the internal zirconia being theoretically in the tetragonal phase only. This is difficult to prove as it would require sectioning of the ceramic to measure the cross-section. This of course would mean measuring a surface that has been exposed to mechanical stress due to the sectioning. Thomson et al [91] attempted to measure the depth of the transformation on similar ZTA materials by SEM analysis of fractured surfaces and Dye penetrant inspection but neither of these techniques were successful. The authors reported the surface transformation as measured by XRD only.

Whatever the mechanism for its formation the presence of a monoclinic layer on the surface of the ceramic may effect its mechanical properties. The 3-4% volume increase associated with the tetragonal to monoclinic transformation will result in change occurring in the ZTA ceramic:

1. the volume increase will impart a compressive layer on the surface [77]. This may improve the mechanical strength and wear resistance of the ceramic,
2. the volume increase could cause micro-cracks around the zirconia grains in the matrix. These in turn would lead to ingress of water and further transformation and micro-cracking, thus reducing the mechanical strength of the ceramic.

Flexural strength testing was carried out to investigate the second point above. As reported in tables 8 & 9 there was no loss of mechanical strength with either ceramic. The AZTA material as-received had a flexural strength of 1188.2 ± 136.4 MPa and 1203.3 ± 101.15 MPa after 12 months real time ageing. Similarly, the BZTA showed a mean flexural strength of 823.8 ± 136.4 MPa before ageing and 741.6 ± 122.2 MPa after 12 months real time ageing. In both cases, there was statistically no difference in the results. This is further confirmation that the monoclinic content of the AZTA material is stable and that the BZTA does not form any monoclinic phase. This would imply either that the aforementioned volume increase was absorbed by the alumina matrix without

any microcracking occurring, or the monoclinic phase was formed in the starting powder prior to densification.

The ageing results presented in the literature for ZTA materials are mixed. For the most part authors have indicated problems with using ZTA for biomedical applications due to a decrease in mechanical properties after ageing trials [89,90,91,91]. The most comprehensive work on the subject was completed by Thomson et al. Their work needs to be divided into two stages in order to understand the relevance of their findings and how they evolved. The first materials investigated by the authors were laboratory produced and were probably suboptimal with regard to density, zirconia distribution and starting powder purity. None of these critical parameters were reported in the first study [89]. The ZTA material had an as-fired monoclinic content of 5% that increased to over 25% after 19 months real time ageing in Ringer's solution at 37°C. Their flexural strength decreased from 448 ± 37 MPa to 397 ± 52 MPa. This is certainly not what was found in the current study when testing the AZTA and BZTA materials. Even though the real time testing for these materials did not extend to 19 months, it is clear that there is no measurable transformation observable at 12 months real time ageing. Thomson [89] shows the material to have reached 25 % monoclinic transformation by 12 months.

Further, the accelerating ageing used to measure the AZTA and BZTA materials has been shown to be equivalent to 20 years *in-vivo* ageing [81]. The zirconia control in this test, which is made from the same starting powder used to make the BZTA, showed a 5% increase in monoclinic content after ageing. The AZTA and the BZTA material did not change after this ageing. This would suggest that the alumina matrix is restricting the transformation of the zirconia grains, even under extreme ageing conditions. The high modulus of the alumina 400 GPa when compared with the zirconia at 200 GPa may be of benefit in achieving this [89].

Therefore, the ZTA results obtained by Thomson in his first study cannot be compared to those obtained for the AZTA and BZTA ceramics in this study. However, The authors went on to look at commercially produced ZTA ceramics in two subsequent studies [90,91]. These were supplied by a biomedical ceramic supplier Morgan and Matroc in the UK. The results show that these ceramics were very resistant to ageing in different aqueous based solutions. The only solution to cause significant ageing was 20% HCl.

Mandrino et al [97] showed ZTA materials maintained their flexural strength after 64 weeks *in-vivo* ageing. Again, the materials were laboratory produced however this time the authors present the relevant material properties such as density and Youngs modulus. The material's strength was maintained at ~ 400 MPa and no ageing occurred. These materials had 2 mol % Y stabilising agent as opposed to 3 mol % for the AZTA and BZTA ceramics in this study. This would indicate that, when produced to high standards, the ZTA materials are extremely stable.

## 6.4 Summary.

The ceramic microstructure has been the main influence on the mechanical strength, toughness, and stability of the ZTA materials. As with the development of the first generation of alumina ceramics for biomedical applications, it is similarly critical in the development of these fourth generation ceramics.

The AZTA material had a fine dispersion of zirconia throughout the alumina matrix, which resulted in a strong grain refining effect on the alumina grains. This imparts high flexural strength and toughness to the material. The BZTA material had an agglomerated dispersion of zirconia grains throughout the matrix, which resulted in a less refined alumina grain structure and subsequently lower flexural strength and fracture toughness values. Ultimate compression testing confirmed the ZTA materials are capable of performing above the requirements for standards orthopaedic applications.

Both ceramics were stable in aqueous environments under both accelerated ageing and real time ageing. Up to 30% of the zirconia grains in the AZTA material were monoclinic. This however did not change after ageing as confirmed by XRD and flexural strength testing.

Ultimately then will these improvements translate to substantial clinical benefits? The ZTA materials are a significant improvement over the currently used third generation alumina material in terms of mechanical properties. They are 50% to 70% stronger and 10% to 20% tougher, which will logically give added benefits in terms of a more user-friendly material, fracture resistance and allow greater flexibility in terms of range of applications.

## 6.5 Tribology.

### 6.5.1 Introduction.

The previous sections exclusively covered the static engineering design material properties of the ZTA ceramics. However, in developing a new material for biomedical bearing applications it is essential that the material is tested in its final design form in as close as possible, the conditions it will encounter *in-vivo.* The material needs to be tested in hip friction and wear simulators under physiological loading and activity levels.

### 6.5.2 Friction.

The friction results for the various bearing combinations tested showed a marked difference between using a polyethylene liner and an all-ceramic construct. The friction factors for the metal polyethylene and ceramic polyethylene were comparable. They both fall in the range of 0.035 to 0.025 across the range of viscosities tested. In fact, the alumina polyethylene combination showed slightly higher friction factor values than the metal polyethylene combination. This was probably due to variations in the cup/head clearances. Looking at the Stribeck curves it was clear that the friction factors were decreasing as the viscosity was increased indicating a mixed lubrication regime. This means that there was contact at all stages of the walking cycle between the asperities on the polyethylene surface and the asperities on the ceramic surface. This was the main reason why there was no apparent improvement in friction factors when using a ceramic head instead of a metal head. Even though the ceramic is smoother than the metal, the polyethylene roughness was an order of magnitude greater than both these surfaces.

The ceramic-on-ceramic bearings operated at much lower levels of friction. All ceramic bearings tested showed friction factors in the range 0.015 to below 0.005 for the viscosity range used. There was very little difference noted between the alumina –on-alumina bearing and the ZTA-on-ZTA bearings. The Stribeck curves practically mapped each other and show a decreasing trend as the viscosity was increased. However, this time the Stribeck plot falls off very steeply between 3.0 and 37.21 Cp and then starts to level off. This indicates that, unlike the metal/ceramic polyethylene bearings, the ceramic-on-ceramic bearings are approaching full fluid film lubrication at lower fluid viscosities. This is due to a combination of low radial clearances between the ceramic

couples, extremely low surface roughness values and high modulus of the ceramic components.

It was not surprising then that the alumina bearings had similar friction factors to the ZTA bearings; there was very little difference in terms of surface roughness, radial clearance and probably surface hydrophillicity between the two materials. The zirconia additions to the matrix do not effect the friction performance of the material.

The alumina-on-alumina bearing that was tested after hip simulator testing gives an interesting insight into how these ceramics are likely to behave with respect to friction factors *in-vivo.* The couple shows the lowest friction factors of all components tested. The Stribeck curve started below a friction factor of 0.005 and remained level as the viscosity was increased indicating that the couple was very close to operating in full fluid film lubrication conditions. This couple was not friction tested prior to the hip simulator testing, nor was the surface roughness or radial clearance known. However, when the surface roughness ($S_a$) of these components was compared to that of a representative as-received component it was found to be 70% lower. The wear cycles have reduced the roughness of the components to a level where there are very few asperities on the surface thus reducing the friction factors. This was further evidence that the bearing system was not quite operating in a full fluid film regime but in a mixed mode where there was some contact between the surfaces, hence the polishing affect. Green et al [117] looked at precisely this when they examined alumina heads before and after hip simulator testing using an atomic force microscope (AFM) to measure roughness. The as-received roughness values presented were very close to the values measured in this study, 3.45 ± 0.61 nm and 3.4 ± 0.41 nm respectively. However, the authors found that this value increased after simulator wear testing. As the wear test proceeded, the average area surface roughness of the femoral heads increased from 3.35 to 7.58nm. The authors found that whilst the polishing scratches seen on the as received heads were being polished away, grain pull-out was occurring at the pole of the heads. This grain pull-out was extensive and accounted for the roughness increase reported. No grain pull-out was observed on the main articulation surface of the heads measured in this study. The ceramics used by Green [117] were from another ceramic supplier to that used in this study and the amount of grain pull-out seen with this material would cause concern. However, the authors also concluded that these bearings were clearly operating in a mixed lubrication regime.

The findings by Green et al [117] are also in complete disagreement with the work presented by Rehman et al [118]. The latter looked at the lambda ratio, defined as the ratio between the theoretical fluid film thickness to the composite roughness of the head and cup, for alumina, zirconia and ZTA couples. The composite roughness values presented showed all the ceramic bearings to have a decrease in composite roughness after wear testing. The authors concluded that this occurred to such an extent that the alumina bearing may have moved from a mixed lubrication regime to a full fluid film regime.

Figure 56, shows the friction factors for the different bearings at a viscosity of 9 Cp which is approximately that of healthy synovium. This graph grades the systems in terms of reducing friction factors and illustrates the large gap between the metal/ceramic polyethylene bearings and the ceramic bearings. One interesting point to note is the slightly lower friction factor recorded for the ZTA/ZTA combination when compared to the Al/Al combination. This was not anyway significant, but it may be interesting when considering the wear behaviour of these couples.

### 6.5.3 Simulator Wear.

Simulator wear testing is the closest *in-vitro* test that approaches the *in-vivo* demands placed on orthopaedic bearings. Standard simulator wear results for ceramic bearings are well reported [22] and tend to be largely indifferent as they report the same low wear results no matter what the ceramic material combination tested. These wear rates are typically lower than those reported clinically for alumina -on-alumina [124].

When testing the new ceramic bearing material, ZTA, the objective was to test the material under non-ideal, aggressive simulation conditions. Based on clinical investigations conducted by Mallory [124] microseparation of the head and cup was introduced into the walking cycle of the hip simulator. This resulted in line contact between the head and the rim of the cup for a fraction of a second during the simulator walking cycle and has been proven to reproduce clinical wear rates, wear scars and debris for the first time in a hip simulator [125]. The development of this simulator testing coincided with the development of the ZTA materials.

Initial trials were carried out using standard simulator conditions for three million cycles followed by microseparation conditions for over one million cycles. The results for the

standard simulation testing showed the ZTA materials to have a wear rate slightly lower than the alumina-on-alumina bearings, 0.03 $mm^3/10^6$ cycles as opposed to 0.05 $mm^3/10^6$ cycles. This was not a significant difference however it does seem to echo the difference seen in the friction factors for the two combinations. The results corresponded well with other authors working on these materials. Rehman et al [118], in a recent study, reported the wear rate of ZTA/ZTA as 0.025 $mm/10^6$ cycles for standard hip simulator conditions. They also reported a wear rate for alumina that was higher than ZTA at 0.076 $mm^3/10^6$ cycles.

Microseparation was introduced for a further two million cycles following the standard simulation. This resulted in an increase in the wear rate for all the couples, Figure 58, with the ZTA materials wearing less than the alumina couples. The wear rates for this study are shown graphically in Figure 59, and it can be seen that the most wear occurred during the first half a million cycles and then all components show a levelling off of the wear rate.

The surface roughness measurements for these heads illustrated clearly the difference in alumina bearings and ZTA bearings when it came to resisting damage due to the action of microseparation. The alumina components showed a $S_a$ value of between 0.17 and 0.19 µm at the centre of the wear stripe where as the ZTA materials remained below 0.05 µm in the same damaged areas, Table 19.

The SEM analysis, on alumina scars only, showed the type of damage caused by this testing. The damage could be divided into two regions:

1. an area of severe inter-granular fracture and grain pull -out at the centre of the scar, Figure 63,
2. an area of individual grain pull-out at the edge of the scar, Figure 62.

The second simulator run concentrated on running the microseparation conditions for a full five million cycles for alumina-on-alumina and on a mixed bearing of AZTA -on-alumina. The microseparation parameters were also changed slightly for this run in that a more consistent separation distance was achieved in each cycle thus making the test even more severe on the bearings.

The wear rates showed some clear differences between the two groups. Figure 66 shows the AZTA/Al couples to be wearing less than the Al/Al couples. In the first million

cycles, the AZTA/Al couples had an average volumetric wear of 0.98 $mm^3$ as opposed to 3.98 $mm^3$ for the Al/Al couples, Table 23. This difference is further illustrated in figure 67 which plots the average cumulative wear for both bearing combinations against millions of cycles. Also included in this graph are results for alumina-on alumina couples with no microseparation. The results showed the ZTA heads were more resistant to microseparation damage than the alumina heads. This was further illustrated by the roughness analysis on the wear scars, Table 24.

The dimensional measurement of the resulting wear scars showed very little difference in terms of wear scar width however the alumina scars were deeper, Table 25. The alumina wear scar depths were on average 89.3 μm as opposed to 37.6 μm for the ZTA scars.

The ZTA wear scars, when examined under the SEM, were visibly different to those previously reported for alumina. Even though the scar damage could be divided into the same two areas as previously, this time the grain pull-out consisted of much smaller holes reflecting the finer grain size, Figure 70. Further, the damage within the ZTA scar showed a more polished appearance with a more intra-granular type failure mode evident. The ZTA material was clearly much more resistant to damage of this type than the alumina. The increase in toughness measured for the ZTA over the alumina has resulted it being more resistant to damage in the adverse wear situation of microseparation. Any level of performance enhancement that extends the wear resistance of a bearing system will greatly extend the lifetime of the bearing.

An observation on the behaviour of these bearings is the wear rate is not the same throughout the five million cycles. The wear can be divided into a high wear state for the first 1-2 million cycles after which it reached a steady state with only a minor increase in wear. This was an important result as it meant that this microseparation will not lead to run away wear requiring early clinical intervention for these components. When this adverse situation occurs the scars will form quickly and as they develop, the line contact becomes increasingly conforming, the contact stress is reduced and a steady state wear rate will be achieved. The fact that these stripes are formed outside the main bearing contact area also helps this situation. Figure 72 shows the different stages of the wear process as a high wear or bedding-in stage, a steady state stage and then the overall average wear rate for the couples. It is clear that the ZTA-on-alumina couple was wearing much less than the alumina -on- alumina couple in this study .

The third and final wear study looked at the wear behaviour of AZTA-on-AZTA for five million cycles and a mixed bearing zirconia-on-alumina, a combination that has received a lot of *in-vitro* and *in vivo* attention.

The wear rates for the AZTA-on-AZTA combination were lower than those previously reported for the AZTA-on-alumina component in study two. They showed an initial volumetric wear of 0.319 $mm^3$ as opposed to 0.98 $mm^3$ measured for AZTA-on-alumina. This further decrease in wear was due to the use of all-ZTA bearings thus conferring resistance to damage on both the cup and the head.

The wear results for the zirconia-on-alumina combination are spectacular. The bearings were not resistant to microseparation damage with runaway wear seen in all three couples. The volumetric wear for these components was so high, 10.77 $mm^3$ for the first million cycles, that two tests on two of the three components had to be stopped due to component fracture. One station had a fractured zirconia head after three million cycles and unusually, a second had a fractured cup after two million cycles. Figure 74 b, and Figure 75, shows that the majority (90%) of the wear was occurring on the zirconia head as opposed to an even distribution for the AZTA-on-AZTA bearing.

The wear stripe dimensions for the components show the stripe widths to be approximately the same for all components ~ 5-8 μm, however the stripe depth for the zirconia heads ranged between 130 μm and 350μm. The zirconia resistance to this type of edge loading is by far the lowest of all the components tested under microseparation conditions. This would suggest that toughness and high hardness are the material properties required to resist this type of damage.

The ZTA materials proved to have the best combination of these properties and wore much less than any of the bearings tested. A summary of the extensive simulator testing completed is presented in Figure 82. The bearings can be graded in order of lowest wear rate first as : ZTA/ZTA, ZTA/AL, Al/Al .

Therefore the simulator testing has been successful in two respects, the test design has simulated the worst case clinical conditions for bearings through the application of microseparation and the results have shown the various ceramic materials can be graded according to their relative wear rates under these conditions. This is unique in relation to extensive work reported on ceramic *in-vitro* wear in the literature.

### 6.5.4. Clinical wear

Unique access to a series of explanted alumina-on alumina components presented the opportunity to study the clinical effect of microseparation on these bearings. The patients studied were from one surgical group and formed a small percentage of a large number of successful implantations.

These patients all had surgically related complications that emphasize the fact that in the clinical application the conditions are not always ideal for bearing surfaces. A number of patients had some form of fracture and indeed two hips had subsided by more than two centimetres distally. The analysis showed eleven out of sixteen hips had wear scars present on both the heads and cups.

The mechanism of formation of the wear pattern for at least two of these cases correlated with the heel strike theory simulated in the hip simulators. However, the remaining wear scars were formed during the sit to stand patient activity. The position and alignment of the scars on the heads and cups for these components only match up when the femur is at 90° to the pelvis. The patient when sitting will rest mainly on the pelvis allowing the main hip muscles to relax, the ceramic components will sublux slightly to a inferior - posterior position. The head and cup clearance on these components is so small that a subluxation of 40-50 μm is enough to bring the head into line contact with the rim of the cup. As the hip is in the relaxed sitting position and the patient moves to stand up, the main hip muscles flex and the head and cup relocate after first loading on the rim. It is this line or point loading on the ceramic that starts the wear scar formation. Incidentally, the head and cup never separate in either the hip simulator trials or in the clinical situation, therefore microseparation is a misleading term in this regard.

This has further validated the case for harsh, non-standard wear simulation in the laboratory. Even under these conditions, the alumina performs well showing no run away wear and even though the wear rate has increased, it is still orders of magnitude lower than metal polyethylene wear rates. The ZTA bearings showed even lower wear rates in microseparation testing. The zirconia bearings failed under these test conditions.

# 7.0 Conclusions

Research into the reduction of clinical wear of bearing surfaces is of extreme importance for the longevity of future orthopaedic implants. Ceramic-on-ceramic bearing surfaces have been instrumental in ensuring low wear options are available for younger active patients. These bearings have performed extremely well in this application for over thirty years. However, clinical demand on bearing surfaces has increased, and surgeons are implanting the materials into even younger more active patients. All patients are living longer healthy active lives further increasing the clinical demands. Orthopaedic research cannot afford to stand still with regard to meeting this demand. The current third generation ceramics will be pushed to the edge of their performance design limits and in some cases these will be exceeded.

Development of fourth generation ceramics is concerned with looking at increasing the possible clinical operating range of the current bearing materials to meet this challenge. ZTA has proven to be an excellent candidate for this application and the following conclusions can be made:

- The mechanical properties measured showed the ZTA ceramic materials to be stronger, tougher and in the case of zirconia more stable than the currently used ceramic bearing materials. The microstructure was the main factor that influenced the subsequent mechanical properties. The addition of 25 wt. % zirconia has resulted in a strong grain refining effect on the alumina. The two ZTA materials showed that the alumina grains are sub micron in the case of AZTA and just above this for the BZTA material. This has resulted in flexural strength increases of between 50% and 75% over alumina. The toughness of both ZTAs was 20 to 25% higher than alumina. These strength and toughness increases have resulted in up to 12 % improvements in ultimate compression testing of the final ballheads on cobalt chrome spigots.

- The XRD analysis of the ZTAs showed differences in the phase compositions of their surfaces. The AZTA material has up to 30% monoclinic phase on its surface. The BZTA material has no monoclinic phase present. Neither of the materials

however shows any further tetragonal to monoclinic transformation after both accelerated and real time ageing.

- Friction testing of the bearings showed the ceramic materials performed under full fluid film lubrication regimes unlike the metal polyethylene bearings which operates in a mixed lubrication regime. However, the friction factors for the ceramic-on-ceramic bearings were an order of magnitude lower than the metal polyethylene bearings. The ZTA materials showed slightly lower friction factors than the alumina-on-alumina bearings, however this difference was not significant. Friction testing of a simulator worn head and cup showed the lowest results. This was due to the benign polishing that occurs between the components reducing the surface roughness hence decreasing the friction factor.

- Hip simulator wear testing was carried out in both standard and microseparation conditions. The ZTA-on-ZTA bearings had wear rates as low as or maybe lower than alumina-on-alumina bearings in standard hip simulation testing. All components showed increased wear rates and the formation of wear scars when microseparation was introduced into the hip simulators. The ZTA bearings showed significantly lower wear rates in microseparation than alumina. The combination of higher toughness and high hardness of the ZTA materials has resulted in superior resistance to microseparation loading conditions than any other bearing materials tested in this study. The zirconia-on-zirconia bearings were the only bearings to show runaway wear to the point of component fractures in microseparation testing. This bearing should be contra-indicated for clinical use.

- The clinically explanted heads showed a high incidence of wear scars present on both the heads and cups. Two different mechanisms for the formation of these wear scars were identified. On the heads that came from patients with large stem subsidence the wear scars were formed during the walking cycle at heel strike as simulated in the wear trials. There were two such cases, the remaining nine components were well fixed with no clinical subsidence reported. The orientation of the wear scars present on these components showed that they were formed when the leg was in 90° of flexion. This would indicate that the main activity responsible for the formation of these scars is the sitting to standing action of the patient.

- ZTA is a suitable material for orthopaedic bearing applications. The material represents a clear and measurable advantage over the existing clinically used ceramics in terms of strength, fracture toughness and wear resistance. These will translate into real advantages in terms of clinical outcomes and allow added benefit to patients in terms of safer, longer lasting hip replacements.

## 8.0 Further Work

The ZTA ceramic materials delivered the required properties for orthopaedic applications, however there is some outstanding analysis that if completed will enhance our knowledge on how these materials will behave in-vivo.

More in-depth analysis needs to be completed on the origin of the monoclinic phase in the AZTA material. Glancing angle XRD needs to be run on the samples as this technique will measure the crystalline phases as a function of depth. Sectioning the components and doing XRD is not an option as previously discussed. Ideally, the starting raw material used to manufacture the ceramic should be analysed.

The AZTA material contains a small percentage of strontium. This is reported by the manufacturer to be present in the matrix as a platelet shaped grain 5 microns long and 1 micron wide. This was not observed in any of the extensive SEM analysis carried out in this work. Further work will be required in determining how this strontium mixes in the ZTA and what form it takes in the microstructure.

## 9.0 References


1 Black, J,"Prospects for alternate bearing surfaces in total replacement arthroplasty of the hip." Performance of the wear couple, proceedings of the 2nd. Symposium on ceramic wear couple, Stuttgart, 8, 1997.

2 Amstutz, HC, Campbell, P, Kossovsky, N and Clarke, IC, "Mechanism and clinical significance of wear debris induced osteolysis", Clinical Orthopaedics, 276, 7, 1992.

3 Maloney, WJ, Jasty, M, Harris, WH, "Bone lysis in a well fixed cemented femoral components", Journal of Bone and Joint Surgery, 72B, 966, 1990.

4 Schmalzreid, TP, Jasty, M, Harris, WH, "Periprosthetic bone loss in total hip arthroplasty. Polyethylene wear debris and the concept of the effective joint space" The Journal of the Bone and Joint Surgery, American volume, 74, Issue 6, 849, 1992.

5 Mc Kellop, H, Shen, FW, Lu, B, Campbell, P, Salovey, R, " Effect of sterilization method and other modifications on the wear resistance of acetabular cups made of ultra-high molecular weight polyethylene" The Journal of Bone and Joint Surgery, American volume, 82-A, 12, 2000.

6 Lerf, R, Schmotzer, H, Weller, M, " The effect of post irradiation treatments on the properties of cross linked UHMWPE" Conference proceedings, IMechE, Engineers & Surgeons –Joined at the hip, Savoy Place, London, UK, 2002.

7 Ingham, E, Fisher, J, "Biological reactions to wear debris in total joint replacement", Proceedings of the Institution of Mechanical Engineers, 214 Part H, 21, 2000.

8 Willmann, G, " Biolox forte heads and cups for THR – What surgeons should know", Proceedings of the second symposium on the wear of the ceramic couple, Stuttgart, Germany, 2000.

9 Chevalier, J, Drouin, JM, Cales, B, " Low temperature ageing behaviour of zirconia hip joint heads", Bioceramics, 10, 1997.

10 D'Antonio, J, Capello, W, Manley, M, Bierbaum, B, " New experience with alumina on alumina ceramic bearings for total hip arthroplasty", The Journal of Arthroplasty, 17, 4, 2002.

11 Wise, DL, Trantolo, DJ, Altobelli, DE, Schwartz, ER, "Encyclopedic handbook of biomaterials and bioengineering", Marcel Dekker Inc, 1, 1st Edition, 415, 1995.

12 Cales, B, Stefani, Y, Liley, E, " Long term *in-vivo* and *in-vitro* ageing of a zirconia ceramic used in orthopaedy", 19th annual meeting Society for Biomaterials, 2000.

13 Swab, JJ, "Low temperature degradation of Y-TZP materials", Journal of Materials Science, 36, 6706, 1991.

14 Wang, J, Stevens, R, " Review Zirconia toughened alumina (ZTA) ceramics", Journal of Materials Science, 24, 3421, 1989.

15 Hummer, CD, Rothman, RH, Hozack, WJ, "Catastrophic failure of modular zirconia ceramic femoral head components after total hip arthroplasty", The Journal of Arthroplasty, 10, No. 6, 1995.

16 Ashby, MF, Jones, RH, "Engineering materials 2" International series on materials science and technology, Volume 39, Pergamon, 4th Edition, 1994.

17 Ricardo, JH, Willman, G, "Ceramics in total hip arthroplasty: history, mechanical properties, clinical results, and current manufacturing state of the art", Seminars in Arthroplasty, 9, (2), 114, 1998.

18 Higuchi, F, Shiba, N, Inoue, A, Wakebe, I, "Fracture of an alumina ceramic head in total hip arthroplasty", The Journal of Arthroplasty, 10, 6, 1995.

19 Krikler, S, Schatzker, J, "Ceramic head failure", The Journal of Arthroplasty, 10, 6, 1995.

20 Hadley, G, Flynn, W Chitranjan, SR, Thomas, PS, "Fracture of a femoral head after ceramic on polyethylene total hip arthroplasty", The Journal of Arthroplasty, 10, 6, 1995.

21 Pulliam, I, Trousdale, T, "Fracture of a ceramic head after a revision operation" Journal of Bone and Joint Surgery, 79-A, 1, 1997.

22 Nevelos, J E, "The tribology of ceramic-ceramic hip joints", PhD thesis, Department of Mechanical Engineering, University of Leeds, 2000.

23 Mittelmeier, H, Heisel, J, "Sixteen-years experience with ceramic hip prostheses", Clinical Orthopaedics, 282, 64, 1992.

24. Schmalzreid, TP, Kwong, LM, Jasty, M, Sedlacek, RC, Haire, TC, OConnor, DO, Bragdon, CR, Kabo, JM, Malcolm, AJ, Harris WH, "The mechanism of loosening of cemented acetabular components in total hip arthroplasty. Analysis of specimens retrieved at autopsy", Clinical Orthopaedics. 274, 60, 1992.

25 Schmalzried, TP, Guttmann, D, Grecula, M, Amstutz HC, "The relationship between the design, position, and articular wear of the acetabular components inserted without cement and the development of pelvis osteolysis", The Journal of Bone and Joint Surgery, 76, (5), 677,1994.

26 Wang, A, Stark, C, Dumbleton, JH, "Mechanistic and morphological origins of ultra-high molecular weight polyethylene wear debris in total joint replacement prostheses" Proceedings of the Institutes of Mechanical Engineers, Part H: Journal of Engineering in Medicine, 210, 1996.

27 Ingham, E, Fisher, J, "Biological response to wear debris in total joint replacement" Proceedings of the Institutes of Mechanical Engineers, Part H: Journal of Engineering in Medicine, 214, 1999.

28 Dumbleton, JH, Manley, T, Edidin A, "A literature review of the association between wear rate and osteolysis in total hip arthroplasty", The Journal of Arthroplasty 17, 5, 2002.

29 Insley, GM, Streicher, RM, "Ceramic-on ceramic bearing options for orthopaedic applications", Technical presentation, Stryker Howmedica Osteonics, 2000.

30 Black, J, "Prospects for alternate bearings in total replacement arthroplasty of the hip", Proceedings of the 2nd Symposium on Ceramic Wear Couple, Ferdinand Enke Verlag Stuttgart, 1997.

31 Toni, A, Sudanese, S, Terzi, G, Brizio, S, Paderni, G, "Ceramic in total hip arthroplasty", Proceedings of the 2nd Symposium on Ceramic Wear Couple, Ferdinand Enke Verlag Stuttgart, 1997.

32 Ashby, MF, Jones, DRH, "Engineering materials 2: an introduction to microstructure, processing and design", International Series on Materials Science and Technology, Pergamon, 39,1994.

33 Gee, MG, "Wear testing and ceramics", Proceedings of the Institutes of Mechanical Engineers, 208, 1994.

34 Gee, MG, Almond, A, "The effect of surface finish on the sliding wear of alumina", Journal of Materials Science 25, 296, 1990.

35 Saikko, V, Pfaff, G, "Wear of alumina-alumina total hip joints studied with a hip joint simulator", Proceedings of the 2nd Symposium on Ceramic Wear Couple, Ferdinand Enke Verlag Stuttgart, 1997.

36 Garvie, RV, Swain, MV, Journal .of Materials Science, 20, 1193, 1985.

37 Fisher, J, Besong, A A, Firkins, PJ, Barbour, PSM, Nevelos, JL, Stone, MH, Ingham, E, "Wear debris generation in UHMWPE on ceramic, metal on metal and ceramic on ceramic hip prostheses", Sixth World Biomaterials Congress Transactions, 871, 2000.

38 Hatton, A, Ingham, E, Nevelos, JL, Fisher J, Nevelos, A, "Histological analysis of tissue from revised uncemented ceramic on ceramic total hip arthroplasties", Sixth World Biomaterials Congress Transactions, 1188, 2000.

39 Ingham, E, Hatton, A, Matthews, JB, Nevelos, JE, Fisher, J, "Osteolytic potential of clinically relevant alumina ceramic wear debris generated under microseparation conditions in a hip joint simulator", 49th Annual Meeting, Orthopaedic Research Society, 2003.

40 Heros, R, Willmann, G, "Ceramics in total hip arthroplasty: history, mechanical properties, clinical results and current manufacturing state of the art", Seminars of Arthroplasty, 9, 114,1998.

41 Sedel, L, Lerouge, S, "Long term results of all alumina bearings" Proceedings of the 2nd Symposium on Ceramic Wear Couple, Ferdinand Enke Verlag Stuttgart, 1997.

42 Insley, GM, Streicher, RM, "Ceramic-on ceramic bearing options for orthopaedic applications", Technical presentation, Stryker Howmedica Osteonics, 2003.

43 Willmann, G, Chamier, WV, "The improvements in material properties of Biolox offers benefits for THR", Bioceramics in Orthopaedics-New Applications, Enke Verlag, Stuttgart, 1998.

44 Siverhus, SW, "Design considerations and preliminary results with the Osteonics acetabular cup system", Bioceramics in Orthopaedics: New Applications,

Proceedings from the 3rd International Symposium on Ceramic Joint Couple, Ferdinand Enke Verlag Stuttgart, 1998.

45 D'Antonio, JA, Capello, WN, Manley, M, "New experience with alumina/alumina ceramic bearing for total hip arthroplasty", Internal communication, Stryker Howmedica Osteonics, 2000.

46 "Guidance document for the preparation of premarket notification for ceramic ball hip systems" US food and Drug Administration, Center for Devices and Radiological Health, 1995.

47 Sedel, L, "Clinical experience with all ceramic prosthesis", Royal Academy of Engineering, Conference Proceedings: Joint Replacement, Once is Forever, 43, 2000.

48 Blomer, W, "Design aspects of modular inlay fixation", Bioceramics in Orthopaedics: New Applications, Proceedings from the 3rd International Symposium on Ceramic Joint Couple, Ferdinand Enke Verlag Stuttgart, 1998.

49 The picture archive, Biolox Forte, Fact book, edition 1, Ceramtec Plochingen Germany.

50 Cales, B, "Zirconia ceramic for improved hp prosthesis-a review" 6th Biomaterials Symposium, Gottinngen, Germany, 1994.

51 Willmann, G, "Medical grade Zirconia" Orthopaedics International, 2, 1, 66, 1994.

52 Stevens, R, "Zirconia and zirconia ceramics", Magnesium Elektron Ltd., 12, 1986.

53 Piconi, C, Maccauro, G., "Zirconia as a ceramic biomaterial", Biomaterials, 20, 1, 1999.

54 Wang, J, Stevens, R, "Review- zirconia-toughened alumina (ZTA) ceramics", Journal of Materials Science, 24, 3421, 1989.

55 "Non metallic materials for surgical implants, part 6, specification for ceramic materials based on yttria stabilized tetragonal zirconia", ISO 13356, 1997.

56 Drouin, JM, Cales, B, "Yttria-stabilised zirconia ceramic for improved hip joint head", Bioceramics, 7, 1994.

57 Willert, G, "From alumina to zirconia hip joint heads", 6th World Biomaterials Congress, Hawaii, US, Workshop 7, 2000.

58 Cales, B, "15 years experience with zirconia hip joint heads: main characteristics, advantages and recommendations for use", 6th World Biomaterials Congress, Hawaii, US, Workshop 7, 2000.

59 Derbyshire, B, Fisher, J, Dowson, D, Hardaker, C, Brummitt, K, " Comparative study of the wear of UHMWPE with zirconia ceramic and stainless steel femoral heads in artificial hip joints", Med. Eng. Phys., 16, 229, 1994.

60 Mc Kellop, H, Benya, P, Lu, B, Park, SH, "Friction, Lubrication and wear of cobalt-chromium, alumina and zirconia hip prostheses compared on a joint simulator", Orthopaedic Research Society Proceedings, 402, 1992.

61 Davidson, JA, "Characteristics of metal and ceramic total hip bearing surfaces and their effect on long term ultra-high molecular weight polyethylene wear", Clinical Orthopaedics and Related Research, 294, 361, 1993.

62 Minakawa, H, Ingham, E, Tipper JL, Stone, M, Wroblewski, BM, Fisher, J, "Why do ceramic femoral heads produce lower polyethylene wear in artificial joints?" Proceedings of the International Conference on New Frontiers in Biomechanical Engineering, Japan, 331, 1997.

63 Bigsby, RJ, Hardaker, CS, Fisher, J, "Wear of ultra-high molecular weight polyethylene acetabular cups in a physiological hip joint simulator in the anatomical

position using bovine serum as a lubricant", Proceedings of the Institute of Mechanical Engineers, 211, 265, 1997.

64 Rieger, W, "Medical applications of ceramics", High-Tech Ceramics: Viewpoints and perspectives, Academic Press Ltd., 1989.

65 Amin, KE, Nag, N, "Tribological characteristics of zirconia-yttria ceramics", American Ceramic Bulletin, 74, 5, 1995.

66 Willmann, G, "Experience on zirconia ceramic femoral head", 6th World Biomaterials Congress, Hawaii, US, Workshop 7, 2000.

67 Willmann, G, Fruh, HJ, Pfaff, HG "Wear characteristics of sliding pairs of zirconia (y-TZP) for hip endoprostheses", Biomaterials 17, 2157, 1996.

68 Clarke, IC, "Zirconia simulated wear performance up to 15MC in serum lubricant", 6th World Biomaterials Congress, Hawaii, US, Workshop 7, 2000.

69 Rieker, C, "Comparison of two hard-hard bearing systems on a simulator" 6th World Biomaterials Congress, Hawaii, US, Workshop 7, 2000.

70 Banon, F, "Experience with ceramic heads and friction with polyethylene and alumina cups in hip surgery: A new couple zirconia / alumina – about 163 cases", 6th World Biomaterials Congress, Hawaii, US, Workshop 7, 2000.

71 Pitto, RP, "Hybrid ceramic-ceramic articulation in hip arthroplasty with zirconia femoral heads and alumina acetabular liners. A randomized clinical trial", 6th World Biomaterials Congress, Hawaii, US, Workshop 7, 2000.

72 Pitto, RP, Blanquaert, D, Hohmann, D, " Alternative bearing surfaces in total hip arthroplasty: zirconia-alumina pairing. Contribution or caveat?" Acta Orthopaedics Belgium, 68(3), 242, 2002.

73 Nevelos, JE, Doyle, C, Ingham, E, Nevelos, A, Fisher, J, "Wear of hipped and non hipped alumina-on-alumina bearings under standard and harsh simulator conditions" Trans., Orthopaedic Research Society, 25, 28, 2000.

74 Kaddick, C, Pfaff, G, "A wear study of the alumina/zirconia system", Reliability and long term results of orthopaedic ceramics, Georg Thieme Verlag, Stuttgart, 1999.

75 Doyle, C, "Microscopy study of explanted and as manufactured zirconia heads." Internal report, Stryker Howmedica Osteonics, 1995.

76 Clarke, IC, Mannaka, M, Green, DD, Pezzotti, G, Kim, YH, Ries, M, Sugano, N, Sedel, L, Delauney, C, Nissan, BB, Gustafson, GA, "Current status of zirconia total hip implants- clinical and laboratory studies", American Academy of Orthopaedic Surgeons, SE-203, 2003.

77 Swab, JJ, Katz, RN, Starita, JC, "Effects of oxygen non-stoichiometry on the high temperature performance of a yttria tetragonal zirconia polycrystal material", Ceramic Engineering Science Proceedings, 9, 1305, 1988.

78 Lange, FF, Dunlop, GL, Davis BI, " Degradation during aging of transformation – toughened $ZrO_2$-$Y_2O_3$ materials at 250°C", Journal of American Ceramic Society, 69, (3), 237, 1986.

79 Masaki, T, Nakajima, K, Shinjo, K, " High temperature mechanical properties of Y-PSZ HIPed under an oxygen containing atmosphere", Journal of Materials Science Letters, 5, 1115, 1986.

80 Cales, B, Stefani, Y, Lilley, E, " Long-term *in vivo* and *in vitro* aging of a zirconia ceramic used in orthopaedy", Journal of Biomedical Materials Research, 28, p 619, 1994.

81 Cales, B, Stefani, Y, "Long term stability of a surgical grade zirconia ceramic." Bioceramics, 7, 221, 1994.

82 Lawson, S, " Environmental degradation of zirconia ceramics", Journal of the European Ceramic Society, 15, 485,1995.

83 Lilley, E, "Review of low temperature degradation in zirconia (y-TZP)", Ceramic Transactions, 10, 1990.

84 Cales, B, Stefani, Y, "Mechanical properties and surface analysis of retrieved zirconia hip joint heads after an implantation time of two to three years", Journal of Materials Science: Materials in Medicine, 5, 376, 1994.

85 Cales, B, Stefani, Y, Olagnon, C, Fantozzi, G, "Mechanical characterisation of a Zirconia ceramic used as a implant material", Bioceramics, 6, 1993.

86 Shimizu, K, Oka, M, Kumar, P, Kotoura, Y, Yamamuro, T, Makinouchi, K, Nakamura, T, " Time-dependent changes in the mechanical properties of zirconia ceramic", Journal of Biomedical Materials Research, 27, 729, 1993.

87 Christel, P, Meunier, A, Heller, M, Torre, JP Peille, CN, " Mechanical properties and short term *in-vivo* evaluation of yttrium-oxide-partially –stabilised zirconia", Journal of Biomedical Materials Research, 23, 45, 1989.

88 Murray, MGS, Pryce, AW, Stuart, JW, " A comparison of Zyranox zirconia femoral heads before and 1.5 years of implantation", Fourth Euro Ceramics, 6, 37. 1995.

89 Thomson I, Rawlings, RD, " Mechanical behaviour of zirconia and zirconia toughened alumina in a simulated body environment", Biomaterials, 11, 1990.

90 Thomson, I, Rawlings, RD, "Effects of liquid environments on zirconia-toughened alumina", Journal of Materials Science, 27, 2823, 1992.

91 Thomson, I, Rawlings, RD, " Effects of liquid environments on zirconia toughened alumina", Journal of Materials Science, 27, 2831, 1992.

92 Drummond, JL, "*In-vitro* ageing of yttria stabilised zirconia." Journal of the American Ceramic Society, 72, 4, 675, 1989.

93 Leriche, A, Moortgat, G, Cambier, F, Homerin, P, Thevenot, F, Orange, G, Fantozzi, G, "Preparation and characterisation of a dispersion toughened ceramic for thermomechanical uses (ZTA). Part I: material preparation. Characterisation of microstructure", Journal of the European Ceramic Society, 9, 169, 1992.

94 Orange, G, Fantozzi, G, Homerin, P, Thevenot, F, Leriche, A, Cambier, F, "Preparation and characterisation of a dispersion toughened ceramic for thermomechanical uses (ZTA). Part II: Thermomechanical characterisation. Effect of microstructure and temperature on toughening mechanisms", Journal of the European Ceramic Society, 9, 177, 1992.

95 Orange, G, Fantozzi, G, "Comportments mecaniques de composites ceramiques a dispersoides" Materiaux et Techniques, 29, 1998.

96 Trabelsi, R, Treheux, D, Orange, G, Fantozzi, G, Homerin, P, Theievenot, F, "Relationship between mechanical properties and wear resistance of alumina-zirconia ceramic composites" Conference proceedings, Franco-Allemande sur les Ceramiques Techniques Achen/Aix La Chapelle, 1987.

97 Mandrino, A, Moyen, B, Ben Abdallah, A, Treheux, D, Orange, D, " Aluminas with dispersoides. Tribology properties and *in-vivo* ageing", Biomaterials, 11, 1990,

98 Wang, J, Rainforth, WM, Wadsworth, I, Stevens, R, "The effects of notch width on the SENB toughness for oxide ceramics", Journal of the European Ceramic Society, 10, 21, 1992.

99 Anstis, GR, Chantikul, P, Lawn, BR, Marshall, DB, "A critical evaluation of indentation techniques for measuring fracture toughness: I, strength method", Journal of the American Ceramic Society, 64, 9, 539, 1981.

100 Chantikul, P, Anstis, GR, Lawn, BR, Marshall, DB, "A critical evaluation of indentation techniques for measuring fracture toughness: II, direct crack measurement", Journal of the American Ceramic Society, 64, (9), 533, 1981.

101 Lawn, B, Wilshaw, R, "Review indentation fracture: principles and applications", Journal of materials Science, 10, 1049, 1975.

102 Mukhopadhyay, AK, Datta, SK, Chakraborty, D, "Fracture toughness of structural ceramics", Ceramics International, 25, 447, 1999.

103 Sherman, D, "Fracture toughness evaluation of small thin ceramic specimens", Journal of the American Ceramic Society, 80, 7, 1904, 1997.

104 Tikare, V, Choi, SR, "Combined mode I-mode II fracture of 12-mol%-ceria-doped tetragonal zirconia polycrystalline ceramic", Journal of the American Ceramic Society, 80,(6), 1624, 1997.

105 Nose, T, Fiji, T, "Evaluation of fracture toughness for ceramic materials by a single-edge-precracked –beam method", Journal of the American Ceramic Society, 71, (5), 328, 1988.

106 De Aza, AH, Chevalier, J, Fantozzi, G, Schehl, M, Torrecillas, R, "Crack growth resistance of alumina, zirconia and zirconia toughened alumina ceramics for joint prostheses", Biomaterials, 23, 937, 2002.

107 Yao, JQ, Unsworth, A, "Asperity lubrication in human joints", Proc. Instn. Mech. Engnrs., vol 201, IMechE 1993.

108 Unsworth, A, " Recent developments in the tribology of artificial joints", Tribology International, 28, 7, 1995.

109 Hall, RM, Unsworth, A, " Review Friction in hip prosthesis", Biomaterials, 18, 1017, 1997.

110 Sawae, Y, Murakami, T, Chen, J, " Effect of synovia constituents on friction and wear of ultra high molecular weight polyethylene sliding against prosthetic joint materials", Wear, 216, 213, 1998.

111 Young, SK, Lotito, MA, Keller, TS, " Friction reduction in total joint arthroplasty" Wear, 222, 29, 1998.

112 Zhou, YS, Ohashi, M, Ikeuchi, K, " Start up and steady state friction of alumina against alumina", Wear, 210, 112, 1997.

113 Scholes, SC, Unsworth, A, Hall, RM, Scott, R, " The effects of material combination and lubricant on the friction of total hip prostheses", Wear, 241, 209, 2000.

114 Unsworth, A, Hall, RM, Burgess, IC, Wroblewski, BM, Streicher, RM, Semlitsch, M, " Frictional resistance of new and explanted artificial hip joints", Wear 190, 226, 1995.

115 Dowson, D, Goldsmith, AAJ, Mc Nie, CM, Smith SL " A tribological study of metal-on-metal total replacement hip joints", Friction and Lubrication and Wear of Artificial Joints, Professional Engineering Publishing, 41, 2002.

116 Scholes, SC, Smith, SL, Ash, HE, Unsworth, A, " The lubrication and friction of conventional UHMWPE, novel compliant layer and hard bearing surfaces for use in total hip prostheses", Friction and Lubrication and Wear of Artificial Joints, Professional Engineering Publishing, 59, 2002.

117 SM, Green, "Nanoscale wear degradation of alumina femoral head bearing surfaces assessed using an atomic force microscope", International Conference, Engineers and Surgeons – Joined at the Hip, 2, 7-11, 2002.

118 Rehman, S, Smith, SL, Goldsmith, AAJ, Hardaker, CS, Isaac, G, Dowson, D, "Evaluation of a new ceramic bearing surface", International Conference, Engineers and Surgeons – Joined at the Hip, 2, 7-11, 2002

119 Amstutz, HC, Campbell, P, Kossovsky, N and Clarke, IC "Mechanism and clinical significance of wear debris induced osteolysis", Clinical Orthopaedics, 276, 7-18, 1992.

120 Maloney, WJ, Jasty, M, Rosenberg, A and Harris, WH, "Bone Lysis in well fixed cemented femoral components" Journal of Bone and Joint Surgery, 72B, 966, 1990.

121 Nevelos, J E, Ingham, E, Doyle, C, Fisher J, Nevelos AB, "Analysis of retrieved alumina ceramic components from Mittelmeier total hip prostheses", Journal of Biomaterials 20, 1833, 2000.

122 Fisher, J, Besong, AA, Firkins, PJ, Barbour, PS.M., Nevelos, J.E., Tipper, JL, Stone, H, Ingham, E, Trans 45th Orthopaedic Research Society, Proceedings of the 6th World Congress of Biomaterials, 871, 2000.

123 Nevelos, JE, Ingham, E, Doyle, C, Streicher, R, Nevelos, AB, Walter, W, Fisher, J, "Microseparation of the centres of alumina-alumina artificial hip joints during simulator testing produces clinically relevant wear rates and patterns", Journal of Arthroplasty, 15, 793, 2000.

124 Mallory, TH; Dennis, DA; Northcut, EJ; Lombardi Jr. AV; Herrington, SM, "Do total hip arthroplasty piston during leg length maneuvers and Gait? An In vivo determination of total hip arthroplasty separation during abduction/Adduction leg lift and gait.

125 Stewart T; Tipper J; Streicher R; Ingham E; Fisher J, "Long term wear of HIPed alumina-on-alumina bearings for THR under microseparation conditions" Journal of Material Science. (In Press).

## 10.0 Publications

1 Insley, G, Turner I, Fisher, J., Streicher R., "The next generation bearing – zirconia toughened alumina", Orthopaedic Research Society, 47th annual meeting, San Francisco, 2001, poster presentation.

2 Insley, G, Turner I, Fisher, J., Streicher R., "New developments in hard bearing materials for orthopaedic joint applications" Combined meeting of the Orthopaedic Research Societies of the USA, Canada, Europe and Japan, Rhodes, Greece, 2001, podium presentation.

3 Stewart , T., Fisher, J., Ingham, E., Insley, G., Streicher, R., "Wear of toughened alumina heads against hiped alumina inserts in a hip simulator undergoing swing phase microseparation" Orthopaedic Research Society, 48th annual meeting, Texas, 2002, podium presentation.

4 Insley, G, Turner I, Fisher, J., Streicher R., "*In-vitro* testing and validation of zirconia toughened alumina" Bioceramics in Joint Arthroplasty, Proceedings 7th International Biolox Symposium, 2002, podium presentation, white paper.

5 Insley, G, Stewart T, Nevelos, J., Fisher, J., Streicher, R.M., "Wear of ceramic-ceramic hip prostheses under microseparation simulation conditions" Friction, lubrication and wear of artificial joints, Professional Engineering Publishing , 2002.

Streicher, R.M. (2)
Alte Landstr. 36C,
CH-8802,Kilchberg,
Switzerland
0041-17156361 / Fax: 0041-17156362 /
rms@bluewin.ch

**Preferences and Keywords**

Total Joint Arthroplasty;Ceramic;Mechanical Properties;Wear;Aging

ABSTRACT NO.
PAPER NO.
Check One: _ Clinical _ Biology _ Engineering
**Disclosure**
(E-Stryker Howmedica Osteonics) (A-Stryker Howmedica Osteonics) (E-Stryker Howmedica Osteonics)

# THE NEXT GENERATION BEARING - ZIRCONIA TOUGHENED ALUMINA

*Insley, G (E-Stryker Howmedica Osteonics); ***Turner, I; ****Fisher, J (A-Stryker Howmedica Osteonics); +**Streicher, R (E-Stryker Howmedica Osteonics)
*Stryker Howmedica Osteonics, Limerick, Ireland.. +**Stryker Howmedica Osteonics, Rutherford, US. Alte Landstr. 36C,, CH-8802,Kilchberg,, Switzerland, 0041-17156361, Fax: 0041-17156362, rms@bluewin.ch

## Introduction

Alpha-Alumina and partially stabilized Zirconia (YPSZ) are accepted and standardized ceramic materials in clinical use today, and have a long clinical history in hip joint replacement in articulation with Polyethylene or themselves (Alumina). Although effective, both materials have specific potential disadvantages. Alumina exhibits excellent hardness and wear properties, however it is a brittle material with a risk of fracture. Also certain design restrictions apply to Alumina due to this property. Zirconia has only 50% of Alumina's hardness but transformation toughening improves fracture resistance. Therefore, its overall toughness and bending strength are substantially higher than Alumina. However because Zirconia is in a meta-stable form, phase transition can occur and affect its overall stability. The poor thermal conductivity of Zirconia that increases this phenomenon is also of concern. Therefore the ideal ceramic would be a material that combines the best properties of Zirconia and Alumina.

The objective of this study is to investigate the feasibility of a new Alumina based ceramic material with improved toughness for hip joint articulation applications against PE, itself or Alumina. This objective can be met by increasing the toughness and bending strength of Alumina, through the addition of Zirconia, whilst maintaining all other properties such as wear, hardness, stability and chemical inertness. Additions of approximately 25% Zirconia to Alumina during the manufacturing process have been shown promising to achieve the objectives (Zirconia Toughened Alumina, ZTA [1]).

## Materials and Methods

Two candidate Zirconia Toughened Alumina (ZTA) ceramics were obtained. The samples were supplied in the form of bars (45 x 4 x 3 mm), flat polished coupons and ball heads as well as inserts for modular cups (28 mm). At least 10 samples per test were used.

One ZTA (NZTA) had a composition of 75% Alumina and 25% Zironia, the other one, (CZTA) had a composition of 74% Alumina, 24% Zirconia and 1% mixed oxides. To characterize the two new ZTA's several methods were used. Alumina served for all tests as a reference. Mechanical testing involved: hardness (HV), flexural strength (ASTM C1161) and indentation fracture toughness determination. X-ray diffraction (XRD) was used to measure the cyrstalline phase composition of the ZTA's and was also used to monitor any transformation during aging. Aging was conducted in two ways; by accelerated aging (5 hrs at 134°C in a steam autoclave, equivalent to 20 years in vivo) and real time aging for one year (Ringer's solution at 37°C) at intervals of 6 months. Wear simulator testing has been carried out applying a six-station physiological hip simulator, described elsewhere. The simulator testing was done using standard conditions and in micro-separation mode [2]. All test data was analyzed by descriptive statistics where applicable.

## Results

The results obtained for the unaged specimen are summarized in table 1. One candidate material (NZTA) has a significantly lower flexural strength than the other one (CZTA). However even this value is between 50% to 75% stronger than Alumina; statistically significant at $p < 0.05$. The indentation fracture toughness was measured and gave a $K_{IC}$ of 4.1 $MPa*m^{½}$ for both ZTA materials as opposed to 2.78 $MPa*m^{½}$ for Alumina. The ZTA ceramics maintain almost the same hardness values as the base Alumina,, statistically not significant at $p > 0.05$.

| Test | Units | Alumina | CZTA | NZTA |
|---|---|---|---|---|
| **Flexural Strength** | MPa | 466 ± 106 | 1203 ± 101 | 800 ± 131 |
| **Fracture toughness** | $MPa*m^{½}$ Indentation | 2.78 | 4.1 | 4.1 |
| **Hardness** | HV(30) | 1878 ± 60 | 1840 ± 60 | 1840 ± 60 |

**Table1. Mechanical test results for the unaged ZTA ceramics**

The two ZTA ceramics differ in the crystalline form of Zirconia seen at the surface when measured by XRD. NZTA contains Zirconia in a purely tetragonal crystalline form with no measurable monoclinic phase present. CZTA contains Zirconia with up to 35% of the monoclinic phase present at the surface. No further transformation in the Zirconia phase was observed after accelerated aging and up to 12 months real time aging for both ZTAs'. This indicates the ZTA is a chemically stable ceramic.

The wear testing, in standard simulator mode, showed that both ZTA - ZTA couples articulating against themselves have even lower wear than Alumina – Alumina couples, this wear rate being reported elsewhere [3]. Using the micro separation simulator set-up, similar results for both ZTA - ZTA combinations were obtained. Although the overall wear rate was increased in this mode, it also reached a steady state after 1 million cycles. ZTA's wore also in this test set-up – statistically not significant – less than the Alumina – Alumina combination.

## Discussion

The objective of this innovation was to increase the toughness and bending strength of Alumina. This was achieved through the addition of ca. 25% Zirconia to the Alumina matrix. The hardness is not affected but the toughness and the flexural strength of the ceramic has been increased by up to 50% thus reducing the risk of fracture with such ceramic implant components. This two different ZTA's demonstrate their ability to achieve superior properties to Alumina and maintain them during accelerated and normal aging. The wear properties under standard and adverse tribological conditions also demonstrate improvement over Alumina, although statistically not significant. Zirconia Toughened Alumina looks promising for the next generation of fracture and wear resistant ceramic bearings for hip joint prostheses.

[1] G.Orange, G.Fantozzi, P.Homerin, F. Thevenot; Journal of European Ceramic Society, 9 (1992) 177-185.

[2] J.E.Nevelos et al; Journal of Arthroplasty, 2000, in press.

[3] J.E.Nevelos et al; ORS, 46th Annual Meeting, Orlando, FL/March, 12-15, 2000.

***University of Bath, Bath, UK.
****University of Leeds, Leeds, U.K..

Streicher, R.M. (2)
Alte Landstr.36C,
CH-8802,Kilchberg,
Switzerland
0041-17156361 / Fax: 0041-17156362 /
rms@bluewin.ch

Additional Info and Keywords

Total Joint Arthroplasty;Hip;Ceramic;Mechanical Properties;Wear

ABSTRACT NO. _____
PAPER NO. _____

Disclosure
(E-Stryker Howmedica Osteonics) (A-Stryker Howmedica Osteonics) (E-Stryker Howmedica Osteonics)

# NEW DEVELOPMENTS IN HARD BEARING MATERIALS FOR ORTHOPAEDIC JOINT APPLICATIONS

*Insley, G (E-Stryker Howmedica Osteonics); ***Turner, I; ****Fisher, J (A-Stryker Howmedica Osteonics); +**Streicher, R (E-Stryker Howmedica Osteonics)
*Stryker Howmedica Osteonics, Limerick, Ireland. +**Stryker Howmedica Osteonics, Rutherford, US. Alte Landstr.36C,, CH-8802,Kilchberg,, Switzerland, 0041-17156361, Fax: 0041-17156362, rms@bluewin.ch

## Introduction

Alpha-Alumina and partially stabilized Zirconia (YPSZ) are accepted and standardized ceramic materials in clinical use today, and have a long clinical history in hip joint replacement in articulation with Polyethylene or themselves (Alumina). Although effective, both materials have specific potential disadvantages. Alumina exhibits excellent hardness and wear properties, however it is a brittle material with a risk of fracture. Also certain design restrictions apply to Alumina due to this property. Zirconia has only 50% of Alumina's hardness but transformation toughening improves fracture resistance. Therefore, its overall toughness and bending strength are substantially higher than Alumina. However because Zirconia is in a meta-stable form, phase transition can occur and affect its overall stability. The poor thermal conductivity of Zirconia that increases this phenomenon is also of concern. Therefore the ideal ceramic would be a material that combines the best properties of Zirconia and Alumina. ZTA ( zirconia toughened Alumina ) does exactly this.

The objective of this study is to characterise two candidate ZTA materials in terms of the properties required for orthopaedic bearing applications.

## Materials and Methods

Two candidate Zirconia Toughened Alumina (ZTA) ceramics were obtained. The samples were supplied in the form of bars (45 x 4 x 3 mm), flat polished coupons and ball heads as well as inserts for modular cups (28 mm). At least 10 samples per test were used.

One ZTA (NZTA) had a composition of 75% Alumina and 25% Zironia, the other one, (CZTA) had a composition of 74% Alumina, 24% Zirconia and 1% mixed oxides. To characterize the two new ZTA's several methods were used. Alumina served for all tests as a reference. Mechanical testing involved: hardness (HV), flexural strength (ASTM C1161) and indentation fracture toughness determination. X-ray diffraction (XRD) was used to measure the crystalline phase composition of the ZTA's and was also used to monitor any transformation during aging. Aging was conducted in two ways; by accelerated aging (5 hrs at 134°C in a steam autoclave, equivalent to 20 years in vivo) and real time aging for one year (Ringer's solution at 37°C) at intervals of 6 months. Microstructural analysis involved thermal etching the samples at 1500°C for 15 minutes and then analysing the ceramics using a scanning electron microscope. Wear simulator testing has been carried out applying a six-station physiological hip simulator, described elsewhere. The simulator testing was done using standard conditions and in micro-separation mode [1]. All test data was analyzed by descriptive statistics where applicable.

## Results

The results obtained for the unaged specimen are summarized in table 1. One candidate material (NZTA) has a significantly lower flexural strength than the other one (CZTA). However even this value is between 50% to 75% stronger than Alumina; statistically significant at $p < 0.05$. The main reason for this difference can be explained by considering the microstructure of these ceramics. The CZTA material has a much finer grain size as outlined in table 1, thus giving it superior strength properties. The indentation fracture toughness was measured and gave a $K_{IC}$ of 4.1 MPa*$m^{½}$ for both ZTA materials as opposed to 2.78 MPa *$m^{½}$ for Alumina. The ZTA ceramics maintain almost the same hardness values as the base Alumina, statistically not significant at $p > 0.05$.

| Test | Units | Alumina | CZTA | NZTA |
|---|---|---|---|---|
| Flexural Strength | MPa | 466 ± 106 | 1203 ± 101 | 800 ± 131 |
| Fracture toughness | MPa*$m^{½}$ Indentation | 2.78 | 4.1 | 4.1 |
| Hardness | HV(30) | 1878 ± 60 | 1840 ± 60 | 1840 ± 60 |
| Grain size | µm | 4.3 | 0.8–Al<br>0.08 - Zr | > 3.0 – Al<br>> 0.8 - Zr |

**Table1. Mechanical test results for the unaged ZTA ceramics**

The two ZTA ceramics differ in the crystalline form of Zirconia seen at the surface when measured by XRD. NZTA contains Zirconia in a purely tetragonal crystalline form with no measurable monoclinic phase present. CZTA contains Zirconia with up to 35% of the monoclinic phase present at the surface. No further transformation in the Zirconia phase was observed after accelerated aging and up to 12 months real time aging for both ZTAs'. This indicates the ZTA is a chemically stable ceramic.

The wear testing, in standard simulator mode, showed that both ZTA - ZTA couples articulating against themselves have even lower wear than Alumina – Alumina couples, this wear rate being reported elsewhere [2]. Using the micro separation simulator set-up, similar results for both ZTA - ZTA combinations were obtained. Although the overall wear rate was increased in this mode, it also reached a steady state after 1 million cycles. ZTA's wore also in this test set-up – statistically not significant – less than the Alumina – Alumina combination.

## Discussion

The objective of this innovation was to characterise ZTA ceramics for orthopaedic bearing applications. This was achieved. The hardness, toughness and the flexural strength of the ceramic is up to 50% stronger than Alumina thus reducing the risk of fracture with such ceramic implant components. These two different ZTA's demonstrate their ability to achieve superior properties to Alumina and maintain them during accelerated and normal aging. The wear properties under standard and adverse tribological conditions also demonstrate improvement over Alumina, although statistically not significant. Zirconia Toughened Alumina looks promising for the next generation of fracture and wear resistant ceramic bearings for hip joint prostheses.

[1] J.E.Nevelos et al; Journal of Arthroplasty, 2000, in press.

[2] J.E.Nevelos et al; ORS, 46th Annual Meeting, Orlando, FL/March, 12-15, 2000.

***University of Bath, Bath, UK.
****University of Leeds, Leeds, UK.

Stewart, Todd (1)
The School of Mechanical Engineering
The University of Leeds
Leeds, LS2 9JT
United Kingdom44 113 2332125 / Fax: 44 113 2424611 / T.D.Stewart@leeds.ac.uk

**Additional Info and Keywords**

Hip;Wear;Microseparation;Ceramic on Ceramic;Zirconia Toughened Alumina (ZTA)

ABSTRACT NO. _____
PAPER NO. _____

**Disclosure**
(A-Stryker Howmedica Osteonics and The Arthritis Research Campaign)

# WEAR OF ZIRCONIA TOUGHENED ALUMINA HEADS AGAINST HIPED ALUMINA INSERTS IN A HIP SIMULATOR UNDERGOING SWING PHASE MICROSEPARATION

+*Stewart, T (A-Stryker Howmedica Osteonics and The Arthritis Research Campaign); *Fisher, J; **Ingham, E; ***Insley, G; ***Streicher, R
+*The School of Mechanical Engineering, The University of Leeds, Leeds, LS2 9JT, UK. 44 113 2332125, Fax: 44 113 2424611, T.D.Stewart@leeds.ac.uk

**Introduction** Recently Zirconia Toughened Alumina (ZTA) femoral heads have been introduced for hip prostheses as an alternative to the current generation of Hot Isostatic Pressed Alumina. ZTA is reported to offer improved toughness compared to alumina ceramic without a significant reduction in hardness, making it a potentially more flexible for the design of ceramic–ceramic hip prostheses (1). There is, however, no published data on the wear of ZTA on Alumina under microseparation conditions that have been shown for Alumina on Alumina to provide clinically relevant wear rates, wear mechanisms and wear debris (2, 3). The purpose of this study was to evaluate the long-term wear performance of Zirconia Toughened Alumina heads against HIPed Alumina inserts in a hip joint simulator incorporating swing phase microseparation.

**Materials and Methods** Two commercially available materials were tested Zirconia Toughened Alumina (ZTA) and 3rd Generation Hot Isostatic Pressed (HIPed) Alumina. The ZTA ceramic was Biolox Delta and the HIPed Alumina ceramic was Biolox Forte, both were manufactured by CeramTec. In the hip simulator three Biolox Delta ZTA heads were tested against Biolox Forte HIPed Alumina inserts (ZTA/AL) and three Biolox Forte HIPed Alumina heads were tested against Biolox Forte Alumina inserts (AL/AL). A six station hip joint simulator was used providing a physiological twin peak time dependant loading curve with an elliptical wear path. Inserts were positioned anatomically 'on top' inclined at 45° to the horizontal axis. Heads underwent flexion/extension +30° to -15° and the insert internal/external rotation ±10°.

The procedure of microseparation involved applying a small lateral to medial load to the acetabular insert with a spring, which, during the swing phase when the joint load was reduced, produced a medial (200- 500µm) and superior translation of the insert relative to the head resulting in impact between the head and the superior rim of the insert (4). Severity of conditions was altered by adjusting the swing phase load in the simulator which, when reduced from 400N for mild conditions to 50N for severe conditions, made it easier for the medial separation force to both overcome friction and to produce superior translation between the head and insert. This, in turn, increased the velocity of the insert and upon impact with the head produced an increased momentum and impact energy which resulted in a more severe microseparation condition. The variable swing phase load, therefore, may be representative of varying degrees of joint laxity.

**Results** The simulator produced a regular pattern of micro-separation. A stripe of wear was formed on all of the heads of both ZTA on Alumina and HIPed Alumina on Alumina bearing combinations, which increased the surface roughness Ra from < 0.005 µm to between 0.02 and 0.13 µm. Wear volumes are shown in Figure 1. It can be seen that in the microseparation mode the wear of HIPed Alumina on Alumina increased considerably compared to previously tested HIPed Alumina on Alumina under standard conditions with no microseparation. Under severe microseparation conditions the wear rates of the ZTA on Alumina was significantly less than the wear of HIPed Alumina on Alumina. Wear rates under standard and micro-separation conditions are shown in Figure 2. A bedding-in wear rate of 0.99 mm³/million cycles was observed during the initial 1 million cycles corresponding to the formation of stripe of wear on the ZTA femoral heads and a matching area on the rim of the HIPed Alumina acetabular inserts. The wear rate then reduced to a lower steady state level of 0.37 mm³/million cycles for the remainder of the study resulting in an overall average wear rate of 0.49 mm³/million cycles. The wear of ZTA on Alumina was significantly lower than the wear of HIPed Alumina on Alumina where bedding-in, steady state and overall wear rates of 4.0, 1.31, and 1.85 mm³/million cycles were observed respectively.

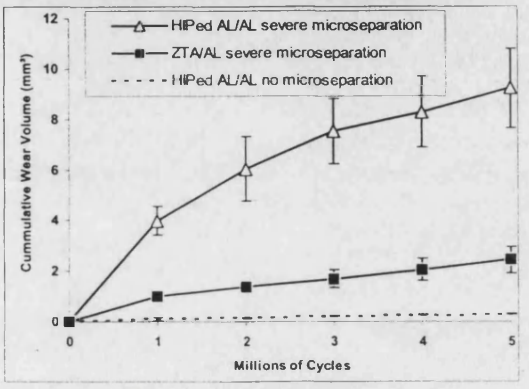


Figure 1. Wear Volumes ±SE, n=3

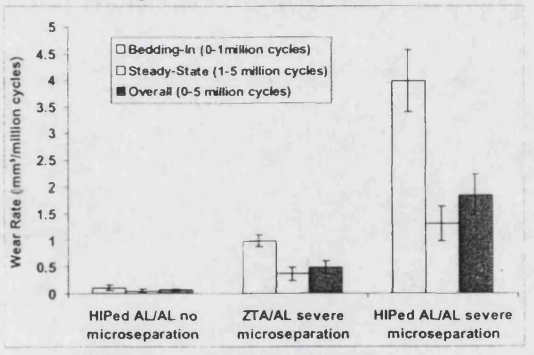


Figure 2. Average Wear Rates ±SE, n=3

**Discussion** Long term *in-vitro* microseparation of Zirconia Toughened Alumina heads against HIPed Alumina ceramic inserts produced an overall average wear rate of 0.49 mm³/million cycles under severe conditions. This was three times lower than observed with HIPed Alumina ceramic bearings under the same severe conditions which produced an overall average wear rate of 1.84 mm³/million cycles. A characteristic stripe of wear was observed on all femoral heads with a corresponding area on the rim of the acetabular inserts. Wear was characterised by an initially higher bedding-in period during the initial 1 million cycles which reduced to a lower steady state level for the remaining 4 million cycles with no runaway wear observed.

The results suggest that the Zirconia Toughened Alumina femoral heads articulating against HIPed Alumina acetabular inserts have better resistance to microseparation damage and wear compared to HIPed Alumina on Alumina. This may be due to the improved mechanical properties of the ZTA femoral head.

**Acknowledgements** The research was funded by Stryker Howmedica Osteonics and the Arthritis Research Campaign.

**Division of Microbiology, The University of Leeds, Leeds, LS2 9JT, UK.
***Stryker Howmedica Osteonics, Alte Landstr. 36C, CH-8802 Kilchberg, Switzerland.

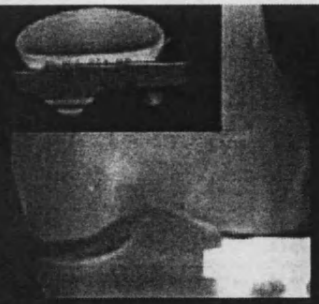

Garino/ Willmann

Bioceramics in Joint Arthoplasty

# Bioceramics in Joint Arthoplasty

## Proceedings 7th International BIOLOX® Symposium March 15/16 2002

Ceramic acetabular cups have been used successfully for more than thirty years in total hip arthroplasty. Pioneering one piece designs are no longer used as a result of mechanical loosening complications related to their design. These early concepts were replaced in the late 80's with modular ceramic inserts used in conjunction with proven non-cemented hemispherical shells and have addressed well these early design related problems.

Throughout this evolution, the performance and reliability of the ceramic components has been excellent. As a result of this and in answer to the challenge created by wear debris generated osteolysis, a renewed interest has surfaced in the ceramic on ceramic articulation. This renaissance has created a new alternative for the young and active patients in search of a more durable and longer term option Total Hip Replacement.

The objective of the 7th BIOLOX® Symposium has been to assemble experts and have them present the current state-of-the-art in the alternative bearing area along with their clinical experience with current generation of ceramic inserts.

In addition a special chapter has been included which reviews the status and the options of ceramics for total knee replacement.

Edited by
Jonathan P. Garino
Gerd Willmann

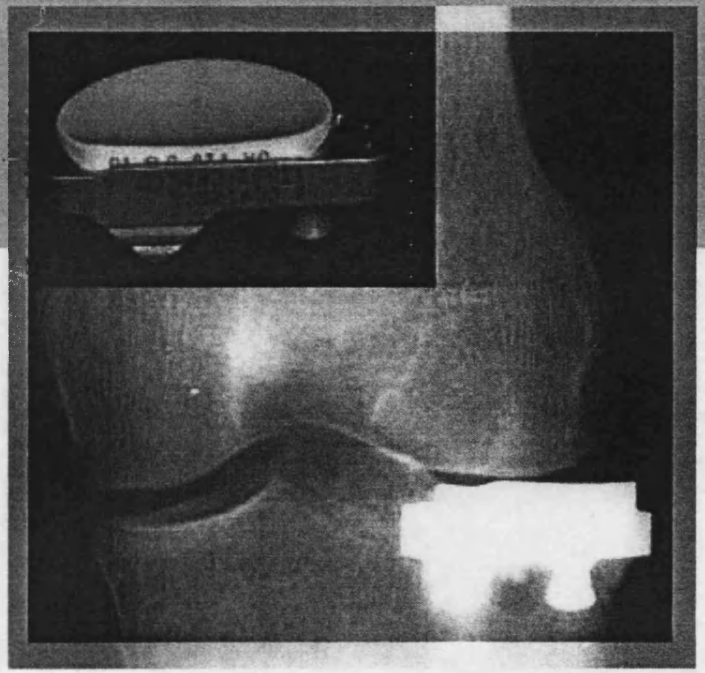

ISBN 3-13-132651-4

Unsere Homepage:

Thieme

lox Forte' alumina/alumina hip joints in a physiological simulator. In 45th Annual Meeting, 45th ORS, 1999; p. 857.
14 Stewart T, Williams S, Ingham E Stone M and Fisher, J. Wear of metal-metal and ceramic-ceramic hip prostheses with swing-phase micro separation. In 48th ORS, 2002: p. 128.
15 Kaddich C. and Pfaff, HG. Wear study in the alumina-zirconia system. In Bioceramics in Hip Joint Replacement, Eds: G. Willmann and K. Zweymüller, Proc 5th International CeramTec Symp, 2000: 146–150.
16 Clarke, I. C., Schroeder, D., Williams, P. A., Good, V., Anissian, L., Stark, A., Oonishi, H., Schuldies, J. and Gustafson, A. Ultra-low wear rates for rigid = on-rigid bearings in total hip replacements. Proc. Instn. Mech. Engrs. 2000; 214: 333–347.
17 ISO/DIS 14242-1: 1999–2006: Implants for surgery – wear of total hip prostheses – Part 1: loading and displacement parameters for wear testing machines and corresponding environmental conditions for test.
18 Kawanabe, K., Clarke, I. C., Good, V. and Yamamoto, K. Hydraulic pressure for removal of femoral heads – A novel technique. Submitted for publication, 2002.
19 Clarke IC, Chan, W., Essner, A., Good, V., Kaddich, C., Lappalainen R., Laurent, M., McKellop, H., McGarry, W., Schroeder, D., Selenius, M., Shen, MC., Ueno, MC., Wang, A. and Yao, J. Multi-laboratory simulator studies on effects of serum proteins on PTFE cup wear. Wear 2001; 250: 188–198.
20 Clarke, Ic., Oonishi, H., Anissian, L., Williams, P., Stark, A., and Gustafson, A. Serum protection important for all-metal and all-ceramic (rigid-rigid) bearings in hip simulator studies. In 48th Annual Meeting of the Orthopaedic Research Society, 2002, 1017.
21 Schmalzried, T. P., Szuszczewicz, E. S., Northfield, M., Akizuki, K., Frankel, R., Belcher, G. and Amstutz, H. C. Quantitative Assessment of Walking Activity after Total Hip or Knee Replacement. J Bone Jt. Surg., 1998; 80 A: 54–59.

## 1.5 In-Vitro Testing and Validation of Zirconia Toughened Alumina (ZTA)

G. M. Insley, I. Turner, J. Fisher, R. M. Streicher

### Introduction

Alumina and partially stabilized zirconia (YPSZ) are accepted and standardized ceramic materials in clinical use today. These ceramics have a long clinical history in hip joint replacement in articulation with polyethylene or, in the case of alumina, in articulation with itself.

Although effective, both materials have specific potential disadvantages. Alumina exhibits excellent hardness and wear properties, however it is a brittle material with a risk of fracture. This risk is low, typically 1 in 25 000, depending on what series examined [1] however this is a problem. This hard but brittle combination of material properties also means that certain design restrictions apply to alumina.

Zirconia has only 50% of alumina's hardness but transformation toughening improves its fracture resistance. Therefore, its overall toughness and bending strength are substantially higher than alumina. However because zirconia is in a meta-stable form, phase transition can occur and affect its overall stability. The poor thermal conductivity of zirconia that increases this phenomenon is also of concern.

Therefore the ideal ceramic would be a material that combines the best properties of zirconia and alumina. ZTA (zirconia toughened alumina) is a next generation ceramic that does exactly this.

Any new ceramic material proposed for joint articulation needs to be rigorously tested to prove that it can at least perform as good as the current generation ceramics. Indeed, if they are proposed as being the next generation, then they have to have distinct advantages to merit this description. The objective of this study is to characterise two candidate ZTA materials in terms of the properties required for orthopaedic bearing applications. The test methods are designed where possible to test the ceramic in simulated adverse clinical conditions and compare their performance to the current standard ceramics.

## Materials and Methods

Two candidate zirconia toughened alumina (ZTA) ceramics were obtained. The samples were supplied in the form of bars (45 × 4 × 3 mm), flat polished coupons and ball heads as well as inserts for modular cups (28 mm). At least 10 samples per test were used. Alumina (commercial Biolox Forte, Ceramtec, Germany) served for all tests as a reference.

One ZTA (NZTA) had a composition of 75% alumina and 25% zirconia, and was a batch-processed material. The other ZTA, (CZTA) had a composition of 74% alumina, 24% zirconia and 1% mixed oxides.

To characterize the two new ZTA's several methods were used. Mechanical testing involved: hardness (HV), flexural strength (ASTM C1161), ultimate compression strength (UCS) (ISO 7206-5) and indentation fracture toughness determination. X-ray diffraction (XRD) was used to measure the crystalline phase composition of the ZTA's and was also used to monitor any tetragonal to monoclinic transformation during aging. Aging was conducted in two ways; by accelerated aging (5 hrs at 134 °C in a steam autoclave, equivalent to 20 years in vivo) and real time aging for one year (Ringer's solution at 37 °C) at intervals of 6 months.

Microstructural analysis involved thermal etching the samples at 1500 °C for 15 minutes and then analysing the ceramics using a scanning electron microscope.

Wear simulator testing was carried out applying a six-station physiological hip simulator, described elsewhere [2]. The simulator testing was done using standard conditions and in microseparation mode. Under standard conditions the Leeds MKII simulator applies a small positive swing phase load, which ensures the head remains located correctly in the insert. To provide microseparation of the head and cup a small lateral to medial load was applied with a spring. Microseparation conditions were varied by altering the swing phase load from 400 N for mild to 50 N for severe separation. The medio-lateral separation load was regularly adjusted in each of the six stations to provide between 200 and 500 µm of medio-lateral motion.

All test data was analyzed by descriptive statistics where applicable.

## Results

### Mechanical properties

The results obtained for the unaged specimen are summarized in (Table **1**). One candidate material (NZTA) has a significantly lower flexural strength than the other one (CZTA). However, even this value is between 50% to 75% stronger than Alumina; statistically significant at $p < 0.05$. The main reason for this difference can be explained by considering the microstructure of these ceramics. The CZTA material has a much finer grain size (Table **1**), thus giving it superior strength properties. A further reason for the difference in strength is the dispersion of the zirconia grains in the alumina matrix. The NZTA is a batch-processed material and as can be seen from (Fig. **1 a**) its microstructure has not been optimised. There are large agglomerates of zirconia grains throughout the alumina matrix. The commercially processed CZTA has a much finer dispersion of zirconia grains (Fig. **1 b**).

The indentation fracture toughness was measured and gave a $K_{IC}$ of 4.1 MPa × $m^{½}$ for both ZTA materials as opposed to 2.78 MPa × $m^{½}$ for alumina. The ZTA ceramics maintain almost the same hardness values as the base alumina, statistically not significant at $p > 0.05$.

The ultimate compression strength (UCS) showed that both ZTA materials surpass the FDA

Table 1 Mechanical test results for alumina & unaged ZTA ceramics

| Test | Units | Alumina | CZTA | NZTA |
|---|---|---|---|---|
| Flexural Strength | MPa | 466 ± 106 | 1203 ± 101 | 800 ± 131 |
| Fracture toughness | MPa × $m^{½}$ Indentation | 2.78 | 4.1 | 4.1 |
| Hardness | HV (30) | 1878 ± 60 | 1840 ± 60 | 1840 ± 60 |
| Grain size | µm | < 2 | Al – 0.872 ± 0.26<br>Zr – 0.355 ± 0.09 | Al – 1105 ± 0.45<br>Zr – 0.265 ± 0.05 |

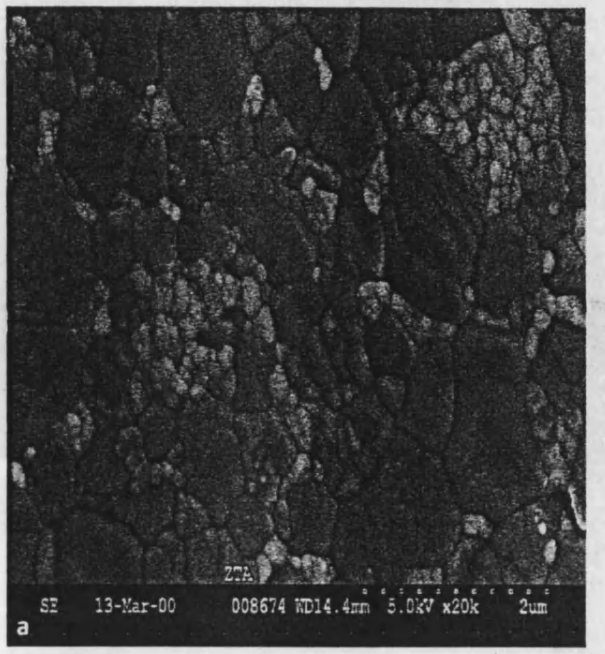


Fig. **1 a** NZTA microstructure.

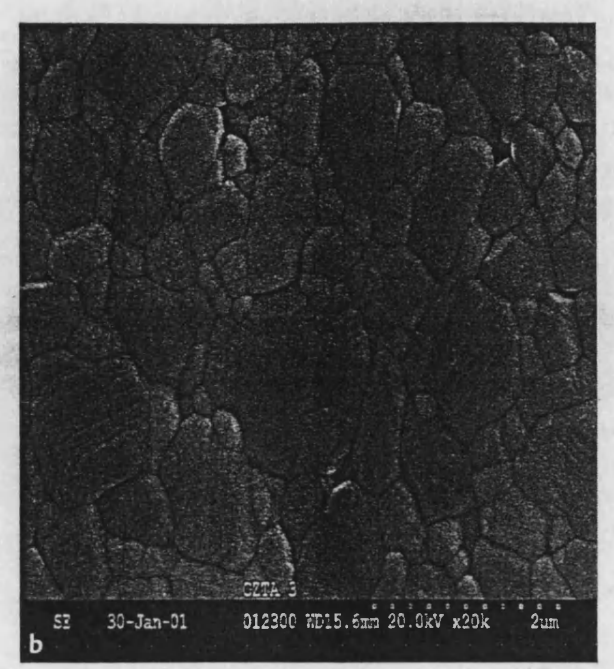


Fig. **1 b** CZTA microstructure.

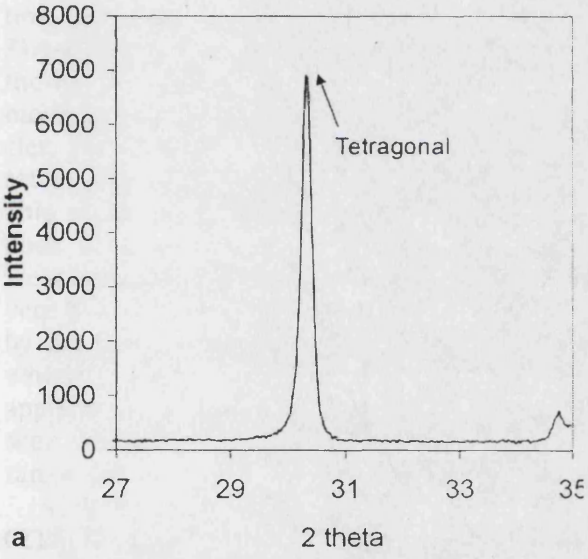


Fig. **2 a** NZTA as received and aged.

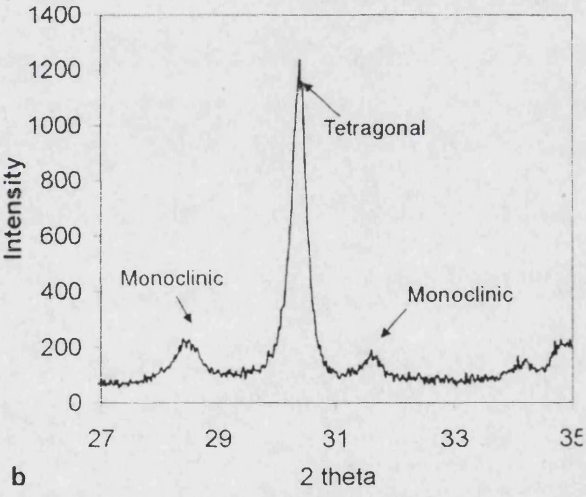


Fig. **2 b** CZTA as received and aged.

requirement of 46 KN for all spigot materials tested on both the femoral heads and the cups.

### Aging properties

The two ZTA ceramics differ in the crystalline form of Zirconia seen at the surface when measured by x-ray diffraction (XRD). NZTA contains Zirconia in a purely tetragonal crystalline form with no measurable monoclinic phase present (Fig. **2 a**). CZTA contains Zirconia with up to 35% of the monoclinic phase present at the surface (Fig. **2 b**). No further transformation in the Zirconia phase was observed after accelerated aging and up to 12 months real time aging for both ZTAs'. This indicates the ZTA is a chemically stable ceramic.

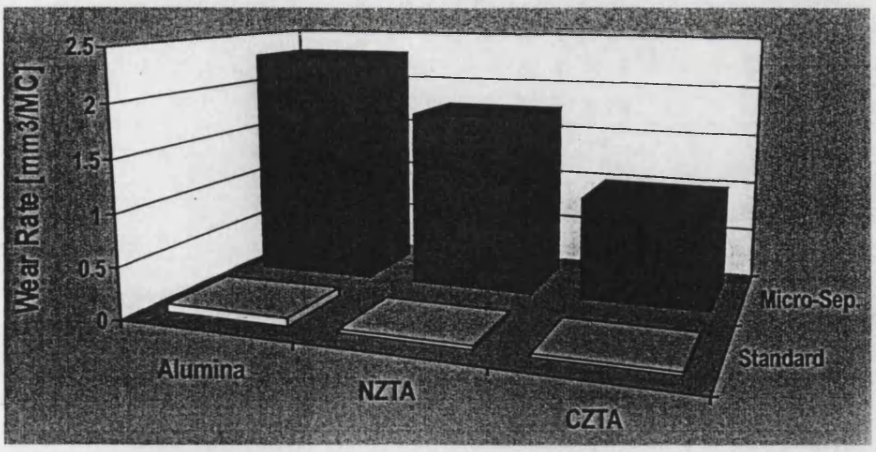


Fig. **3** Wear results for Al, NZTA and CZTA in both normal and microseparation mode.

### Wear

The wear testing, in standard simulator mode, showed that both ZTA couples articulating against themselves have even lower wear than alumina – alumina couples, this wear rate being reported elsewhere [2]. Using the micro separation simulator set-up, similar results for both ZTA-ZTA combinations were obtained (Fig. **3**). Although the overall wear rate was increased in this mode, it reached a steady state after 1 million cycles. The ZTA's also performed better in this test set-up than the alumina – alumina combination. This result is statistically not significant but it does illustrate that these materials are more wear resistant than the alumina even in this severe hip simulation mode. This can be explained by the finer grain structure of the ZTA material, which is more resistant to damage caused by the application of high point stresses such as that seen when the head contacts the rim of the ceramic cup.

Very low wear rates were also measured on a CZTA/Al couple in severe microseparation mode. The Zirconia Toughened Alumina heads against HIPed alumina inserts produced an average wear rate of 0.61 $mm^3$/million cycles under these severe conditions, three times lower than the wear rate of HIPed alumina on alumina (Fig. **4**).

A characteristic stripe of wear was observed on all femoral heads with a corresponding area of damage on the rim of the acetabular inserts.

Extremely low wear (< 0.1 $mm^3$/million cycles) has been reported for zirconia femoral heads articulating against alumina inserts for hip prostheses under normal laboratory hip simulation conditions. This bearing combination has been recently introduced into clinical use [3, 4]. These in-vitro testing conditions, however, produce wear by relief polishing of the ceramic grains and are not indicative of the wear of explanted devices which, for alumina prostheses have shown wear rates an order of magnitude higher (~ 1 $mm^3$/million cycles) with areas of intragranular fracture [5].

When tested in microseparation, the zirconia on alumina couple had wear volumes significantly greater than the ZTA on ZTA couple in hip simulation tests with severe microseparation (Fig. **5**). Additionally the elevated wear of Zirconia on Alumina led to fracture of the rim of one Alumina insert after ~ 2 million cycles and fracture of one Zirconia head after ~ 2.4 million cycles leaving only one joint of three to survive the full 5 million cycle test duration.

## Discussion

The current generation ceramic materials used in orthopaedics have a long and successful clinical history offering many advantages for clinical use in younger more active patients. However, there are certain disadvantages with these materials i.e. risk of fracture.

Scientists and clinicians are constantly looking to improve orthopaedic materials to achieve even more successful clinical outcomes in the future.

Zirconia toughened alumina is a next generation ceramic material for hip joint articulation applications and has undergone extensive in-vitro validation testing with good results.

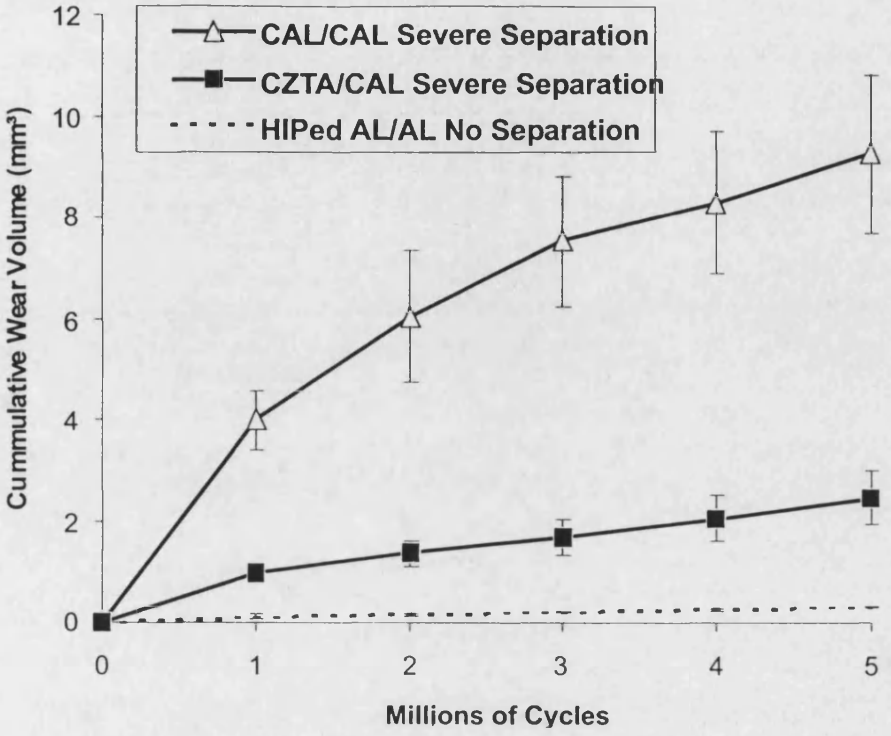


Fig. 4 Average cumul tive volumetric wear o ZTA/Al and Al/Al in mic separation mode.

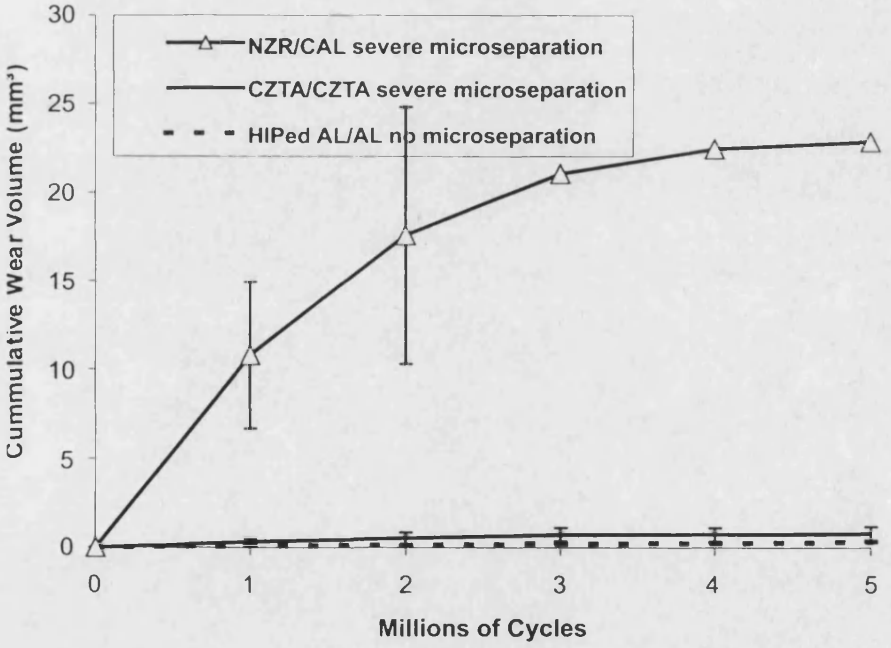


Fig. 5 Average cumul tive volumetric wear fo Zr/Al and CZTA/CZTA ir microseparation mode.

The ZTA is tougher, more fracture resistant than alumina whilst not having the ageing concerns associated with zirconia. The wear properties under standard and adverse tribological conditions demonstrate improvement over alumina, although statistically not significant. When ZTA is used in articulation against alumina cups the wear rate is significantly lower than that seen with alumina-on-alumina. The wear properties of the ZTA materials are significantly better t the catastrophic wear measured in the zirc on alumina couple, under the same severe mi separation testing conditions, and should be c tra-indicated for clinical use.

Zirconia Toughened Alumina looks promis for the next generation of fracture and wear sistant ceramic bearings for hip joint prosthes

### References

1 R. J. Heros, G. Willmann, Ceramics in Total Hip Arthroplasty: History, Mechanical Properties, Clinical Results and Current Manufacturing State of the Art, Seminars in Arthroplasty, Vol. 9, No. 2, (April), 1998: pp 114–122.

2 T Stewart, J L Tipper, R Streicher, E Ingham, J Fisher, Long Term Wear of HIPed Alumina on Alumina Bearings for THR Under Microseparation conditions, J. of Material Science, 12, 1053–1056, 2001.

3 F Villermaux *et al*, Trans. Soc. Biomat, 135, 1999.

4 C. Kaddick *et al*, 4th CeramTec Symposium, 96–101, 1999

5 J E Nevelos, E Ingham, C Doyle, R Streicher, A B Nevelos, W Walter, J Fisher, "Microseparation of the centres of Alumina-Alumina artificial hip joints during simulator testing produces clinically relevant wear rates and patterns". Journal of Arthroplasty, 15, 793–795, 2000.


# 1.6 Wear of Polyethylene Against Scratched Metallic Femoral Heads in Hip Prostheses

T. D. Stewart, J. L.Tipper, M. H. Stone, E. Ingham, J. Fisher

## Introduction

Polyethylene acetabular cups articulating on metal or ceramic femoral heads have been used as the articulating couple in the majority of hip prostheses implanted over the last forty years. Polyethylene wear debris generated at the articulating surfaces, has been found to accumulate in periprosthetic tissues and lead to adverse cellular reactions, osteolysis and loosening. There is currently much interest in reducing the wear rate of the polyethylene acetabular cups. Minakawa *et al* showed a significant difference in the surface roughness of explanted femoral heads (1). Both cobalt chrome and stainless steel femoral heads showed damage and scratching which significantly increased their surface roughness. In contrast explanted ceramic femoral heads showed little damage and retained their smooth highly polished surface finish.

The aim of this study was to investigate the effect of damage to metallic femoral heads on the wear rates of polyethylene acetabular cups.

## Materials and Methods

This paper combines both analysis of explants and laboratory simulator studies.

### Explanted Prostheses

Eighteen Charnley hip prostheses with polyethylene acetabular cups and stainless steel femoral heads were explanted from patients after between 10 and 19 years (2). The mean implant life was 12.9 years. Femoral head surface roughness was measured with a Form Talysurf 6 profilometer. Average surface roughness $R_a$ and average peak height of scratches above the mean line $R_{pm}$ were determined. Heads were measured in the articulating zone in areas of visually identified scratching. Heads were divided into two groups low damage $R_{pm} < 0.2\,\mu m$ and high damage $R_{pm} > 0.2\,\mu m$.

Wear of the respective acetabular cups was measured with a computer controlled measuring machine. Linear penetration and volumetric wear rates were determined for each of the cups and average for the low wear and high wear rate groups determined (2).

### Hip Simulator Studies

Three separate hip joint simulator studies were carried out using both smooth, as manufactured femoral heads and deliberately scratched femoral heads, where three discrete scratches were applied to replicate the third body damage found on explanted prostheses. In each case prostheses were run in the Leeds PA hip joint simulators for a period of three million cycles and then the heads

# Wear of Ceramic-Ceramic Hip Prostheses under Microseparation Simulation Conditions

*G.M.Insley[1], T. Stewart[2], J. Nevelos[2], J Fisher[2] and R.M.Streicher[3].*

[1]Stryker SA, Scientific and Clinical Affairs, Limerick, Ireland.
[2]School of Mechanical Engineering, University of Leeds, LS2 9JT UK
[3]Stryker SA, Scientific and Clinical Affairs, Thalwil, Switzerland

## 1. INTRODUCTION.

The majority of total hip prostheses currently implanted consist of a metal femoral head i.e. (cobalt chrome, nitrogen-strengthened stainless steel) articulating against an ultra high molecular weight polyethylene (UHMWPE) acetabular cup. Typical wear rates of 40-100 $mm^3$ per year have been reported corresponding to a linear penetration rate of the femoral head into the acetabular component of less than 0.25mm per year [1]. Even though the majority of these implants are successful there is a growing volume of evidence showing that wear debris from this combination leads to the eventual failure of the prosthesis [2,3]. It is generally believed that UHMWPE wear debris generated at the articulating surface enters the periprosthetic tissue where it triggers a number of defence mechanisms in the bone cells. The end result is osteoclastic bone resorption, leading to osteolysis and eventual loosening of the prosthesis. It is not the volume of wear particles that is important in this mechanism but the number of particles and their size range. Research has shown that particles in the size range 0.2-0.8 μm cause the highest biological response in the body [1].

The growing need to treat younger, more active patients has led to alternative bearing materials. Examples are the hard-on-hard bearing combinations of ceramic-on-ceramic and metal-on-metal. Ceramic-on-ceramic replacement hip joints have been in use since 1970. The earliest examples of ceramic-on-ceramic total hip replacements and surface replacements were those designed by Boutin, Griss, Salzer and Mittelmeier. These involved alumina femoral heads articulating against alumina acetabular cups, and were designed to provide low wear and good durability. Alumina ceramics are compounds in their highest oxidation state, making them chemically inert. Additionally ceramics are very hard (alumina has a Vickers hardness of 1900 $Kgfmm^{-2}$), and are also hydrophilic which means that the surfaces have very good wettability. Furthermore, it is possible to polish ceramics to a very smooth finish with surface roughnesses ($R_a$) of < 0.005 μm. These factors combine to give ceramic counterfaces excellent tribological properties with potential for fluid film lubrication during walking [4]. The wettability and the smoothness of the ceramic surfaces aids in this lubrication, while the hardness and low friction of the surfaces resist damage and wear.

Wear rates of early alumina/alumina hip prostheses manufactured from first generation alumina have been shown to be low *in vivo*, ranging from 1 to 5 $mm^3$ per year [5]. The vast majority of retrieved components showed similar characteristic features within the worn bearing surfaces. These included:

An elliptical wear stripe on the head with maximum penetration up to 100μm
A worn area in the cup with evidence of rim wear.
An intergranular fracture wear mechanism.

Characteristically these early prostheses were revised for loosening of the acetabular cups, which was partly attributed to the poor fixation of the acetabular component to the bone.

In contrast, simulator testing of ceramic-on-ceramic hip prostheses yielded extremely low wear rates (< 0.1mm$^3$ per million cycles), an order of magnitude lower than those reported *in vivo*. Bearing surfaces were undamaged, with no noticeable change in surface roughness [6].

The wear stripes found in first generation alumina ceramics were believed to be related to the inferior quality of the ceramic material. Developments such as hot isostatic pressing (HIPing) and grain refinement, to increase the density and strength of the alumina, were considered to alleviate this problem. However, recently two modern alumina/alumina hip prostheses manufactured from second generation HIPed alumina retrieved after only one year showed wear patterns similar to those found in the early retrieved components, with a small elliptical wear stripe on the femoral head 2-5 µm deep and a small amount of wear on the rim of the acetabular cup. These two prostheses (Figure 1) were both revised due to trauma and were anatomically positioned and well fixed prior to revision [7]. Wear volumes for these components have been measured to be approximately 0.5 mm$^3$.

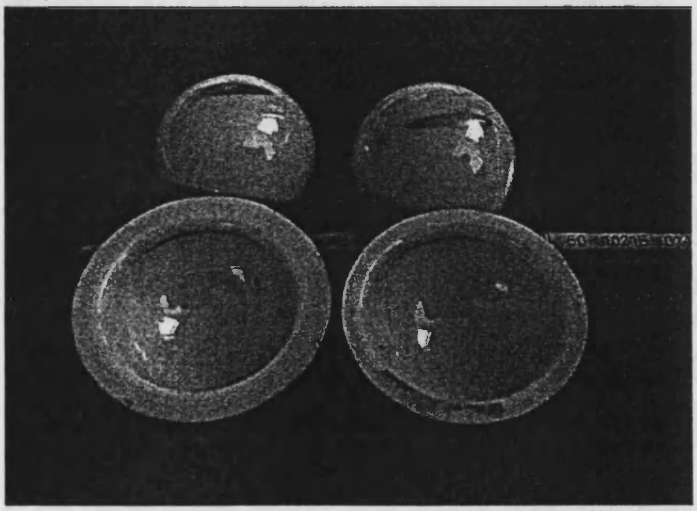

**Figure 1. Wear stripes on explanted HIPed alumina/alumina components after 1 year in vivo. The wear on the head and insert has been emphasised by rubbing with a graphite pencil.**

Wear patterns and mechanisms found clinically were not replicated in standard *in vitro* simulator tests.

Mallory *et al* [8] found by examining the fluoroscopic images of ten patients walking on a treadmill that the head and cup separate by a small amount during the swing phase. They found that the maximum separation was 2.8 mm and the minimum was 0.8 mm with an average separation seen at 1.2 mm. They also found that while the femoral head separated from the cup it remained in contact with the rim and postulated that high contact stresses would occur at this point with the application of load at heel-strike.

From this research it was hypothesized that microseparation of the head and cup could occur with any joint replacement and that this could be a factor in wear initiation for ceramic – ceramic systems as seen *in vivo*. Typically with these systems there is a very small clearance between the head and cup, of the order of 40 μm, and it is these tight clearances that allow the femoral head to contact the rim of the cup with only limited translation (Figure 2). Contact would occur with lateral and inferior displacements of less than 1 mm for a well-positioned prosthesis. Upon heel strike the head will translate superiorly and contact the rim before relocating. This rim contact will occur under very high stress and may initiate surface damage and hence accelerate wear [7].


**Figure 2.Schematic diagram showing of the stages of microseparation during the walking cycle**

This paper describes the wear of current and future ceramic-on-ceramic bearing couples under microseparation conditions in a laboratory.

## 2. MICROSEPARATION

*In vitro* microseparation was first reproduced by Nevelos *et al* (2000) using the Leeds mark II physiological hip joint simulator [7]. Under standard conditions this simulator applied a small positive swing phase load that ensured that the head remained located correctly in the cup throughout the gait cycle. To achieve joint separation a small lateral to medial load was applied to the acetabular insert, which, during the swing phase when the joint load was reduced, produced medial and superior translation of the insert relative to the head. Joint separation was limited by the radial clearance between the articulating components and ceased when the superior rim of the insert contacted the head after approximately 0.5 mm of translation. Further impact of the head and cup occurred with reapplication of the joint load at heel-strike. The load was momentarily supported by the small contact at the rim before the head relocated in the insert, thus modeling the clinical observations shown in Figure 2.

The microseparation technique reproduced for the first time clinically relevant levels of wear in ceramic-ceramic hip prostheses. The technique produced stripe wear with alumina/alumina via a similar intergranular fracture wear mechanism (Figure 3) to that seen *in vivo*. For additional validation of the technique, debris collected from the simulator were compared to debris from

retrieved tissues; both were found to contain predominantly nanometer - sized ceramic debris with the addition of a few larger ceramic particles attributed to microseparation.

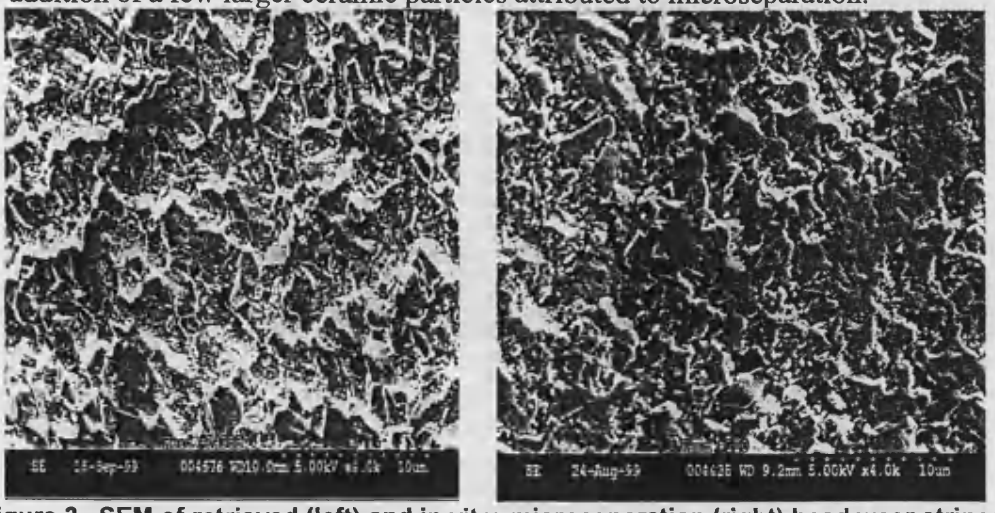

**Figure 3. SEM of retrieved (left) and in vitro microseparation (right) head wear stripes.**

Further research by Stewart *et al* (2001) showed that when the swing phase load in the simulator was reduced it becomes easier for the medial separation force both to overcome friction and to produce superior translation between the head and insert [9]. This increased the velocity of the insert and upon impact of the insert and head produced an increased momentum and impact energy, which resulted in a more severe microseparation condition. Therefore, by decreasing the swing phase load greater levels of joint laxity were modelled.

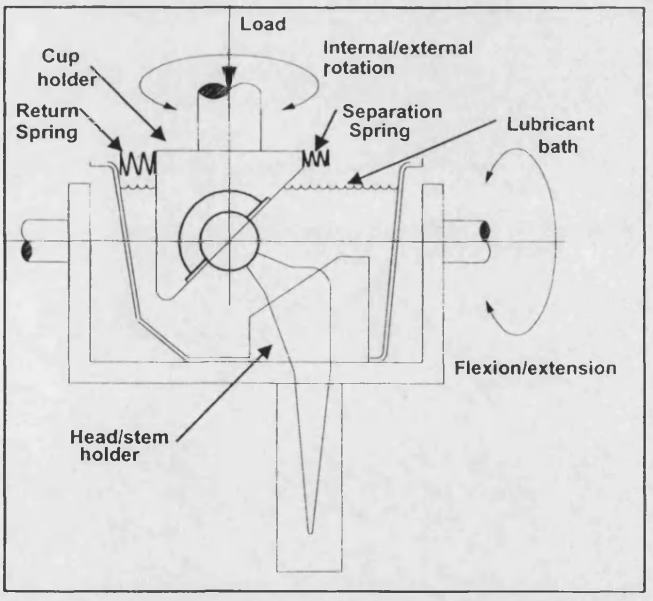


**Figure 4. Schematic diagram of the Leeds Mk II physiological hip joint simulator with microseparation.**

## 3. CERAMICS FOR HIP PROSTHESES

Alumina ceramic has been improved over the past 30 years and the introduction of hot isostatic pressing and grain refinement resulted in improved material properties, as shown in Table 1 [10].

**Table 1. Ceramic materials for hip prostheses**

| Ceramic | 1st generation alumina | 3rd generation alumina | Zirconia toughened alumina |
|---|---|---|---|
| Grain Size (μm) | <10 | <2 | <2 |
| Flexural Strength (MPa) | 400 | 580 | 1150 |
| Density (Mg $m^{-3}$) | 3.95 | 3.98 | 4.36 |
| Hardness (HV) | | 2300 | 1975 |
| Fracture Toughness (MPa $m^{1/2}$) | | 4.3 | 8.5 |
| Roughness $R_a$ (μm) | <0.05 | <0.005 | <0.005 |

One of the main disadvantages of ceramics in joint replacement has been their brittleness. Although the current reported fracture rate is low, typically 1 in 25000 [9] this remains a concern for some surgeons.

The addition of ~ 25 wt. % zirconia to the alumina matrix during manufacture has been shown to increase the fracture toughness and flexural strength of the alumina [10,11,12]. Two zirconia toughened aluminas (ZTAs) are currently available, one containing 74 wt. % alumina, 24 wt % zirconia and 1% mixed oxides, and another consisting of 75 wt. % alumina and 25 wt. % zirconia.

## 4. CERAMIC WEAR

The volumetric wear from standard simulator testing of alumina ceramic - on - ceramic bearings has generally been reported as < 0.1 $mm^3$ per million cycles. Microseparation simulation has been shown to increase this by a factor of 10, approaching clinical levels of wear as seen in retrieved first generation alumina hip prostheses (Figure 5).

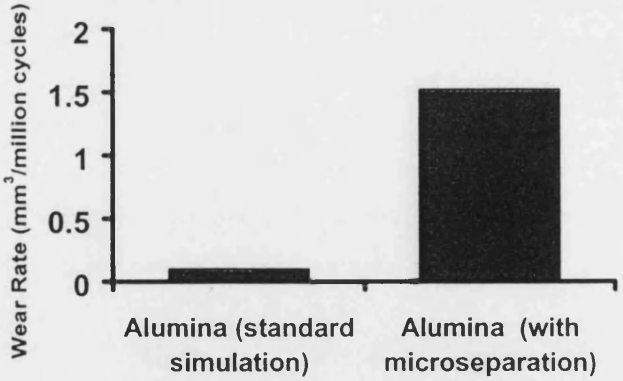


**Figure 5. In vitro ceramic wear; comparison of standard and microseparation simulator tests [7].**

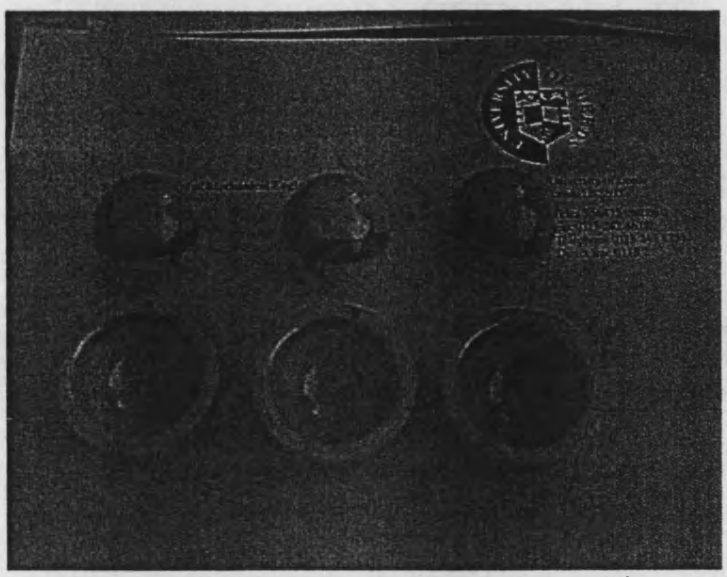

**Figure 7. Wear stripes on the alumina/alumina components after 5 million cycles in the Leeds hip simulator under microseparation conditions.**

Scanning electron microscopy (SEM) was used to examine the wear scars at a microscopic level. The scars produced by microseparation testing were remarkably similar to the wear scars seen on the explanted ceramics (Figure 3) and a similar grain boundary fracture wear mechanism was observed.

Wear debris collected and analysed from microseparation simulation of alumina/alumina were generally very small with a mean particle size of approximately 40 nm, as shown in Figure 8. This was similar to the debris collected from normal simulator tests with a mean particle size of 30 nm. The size range of these particles showed that the microseparation debris also contains a few larger particles that are not seen in normal simulation. Typically these were in the range of 100 to 3000 nm and compare well to the larger particles seen in the surrounding tissue of retrieved ceramic components.

Microseparation simulator studies have only, as yet, been reported from one centre. The findings so far support its use as a means to evaluate ceramic bearing materials in a more physiologically realistic manner.

Long term testing has been reported for the current generation of alumina hip prostheses [9] with typical wear behaviour as shown in Figure 6.

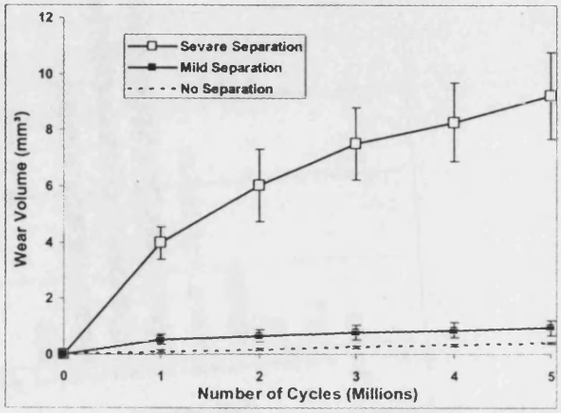


**Figure 6. Wear volumes ± Standard error, n=3 for each group.**

For the current Alumina materials under severe microseparation wear, was characterised by an initially higher wear period during which a characteristic wear stripe on the femoral head and the rim wear on the cup were initiated. The wear then decreased to a lower steady - state value with no signs of run-away wear observed. The severity of testing made a significant difference to the resulting wear rates of the alumina material, emphasising the need for careful control of experiments.

Worn surfaces appeared as shown in Figure 7, in which the wear on the head and insert has been emphasised by rubbing with a graphite pencil.

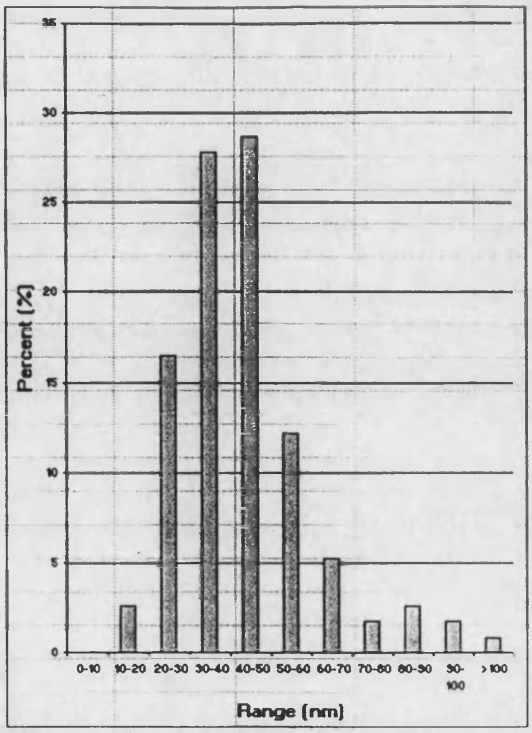


**Figure 8. Particle size distribution for wear debris from HIPed alumina tested in the simulator under microseparation conditions.**

Preliminary simulator studies have also been completed for two different ZTA materials under standard and microseparation conditions shown in Figure 9. The materials were tested in a concurrent study with HIPed alumina as a control, for a duration of 1 million cycles.

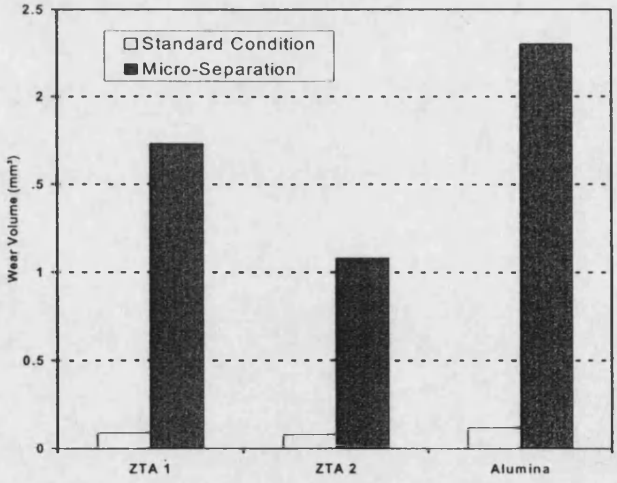


**Figure 9. Wear Volume of two ZTA materials in standard and microseparation simulator testing conditions compared to alumina.**

Under normal simulation conditions both ZTA materials showed slightly less wear than alumina/alumina. Under microseparation mode, the wear for all couples increased. However, the ZTA/ZTA couples wore less than the equivalent alumina/alumina couple.

## 5. Conclusions.

Standard simulator kinematics are not sufficient to reproduce the wear rates and mechanisms of alumina ceramic hip prostheses which are found in the clinical situation. However, simulation of a microseparation between the femoral head and acetabular cup during the swing phase in the hip joint simulator has reproduced clinically relevant wear rates, wear patterns, wear mechanisms and wear debris for alumina/alumina bearings.

Despite the increase in wear volume produced by the microseparation of ceramic-ceramic bearings the wear still remains significantly lower than the wear of traditional metal on UHMWPE bearings.

Preliminary results using zirconia toughened alumina composite ceramics show slightly lower wear than the alumina/alumina couple.

## References


[1] Ingham, E. and Fisher, J. Biological reactions to wear debris in total joint replacement. Proc. Instn. Mech. Engrs. Vol 214 Part H, 2000, 21-37.

[2] Amstutz, H.C.; Campbell, P.; Kossovsky, N. and Clarke I.C. Mechanism and clinical significance of wear debris induced osteolysis. Clin. Orthop.; 1992, 276, 7-18.

[3] Maloney, W.J., Jasty, M., Rosenberg, A. and Harris, W.H. Bone lysis in well fixed cemented femoral components. J. Bone Jt. Surgery, 1990, 72B, 966-970.

[4] Z M Jin, D Dowson, and J Fisher. Analysis of fluid film lubrication in artificial hip joint replacements with surfaces of high elastic modulus. Proc. Instn. Mech. Engrs. Vol H 211, 247-256, 1997.

[5] J. E. Nevelos, E. Ingham, C. Doyle, J. Fisher and A. B. Nevelos, "Analysis of retrieved Alumina ceramic components from Mittelmeier total hip prostheses". Journal of Biomaterials 20, 1833-1840, 2000.

[6] J. Fisher, A. A. Besong, P. J. Firkins, P. S. M Barbour, J. E. Nevelos, J. L. Tipper, M. H. Stone and E. Ingham, Trans 45th Orthopaedic Research Society, Proceedings of the 6th World Congress of Biomaterials, 871, 2000.

[7] J. E. Nevelos, E. Ingham, C. Doyle, R. Streicher, A. B. Nevelos, W. Walter and J. Fisher, Microseparation of the centres of Alumina-Alumina artificial hip joints during simulator testing produces clinically relevant wear rates and patterns. Journal of Arthroplasty, 15, 793-795, 2000.

[8] T.H. Mallory, D.A. Dennis, E.J. Northcut, A.V. Lombardi Jr., and S.M. Herrington, Do total hip arthoplasty piston during leg length maneuvers and Gait? An in-vivo determination of total hip athroplasty separation during abduction/Adduction leg lift and gait. Scientific Exhibit 66, AAOS, Los Angeles, CA, USA, 1999.

[9] T. Stewart, J. Tipper, R. Streicher, E. Ingham and J. Fisher, Long Term Wear of HIPed Alumina on Alumina Bearings for THR Under Microseparation Conditions Journal of Material Science. In Press.

[10] R. Rack, H.G. Pfaff, A new ceramic material for orthopaedics. Proceedings of the 5th International Biolox Symposium, March 23/24, 141-145 (2000) Published by Thieme.

[11] J. Wang, R. Stevens, Zirconia Toughened Alumina (ZTA) ceramics. Journal of Materials Science 24 (1989) 3421-3440.

[12] G. Orange, G. Fantozzi, Comportement mecanique de composites ceramiques a dispersoides. Materiaux et Techniques – Mars (1988), 29 - 39.

# Wear of Ceramic-Ceramic Hip Prostheses under Microseparation Simulation Conditions

*G.M.Insley[1], T. Stewart[2], J. Nevelos[2], J Fisher[2] and R.M.Streicher[3].*

[1]Stryker SA, Scientific and Clinical Affairs, Limerick, Ireland.
[2]School of Mechanical Engineering, University of Leeds, LS2 9JT UK
[3]Stryker SA, Scientific and Clinical Affairs, Thalwil, Switzerland

## 1. INTRODUCTION.

The majority of total hip prostheses currently implanted consist of a metal femoral head i.e. (cobalt chrome, nitrogen-strengthened stainless steel) articulating against an ultra high molecular weight polyethylene (UHMWPE) acetabular cup. Typical wear rates of 40-100 $mm^3$ per year have been reported corresponding to a linear penetration rate of the femoral head into the acetabular component of less than 0.25mm per year [1]. Even though the majority of these implants are successful there is a growing volume of evidence showing that wear debris from this combination leads to the eventual failure of the prosthesis [2,3]. It is generally believed that UHMWPE wear debris generated at the articulating surface enters the periprosthetic tissue where it triggers a number of defence mechanisms in the bone cells. The end result is osteoclastic bone resorption, leading to osteolysis and eventual loosening of the prosthesis. It is not the volume of wear particles that is important in this mechanism but the number of particles and their size range. Research has shown that particles in the size range 0.2-0.8 μm cause the highest biological response in the body [1].

The growing need to treat younger, more active patients has led to alternative bearing materials. Examples are the hard-on-hard bearing combinations of ceramic-on-ceramic and metal-on-metal. Ceramic-on-ceramic replacement hip joints have been in use since 1970. The earliest examples of ceramic-on-ceramic total hip replacements and surface replacements were those designed by Boutin, Griss, Salzer and Mittelmeier. These involved alumina femoral heads articulating against alumina acetabular cups, and were designed to provide low wear and good durability. Alumina ceramics are compounds in their highest oxidation state, making them chemically inert. Additionally ceramics are very hard (alumina has a Vickers hardness of 1900 $Kgfmm^{-2}$), and are also hydrophilic which means that the surfaces have very good wettability. Furthermore, it is possible to polish ceramics to a very smooth finish with surface roughnesses ($R_a$) of < 0.005 μm. These factors combine to give ceramic counterfaces excellent tribological properties with potential for fluid film lubrication during walking [4]. The wettability and the smoothness of the ceramic surfaces aids in this lubrication, while the hardness and low friction of the surfaces resist damage and wear.

Wear rates of early alumina/alumina hip prostheses manufactured from first generation alumina have been shown to be low *in vivo*, ranging from 1 to 5 $mm^3$ per year [5]. The vast majority of retrieved components showed similar characteristic features within the worn bearing surfaces. These included:

An elliptical wear stripe on the head with maximum penetration up to 100μm
A worn area in the cup with evidence of rim wear.
An intergranular fracture wear mechanism.

Characteristically these early prostheses were revised for loosening of the acetabular cups, which was partly attributed to the poor fixation of the acetabular component to the bone.

In contrast, simulator testing of ceramic-on-ceramic hip prostheses yielded extremely low wear rates (< 0.1mm$^3$ per million cycles), an order of magnitude lower than those reported *in vivo*. Bearing surfaces were undamaged, with no noticeable change in surface roughness [6].

The wear stripes found in first generation alumina ceramics were believed to be related to the inferior quality of the ceramic material. Developments such as hot isostatic pressing (HIPing) and grain refinement, to increase the density and strength of the alumina, were considered to alleviate this problem. However, recently two modern alumina/alumina hip prostheses manufactured from second generation HIPed alumina retrieved after only one year showed wear patterns similar to those found in the early retrieved components, with a small elliptical wear stripe on the femoral head 2-5 μm deep and a small amount of wear on the rim of the acetabular cup. These two prostheses (Figure 1) were both revised due to trauma and were anatomically positioned and well fixed prior to revision [7]. Wear volumes for these components have been measured to be approximately 0.5 mm$^3$.

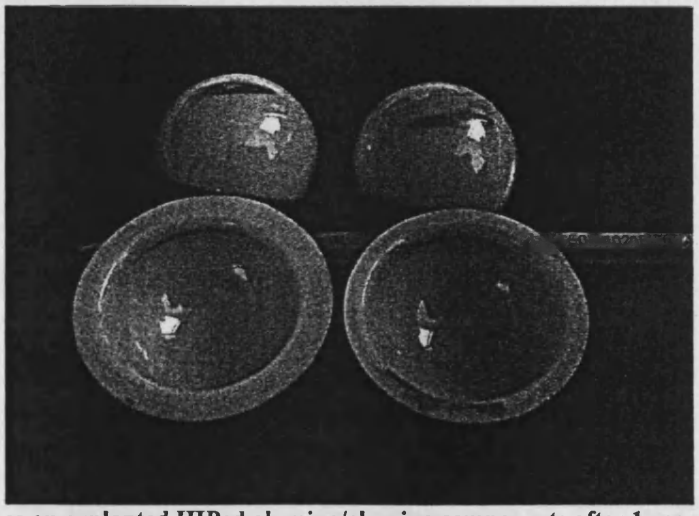

**Figure 1. Wear stripes on explanted HIPed alumina/alumina components after 1 year in vivo. The wear on the head and insert has been emphasised by rubbing with a graphite pencil.**

Wear patterns and mechanisms found clinically were not replicated in standard *in vitro* simulator tests.

Mallory *et al* [8] found by examining the fluoroscopic images of ten patients walking on a treadmill that the head and cup separate by a small amount during the swing phase. They found that the maximum separation was 2.8 mm and the minimum was 0.8 mm with an average separation seen at 1.2 mm. They also found that while the femoral head separated from the cup it remained in contact with the rim and postulated that high contact stresses would occur at this point with the application of load at heel-strike.

From this research it was hypothesized that microseparation of the head and cup could occur with any joint replacement and that this could be a factor in wear initiation for ceramic – ceramic systems as seen *in vivo*. Typically with these systems there is a very small clearance between the head and cup, of the order of 40 µm, and it is these tight clearances that allow the femoral head to contact the rim of the cup with only limited translation (Figure 2). Contact would occur with lateral and inferior displacements of less than 1 mm for a well-positioned prosthesis. Upon heel strike the head will translate superiorly and contact the rim before relocating. This rim contact will occur under very high stress and may initiate surface damage and hence accelerate wear [7].


**Figure 2.Schematic diagram showing of the stages of microseparation during the walking cycle**

This paper describes the wear of current and future ceramic-on-ceramic bearing couples under microseparation conditions in a laboratory.

## 2. MICROSEPARATION

*In vitro* microseparation was first reproduced by Nevelos *et al* (2000) using the Leeds mark II physiological hip joint simulator [7]. Under standard conditions this simulator applied a small positive swing phase load that ensured that the head remained located correctly in the cup throughout the gait cycle. To achieve joint separation a small lateral to medial load was applied to the acetabular insert, which, during the swing phase when the joint load was reduced, produced medial and superior translation of the insert relative to the head. Joint separation was limited by the radial clearance between the articulating components and ceased when the superior rim of the insert contacted the head after approximately 0.5 mm of translation. Further impact of the head and cup occurred with reapplication of the joint load at heel-strike. The load was momentarily supported by the small contact at the rim before the head relocated in the insert, thus modeling the clinical observations shown in Figure 2.

The microseparation technique reproduced for the first time clinically relevant levels of wear in ceramic-ceramic hip prostheses. The technique produced stripe wear with alumina/alumina via a similar intergranular fracture wear mechanism (Figure 3) to that seen *in vivo*. For additional validation of the technique, debris collected from the simulator were compared to debris from

retrieved tissues; both were found to contain predominantly nanometer - sized ceramic debris with the addition of a few larger ceramic particles attributed to microseparation.

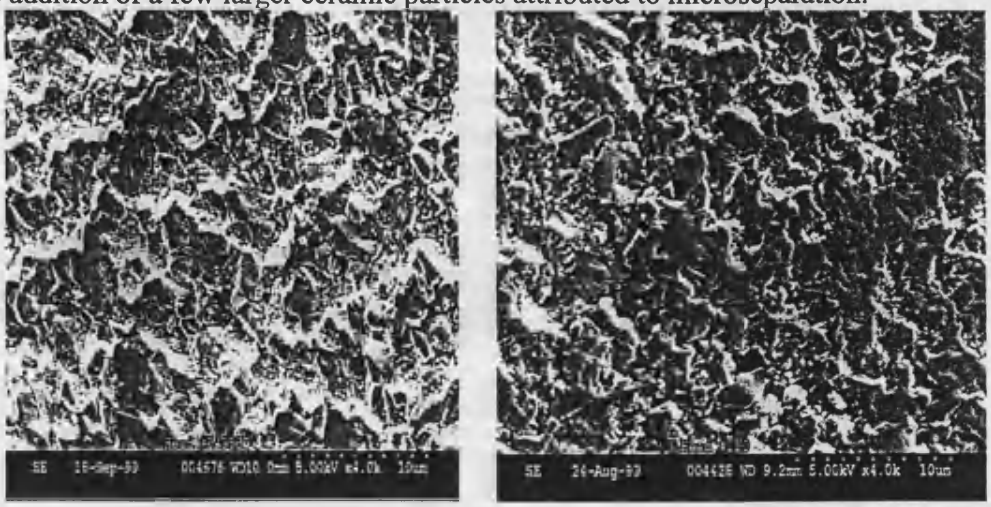

**Figure 3. SEM of retrieved (left) and in vitro microseparation (right) head wear stripes.**

Further research by Stewart *et al* (2001) showed that when the swing phase load in the simulator was reduced it becomes easier for the medial separation force both to overcome friction and to produce superior translation between the head and insert [9]. This increased the velocity of the insert and upon impact of the insert and head produced an increased momentum and impact energy, which resulted in a more severe microseparation condition. Therefore, by decreasing the swing phase load greater levels of joint laxity were modelled.

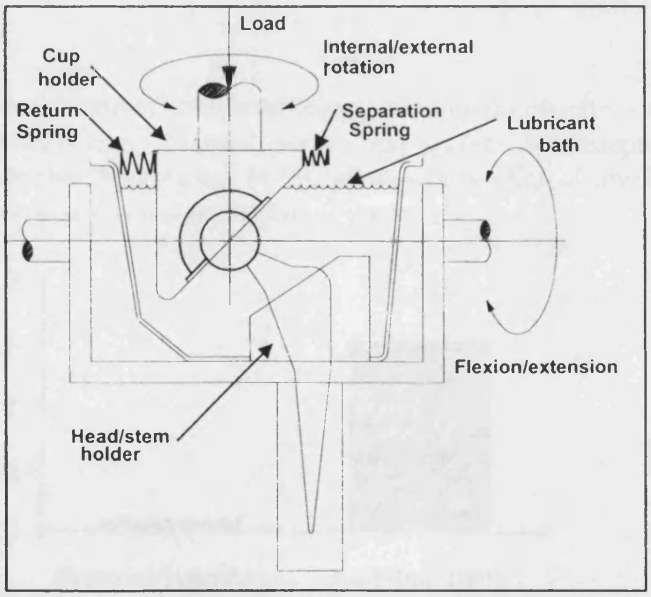


**Figure 4. Schematic diagram of the Leeds Mk II physiological hip joint simulator with microseparation.**

## 3. CERAMICS FOR HIP PROSTHESES

Alumina ceramic has been improved over the past 30 years and the introduction of hot isostatic pressing and grain refinement resulted in improved material properties, as shown in Table 1 [10].

**Table 1. Ceramic materials for hip prostheses**

| Ceramic | 1st generation alumina | 3rd generation alumina | Zirconia toughened alumina |
|---|---|---|---|
| Grain Size (μm) | <10 | <2 | <2 |
| Flexural Strength (MPa) | 400 | 580 | 1150 |
| Density (Mg $m^{-3}$) | 3.95 | 3.98 | 4.36 |
| Hardness (HV) | | 2300 | 1975 |
| Fracture Toughness (MPa $m^{1/2}$) | | 4.3 | 8.5 |
| Roughness $R_a$ (μm) | <0.05 | <0.005 | <0.005 |

One of the main disadvantages of ceramics in joint replacement has been their brittleness. Although the current reported fracture rate is low, typically 1 in 25000 [9] this remains a concern for some surgeons.

The addition of ~ 25 wt. % zirconia to the alumina matrix during manufacture has been shown to increase the fracture toughness and flexural strength of the alumina [10,11,12]. Two zirconia toughened aluminas (ZTAs) are currently available, one containing 74 wt. % alumina, 24 wt % zirconia and 1% mixed oxides, and another consisting of 75 wt. % alumina and 25 wt. % zirconia.

## 4. CERAMIC WEAR

The volumetric wear from standard simulator testing of alumina ceramic - on - ceramic bearings has generally been reported as < 0.1 $mm^3$ per million cycles. Microseparation simulation has been shown to increase this by a factor of 10, approaching clinical levels of wear as seen in retrieved first generation alumina hip prostheses (Figure 5).

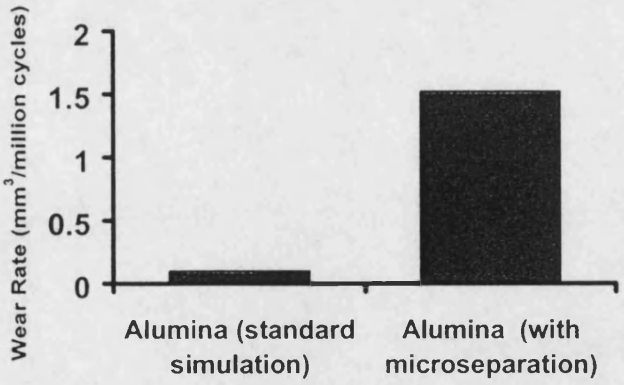


**Figure 5. In vitro ceramic wear; comparison of standard and microseparation simulator tests [7].**

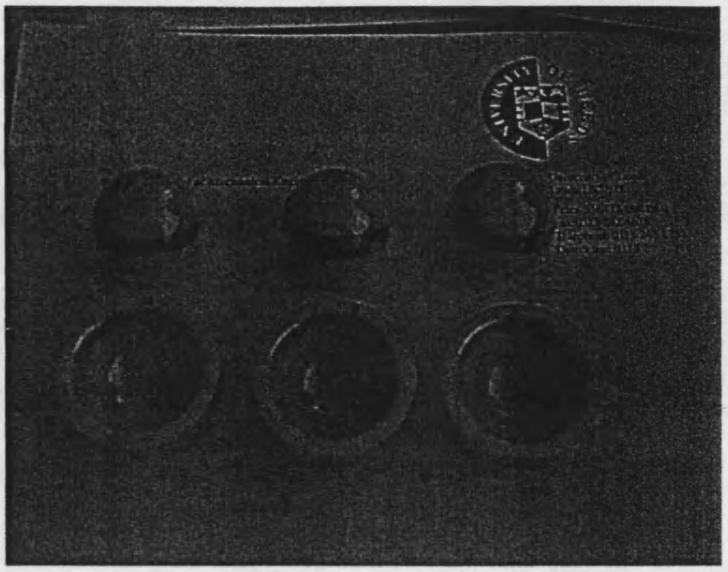

**Figure 7. Wear stripes on the alumina/alumina components after 5 million cycles in the Leeds hip simulator under microseparation conditions.**

Scanning electron microscopy (SEM) was used to examine the wear scars at a microscopic level. The scars produced by microseparation testing were remarkably similar to the wear scars seen on the explanted ceramics (Figure 3) and a similar grain boundary fracture wear mechanism was observed.

Wear debris collected and analysed from microseparation simulation of alumina/alumina were generally very small with a mean particle size of approximately 40 nm, as shown in Figure 8. This was similar to the debris collected from normal simulator tests with a mean particle size of 30 nm. The size range of these particles showed that the microseparation debris also contains a few larger particles that are not seen in normal simulation. Typically these were in the range of 100 to 3000 nm and compare well to the larger particles seen in the surrounding tissue of retrieved ceramic components.

Microseparation simulator studies have only, as yet, been reported from one centre. The findings so far support its use as a means to evaluate ceramic bearing materials in a more physiologically realistic manner.

Long term testing has been reported for the current generation of alumina hip prostheses [9] with typical wear behaviour as shown in Figure 6.

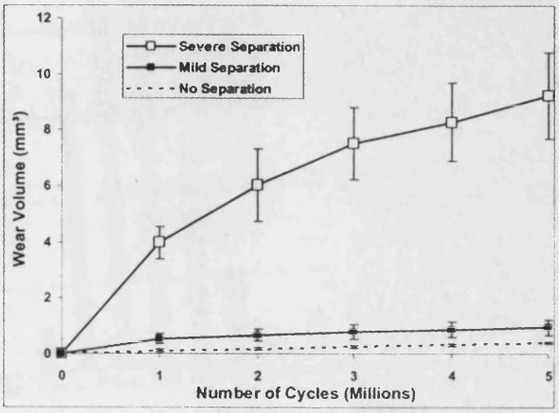


**Figure 6. Wear volumes ± Standard error, n=3 for each group.**

For the current Alumina materials under severe microseparation wear, was characterised by an initially higher wear period during which a characteristic wear stripe on the femoral head and the rim wear on the cup were initiated. The wear then decreased to a lower steady - state value with no signs of run-away wear observed. The severity of testing made a significant difference to the resulting wear rates of the alumina material, emphasising the need for careful control of experiments.

Worn surfaces appeared as shown in Figure 7, in which the wear on the head and insert has been emphasised by rubbing with a graphite pencil.

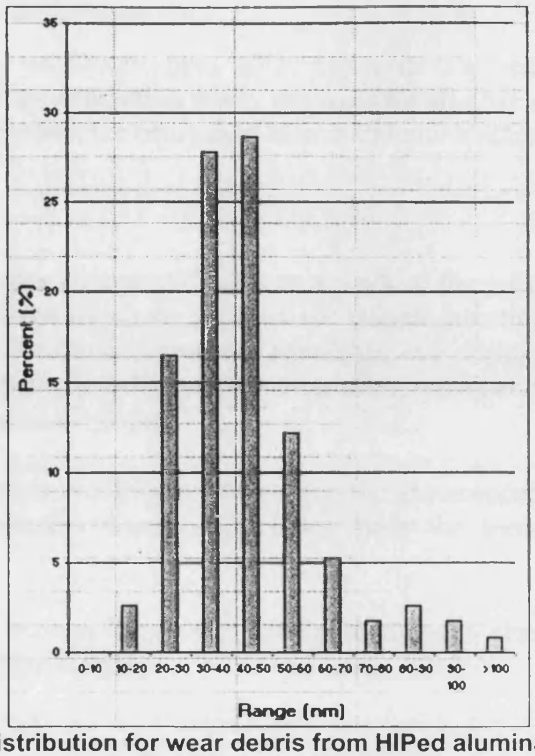


**Figure 8. Particle size distribution for wear debris from HIPed alumina tested in the simulator under microseparation conditions.**

Preliminary simulator studies have also been completed for two different ZTA materials under standard and microseparation conditions shown in Figure 9. The materials were tested in a concurrent study with HIPed alumina as a control, for a duration of 1 million cycles.

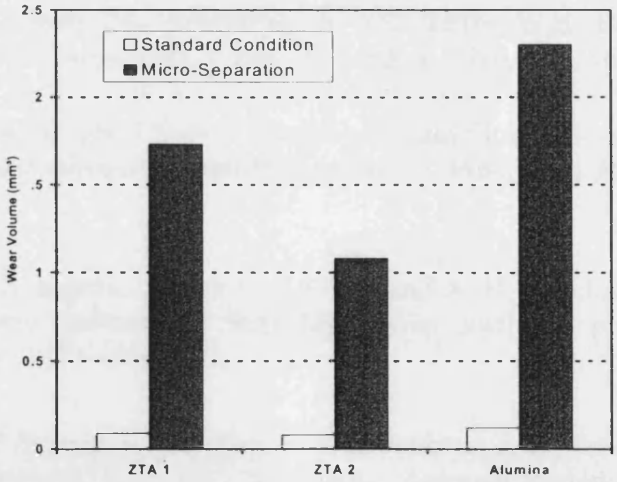


**Figure 9. Wear Volume of two ZTA materials in standard and microseparation simulator testing conditions compared to alumina.**

Under normal simulation conditions both ZTA materials showed slightly less wear than alumina/alumina. Under microseparation mode, the wear for all couples increased. However, the ZTA/ZTA couples wore less than the equivalent alumina/alumina couple.

## 5. Conclusions.

Standard simulator kinematics are not sufficient to reproduce the wear rates and mechanisms of alumina ceramic hip prostheses which are found in the clinical situation. However, simulation of a microseparation between the femoral head and acetabular cup during the swing phase in the hip joint simulator has reproduced clinically relevant wear rates, wear patterns, wear mechanisms and wear debris for alumina/alumina bearings.

Despite the increase in wear volume produced by the microseparation of ceramic-ceramic bearings the wear still remains significantly lower than the wear of traditional metal on UHMWPE bearings.

Preliminary results using zirconia toughened alumina composite ceramics show slightly lower wear than the alumina/alumina couple.

## References


[1] Ingham, E. and Fisher, J. Biological reactions to wear debris in total joint replacement. Proc. Instn. Mech. Engrs. Vol 214 Part H, 2000, 21-37.

[2] Amstutz, H.C.; Campbell, P.; Kossovsky, N. and Clarke I.C. Mechanism and clinical significance of wear debris induced osteolysis. Clin. Orthop.; 1992, 276, 7-18.

[3] Maloney, W.J., Jasty, M., Rosenberg, A. and Harris, W.H. Bone lysis in well fixed cemented femoral components. J. Bone Jt. Surgery, 1990, 72B, 966-970.

[4] Z M Jin, D Dowson, and J Fisher. Analysis of fluid film lubrication in artificial hip joint replacements with surfaces of high elastic modulus. Proc. Instn. Mech. Engrs. Vol H 211, 247-256, 1997.

[5] J. E. Nevelos, E. Ingham, C. Doyle, J. Fisher and A. B. Nevelos, "Analysis of retrieved Alumina ceramic components from Mittelmeier total hip prostheses". Journal of Biomaterials 20, 1833-1840, 2000.

[6] J. Fisher, A. A. Besong, P. J. Firkins, P. S. M Barbour, J. E. Nevelos, J. L. Tipper, M. H. Stone and E. Ingham, Trans 45th Orthopaedic Research Society, Proceedings of the 6th World Congress of Biomaterials, 871, 2000.

[7] J. E. Nevelos, E. Ingham, C. Doyle, R. Streicher, A. B. Nevelos, W. Walter and J. Fisher, Microseparation of the centres of Alumina-Alumina artificial hip joints during simulator testing produces clinically relevant wear rates and patterns. Journal of Arthroplasty, 15, 793-795, 2000.

[8] T.H. Mallory, D.A. Dennis, E.J. Northcut, A.V. Lombardi Jr., and S.M. Herrington, Do total hip arthoplasty piston during leg length maneuvers and Gait? An in-vivo determination of total hip athroplasty separation during abduction/Adduction leg lift and gait. Scientific Exhibit 66, AAOS, Los Angeles, CA, USA, 1999.

[9] T. Stewart, J. Tipper, R. Streicher, E. Ingham and J. Fisher, Long Term Wear of HIPed Alumina on Alumina Bearings for THR Under Microseparation Conditions Journal of Material Science. In Press.

[10] R. Rack, H.G. Pfaff, A new ceramic material for orthopaedics. Proceedings of the 5th International Biolox Symposium, March 23/24, 141-145 (2000) Published by Thieme.

[11] J. Wang, R. Stevens, Zirconia Toughened Alumina (ZTA) ceramics. Journal of Materials Science 24 (1989) 3421-3440.

[12] G. Orange, G. Fantozzi, Comportement mecanique de composites ceramiques a dispersoides. Materiaux et Techniques – Mars (1988), 29 - 39.